A Dissertation

entitled

Migration Ecology of *Vermivora* Warblers

by

Gunnar Robert Kramer

Submitted to the Graduate Faculty as partial fulfillment of the requirements for the

Doctor of Philosophy Degree in

Biology

Dr. Henry M. Streby, Committee Chair

Dr. David E. Andersen, Committee Member

Dr. Jonathon M. Bossenbroek, Committee Member

Dr. David A. Buehler, Committee Member

Dr. Petra B. Wood, Committee Member

Dr. Amy Thompson, Acting Dean
College of Graduate Studies

The University of Toledo

December 2021

An Abstract of

Migration Ecology of *Vermivora* Warblers

by

Gunnar Robert Kramer

Submitted to the Graduate Faculty as partial fulfillment of the requirements for the
Doctor of Philosophy Degree in
Biology

The University of Toledo
December 2021

Conserving and managing migratory species is inherently complicated due largely to their reliance on multiple landscapes at different stages of their annual cycle (Faaborg et al. 2010). The combination and degree to which each life stage (e.g., nascence through independence from adult care), geographical location (e.g., a large estuarine stopover site), or portion of the annual cycle (e.g., the nonbreeding period) influences a population is often unknown. Thus, resulting conservation strategies are often built with information representing a limited portion of a migratory species' annual range (Runge et al. 2014). This trend is concerning as recent studies demonstrate the influence of poorly studied life stages (e.g., the post-fledging period; Streby and Andersen 2011) and carryover effects (e.g., habitat quality and food availability influencing subsequent productivity; Legagneux et al. 2012) on population dynamics of migratory species. Previous research suggests that, like other migratory taxa, global populations of many migratory birds are declining at alarming rates (Robbins et al. 1989, Sauer et al. 1996, Sanderson et al. 2006), presenting an important and time-sensitive opportunity to develop full life-cycle conservation strategies and identify and mitigate key factors driving population declines in migratory species.

This dissertation investigates the migratory ecology of *Vermivora* warblers and synthesizes findings in ecological, evolutionary, and conservation frameworks. *Vermivora* warblers are a species complex composed of two extant species of obligate Nearctic-Neotropical migrant warblers that are extremely closely related (Toews et al. 2016). Golden-winged warblers (*Vermivora chrysoptera*) and blue-winged warblers (*Vermivora cyanoptera*) breed and migrate throughout deciduous forests of eastern North America and occur throughout Central America, with golden-winged warblers also occurring in northern South America during the nonbreeding period (Rosenberg et al. 2016). On the breeding grounds, golden-winged warblers and blue-winged warblers have overlapping distributions and regularly hybridize to produce viable young (Vallender et al. 2007a, Neville et al. 2008). Recent genomic evidence suggests overlap and hybridization has occurred for >1,000 years and that these two species may constitute a single, polymorphic species with differences in their genomes primarily associated with different plumage traits (Toews et al. 2016, Toews et al. 2021). Both species of *Vermivora* and two recognized hybrid phenotypes breed in similar habitat, often with overlapping territories; sing songs with overlapping characteristics; and exhibit nearly identical foraging and reproductive strategies (Rosenberg et al. 2016, Streby et al. 2016a, Kramer et al. 2020).

Despite remarkable genetic, behavioral, and natural history similarities, regional populations of *Vermivora* have experienced starkly contrasting population trajectories since standardized monitoring began in 1966 (Pardiek et al. 2016, Sauer et al. 2017). Golden-winged warblers breeding throughout the Great Lakes region have maintained historical abundances, whereas golden-winged warblers breeding throughout the

Appalachian Mountains region have declined precipitously (Sauer et al. 2017). To date, declines in the Appalachian Mountains have amounted to a loss of 98% of historical abundance and resulted in regional extirpations from many areas where golden-winged warblers were once common (Rosenberg et al. 2016). Hypotheses about the cause of these declines have focused on breeding-grounds factors, namely, habitat loss and hybridization (i.e., genetic swamping), as the primary drivers of declines in Appalachian Mountains populations of golden-winged warblers (Rosenberg et al. 2016). However, habitat loss and hybridization fail to parsimoniously explain the stationary population trends of Great Lakes populations of golden-winged warblers and the stationary population trends of blue-winged warblers throughout their distribution, including in the Appalachian Mountains, where they co-occur with historically declining populations of golden-winged warblers (Streby et al. 2016a). Therefore, describing the nonbreeding distribution and ecology of *Vermivora* warblers may be instrumental in developing effective conservation strategies for declining populations of *Vermivora* and may also provide important ecological and evolutionary insights into the phenomenon of long-distance migration.

In Chapter 1, I described the distribution and migratory connectivity of *Vermivora* populations during the stationary nonbreeding period. Populations of *Vermivora* exhibit geographically varied historical population trends that are poorly explained by breeding-grounds factors despite decades of research. Using analytical methods that I developed to analyze geolocator data, I tested whether breeding populations of *Vermivora* warblers exhibit strong migratory connectivity (i.e., remain isolated during the nonbreeding period) and if population trends are linked to land-use change in population-specific nonbreeding areas. I found that blue-winged warblers exhibited weak migratory connectivity whereas golden-winged warblers exhibited strong migratory connectivity. Moreover, golden-winged warblers from populations that experienced historical population declines occurred in northern South America during the nonbreeding period and were temporally associated with deforestation. Golden-winged warblers from numerically stable breeding populations almost exclusively occurred in Central America during the nonbreeding period in areas that experienced less historical deforestation. I also identified other Nearctic-Neotropical migrant bird species (Passeriformes) with similar distributions and population trends consistent with golden-winged warblers that may be experiencing similar limiting factors as golden-winged warblers.

In Chapter 2, I explored space-use patterns of *Vermivora* populations during autumn and spring migrations. Migration is purported to be the most dangerous period of the annual cycle for many small, migratory songbirds. The availability of suitable stopover sites where migratory individuals stop and refuel and/or the abundance of anthropogenic and natural risk-factors experienced during migration may be limiting populations for many species. I quantified differences in space-use among populations of *Vermivora* warblers during migration with a focus on providing information to improve population-level conservation. Populations of *Vermivora* warblers exhibited variation in space use during migration but these differences were not meaningfully associated with differential exposure to both anthropogenic risk-factors (e.g., light pollution, communication towers, wind energy turbines) and natural risk-factors (e.g., severe storms, hurricanes) at several spatial scales. Thus, there is little evidence that recent variation in population trends of *Vermivora* warblers is linked to risk factors experienced during migration.

Chapter 3 focused on identifying drivers of migratory behavior of individual *Vermivora* warblers at the Gulf of Mexico. Specifically, I determined whether individuals crossed the Gulf of Mexico directly in a single, overwater flight or circumvented the Gulf of Mexico to the west using a primarily overland route with stopover sites along the eastern coast of Mexico. I investigated if weather conditions explained variation in individuals' strategies and if patterns in route-type use exist between species and among populations. Departure across the Gulf of Mexico was associated with different weather conditions in autumn and spring migrations. The predicted favorability of conditions varied geographically and the general distribution of *Vermivora* warblers reflected the favorability of weather conditions for departing across the Gulf of Mexico. Thus, changing climate conditions might affect the favorability of conditions and shape route use by *Vermivora* warblers crossing the Gulf of Mexico in the future.

In Chapter 4, I revisited my results from Chapter 1 and explored the evolutionary origins and implications of migratory connectivity in the Anthropocene. Specifically, I simulated how different selective pressures influence the evolved strength of migratory connectivity. I found that strong migratory connectivity could arise rapidly under specific selection scenarios that resulted in relatively greater fitness for individuals breeding and wintering in specific areas. After strong migratory connectivity evolved, connectivity remained strong even if selection pressures were eliminated. These simulations provide context for understanding the conditions under which strong migratory connectivity evolves and suggest that strong migratory connectivity may constitute an evolutionary trap. This type of previously undefined evolutionary trap may arise when rapidly changing conditions in distinct portions of the annual cycle cause previously adaptive associations to become disentangled from historical fitness outcomes. Understanding the evolutionary constraints of strong migratory connectivity in the Anthropocene will address critical knowledge gaps that can lead to improved conservation and management of migratory species.

This dissertation and the individual chapters within were largely influenced by my experiences studying *Vermivora* warblers and provide timely and pertinent information that will prove useful for the management and conservation of this species complex. More broadly, I believe the themes and results of this dissertation provide important and novel insights into the ecology and management of migratory species across taxa.

Acknowledgments

I am deeply grateful for the guidance and mentorship of my committee. I thank the UToledo College of Graduate Studies for awarding me a Graduate Dean's Fellowship which supported me for the majority of my dissertation. I am especially thankful to Dr. C. Gruden, Dr. A. Bryant-Friedrich, T. Green, and the inaugural GDSF cohort for their mentorship and collaboration during my time as a GDSF Fellow.

I thank S. Fischer, R.K. Pagel, I. Clifton, J. Otten, A. Hulbert, R. Whittington, S. Carter, A. Lindsay, E. West, and the rest of the Refsnider and Streby labs for their friendship and inspiration. The field work that led to this dissertation would not have been possible without the efforts of many dedicated technicians and volunteers. I am especially grateful for the contributions of S. Peterson, C. Ziegler, K. Maley, P. Rodrigues, and A. Pesano. Additionally, I received invaluable logistical support from H. Saloka, W. Ford, and many other collaborators.

Mom, Dad, Louise, Tom, and August: thank you for your unwavering encouragement and enthusiasm. Collin, thank you for your endless love and support throughout all of our adventures.

Table of Contents

List of Tables

List of Figures

Chapter 1

Population Trends in *Vermivora* Warblers are Linked to Strong Migratory Connectivity

This chapter published in *Proceedings of the National Academy of Sciences*:

Kramer, G.R., D.E. Andersen, D.A. Buehler, P.B. Wood, S.M. Peterson, J.A. Lehman, K.R. Aldinger, L.P. Bulluck, S. Harding, J.A. Jones, J.P. Loegering, C. Smalling, R. Vallender, and H.M. Streby. 2018. Population trends in *Vermivora* warblers are linked to strong migratory connectivity. *Proceedings of the National Academy of Sciences* 115:E3192–E3200 https://doi.org/10.1073/pnas.1802174115.

1.1 Abstract

Migratory species can experience limiting factors at different locations and during different periods of their annual cycle. In migratory birds, these factors may be separated by hemispheres. Therefore, identifying the distribution of populations throughout their annual cycle (i.e., migratory connectivity) can reveal the complex ecological and evolutionary relationships that link species and ecosystems across the globe and illuminate where and how limiting factors influence population trends. A growing body of literature continues to identify species that exhibit weak or moderate connectivity wherein individuals from distinct breeding areas co-occur during the nonbreeding period. A detailed account of a broadly distributed species exhibiting strong migratory connectivity in which nonbreeding isolation of populations is associated with differential population trends remains undescribed. Here I present a range-wide assessment of the nonbreeding distribution and migratory connectivity of two broadly dispersed Nearctic-Neotropical migratory songbirds. I used geolocator data to determine the movements of 70 *Vermivora* warblers from sites spanning their breeding distribution in eastern North America and identified links between breeding populations and nonbreeding areas. Unlike blue-winged warblers (*V. cyanoptera*), breeding populations of golden-winged warblers (*V. chrysoptera*) exhibited strong migratory connectivity, which was associated with historical breeding population trends. Overall, historically stable breeding populations of *Vermivora* wintered in Central America, whereas declining breeding populations wintered in northern South America. Identifying the migratory connectivity of additional species will provide insights into the evolution of different migration strategies and the implications of such strategies in today's world.

1.2 Introduction

Populations of migratory species can be limited by factors throughout their annual cycle. The degree to which spatially isolated breeding populations use geographically distinct areas during the nonbreeding period (i.e., migratory connectivity) affects the potential for regionally specific factors to influence population trends (Sherry and Holmes 1996, Webster et al. 2002, Faaborg et al. 2010). Tracking migratory animals to link breeding populations with nonbreeding areas has primarily focused on the migratory behaviors of large mammals and large birds, which have been studied for decades, and even centuries (Wilkes 1845, Maury 1851, Lincoln 1921, Hanson and Smith 1950, Dawbin 1956, Mandel et al. 2008). However, following recent technological advances, it is now possible to track all but the smallest migratory species across time and space (Holland et al. 2006, Stutchbury et al. 2009, Hobson 1999). The value of tracking species throughout the annual cycle is manifold. Identifying the migratory pathways by which animal populations navigate between breeding and nonbreeding areas can reveal population-level differences in route or space-use that may explain differential breeding population trends (Hewson et al. 2016) or signal tradeoffs in life-history strategies (Prop et al. 2003, Hebblewhite and Merrill 2007, Deppe et al. 2015). In migratory birds, the distribution of breeding populations during the nonbreeding period has the potential to be the primary driver of population trends as many long-distance migrant species spend more time on nonbreeding sites than in any other location during the annual cycle (Sillett and Holmes 2002). Furthermore, environmental conditions experienced during the nonbreeding period can have both direct (Taylor and Stutchbury 2017) and indirect effects (Marra et al. 1998) on individuals and, consequently, influence population trends. As such, describing the spatial structure and level of dispersion of a migratory species during the nonbreeding period can identify potential areas that may limit some populations but not others (Fraser et al. 2012, Stanley et al. 2014, Hallowrth et al. 2015), provide insight into the evolutionary history of migratory species (Winger et al. 2014, Burgio et al. 2017, Toews et al. 2017), and aid in the identification of important areas that may be targeted for conservation (Sawyer et al. 2009, Iwamura et al. 2013, Stanley et al. 2014, Richardson et al. 2016, Kramer et al. 2017, Taylor and Stutchbury 2017, Wolfson et al. 2017).

Despite a growing body of information on the behaviors and connectivity of migratory birds, detailed range-wide studies investigating the nonbreeding distribution and migratory connectivity of entire species remain rare (Fraser et al. 2012, Stanley et al. 2014). Weak migratory connectivity is most commonly reported in studies of long-distance migratory bird species worldwide (Hahn et al. 2013, Finch et al. 2015, Hobson et al. 2015, Ouwehand et al. 2016, Finch et al. 2017). Weak connectivity results in nonbreeding areas that are inhabited by individuals from multiple, widely dispersed breeding populations. Strong migratory connectivity, resulting in geographic isolation during the nonbreeding period, is required for differential population trends of geographically distinct breeding populations to be driven by factors away from the breeding grounds. Though the theoretical implications of strong connectivity have been addressed and discussed (Webster et al. 2002), rarely are species' breeding population trends decisively linked to individual populations' occurrence at isolated nonbreeding areas and this information can be particularly important for the conservation of declining and threatened species. Identifying species with populations that might be independently limited by factors outside of the breeding period will contribute to the understanding of the ecological and evolutionary implications of strong migratory connectivity, and why it appears to be uncommon among migratory birds.

I investigated the migratory connectivity of *Vermivora* wood-warblers (Parulidae): a species-complex comprised of two extant species of obligate Nearctic-Neotropical migrant warblers that are extremely closely related (Toews et al. 2016). Golden-winged warblers (*V. chrysoptera*) and blue-winged warblers (*V. cyanoptera*) breed and migrate throughout deciduous forests of eastern North America and occur throughout Central America with golden-winged warblers also occurring in northern South America during the nonbreeding period and recent evidence suggests golden-winged warblers may exhibit strong, range-wide migratory connectivity (Bennett et al. 2017, Kramer et al. 2017). On the breeding grounds, golden-winged warblers and blue-winged warblers have overlapping breeding distributions and regularly hybridize to produce viable young (Vallender et al. 2007a). Recent genomic evidence suggests overlap and hybridization has occurred for >1,000 years and that these two species may constitute a single, polymorphic species with differences in their genomes primarily associated with different plumage traits (Toews et al. 2016). That said, detailed information on the genetic structure of *Vermivora* populations is lacking (Toews et al. 2016). Furthermore, to date there is little evidence of costs to producing hybrid young in this system (Vallender et al. 2007b, Neville et al. 2008). Both species of *Vermivora*, and two recognized hybrid phenotypes breed in similar habitat, often with overlapping territories, sing songs with overlapping characteristics, and exhibit nearly identical foraging and reproductive strategies (Rosenberg 2016, Streby et al. 2016a).

Despite remarkable genetic, behavioral, and natural history similarities, regional populations of *Vermivora* have experienced starkly contrasting population trajectories since standardized monitoring began in 1966 (Pardieck et al. 2016, Sauer et al. 2017). Golden-winged warblers breeding throughout the Great Lakes region have maintained historical abundances, whereas golden-winged warblers breeding throughout the Appalachian Mountains region have declined steadily (Sauer et al. 2017; Fig. 1 – A: D, E). To date, declines in the Appalachian Mountains have amounted to a loss of 98% of historical abundance and resulted in regional extirpations from many areas where golden-winged warblers were once common (Rosenberg et al. 2016). Hypotheses about the cause of these declines have focused on breeding-grounds factors, namely habitat loss and hybridization (i.e., genetic swamping) as the primary drivers of declines in Appalachian Mountain populations of golden-winged warblers (Rosenberg et al. 2016). However, habitat loss and hybridization fail to parsimoniously explain the stationary population trends of Great Lakes populations of golden-winged warblers and the stationary population trends of blue-winged warblers throughout their distribution, including in the Appalachian Mountains where they co-occur with historically declined populations of golden-winged warblers (Streby et al. 2016a). Previous investigations into the migratory connectivity of *Vermivora* warblers have focused exclusively on golden-winged warblers and are equivocal. Assessments of stable isotopes in feathers of golden-winged warblers collected during the nonbreeding period showed a possible overlap among Appalachian and Great Lakes populations in Central America (Hobson et al. 2016), whereas a smaller-scale, light-level geolocator study found no evidence of nonbreeding population overlap among golden-winged warblers at Great Lakes and Appalachian breeding sites (Kramer et al. 2017). Populations of blue-winged warblers, including those breeding sympatrically with declining golden-winged warblers in the Appalachian Mountain region, have remained numerically stable (Sauer et al. 2017; Fig. 1 – A: F–H). This suggests that the limiting factor primarily driving declines of Appalachian golden-winged warblers is likely experienced somewhere outside the breeding period at a time or location that exclusively affects golden-winged warblers that breed in the Appalachian Mountains.

Here, I present the results of a large, range-wide study (Fig. A – 1) tracking individual songbirds and describe the migratory connectivity of two hybridizing migratory species. I used light-level geolocators (hereafter, geolocators; see Appendix A Supplementary Methods) to track individual *Vermivora* warblers throughout their annual cycle and determine links between breeding and nonbreeding areas. Based on differences in breeding population trends (Fig. 1 – 1: A) that are not explained by breeding-grounds factors, I predicted that golden-winged warblers would exhibit strong migratory connectivity with declining populations occurring disparately from numerically stable populations. If there is strong migratory connectivity and isolation among populations during the nonbreeding period, I further predicted that nonbreeding areas used by historically declining populations will have experienced disproportionate rates of forest loss that coincide with population trends. I discuss the implications of the observed migratory connectivity of *Vermivora* warblers in ecological and evolutionary frameworks. Lastly, I identify species that share similar nonbreeding distributions with *Vermivora* and exhibit varied regional population trajectories akin to those seen in golden-winged warblers that I hypothesize may have similarly strong migratory connectivity driving those species' regional population trends.

1.3 Results and Discussion

Geolocator-marked golden-winged warblers (*n* = 41) occurred at sites from Guatemala and southern Mexico to northern Venezuela during the nonbreeding period (Fig. 1 – 2: A). Individuals from historically stable Great Lakes breeding populations (Bird Conservation Region [BCR] S12: Boreal Hardwood Transition; see Materials and Methods; Fig. 1 – 1) were dispersed broadly and almost exclusively throughout Central America during the nonbreeding period (28/29; 97%; Fig. 1 – 2: B–C) though one individual from a breeding site in central Ontario, Canada occurred in northern South America (Fig. 1 – 2: A). Golden-winged warblers from historically declining breeding populations in the Appalachian Mountains (BCR S28: Appalachian Mountains; *n* = 12) occurred at sites exclusively in northern South America, primarily in northern Venezuela (Fig. 1 – 2: D–E) during the nonbreeding period. Blue-winged warblers (*n* = 25), which exhibit historically stable population trends throughout their breeding distribution (BCRs S23, S24, and S28; Prairie Hardwood Transition, Central Hardwoods, and Appalachian Mountains, respectively; Fig. 1 – 1), occurred almost exclusively in Central America during the nonbreeding period (24/25; 96%; Fig. 1 – 2: F). Only one blue-winged warbler from a northern Appalachian Mountain breeding population occurred in northern South America. Phenotypic hybrids (*n* = 4) from breeding populations in the Great Lakes region (*n* = 2) occurred in northern Central America during the nonbreeding period (Fig. 1 – 3: B), whereas hybrids from breeding populations in the Appalachian Mountains (*n* = 2) occurred in northern South America (Fig. 1 – 3: C). Golden-winged warblers from Great Lakes breeding populations and blue-winged warblers overlapped extensively in Central America during the nonbreeding period (Fig. 1 – 2: B–C, Fig. 1 – 2: G–J, Fig. A – 3). However, historically declining Appalachian Mountains populations of golden-winged warblers were isolated from historically stable populations of both golden-winged warblers and blue-winged warblers during the nonbreeding period (Fig. A – 2).

Regional breeding populations of blue-winged warblers (i.e., populations identified by their BCRs) did not occur in isolation from one another during the nonbreeding period (one-way ANOVA $F = 1.3$, df = 3, 20, $P = 0.3$; Fig. A – 3). However, individual blue-winged warblers that spent the nonbreeding period in Central America exhibited a pattern such that individuals from more easterly breeding longitudes tended to occur farther east during the nonbreeding period (Fig. A – 3). Conversely, regionally isolated breeding populations of golden-winged warblers maintained their separation during the nonbreeding period, with the Great Lakes population of golden-winged warblers occurring farther west during the nonbreeding period, on average, than Appalachian Mountain breeding populations ($F = 213.4$, df = 1, 39, $P < 0.0001$; Fig. A – 2, Fig. A – 3). Unsurprisingly, this pattern remained when I considered the relationship between individual breeding longitude and nonbreeding longitude within and between populations of golden-winged warblers (Fig. A – 4).

I found strong evidence to support the hypothesis that population trends of *Vermivora* warblers were associated with distribution and isolation of historically stable and declining populations during the nonbreeding period. Historically stable populations of golden-winged warblers from breeding sites in the Great Lakes region occurred throughout Central America during the nonbreeding period, whereas historically declining populations from breeding sites in the Appalachian Mountains region occurred in northern South America. Notably, blue-winged warblers from breeding sites in the Appalachian Mountains region (i.e., the same region in which golden-winged warblers are declining) occurred in Central America during the nonbreeding period alongside historically stable Great Lakes populations of golden-winged warblers. The remarkable similarities between these two species on the breeding grounds (e.g., nearly identical habitat use, phenology, life-history) and co-occurrence in geographical space suggests that the differential population trends observed between populations of golden-winged warblers and blue-winged warblers breeding in the Appalachian Mountains region are likely driven by factors outside of the breeding period.

Intraspecific migratory connectivity between populations of golden-winged warblers was strong (i.e., individuals from distinct breeding populations used different areas during the nonbreeding period) and I am not aware of any other report of similarly strong connectivity from a range-wide study of distinct breeding populations in another species of migratory songbird. Blue-winged warbler populations exhibited weak connectivity (i.e., individuals from distinct and isolated breeding areas co-occurred during the nonbreeding period) and occurred throughout Central America alongside golden-winged warblers from Great Lakes populations. I found weak connectivity (or high levels of dispersion) within Great Lakes golden-winged warblers and blue-winged warblers, range-wide. For example, individual golden-winged warblers from breeding sites in Minnesota, USA, where ~50% of the global population of golden-winged warblers breed (Rosenberg et al. 2016), were dispersed throughout Central America during the nonbreeding period occurring from southern Mexico to Panama (maximum distance between two individuals >1,500 km). Similarly, blue-winged warblers from breeding sites in Massachusetts, USA, were dispersed during the nonbreeding period from the Yucatan Peninsula, Mexico, to northern Colombia (maximum distance between two individuals ~2,000 km). Without considering the individual that migrated to Colombia, Massachusetts blue-winged warblers were still broadly dispersed (maximum distance between two individuals ~1,000 km). Conversely, populations of golden-winged warblers from breeding sites throughout the Appalachian Mountains were more concentrated in a relatively small area in northeastern Colombia and northwestern Venezuela during the nonbreeding period (maximum distance between two individuals from the same breeding site ~600 km).

European migratory bird species that disperse broadly during the nonbreeding period are less likely to be declining than species with restricted distributions during the nonbreeding period compared to their breeding distributions (Fuller 2016, Gilroy et al. 2016). I observed this trend at the population level with greater nonbreeding dispersion among numerically stable populations (i.e., golden-winged warblers breeding in the Great Lakes, and all populations of blue-winged warblers) compared to declining breeding populations (e.g., golden-winged warblers breeding in the Appalachian Mountains) suggesting that migratory diversity (i.e., within-population variation in migratory routes and/or destinations) may be linked to population trends at both species and population levels. Tracking additional birds may uncover greater dispersion, but golden-winged warblers from Appalachian Mountain breeding populations were overrepresented in the sample based on estimated population size (29% of golden-winged warbler sample but only ~5% of global population; Rosenberg et al. 2016) and therefore I believe that additional sampling will likely confirm low dispersion in this population.

The differential population trends observed in *Vermivora* warblers using Central American vs. South American nonbreeding areas may be caused by a variety of factors. The complexity of the ecological relationships and resource requirements that exist throughout the annual cycle of a migratory species make it unlikely that there is a single driver of these trends. However, the identification of spatial isolation among these populations of *Vermivora* warblers suggests that the drivers of historical declines in populations of Appalachian-breeding golden-winged warblers are linked to their nonbreeding distribution in northern South America, or the migratory pathways they use between breeding and nonbreeding locations. The cause of the precipitous declines of golden-winged warblers that use this region during the nonbreeding period need not be tied to a single factor, but may be the result of a reliance on a region that has experienced extensive anthropogenic exploitation and changes in land use over the past century (Hansen et al. 2010, Dávalos et al. 2011, Runge et al. 2015, Negret et al. 2017).

Aerial photographs and/or satellite imagery covering the entire nonbreeding distribution of *Vermivora* are not available during the period when Appalachian Mountains populations of golden-winged warblers experienced their steepest declines (~1970–1980; Sauer et al. 2017). Furthermore, it is unlikely that golden-winged warblers in the Appalachian Mountain region began declining in 1966, the first year of the Breeding Bird Survey (Rosenberg et al. 2016). Therefore, clearly identifying a mechanism related to these declines is challenging. Using modeled estimates of historical land use and land-cover change (HYDE 3.1; Goldewijk et al. 2010, Goldewijk et al. 2011, Meiyappan and Jain 2012; Fig. A – 5, see Appendix A for detailed description of analysis) for the region, I found that forest-dominated landscapes at appropriate elevations for golden-winged warblers (i.e., 200–2,400 m above sea level [masl]; Rosenberg et al. 2016) were converted to other, non-forest land uses in northern South America at a disproportionate rate compared to Central America (Goldewijk et al. 2010, Goldewijk et al. 2011, Meiyappan and Jain 2012; Fig. 1 – 4). The loss of forest-dominated landscape within the appropriate elevation envelope for golden-winged warblers in northern South America began in the early- to mid-1940s and continued through 1980 (Fig. 1 – 4). Based on the migratory connectivity of *Vermivora*, these dramatic, regional shifts in land use would likely affect primarily golden-winged warblers from Appalachian Mountain breeding populations (Fig. 1 – 2). Simple linear regressions reveal that these predicted changes in the amount of forest-dominated land in population-specific nonbreeding ranges explains significant variation in the breeding population trends of all three groups (blue-winged warblers range-wide, 1966–2010, F =16.3, df = 1, 8, P = 0.004; Great Lakes populations of golden-winged warblers, 1966–2010, F =13.5, df = 1, 8, P = 0.006; and Appalachian Mountain populations of golden-winged warblers, 1966–1990, F =77.7, df = 1, 4, P = 0.0009; Fig. 1 – 4). This evidence provides a parsimonious and temporally synchronized explanation for the observed differences in breeding population trends among these three groups of *Vermivora* warblers.

Certainly, the loss of appropriate humid mid-elevation tropical forest cover types caused by changes in land use, or other consequences of human activities, may have direct effects on the survival of nonbreeding golden-winged warblers (Chandler et al. 2016). But habitat fragmentation, reduced habitat quality, and habitat loss may have nonlethal effects that lead to lower reproductive success and survival of individuals that return to North America to breed (Marra et al. 1998, Harrison et al. 2011). Additionally, golden-winged warblers migrating to northern South America from northern Appalachian Mountain breeding sites travel >5,000 km farther than golden-winged warblers migrating between Central America and Great Lakes breeding sites each year (Kramer et al. 2017). Therefore, northern Appalachian breeding populations of golden-winged warblers may be more sensitive to declines in available food resources, phenology mismatches during migration, and/or higher risk of encountering predators or other obstacles during migration (Sillet and Holmes 2002, Harrison et al. 2011, Legagneux et al. 2012, Loss et al. 2014, Deppe et al. 2015). Conversely, *Vermivora* that occur in Central America during the nonbreeding period migrate shorter distances to breeding sites and are more widely dispersed during the nonbreeding period such that the effects of potentially limiting factors are not likely to be experienced by all individuals of a population. A future productive research focus may be identifying potential limiting factors during migration so as to assess the impact of differential migration strategies on population trends of *Vermivora* warblers.

I did not observe intermediate nonbreeding site affinity in probable first-generation hybrids (identified based on plumage characteristics [Parkes 1951, Toews et al. 2016]). Hybrids with intermediate migratory traits have been described in other species (Delmore and Irwin 2014), but the hybrids I monitored did not occur in areas that I could differentiate from one of the parental types (e.g., hybrids from the Appalachian Mountains did not occur in Panama). However, if hybrids and parental types used nonbreeding areas separated by short distances (i.e., <250 km), I would be unlikely to differentiate those sites due to the spatial-resolution of geolocator data. Future research with higher-resolution technology (i.e., satellite- or Global Positioning System- enabled markers) may be useful in determining if hybrids exhibit intermediate phenotypes in nonbreeding site affinity that are unable to be identified with geolocators. It is challenging to identify meaningful patterns in the nonbreeding distribution of two hybrids captured in the Great Lakes portion of the breeding distribution as there is little differentiation in the nonbreeding ranges of blue-winged warblers and golden-winged warblers breeding in that region. However, the two phenotypic hybrids tracked from the Appalachian Mountains wintered in northern South America where golden-winged warblers from the Appalachian Mountains occur during the nonbreeding period. I note, however, that the sample of hybrids may be influenced by ascertainment bias, in that I only captured and attached geolocators to hybrids that returned to breeding areas after successfully migrating to and from nonbreeding locations, reducing any opportunity to identify migration to poor quality or inappropriate nonbreeding locations that negatively influenced survival or breeding propensity. It is likely that the hybrid individuals originated from interspecific pairings, or extra-pair copulations, between members of the parental species in the Appalachian Mountains region. Given the results of this study, the hybrid offspring of these pairings likely received genetic information from a blue-winged warbler that wintered in Central America and a golden-winged warbler that wintered in northern South America. If a subset of hybrid individuals produced in the Appalachian Mountains with a genetic predisposition to migrate to Central American nonbreeding areas either do not survive (that could be due to a multitude of reasons including possibly due to a recombination of alleles that results in maladaptive migratory orientation, or other post-zygotic barrier), disperse to breeding areas that are outside the Appalachian Mountains (i.e., nonbreeding site affinity and breeding site affinity are genetically linked), or do not exhibit breeding behavior, the sample of hybrids would likely be biased. Further research is required to fully account for the behaviors of hybrid *Vermivora* warblers during their first migration and winter.

It is unlikely that golden-winged warblers are the only broadly dispersed Nearctic-Neotropical migrant songbird species that exhibits strong migratory connectivity and shows population trends consistent with being limited by nonbreeding factors. These results confirm that migratory connectivity and the nonbreeding distribution of species can be linked to breeding population trends. However, range-wide geolocator studies are expensive and logistically challenging and being able to identify potential candidate species that may exhibit these similar relationships without mounting a continent-wide study would be valuable. I therefore identified 25 species of Nearctic-Neotropical migrant passerines that have similar nonbreeding distributions to *Vermivora* warblers and broadly dispersed breeding distributions (see Materials and Methods; Table A.2; Fig. A – 6). Of those 25 species, I identified 16 (64%) that showed structured differences in regional breeding population trajectories that could be caused by nonbreeding factors (Table A.2). Six of those species showed similar patterns in range-wide population trends as golden-winged warblers (declines from 1966–1990, followed by stable trends from ~1990–2015). Without detailed knowledge of the factors affecting population trends of these species, I predict their regionally distinct breeding population trends may be linked to migratory connectivity and nonbreeding distribution similar to what I observed in golden-winged warblers. The Kentucky warbler (*Geothlypis formosa*) stands out as one of the most likely candidates to exhibit strong migratory connectivity based on these assumptions (Table A.2; Fig. A – 6). Kentucky warblers exhibit a dichotomous north-south pattern in their breeding population trends and occur in the same regions as golden-winged warblers during the nonbreeding period. In addition, range-wide declines starting in 1966 have leveled off and global population trends have been stable since ~1990, similar to golden-winged warblers. Kentucky warblers may be another species that exhibits strong migratory connectivity, and like golden-winged warblers, signals of strong connectivity (e.g., coinciding population declines) may be shared among species that occupy similar regions, and are affected by similar limiting factors during the annual cycle.

More complex scenarios may explain the patterns in population trends exhibited by Kentucky warblers and the other species I have promoted as potential candidates to exhibit strong migratory connectivity. There also are factors (e.g., regionally-specific breeding grounds factors) that could obfuscate or mask the purported signals that I used to identify species that may exhibit strong migratory connectivity. Identifying species with strong connectivity and understanding the implications of such strong connectivity is timely and important (Marra et al. 2015). If anthropogenic changes in land-use patterns in northern South America are identified as a key factor driving population declines of golden-winged warblers occurring in that region during the nonbreeding period, then the strong migratory connectivity I observed in golden-winged warblers may constitute an evolutionary trap (Schlaepfer et al. 2002). In this case, anthropogenic factors that are limiting populations may be occurring over a relatively short period and outpacing the natural ability for these populations to adapt. Understanding the implications (Gill et al. 2009, Vansteelant et al. 2017) and diversity (Egevang et al. 2010, Streby et al. 2015a, McKinnon et al. 2017) of patterns in the distribution of migratory species throughout the annual cycle will aid in predicting the effects of continuously changing anthropogenic factors on migratory species, globally (Both et al. 2006).

1.4 Conclusion

I provide details on the distribution and migratory connectivity of two closely-related, Nearctic-Neotropical migrant songbird species, which recent genetic evidence suggests may be plumage morphs of a single species complex. Unlike blue-winged warblers, golden-winged warblers exhibited strong migratory connectivity and identification of systems with structured patterns in migratory phenotypes may aid future research investigating genomic regions associated with specific migratory behaviors. More importantly, I show through a thorough sampling of populations throughout these species' breeding ranges that strong connectivity leading to the isolation and segregation of populations during the nonbreeding period may be associated with patterns in breeding population trends. The observations of strong migratory connectivity in *Vermivora* warblers represent a major advance in understanding the unique drivers shaping migration strategies, the distribution of populations throughout the annual cycle, and ultimately the evolutionary trajectories of migrants in the rapidly changing Anthropocene. Identifying the factors that led to the severe declines and local extirpation of golden-winged warblers in the Appalachian Mountains region will be critical for their long-term conservation. These findings highlight the value of collecting information about the annual movements of species across their distribution and studies like this can aid in the conservation of migratory species, such as *Vermivora* warblers, in the future.

1.5 Materials and Methods

1.5.1 Study Area and General Procedures

I used data collected from golden-winged warblers, blue-winged warblers, and their hybrids across their breeding distributions in eastern North America from 2013–2017. A small portion of these results include a reanalysis of geolocator data (Kramer et al. 2016) reported in Kramer et al. (2017). Study areas were chosen based upon location (i.e., representing the greatest geographic distribution), density of *Vermivora* warblers, and ease of access. *Vermivora* warblers are diverse-forest species that are often associated with young, regenerating forest surrounded by a larger matrix of mature forest and the study sites reflected the full range of land-cover types used by these species (Aldinger et al. 2015). Warblers were captured in mist nets using conspecific call and song broadcasts. Upon initial capture, individuals were classified based on age and sex, assigned a phenotypic species (i.e., typical golden-winged warbler, typical blue-winged warbler, or hybrid) based on plumage traits (Parkes 1951, Toews et al. 2016), weighed, and banded each individual with an U.S. Geological Survey/Canadian Wildlife Service aluminum band and 1–3 plastic color leg bands to aid in future identification. Geolocators (model ML6240, 2-min light-sampling regime; Biotrak Ltd., Wareham, UK) were attached to male *Vermivora* warblers that exhibited territorial or breeding behaviors (i.e., resident, non-migratory behaviors) using an adapted leg-loop harness that was developed and tested on this species complex without any known negative effects (Rappole and Tipton 1991, Peterson et al. 2015, Streby et al. 2015b). All birds were released after processing and monitored for signs of stress during a brief (~1–15 min) acclimation period.

The year following deployment, I returned to the sites and attempted to recapture all marked birds that returned. *Vermivora* warblers exhibit high site fidelity when their breeding habitat is not altered or removed and often return to the same territories year after year (Bulluck et al. 2013, Peterson et al. 2015). Thus, I began searches for returning geolocator-marked birds at the site where they were marked the previous year. Searches for returning individuals included appropriate breeding cover types within ~1–3 km of the deployment site depending on the site and the surrounding landscape. Individuals were lured into mist nets using identical capture methods as those described above. After capture, geolocators were removed individuals were released at the capture location. New geolocators were attached to a subset of individuals that successfully carried a geolocator in 2013 or 2014 to attempt to understand whether individuals use different nonbreeding areas in different years (see *Geolocator Data Analysis* for discussion of how individuals with multiple years of data were treated).

1.5.2 Geolocator Data Analysis

I downloaded and decompressed raw light-level data from geolocators using BASTrack software (Bastrack Ltd., Wareham, UK). All additional processing and analyses were conducted in R (R Core Team 2016). Briefly, I followed the methods described by Kramer et al. (2017) to derive nonbreeding probability density functions for each individual during the tropical dry season (i.e., 1 Jan – 28 Feb). This period represents the nonbreeding period when I assumed individuals were residing on nonbreeding territories and were exposed to the least environmental shading. I used 'FLightR' (Rakhimberdiev et al. 2017) to estimate spatially explicit likelihood surfaces (~0.5° cell size) for each transition period (i.e., sunrise or sunset) from 1 Jan – 28 Feb. I used a subset of data, or data from a different portion of the nonbreeding period if data were unavailable from 1 Jan – 28 Feb (due to geolocator failure, or occlusion of the light sensor; Table A.1). I then averaged all transition-derived likelihood surfaces for each individual to produce an average probability density function showing the most probable regions used by that individual during the nonbreeding period. I transformed individual nonbreeding likelihood surfaces into probability density functions by dividing each likelihood surface by the sum of its surface. I averaged nonbreeding probability density functions of individuals from the same breeding populations to achieve a population-level probability density function representing areas most likely used by an individual warbler from each population during the nonbreeding period.

Because that portion of the Neotropics used during the nonbreeding period by *Vermivora* warblers extends primarily from west to east, I used longitude as a proxy for individual nonbreeding site location in calculations and estimations of overlap. Longitude is more accurate than latitude in geolocator analyses and can be useful for determining movement and location (Rakhimberdiev et al. 2016), especially in terrestrial organisms that are constrained to land during the period of interest but travel through regions that are bounded to the north and south by expansive water (e.g., Central America). To estimate nonbreeding site longitude, I extracted the longitude of the highest probability cell in the probability density function for each individual. I averaged the nonbreeding probability density functions for warblers with 2 years of data ($n = 6$) so that those individuals did not bias estimates of average nonbreeding distribution of populations.

1.5.3 Statistical Analysis

I evaluated differences between the nonbreeding distributions of populations using linear regression and one-way ANOVA and post-hoc Tukey HSD tests in R unless otherwise noted. I considered results of all tests to be significant at $\alpha = 0.05$. I investigated the level of migratory connectivity in populations of *Vermivora* warblers based on Bird Conservation Regions (BCRs) for which annual population-level sampling is conducted and reported annually by the Breeding Bird Survey (Sauer et al. 2017). Golden-winged warbler populations are largely contained within two BCRs: Boreal Hardwood Transition BCR (S12; i.e., Great Lakes population), and Appalachian Mountains BCR (S28; i.e., Appalachian Mountains population). Blue-winged warblers are more widespread but the study sites fell primarily in three BCRs: Prairie Hardwood Transition BCR (S23), Central Hardwoods BCR (S24), and Appalachian Mountains BCR (S28). For both blue-winged warblers and golden-winged warblers, I split the Appalachian Mountains BCR into northern and southern halves (separated at ~ 39° N) to investigate potential differences in the nonbreeding distributions of these groups of

Vermivora. For golden-winged warblers, I also split the Great Lakes population (BCR 12) into eastern and western portions (~ 85° W) for the same purpose.

1.5.4 Predicting Other Species with Nonbreeding Population Structure

I used range data from BirdLife International (2016) to visually inspect the nonbreeding distributions of Nearctic-Neotropical migrant songbird species. I identified species that occurred in both Central America and South America during the nonbreeding period, as observed in golden-winged warblers (Table A.2). I then visually inspected breeding period trend maps from the Breeding Bird Survey (Sauer et al. 2017) and identified species that showed structured, regional variation in population trends. Finally, I visually inspected the survey-wide population trends for those species and noted their general population trends from 1966–1990 and 1991–2015. From 1966 to~1985, the range-wide population trend of golden-winged warblers declined as a result of the loss of individuals from the Appalachian Mountains breeding population. Following that decline, the range-wide population trend stabilized between 1985 and 1990. If other species had strong migratory connectivity similar to that which I observed in golden-winged warblers (i.e., isolated breeding populations occurring separately in Central America and South America during the nonbreeding period), one might expect to see a similar trend over the same period if limiting factors (e.g., deforestation, fragmentation; see Fig. 1 – 4) also were affecting other Nearctic-Neotropical migrant populations. For example, yellow-throated vireos (*Vireo flavifrons*) are broadly dispersed throughout eastern North America during the breeding period and occur in both Central America and northern South America during the nonbreeding period. Eastern populations of yellow-throated vireos tend to be declining more than western populations. However, survey-wide trends of yellow-throated vireos revealed a stationary trend from 1966–1985 switching to increasing population trends from 1986–2010 (Sauer et al. 2017). This suggests that the factors limiting yellow-throated vireos are different than those limiting golden-winged warblers and therefore I predict that it is unlikely that yellow-throated vireos have similar nonbreeding population distribution and migratory connectivity as golden-winged warblers.

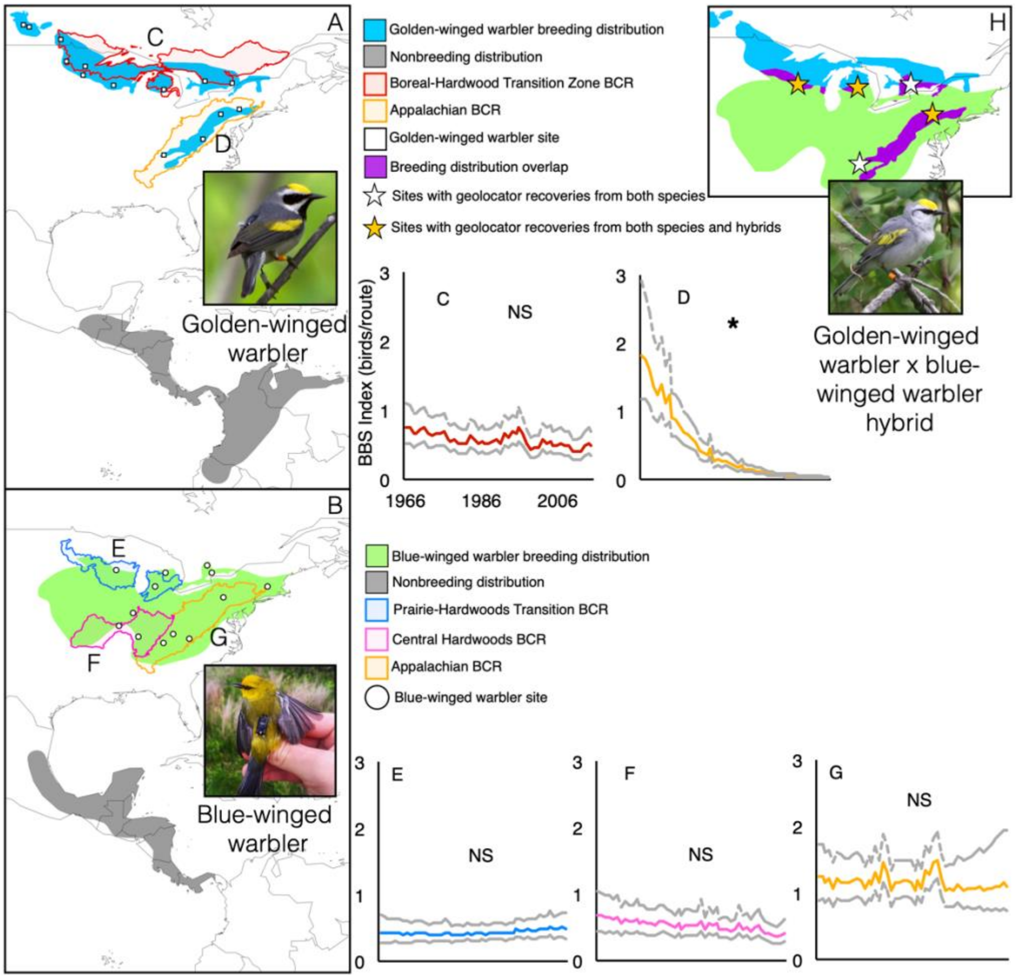

Figure 1 – 1: Breeding and nonbreeding distributions of golden-winged warblers (A) and blue-winged warblers (B) with relevant Bird Conservation Regions (BCRs) outlined and study sites identified. Historical population trends of each species are provided for each relevant BCR from 1966–2015 (Breeding Bird Survey; Sauer et al. 2017). In trend graphs, solid-color lines represent annual indices of golden-winged warblers (C, D) and blue-winged warblers (E–G). Dashed gray lines represent 95% credible intervals around annual indices. Populations are noted as exhibiting non-significant trends (i.e., numerically stable; NS), or significant trends (i.e., increasing or declining; *) depending on whether the 95% credible interval around the trend estimate (from 1966–2015) includes zero. Breeding distribution overlap among golden-winged warblers and blue-winged warblers is presented in (H) and sites with data from both species are identified by white stars and sites with data from golden-winged warblers, blue-winged warblers, and hybrid *Vermivora* warblers are identified by gold stars. Range map information is adapted from BirdLife International (2016) and nonbreeding ranges are buffered by 100 km.

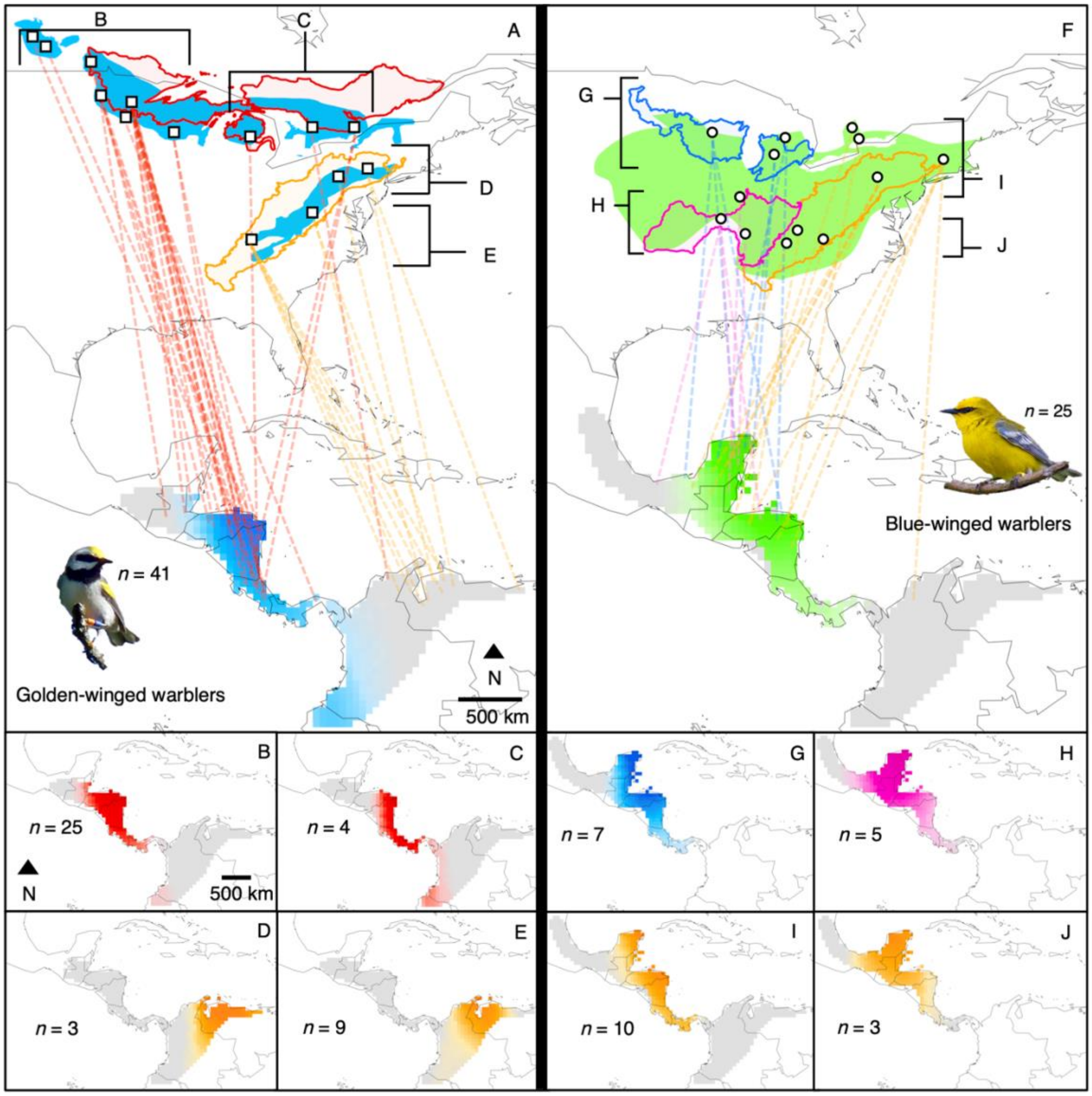

Figure 1 – 2: Species-level average nonbreeding probability density function of blue-winged warblers (A) and golden-winged warblers (B). Dashed lines link individual warblers from breeding sites to their highest probability nonbreeding area. Colors correspond to Bird Conservation Regions (BCRs) in Fig. 1 – 1. Lines do not represent migration routes. Brackets define sites used to create population-level average probability density functions of blue-winged warblers (C–F) and golden-winged warblers (G–J). In all probability density functions, darker colors correspond with higher probability of use and the bottom 50% of probabilities are shown as gray to aid in visualization of core use areas. Range maps adapted from BirdLife International (2016). See Fig. 1 – 1 for description of BCRs.

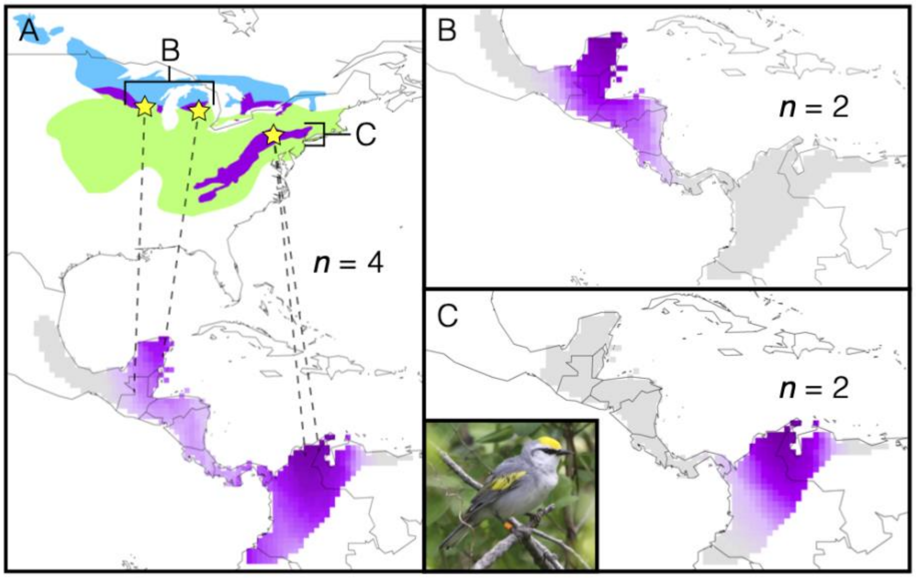

Figure 1 – 3: Average nonbreeding probability density function of all phenotypic *Vermivora* hybrids (*n* = 4; A) and average nonbreeding probability density functions of hybrids from distinct breeding regions in the Great Lakes (B) and Appalachian Mountains (C) regions. Darker colors correspond with higher probability of use and probabilities < 50% of the maximum shown as gray to aid in visualization of core use areas. Lines represent links between individuals' breeding sites and areas of most probable nonbreeding sites but do not represent migration routes. Range maps adapted from BirdLife International (2016).

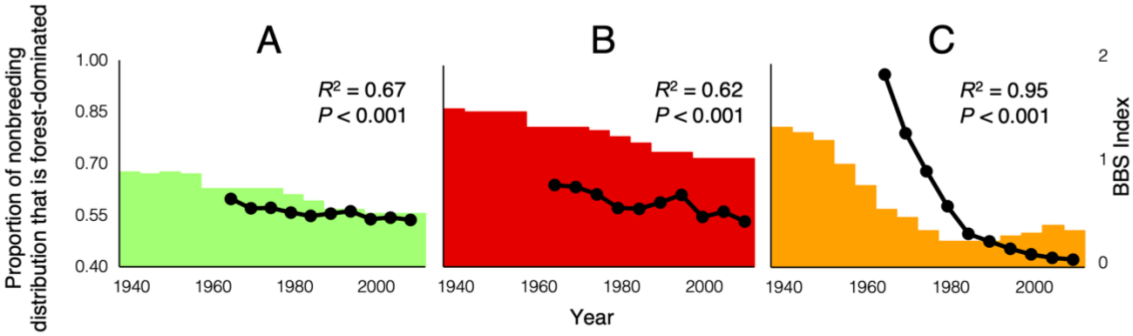

Figure 1 – 4: Bar charts showing the modeled proportion of forest-dominated land cover at 200–2,400 masl in the nonbreeding distribution of blue-winged warblers (A; Central America, southern Mexico), Great Lakes breeding populations of golden-winged warblers (B; Central America), and Appalachian Mountains breeding populations of golden-winged warblers (C; northern South America). Overlaid lines show breeding population trends of each group over the same time scale. Axes for the proportion of forest (left y-axis) and the BBS index (right y-axis) are the same for all respective plots. Summary statistics of simple linear relationships of BBS index as a function of the proportion of forest-dominated land cover are presented. Regressions in blue-winged warblers (A) and Great Lakes breeding populations of golden-winged warblers (B) use all available years. The regression for Appalachian Mountain breeding populations of golden-winged warblers used 1966–1990 during the steepest decline and before the population was effectively reduced to near zero. Land use data from the HYDE 3.1 database (Goldewijk et al. 2010, 2011, Meiyappan and Jain 2012).

Chapter 2

Exposure to Risk Factors Experienced During Migration is not Associated with Recent *Vermivora* Warbler Population Trends

2.1 Abstract

Identifying which factors limit populations of migratory animals is inherently challenging because of their reliance on multiple, often geographically distant regions during their annual cycle. Individuals face a suite of natural and anthropogenic threats (risk factors) associated with increased mortality rate during migration and/or decreased productivity in subsequent breeding seasons, which may drive population trends of some species. Golden-winged warblers (*Vermivora chrysoptera*) and blue-winged warblers (*V. cyanoptera*) are Neotropical-Nearctic migratory songbirds experiencing varied regional population trends linked to strong migratory connectivity and historical forest loss at population-specific nonbreeding areas. Preliminary evidence also suggests populations of *Vermivora* warblers exhibit variation in space use during migration, which may lead to differential exposure to risk factors that may directly or indirectly reduce survival rate or productivity. I used geolocator data from 90 individual *Vermivora* warblers (n = 96 geolocator tracks) tracked from North American breeding locations and Central American nonbreeding locations from 2013–2017 to investigate whether variation in recent breeding population trends was more strongly associated with migration risk-

factors (i.e., natural or anthropogenic threats associated with increased mortality rate during migration and/or carry-over effects that decrease productivity in subsequent breeding periods) or factors associated with breeding and nonbreeding areas. Overall, *Vermivora* warblers exhibited population-specific space use and exposure to anthropogenic and natural risk-factors. However, I found no evidence that recent variation in population trends of *Vermivora* warblers are associated with the amount or intensity of migration risk-factors within populations' seasonal migration core-use areas. Instead, variables associated with migratory connectivity (i.e., breeding and nonbreeding areas) were more strongly associated with recent population trends of *Vermivora* warblers. Maintaining important stopover habitat is critical for the successful conservation of migratory species, but our results suggest that variation in exposure to migration risk-factors is not strongly linked to recent regional variation in *Vermivora* warbler population trends. Therefore, conservation efforts targeting *Vermivora* warblers during breeding and nonbreeding periods may influence population trajectories more than those directed at conditions encountered during migration. However, I caution that geographic variation in projected anthropogenic development leading to land-use changes may differentially affect areas used by different populations of *Vermivora* warblers during migration in the future.

2.2 Introduction

Migratory animals face various threats throughout their annual cycle that may influence their survival and productivity. Identifying which factors contribute to limiting populations of migratory animals is inherently challenging because of their reliance on multiple, often geographically distant regions during their annual cycle (Webster et al.

2002, Newton 2006, Sherry 2018). Populations of migratory species can be limited both directly and indirectly by any number of factors affecting the survival of adults or production of young at breeding sites (Milner-Gulland et al. 2003; Flockhart et al. 2015), the survival of individuals at nonbreeding sites (Mihoub et al. 2010, Kramer et al. 2018a), and the survival of individuals along migration routes between breeding and nonbreeding areas (Berger 2004, Hewson et al. 2016). However, quantifying the relative importance of limiting factors experienced throughout the annual cycle on the abundance or trends of many populations of migratory species remains a challenge due to the often-limited ability to monitor individuals throughout the annual cycle (McKinnon and Love 2018). Moreover, identifying whether distinct populations are regulated by the same, or population-specific factors is critical for directing limited resources to implement effective conservation strategies (Hewson et al. 2016, Studds et al. 2017, Kramer et al. 2018a, Wilson et al. 2018).

In many species, limiting factors occur during breeding or nonbreeding seasons when individuals are relatively stationary and where individuals are reproducing and/or resident for a significant period relative to the migratory portions of their annual cycle (Probst 1986, Milner-Gulland et al. 2003, Flockhart et al. 2015, Heinsohn et al. 2015). However, mortality during migration may be a substantial proportion of annual mortality in some species (Nicholson et al. 1997, Sillett and Holmes 2002), in part due to the myriad threats individuals may face during migration, including those related to negotiating inhospitable barriers (e.g., expansive stretches of open water, deserts, high-elevation mountain ranges; Newton 2007, Seidler et al. 2014), habitat fragmentation or other factors that reduce habitat quality at critical stopover sites (i.e., sites used by individuals to rest and refuel during migration; Studds et al. 2017), phenological mismatch (i.e., climate-change-induced disparity between optimal resource availability and migratory timing; Møller et al. 2008, Jones and Cresswell 2010), increased competition (Hansson and Pettersson 1989, Cohen and Satterfield 2020) and predation risk (Lindström 1989, Hopcraft et al. 2014), and mortality associated with anthropogenic factors (e.g., collision with structures; Jameson and Willis 2014, Loss et al. 2015, Malcolm 2018). Identifying variation in the cumulative exposure of individuals or populations to different migration risk-factors (i.e., those experienced away from areas of prolonged residency) has historically been challenging for many species (Marra et al. 2015). Advancements in tracking technology (e.g., radiotelemetry, Global Positioning System [GPS] tags, and satellite/cellular tags) have recently made it possible to collect landscape-scale movement data from many smaller species (e.g., songbirds and insects; Stutchbury et al. 2009, Knight et al. 2019) providing novel opportunities to identify factors limiting populations of some of the smallest migratory vertebrate and invertebrate species and potentially improving conservation strategies.

I assessed whether variation in exposure to documented migration risk-factors associated with increased mortality rate (i.e., direct effects) and/or decreased productivity (i.e., indirect, carry-over effects) in migratory birds was associated with regional population trends in *Vermivora* wood-warblers (Parulidae). The genus *Vermivora* comprises a complex of two extant Nearctic-Neotropical migrant warbler species (golden-winged warblers [*Vermivora chrysoptera*] and blue-winged warblers [*V. cyanoptera*]) that are extremely closely related and exhibit a range of shared phenotypes (Toews et al. 2016, Kramer et al. 2020). These small (~9 g) songbirds breed and migrate throughout the deciduous forests of eastern North America (Fig. 2 – 1; Rosenberg et al. 2016, Kramer et al. 2017) and during the nonbreeding period, golden-winged warblers occur in Central America and northern South America whereas blue-winged warblers primarily occur in Central America (Kramer et al. 2017, 2018a; Fig. 2 – 1). On the breeding grounds, these two species have overlapping distributions where they regularly hybridize and produce viable young (Vallender et al. 2007a, Baiz et al. 2020, Toews et al. 2021). Populations of blue-winged warblers exhibit relatively weak migratory connectivity in which individuals from across the breeding distribution co-occur throughout Central America during the nonbreeding period (Kramer et al. 2018a). Conversely, golden-winged warblers exhibit strong migratory connectivity in which populations breeding throughout the Great Lakes region (Boreal Hardwoods Transition Bird Conservation Region [BCR]) occur almost exclusively in Central America during the nonbreeding period whereas populations breeding in the Appalachian Mountains (Appalachian Mountains BCR) occur almost exclusively in northern South America (Kramer et al. 2018a; Fig. 2 – 1). Blue-winged warblers have maintained numerically stable population trends since the 1960s with little variation in population trajectories among different breeding population segments (Sauer et al. 2017, Kramer et al. 2018a). Golden-winged warblers experienced historical population declines from the 1960s (when Breeding Bird Survey [BBS] monitoring began; Sauer et al. 2017) until ~1990–2000 resulting in a ~50% reduction in the abundance of golden-winged warblers over that period (Rosenberg et al. 2016). These historical declines were driven by the near extirpation of golden-winged warblers breeding in the Appalachian Mountains BCR (Rosenberg et al. 2016) and were facilitated by habitat loss in population-specific nonbreeding areas (Kramer et al. 2018a). However, conversion of forest to other cover types in northern South America has stabilized since ~1990 relative to historical rates (Goldewijk et al. 2011) and yet populations of golden-winged warblers continue to decline in the Appalachian Mountains (Sauer et al. 2017). Notably, blue-winged warblers across their distribution and golden-winged warblers breeding in the Boreal Hardwood Transition BCR have largely maintained numerically stable population trends (Sauer et al. 2017, Kramer et al. 2018a) suggesting that the factors limiting blue-winged warbler populations and golden-winged warblers breeding in the Boreal Hardwood Transition BCR likely differ from those limiting the golden-winged warbler population breeding in the Appalachian Mountains BCR.

Golden-winged warblers in the Boreal Hardwood Transition BCR have relatively high rates of apparent reproductive success (Streby et al. 2016b; Streby et al. 2018). Rates of reproductive success for golden-winged warblers breeding in the Appalachian Mountains BCR vary among sites but golden-winged warblers at some sites reproduce at rates that should result in population maintenance or growth (Lehman 2017, Aldinger 2018, McNeil 2019). Therefore, recent variation in regional population trends of *Vermivora* warblers (i.e., since 2000) could be linked to factors experienced during migration if declining populations use areas during migration with higher risk of mortality or that experience factors that negatively influence subsequent reproduction relative to numerically stable populations (Newton 2006). Relatively little is known about the movements of individual *Vermivora* warblers during seasonal migration (Bennett et al. 2017, Kramer et al. 2017, Bennett et al. 2019b), although preliminary evidence suggests populations of golden-winged warblers exhibit variation in space use during both autumn and spring migrations (Kramer et al. 2017). The magnitude of variation in space use during migration among populations of *Vermivora* warblers and whether variation in space use is associated with differential exposure to migration risk-factors remains unknown.

Here, I used light-level geolocator data to identify areas used by *Vermivora* warblers during migration. I quantified the level of overlap in space use during migration both between species and among populations. Additionally, I explored four questions related to the importance of migration risk-factors to past and future populations of *Vermivora* warblers (Table 2.1). First, I assessed whether inter- and intraspecific variation in space use during migration was associated with exposure to a suite of natural and anthropogenic migration risk-factors. Second, I quantified the relative importance of migration risk-factors and factors experienced during the breeding or nonbreeding periods in models explaining variation in recent *Vermivora* warbler population trends (i.e., since 2000). Third, I assessed whether migration risk-factors experienced annually, or within seasonal stopover regions bordering the Gulf of Mexico explained additional variation in models of recent *Vermivora* warbler population trends while controlling for breeding and nonbreeding factors. Last, I investigated whether the potential for increased future risk resulting from projected human development could disproportionately affect declining, stationary, or increasing populations in the future (i.e., by 2030). I predicted that *Vermivora* warblers would exhibit both inter- and intraspecific variation in space use during migration and that variation in space use would lead to differential exposure to migratory risk-factors between species and among populations. I hypothesized that populations of blue-winged warblers and numerically stable golden-winged warblers would use similar areas and be exposed to lower levels of migration risk-factors compared to declining populations of golden-winged warblers breeding in the Appalachian Mountains BCR. I also expected projected future anthropogenic development to differentially affect populations of *Vermivora* warblers and that my findings may be useful for improving proactive conservation strategies focused on the complete annual cycle of *Vermivora* warblers.

2.3 Methods

2.3.1 Geolocator Data Collection

I used published geolocator data from 90 individual *Vermivora* warblers (*n* = 96 geolocator tracks; 6 individuals were tracked for 2 years) collected from 2014–2018 (Kramer et al. 2018b, Bennett 2019). Geolocators are a relatively simple tracking technology that record levels of ambient light data at regular intervals (usually 2–5 minutes), which can be used to estimate geographic location based on the seasonal variation in the timing and duration of sunlight across the globe (Hill and Braun 2001, Ekstrom 2004). Most of the geolocator data (76/96 tracks; 79%; Kramer et al. 2018b) were collected from 2014–2018 from *Vermivora* warblers at 26 sites spanning the breeding distributions of both blue- and golden-winged warblers (Fig. 2 – 1; Kramer et al. 2018b). These data were previously used to identify the nonbreeding dispersion and migratory connectivity of *Vermivora* breeding populations (Kramer et al. 2017, Kramer et al. 2018a). I also used geolocator data from 20 individual male golden-winged warblers (20 tracks) collected by Bennett et al. (2019b) from 5 sites in Central America (Fig. 2 – 1; Bennett 2019). I omitted hybrid warblers (*n* = 4 individuals, *n* = 5 geolocator tracks) and one golden-winged warbler that returned with mud caked over the geolocator's light sensor from analysis (Table B.1, B.2).

In total, I analyzed 90 geolocator tracks from 84 individual *Vermivora* warblers: 25 blue-winged warblers (*n* = 26 tracks) and 59 golden-winged warblers (*n* = 64 tracks; Table B.2). I defined populations based on the BCR of an individual's breeding location for figures and in analyses of overlap during migration. However, several study areas occurred in BCRs on the periphery of a species' distribution and I assigned individuals at those sites to the nearest BCR containing other study sites and a greater proportion of the species' distribution. I assigned blue-winged warblers breeding at two sites in southern Ontario, Canada (*n* = 2) and one site in Massachusetts, USA (*n* = 4) to the Appalachian Mountains BCR and golden-winged warblers breeding at two sites in western Manitoba, Canada (*n* = 2) to the Boreal Hardwood Transition BCR. Thus, I classified blue-winged warblers into three populations: Prairie Hardwood Transition BCR (*n* = 7 individuals, *n* = 8 tracks), Central Hardwoods BCR (*n* = 5 individuals and tracks), and the Appalachian Mountains BCR (*n* = 12 individuals, *n* = 13 tracks). I classified golden-winged warblers into two populations: Boreal Hardwood Transition BCR (*n* = 49 individuals, *n* = 51 tracks) and Appalachian Mountains BCR (*n* = 12 individuals, *n* = 13 tracks).

Details on the study sites and field methods used in each study are presented in Kramer et al. (2018a) and Bennett et al. (2019b). Both studies used the same model geolocator (ML6240, 2-min light-sampling regime; Biotrak, Wareham, UK) and modified leg-loop harness to attach geolocators to *Vermivora* warblers (Rappole and Tipton 1991, Streby et al. 2015b). Peterson et al. (2015) found no evidence of any effects of geolocators on the migratory ecology or apparent survival rate of golden-winged warblers marked geolocators using this harnessing method.

2.3.2 Geolocator Data Analysis

I analyzed all geolocator data in R (v. 3.6.1; R Core Team 2019) using the template-fit method in 'FLightR' (v. 4.9: Rakhimberdiev et al. 2015, Rakhimberdiev and Saveliev 2019). The template-fit method derives location estimates from raw light data using the timing and slope of transition events (i.e., sunrises and sunsets; Ekstrom 2004, Rakhimberdiev et al. 2015). I used the package BAStag (Wotherspoon et al. 2016) to identify transition events using a threshold of 1.5 (Kramer et al. 2017, 2018a). I calibrated geolocator data in 'FLightR' using the period that individuals were known (or assumed) to be resident at breeding or nonbreeding deployment sites (Kramer et al. 2018a, 2018b, Bennett et al. 2019b). I followed the workflow of Kramer et al. (2018a) to derive probability density functions using data spanning the duration of an individual's autumn and spring migrations. I analyzed data from each geolocator using the movement model in 'FLightR' (optimized with one million particles) to derive location estimates (i.e., spatially explicit likelihood surfaces) for individual transitions throughout the year.

I used a behavioral mask that allowed migrating *Vermivora* warblers to use over-water routes but prevented them from being stationary >25 km from land (Kramer et al. 2018a, Delancey et al. 2020). I also constrained the maximum distance between subsequent twilights to 1,200 km, which limited the effects of erroneous location estimates, and used the automatic outlier exclusion capability in 'FLightR' to identify and eliminate extreme location estimates during the movement modeling process (Rakhimberdiev and Saveliev 2019). I used the function find.times.distribution in

‘‘FLightR’’ to estimate commencement and termination of seasonal migrations (median date) from known (Kramer et al. 2018a) or estimated (Bennet et al. 2019b) breeding sites to known (Bennett et al. 2019b) or estimated (Kramer et al. 2018a) nonbreeding sites. I then created a daily likelihood surface by multiplying ‘FLightR’-derived likelihood surfaces (~0.5 ° cell size) for each day within the identified migratory period for which I were able to generate a likelihood surface for both sunrise and sunset transitions (generally ~95% of days). I multiplied each day’s sunrise and sunset likelihood surfaces together to create a daily likelihood surface (Kramer et al. 2017, 2018a). The likelihood surface for an individual transition is generally an arc corresponding to the geographic location of the transition between dark and light (or *vice versa*). The likelihood surfaces for sunrises and sunsets are nearly perpendicular and by multiplying the sunrise and sunset likelihood surfaces from a single day, it is possible to effectively pinpoint the estimated location of a geolocator-marked animal (Rakhimberdiev et al. 2015, Kramer et al. 2017). This process assumes that *Vermivora* warblers were stationary or moved relatively short distances (i.e., <250 km) during the day, which is a reasonable assumption as *Vermivora* warblers, like many other migratory songbirds, primarily migrate at night (Lincoln 1935). After creating daily likelihood surfaces for each day that ‘FLightR’ estimated sunrise and sunset likelihood surfaces, I added together an individual’s daily likelihood surfaces spanning each seasonal migration (i.e., all of the daily likelihood surfaces from breeding-site departure to nonbreeding-site arrival [autumn migration] or nonbreeding-site departure to breeding-site arrival [spring migration]). The resulting migration likelihood surface identified areas of relative importance during seasonal migration (i.e., stopover areas; cells with higher likelihoods were associated with a higher probability of being occupied by an individual for a greater duration relative to other locations). I then created a probability density function of each individual's seasonal migration by dividing each migration likelihood surface by its sum. For individuals with 2 years of tracking data, I considered each year as independent because I assumed individuals may not use the same routes and/or stopover sites during different years (or may use them for a different duration; Stanley et al. 2012).

2.3.3 Delineating Space-use by Species and Populations

To identify the general space-use patterns of each species and visualize interspecific variation in space-use, I created average seasonal migration probability density functions for each species by averaging probability density functions of individuals of a given species for each season (i.e., autumn or spring). For example, I summed the autumn probability density functions of all blue-winged warblers in our sample and divided by the sum of the composite surface (i.e., the number of geolocator tracks in each sample; each individual's probability density function sums to 1) to derive the average autumn probability density function for blue-winged warblers. I used the same methods to derive average seasonal migration probability density functions for populations of each species based on BCR.

2.3.4 Quantifying Overlap Within and Among Populations

To quantify variation in space-use among *Vermivora* warblers from different BCRs and determine the degree to which BCR-defined populations overlapped, I identified the core areas used by each population during each season (hereafter, "core-use areas"). Defining a threshold to delineate core-use areas can be useful to differentiate high-probability cells from low-probability cells when analyzing spatially-explicit probability density functions derived from geolocators (e.g., Kramer et al. 2018a). In my analysis of population and seasonal overlap, I defined core-use areas as the top 25th percentile of each population's average seasonal migration probability density function (see above). I considered other thresholds to compare population overlap during exploratory data analysis (i.e., 10th, 50th, 75th, 90th percentiles) but chose to use the 25th percentile in my analysis based on the accuracy of location estimates derived from geolocators (Rakhimberdiev et al. 2016) and because the 25th percentile was the level at which differentiation among populations became readily apparent, aiding in the identification of areas where population-specific conservation efforts may be targeted (Levin 1992).

I quantified the proportion of overlap among populations' seasonal core-use area (e.g., overlap between autumn core-use areas of blue-winged warblers from Central Hardwoods BCR and Appalachian BCR breeding sites) to identify the similarity of space-use patterns among populations within each season. I calculated the total area (km^2) of overlap between two populations' seasonal core-use areas and divided by the total seasonal core-use area of the reference population to derive the proportion of overlap. The proportion of overlap depends on which population's core-use area is the reference (i.e., the denominator). Therefore, I used pairwise comparisons to calculate the proportion of overlap between two core-use areas (i.e., using each core-use area as the reference) and averaged estimates of proportion of overlap when comparing the relative amount of overlap observed between and among populations.

2.3.5 Selection and Analysis of Migration Risk-factors

To determine whether variation in space use among populations of *Vermivora* warblers is associated with variation in exposure to migration risk-factors, I identified natural and anthropogenic factors that exhibit geographic variation in occurrence and/or intensity and are known or hypothesized to be associated with increased risk of mortality and/or decreased productivity in migrating birds (Table 2.2, Appendix B Supplementary Methods). I limited the number of potential variables in my analysis by using those that I predicted could affect populations' trajectories due to the combination of their geographical extent and potential for causing mortality or reducing productivity. When possible, I selected variables that aggregated correlated risk factors. Specifically, I used the variable "human footprint" (Venter et al. 2016, 2018) as a proxy for a suite of highly correlated risk factors associated with urbanization and development (i.e., population density, artificial light at night, built-up area, road density; Table 2.2). Individual-level exposure to migration risk-factors was derived from georeferenced data that I downloaded as rasters or transformed from vectors (i.e., points) to rasters in R using the 'raster' package (Hijmans 2020; Table 2.2). I clipped and resampled all rasters to standardize the extent (i.e., y = 0, 60; x = -120, -60) and resolution (~0.5° × 0.5°).) because the resolution of all migration risk-factor data was finer (i.e., more precise) than the resolution of the geolocator-derived probability density functions (~0.5°; Table 2.2). I also calculated a combined (overall) measure of the relative intensity of migration risk-factors by standardizing each migration risk-factor raster (i.e., minimum and maximum values set to 0 and 1, respectively). I summed standardized migration risk-factor layers to create a single raster layer (assigning equal weight to individual migration risk-factors) and explored whether population trends of *Vermivora* warblers were associated with this combined measure of relative exposure to migration risk-factors (Table 2.1). I did not differentiate between risk factors associated with direct effects (i.e., increased mortality) and those associated with indirect effects (i.e., carry-over effects) in my analysis because each factor I considered could reasonably cause either type of effect. Consequently, my analyses assessed the relationship between population trajectory and the cumulative effects (i.e., both direct and indirect) associated with exposure to migration risk-factors. Other potential risk factors exist that I did not directly account for (e.g., exposure to disease, resource availability, predation risk). However, the risk factors I included in my analysis are among the most frequently proposed threats to migratory birds and most can be mitigated through targeted conservation actions (Newton 2006, Loss et al. 2015).

2.3.6 Variation in Population-specific Exposure to Migration Risk-factors

I quantified the exposure of individual *Vermivora* warblers to each migration risk-factor (plus the raster representing overall exposure) by summing the values of cells of each migration risk-factor's raster that were contained within the individual warbler's seasonal core-use area. As in my analysis of population overlap (above), I considered other thresholds (i.e., 10th percentile, 50th percentile) for delineating core-use areas in my investigation of the associations between population trajectory and migration risk-factors. Here, I present the results of my analysis using the 25th percentile threshold to identify core-use areas because the relative exposure of populations to different risk factors and the direction and strength of modeled relationships (see below) did not meaningfully differ among thresholds (Fig. B – 2). Completion of an annual cycle requires an individual to undergo both autumn and spring migration. Therefore, I summed the values of each migration risk-factor extracted from an individual's autumn and spring core-use areas to derive the total annual exposure for each warbler to each risk factor.

For this analysis, I excluded individuals with geolocators that did not record both autumn and spring migration (*n* = 8). I compared population means to assess whether different populations of both species (i.e., three populations of blue-winged warblers and two populations of golden-winged warblers; based on BCR) were more or less exposed to individual migration risk-factors using one-way analysis of variance (ANOVA) and considered differences to be significant using $\alpha = 0.05$. If I detected a difference between populations with an ANOVA, I conducted a Tukey's post hoc test to determine the comparison(s) that differed and the direction of the difference. Additional sampling in some of the populations with relatively fewer geolocator tracks could increase statistical power. However, power analyses suggested that I would be likely to detect small-to-moderate effect sizes in all of my analyses (Fig. B – 1; Table B.3, B.4).

2.3.7 Linking Population Trends with Exposure to Migration Risk-factors

To determine whether variation in recent population trajectories of *Vermivora* warblers (i.e., since 2000) was more strongly associated with variation in exposure to migration risk-factors or factors associated with breeding and/or nonbreeding periods (i.e., migratory connectivity), I performed a partial least squares (PLS) regression analysis using the 'caret' package in R (Kassambara and Mundt 2019). I used PLS regression analysis because it is effective at reducing the multidimensionality of large sets of explanatory variables by creating a new set of latent, orthogonal (i.e., independent) explanatory variables, thus also addressing multicollinearity (Carrascal et al. 2009). Additionally, PLS regression analysis provides similar results to those obtained through related methods (e.g., multiple regression, principal components regression) but may outperform these other methods in identifying the effect size and relative importance of explanatory variables in modeling the response variable (Carrascal et al. 2009). I tested for multicollinearity in my data by calculating the variable inflation factor (VIF) of each explanatory variable using the ‘mctest’ package in R (Imdadullah et al. 2016, Imdadullah and Aslam 2018).

I used the site-level population trajectory of each species since 2000 as the response variable. Specifically, I extracted the BBS-estimated population trajectory from 2000–2016 at each breeding-grounds deployment site and at each geolocator-estimated breeding site (for individuals tracked from their nonbreeding sites; Fig. 2 – 1, Table B.1). The BBS derives estimates of population trajectory from route-level data (cell size ~0.38°) using an inverse-distance, weighted average approach wherein a route’s influence decreased as the distance to the point of interest increased (see Sauer et al. 2017 for full details). Using site-level estimates of population trajectory allowed me to assess whether finer-scale variation within broader regional populations (i.e., BCR’s; Fig. 2 – 1) was more strongly associated with factors experienced during migration or during stationary breeding and nonbreeding periods as has been observed in other systems (e.g., Hewson et al. 2016).

I analyzed the relationship between the response variable (population trajectory since 2000) and 12 explanatory variables associated with breeding and/or nonbreeding factors, including migratory connectivity terms (*n* = 4; breeding-site longitude, breeding-site latitude, nonbreeding-site longitude, nonbreeding-site latitude; Table 2.2) and risk factors experienced during migration (*n* = 8; forest and shrub cover, net change in forest and shrub cover 2000-2015, tornados, hurricanes, agricultural cover, human footprint, wind energy development, communications towers; Table 2.2). I did not include the variable for overall exposure in the PLS model because my goal was to assess the relative importance of individual migration risk-factors and migratory connectivity terms in explaining variation in *Vermivora* warbler population trends. To train the PLS model and determine the number of latent variables (i.e., components) to include, I scaled and centered all explanatory variables and chose the number of latent variables that resulted in the lowest root mean squared error following 5-fold cross-validation to avoid overfitting (allowing for a maximum of 12 latent variables; Sawatsky et al. 2015). I also incorporated test set validation in which I assessed model performance using 80% of the dataset to train the PLS regression model and compared model predictions to observed values in the withheld (test) portion of the dataset (Sawatsky et al. 2015). I estimated the variable importance for the projection (VIP) score and absolute value of coefficients in our PLS regression model predicting recent population trajectories in *Vermivora* warblers to determine whether terms related to migration risk-factors, factors experienced during stationary breeding and/or nonbreeding periods, or some combination of factors throughout the annual cycle were associated with variation in recent population trajectories. I considered variables with a VIP score > 0.8 and coefficient values > 1.0 as influential in our PLS model (Sawatsky et al. 2015).

I also used an information-theoretic modeling approach to determine whether migration risk-factors experienced annually, or in stopover regions prior to crossing the Gulf of Mexico during autumn or spring explained additional variation in recent *Vermivora* warbler population trends after accounting for breeding and nonbreeding location which are known, or predicted to be associated with variation in population trends (i.e., breeding and nonbreeding latitude and longitudes; Kramer et al. 2018a; Appendix B Supplementary Methods, Fig. B – 2). Briefly, I constructed generalized linear models within a hierarchical modeling framework to determine whether adding singular migration risk-factor parameters (including the variable for overall exposure to migration risk-factors) to a base model consisting of breeding latitude, breeding longitude, nonbreeding latitude, and nonbreeding longitude explained additional variation in *Vermivora* warbler population trends (Appendix B Supplementary Methods). I considered migration risk-factor variables to be uninformative if the more complex model (i.e., base model plus single migration risk-factor parameter) was < 2 ΔAIC_c from the base model (Arnold 2010).

2.3.8 Analysis of Future Threats

I assessed the likelihood that future threats related to land-use change within populations' migration core-use areas would affect *Vermivora* warblers using a georeferenced dataset of the projected development potential (i.e., the land suitability for development of different anthropogenic land uses from 2015–2030; Development Threat Indices, v1 [2015]; Oakleaf et al. 2015, 2019). The spatially explicit (cell size ~0.008°) future development potential for nine anthropogenic land uses was derived from publicly available data and based on the amount of unexploited resources and/or past trends in land-use change to inform future development potential (see Oakleaf et al. 2015 for details). This dataset provided modeled estimates of the projected future suitability of land to be converted to nine different anthropogenic land-use categories (Oakleaf et al. 2015). For analyses, I collapsed the nine different anthropogenic land-use types into six categories: solar energy, urban expansion, agricultural expansion, wind energy, biofuel, and mining (composite of mining, coal mining, conventional oil and gas mining, and unconventional oil and gas mining; see Oakleaf et al. 2015 for details and definitions). I used identical methods as those described above to standardize the extent and resolution of each raster containing the georeferenced development potential for the six land-use types. I estimated the potential future exposure of individual warblers to anthropogenic development within seasonal migration core-use areas by summing the development threat values (scaled from 0–100 for each cell) of each land-use type ($n = 6$) contained within an individual's seasonal migration core-use area (i.e., autumn or spring). I calculated the cumulative potential annual exposure for individual warblers by summing the seasonal exposure of each future development threat from autumn and spring. As in the previous analysis, I excluded individuals with geolocators that did not record both autumn and spring migrations.

I performed a multilevel logistic regression with the package 'lme4' in R (Bates et al. 2015) to determine if the six different types of anthropogenic development associated with increased migration risk-factors may disproportionately affect stationary or increasing vs. declining populations of *Vermivora* warblers in the future. I classified *Vermivora* warblers into two groups based on population trajectory: stationary or increasing (1) vs. declining (0) based on the site-level population trend since 2000 derived from BBS data (Sauer et al. 2017). I considered 95% confidence intervals around odds ratio estimates to determine whether future development potential associated with six types of land-use changes were more likely to occur in the migration core-use areas of populations currently exhibiting stationary or increasing trends (i.e., odds ratio and 95% confidence interval >1), declining trends (i.e., odds ratio and 95% confidence interval

<1), or likely to affect stationary or increasing and declining populations equally (i.e., 95% confidence interval included 1).

2.4 Results

2.4.1 Interspecific Variation in Space-use

Blue-winged warblers and golden-winged warblers exhibited different patterns in space-use during migration (Fig. 2 – 2). During autumn migration, both species used similar areas along the northern coast of the Gulf of Mexico: primarily eastern Louisiana, Mississippi, Alabama, and western Florida (Fig. 2 – 2). However, golden-winged warblers also used areas in Belize, Honduras, and Nicaragua in Central America (Fig. 2 – 2). During spring migration, blue-winged warblers used the Yucatán Peninsula and areas along the northern coast of the Gulf of Mexico (i.e., eastern Louisiana, Mississippi, Alabama, and western Florida; Fig. 2 – 2) whereas golden-winged warblers used areas farther west along the northern coast of the Gulf of Mexico (i.e., eastern Texas and Louisiana) in addition to portions of the central US (i.e., Ozark Mountain region; Fig. 2 – 2).

2.4.2 Intraspecific Variation in Space-use

Vermivora warblers exhibited intraspecific variation (i.e., within the same species but among populations from different BCRs) in core-use areas during migration (Fig. 2 – 3: A). During autumn migration, blue-winged warblers from more eastern breeding sites (i.e., in the Appalachian Mountains BCR) used areas farther east than western-breeding blue-winged warblers; however, there was still extensive overlap in core-use areas among populations defined by BCR (mean proportion of overlap = 0.56 ± 0.13 SD, $n = 6$ pairwise comparisons; range = 0.37-0.70). During spring migration, blue-winged warblers migrating to breeding sites in the Appalachian Mountains BCR used areas in the Yucatán Peninsula and the south-central US whereas the two western-breeding populations primarily used areas in the south-central US (Fig. 2 – 3: A). Intraspecific variation in core-use areas during both autumn and spring migration was most pronounced in golden-winged warblers with individuals breeding at sites in the Appalachian Mountains BCR occurring farther east in the US and in Central America relative to individuals breeding at sites in the Boreal Hardwoods Transition BCR (Fig. 2 – 3: A). The proportion of overlap of core-use areas between populations of golden-winged warblers was low during autumn (0.28 ± 0.7 SD, *n* = 2 pairwise comparisons) migration and there was no overlap between core-use areas during spring migration (*n* = 2 pairwise comparisons; Fig. 2 – 3: A).

The proportion of seasonal overlap (i.e., the overlap between autumn and spring core-use areas of a single population) within blue-winged warbler populations was moderate and similar (range = 0.56-0.68; Fig. 2 – 3: A). Notably, the two populations of golden-winged warblers exhibited both the highest (0.78; Appalachian Mountain BCR) and lowest (0.19; Boreal Hardwoods Transition BCR) proportion of seasonal overlap within *Vermivora* warblers (Fig. 2 – 3: A).

2.4.3 Variation in Population-specific Exposure to Migration Risk-factors

Blue-winged warblers from Prairie Hardwood Transition BCR breeding sites exhibited greater exposure to the summed combination of all migration risk-factors (*n* = 8; “overall”) relative to blue-winged warblers from Appalachian Mountains BCR breeding sites and golden-winged warblers from Boreal Hardwood Transition BCR breeding sites (Fig. 2 – 3: B). I observed high levels of within-population variation in space use but little evidence of differences in the mean exposure to predicted migration risk-factors among *Vermivora* warbler populations. Golden-winged warblers that migrated between the Appalachian Mountains BCR and northern South America had core-use areas with greater amount of relative forest and shrub cover, relatively less agricultural cover, and a lower frequency of tornadic storms compared to golden-winged warblers that primarily migrated between the Boreal Hardwoods Transition BCR and Central America (Fig. B – 3: A, B).

2.4.4 Linking Population Trends with Exposure to Migration Risk-factors

I detected moderate to high multicollinearity among explanatory variables (i.e., natural and anthropogenic migratory risk-factors, migratory connectivity factors; variable inflation factor [VIF] range = 2.4-19.2; Table B.5), warranting use of PLS regression analysis. The PLS regression model with the lowest root mean squared error after 5-fold cross-validation was comprised of two components that cumulatively explained 42% of the variance in the 12 explanatory variables and 59% of the variance in the response variable (population trajectory since 2000) in the training dataset (test-set validation R^2 = 0.55; Fig. B – 4).

The relative importance of standardized, explanatory variables (n = 12) included in PLS regression analysis suggested that factors related to migratory connectivity (i.e., breeding longitude, breeding latitude, nonbreeding longitude, nonbreeding latitude) were most important for explaining variation in recent population trends of *Vermivora* warblers (i.e., population trajectory since 2000; Fig. 2 – 4). Specifically, the variables for breeding latitude and nonbreeding longitude had relatively high regression coefficients (absolute value) and variable importance in the projection (VIP) scores suggesting that these variables were influential in the model. None (0/8) of the explanatory variables related to migration risk-factors had regression coefficients (absolute value) > 0.70 or VIP scores > 0.50 (Fig. 2 – 4, Fig. B – 5). Additionally, none of the generalized linear models assessing associations between migration risk-factors (annual exposure, Table B.6; seasonal pre-Gulf exposure, Table B.7) and *Vermivora* warbler population trends outperformed the base model containing breeding and nonbreeding latitude and longitude terms (results were similar when I considered 10th and 50th percentiles; Table B.8, B.9, B.10).

2.4.5 Analysis of Future Threats

Spatial variation in the projected threat of anthropogenic factors in migration core-use areas may lead to different factors affecting currently stationary and increasing, or declining populations of *Vermivora* warblers in the future (i.e., by 2030; Fig. 2 – 5). Specifically, potential land-use change associated with mining (coal, conventional oil and gas, unconventional oil and gas, and other types of mining) may be more likely to occur within the migration core-use areas of currently stationary or increasing populations of *Vermivora* warblers (odds ratio = 5.0 [1.7-14.7 95% CI]) relative to declining populations. Conversely, areas with a high potential for solar energy development (odds ratio = 0.2 [0.1-0.7 95% CI]) and urban expansion (odds ratio = 0.3 [0.1-0.9 95% CI]) may be more likely to occur within migration core-use areas of *Vermivora* warblers with currently declining population trajectories. Projected agricultural development (odds ratio = 0.9 [0.4-2.0 95% CI]), wind energy development (odds ratio = 1.5 [0.8-2.9 95% CI]), and biofuel energy development (odds ratio = 2.1 [0.8-5.2 95% CI]) are likely to occur in areas used equally by both stationary and increasing, and declining populations of *Vermivora* warblers during migration.

2.5 Discussion

Populations of *Vermivora* warblers exhibited variation in space use during migration. Notably, the greatest observed differences in space use were between numerically stable (Boreal Hardwoods Transition BCR) and declining (Appalachian Mountains BCR) populations of golden-winged warblers during spring migration (Fig. 2 – 3: A). Generally, variation in space use did not correspond with variation in relative exposure to migration risk-factors. However, golden-winged warblers breeding in the Appalachian Mountains BCR migrated through areas with more forest and shrub cover and experienced greater risk of exposure to hurricanes (during fall migration) relative to golden-winged warblers from Boreal Hardwood Transition BCR breeding sites. Golden-winged warblers tend to be associated with forest and shrub cover types during migration (Rohrbaugh et al. 2016) and therefore I predicted populations migrating through areas with more forest and shrub cover would be more likely to be stationary or increasing (Table 2.2). I observed the opposite relationship in that the population associated with the greatest amount of forest and shrub cover during migration (i.e., Appalachian Mountains BCR golden-winged warblers) exhibited declining population trends suggesting that populations of *Vermivora* warblers are not currently limited by availability of appropriate stopover habitat along seasonal migration routes. However, the data I used to quantify the amount of forest and shrub cover on the landscape does not account for factors such as habitat quality, pollution, or variation in predator density/richness, which may vary spatially and influence mortality rate (Gandini et al. 1994, Nicholson et al. 1997, Weber et al. 1999) or decrease future productivity (Legagneux et al. 2011). Golden-winged warblers from Appalachian Mountain BCR breeding sites also used areas that experienced more hurricanes relative to golden-winged warblers migrating to and from Boreal Hardwood Transition BCR breeding sites. However, numerically stable populations of blue-winged warblers migrated through areas with hurricane frequencies similar to declining populations of golden-winged warblers from Appalachian Mountain BCR breeding sites and therefore hurricanes are probably not driving recent declines of golden-winged warblers from Appalachian Mountains BCR breeding sites. Furthermore, golden-winged warblers may be able to detect and avoid strong, non-hurricane storms on the breeding grounds and during spring migration (Streby et al. 2015a) and therefore may be able to detect and avoid hurricanes during autumn migration.

The lack of evidence supporting the hypothesis that variation in recent *Vermivora* population trends is associated with landscape-level variation in exposure to migration risk-factors suggests that the factor(s) currently limiting populations are occurring elsewhere during the annual cycle (e.g., the breeding or nonbreeding grounds; Rohrbaugh et al. 2016, Kramer et al. 2018a). Factors associated with migratory connectivity of *Vermivora* warblers (i.e., breeding and nonbreeding sites) were more strongly associated with differential population trends in *Vermivora* warblers in my PLS regression analysis. Therefore, localized nonbreeding habitat loss (Kramer et al. 2018a) or factors associated with reproduction on the breeding grounds (e.g., low fledgling survival; Lehman 2017) may be driving recent declines in populations of golden-winged warblers from Appalachian Mountains BCR breeding sites. There is geographic variation in reproductive success of local populations of golden-winged warblers breeding within the Appalachian Mountains BCR (Lehman 2017, McNeil 2019). At some sites, golden-winged warblers are apparently reproducing at rates that should lead to population increases (Aldinger 2018, McNeil 2019) whereas others are reproducing at lower rates that correspond with population declines (Lehman 2017). Whether ongoing population declines in the Appalachian Mountain BCR population segment of golden-winged warblers are driven by low reproduction, habitat loss at northern South American nonbreeding sites, or some other factor or combination of factors will likely require additional study. Moreover, demographic information on golden-winged warblers in the Appalachian Mountains BCR comes from several well-studied sites that are often managed to benefit golden-winged warblers. Therefore, it is unclear whether the trends observed at these sites are representative of the broader Appalachian Mountain population, and whether these sites are population sources or sinks (Lloyd et al. 2005, Aldinger 2018). Additional information on golden-winged warbler metapopulation dynamics within the Appalachian Mountains BCR may further inform conservation efforts and identify regions where targeted management may be warranted.

Although the existence of migration indicates that a migratory life-cycle likely confers, or historically conferred greater fitness than a stationary one for many taxa, migration is thought to be an exceptionally challenging portion of the annual cycle for many migratory species and a period with elevated mortality rate relative to stationary periods of the annual cycle (Nicholson et al. 1997, Sillett and Holmes 2002). Mortality during migration is known to be associated with population trends in other migratory species. For example, common cuckoos (*Cuculus canorus*) using the shorter of two routes to cross the Sahara during migration between European breeding sites and sub-Saharan nonbreeding sites experienced greater mortality relative to individuals using the longer route and breeding populations with a greater proportion of individuals using the shorter, more dangerous route were more likely to exhibit declining population trends (Hewson et al. 2016). Stochastic weather events may also affect species during migration (Newton 2007, O'Shea et al. 2016). Severe storms, hurricanes, and other inclement weather that occur during migration can cause mortality in migrating birds, especially when migrants encounter severe weather while traversing an inhospitable barrier (e.g., the Gulf of Mexico; Newton 2007, Yang et al. 2021). The abundance of chimney swifts (*Chaetura pelagica*) at breeding sites in Québec, Canada declined by an average of 62% the year after a hurricane developed and intercepted swifts along their autumn migration route causing mass mortalities (Dionne et al. 2008). Migratory birds also frequently collide with and are killed at communications towers, buildings, and wind turbines (Loss et al. 2015). Estimated mortality of migratory birds at buildings (372–1,030 million birds in the US and Canada, annually; Machtans et al. 2013, Loss et al. 2014), communications towers (~7 million birds in the US; Longcore et al. 2013), and wind turbines (< 1 million birds in the US, annually; Smallwood 2013, Loss et al. 2013) vary by orders of magnitude and are staggering. However, the effects of anthropogenic mortality on the overall population trends of many migratory bird species are poorly understood and an area of rapidly developing research. Longcore et al. (2013) suggested annual mortality at communications towers alone may constitute >1% of 13 migratory species' estimated total population size, including golden-winged warblers. Golden-winged warblers have been described as super-colliders (i.e., experienced collision mortality more frequently than would be expected by chance based on population size and distribution; Arnold and Zink 2008). However, Arnold and Zink (2008) found no evidence that collision mortality experienced by golden-winged warblers and other super-collider species led to discernable changes in breeding population abundance trends. Similarly, I found limited evidence for population-level effects of a suite of natural and anthropogenic migration mortality risk-factors on the population trends of *Vermivora* warblers suggesting mortality experienced during migration may be similar among populations or that the magnitude of population-level differences in mortality rate during migration are not great enough to be captured in Breeding Bird Survey trends.

The geolocator datasets were comprised almost entirely of male *Vermivora* warblers because they are easier to capture and exhibit greater inter-annual site fidelity (Peterson et al. 2015, Kramer et al. 2018a) than females. However, population dynamics may be more sensitive to variation in survivorship of female *Vermivora* warblers during migration if females exhibit different migratory strategies that increase their exposure to mortality risk-factors relative to males (Bennett et al. 2019a, Fischer 2020). Thus, efforts to understand the distribution, abundance, and survivorship of female *Vermivora* warblers throughout the annual cycle may help further refine conservation strategies (Bennett et al. 2019a, Fischer 2020). Additionally, I only recovered geolocator data from individual *Vermivora* warblers that successfully completed both autumn and spring migrations. Thus, I was unable to identify when and where mortality occurred during the annual cycle for individuals that did not return to their initial capture locations with functioning geolocators. Moreover, the relationship between putative risk factors and mortality rate in migrating *Vermivora* warblers may be acting on a finer scale than I was able to assess.

Alternatively, the spatial arrangement of migration risk-factors relative to major migration barriers (e.g., the Gulf of Mexico) may be important to consider in future efforts exploring the relationship between migration risk-factors and the population trends of migratory species. For example, the relatively high occurrence of migration risk-factors in Florida (Fig. 2 – 3: B) could represent a greater risk (i.e., be more strongly associated with increased mortality rate) than other areas with similarly high occurrences of migration risk-factors but farther from the Gulf of Mexico (e.g., Iowa) if *Vermivora* warblers that stop-over in Florida prior to crossing the Gulf of Mexico are unable to sufficiently refuel and therefore initiate a trans-Gulf flight with insufficient energy reserves. However, I found no evidence of associations between variation in exposure to migration risk-factors in stopover regions near the Gulf of Mexico and *Vermivora* warbler population trends. Future efforts to quantify the relationships between migration risk-factors and survivorship of *Vermivora* warblers at a finer resolution (i.e., with radiotelemetry or GPS tags) may provide additional insight into the factors causing mortality during migration and patterns in their geographic arrangement that could provide opportunities for conservation (Hewson et al. 2016). Despite increases in the use of tracking technology to monitor migratory species (Marra et al. 2015), range-wide and multi-species assessments remain uncommon (Knight et al. 2018, Kramer et al. 2018a, Hill and Renfrew 2019, Renfrew et al. 2019, Rushing et al. 2020). My results highlight the importance of tracking multiple species across their distributions to better disentangle the relative importance of drivers of population trends.

The conservation of stopover sites and areas used by species during migration is critical for the long-term maintenance of migratory species (Weber et al. 1999, Wilcove and Wikelski 2008). However, my results suggest populations of *Vermivora* warblers are currently not limited by the availability of appropriate stopover habitat at the landscape scale. Habitat loss at stopover sites can negatively affect populations if suitable sites are far apart and/or limited in quality or abundance (Weber et al. 1999). Species that rely on the availability of predictable resources at fewer stopover sites within an otherwise inhospitable landscape (e.g., shorebirds) may be more susceptible to habitat loss and reduced habitat quality at those stopover sites and conservation of those specific stopover sites may be critical for managing those species (Weber et al. 1999; Studds et al. 2017). *Vermivora* warblers likely have access to sufficient forest- and shrub-dominated landscapes during migration such that targeted conservation of individual sites may not be fruitful. Instead, ensuring that sufficient forest and shrub cover exists broadly within population-specific core-use areas may be an effective conservation strategy for *Vermivora* warblers. Determining whether blue-winged and golden-winged warblers use similar land-cover types during migration, or respond similarly to management intended to create stopover habitat may be important to avoid creating landscapes that benefit one species over the other (e.g., Kramer et al. 2019). Furthermore, continued monitoring of *Vermivora* warbler populations may aid in identifying and mitigating the negative effects of future anthropogenic mortality risk-factors that may differentially affect populations during migration. Lastly, recognizing that migratory behavior in *Vermivora* warblers is a complex and evolving phenomenon and investigating how changes to the climate or landscape may lead to evolutionary tradeoffs may be valuable for long-term conservation planning (Winger et al. 2019).

Table 2.1: Modeling approaches, response variables, and explanatory variables used to address different research questions in this study. The variable "overall" was calculated by summing standardizing individual migration risk-factor rasters (*n* = 8; assigning equal weight to all risk factors).

Research question	Modeling approach	Response variable(s)	Explanatory variable(s)
Do populations of *Vermivora* warblers (defined by Bird Conservation Region [BCR]) exhibit variation in exposure to different anthropogenic and natural migration risk-factors?	One-way analysis of variance (ANOVA) and *post hoc* Tukey test	Annual relative exposure to migration risk-factors (*n* = 9) within individuals' 25th percentile core-use areas (*n* = 81): forest and shrub cover, net change in forest cover 2000–2010, agricultural cover, human footprint, wind energy, communications towers, tornados, hurricanes, overall.	Species and Bird Conservation Region (BCR): blue-winged warblers (*n* = 3 BCRs; Prairie Hardwood Transition BCR [BW PHT], Central Hardwoods BCR [BW CH], Appalachian Mountains BCR [BW AM]); golden-winged warblers (*n* = 2 BCRs; Boreal Hardwood Transition BCR [GW BHT], Appalachian Mountains BCR [GW AM]).
Are migration risk-factors, or breeding and nonbreeding factors more strongly associated with recent population trends of *Vermivora* warblers?	Partial least squares (PLS) regression	Individuals' estimated site-level Breeding Bird Survey population trend (*n* = 81; since 2000; cell size ~0.38°).	Migratory connectivity factors (*n* = 4): breeding latitude, breeding longitude, nonbreeding latitude, nonbreeding longitude. Annual relative exposure to migration risk-factors (*n* = 8): forest and shrub cover, net change in forest cover 2000–2010, agricultural cover, human footprint, wind energy, communications towers, tornados, hurricanes.

Research question	Modeling approach	Response variable(s)	Explanatory variable(s)
Does annual relative exposure to migration risk-factors explain additional variation in recent population trends of *Vermivora* warblers after controlling for breeding and nonbreeding factors?	Hierarchical generalized linear regression	Individuals' estimated site-level Breeding Bird Survey population trend (*n* = 81; since 2000; cell size ~0.38°).	Annual relative exposure to migration risk-factors (*n* = 9): forest and shrub cover, net change in forest cover 2000–2010, agricultural cover, human footprint, wind energy, communications towers, tornados, hurricanes, overall.
Does seasonal relative exposure to migration risk-factors in stopover regions (adjacent to the Gulf of Mexico) explain additional variation in recent population trends of *Vermivora* warblers after controlling for breeding and nonbreeding factors?	Hierarchical generalized linear regression	Individuals' estimated site-level Breeding Bird Survey population trend (*n* = 81; since 2000; cell size ~0.38°).	Seasonal relative exposure to migration risk-factors (*n* = 9) prior to crossing the Gulf of Mexico: forest and shrub cover, net change in forest cover 2000–2010, agricultural cover, human footprint, wind energy, communications towers, tornados, hurricanes, overall.
Do suitable areas for future development of a suite of anthropogenic land-use types disproportionately affect areas used by stable or increasing vs. declining populations of *Vermivora* warblers during migration?	Multiple logistic regression	Binomial classification of individuals' estimated site-level Breeding Bird Survey population trend (*n* = 81; since 2000; cell size ~0.38°; population trend ≥ 0 = "1", population trend < 0 = "0").	Suitability of landscape for future conversion to anthropogenic land-use types (*n* = 6): solar energy, urban cover, agricultural cover, wind energy, biofuel, and mining.

Table 2.2: Natural and anthropogenic risk-factors known or hypothesized to affect mortality rate and/or future reproduction in migrating birds that I included in my analyses. The expected relationship between population trajectories of *Vermivora* warblers from 2000–2015 (cell size ~0.38°, Breeding Bird Survey; Sauer et al. 2017) and potential migration risk-factors describe the expected direction (i.e., positive or negative) an effect would have if it was strong enough to lead to a measurable change in the population trajectory of different groups of *Vermivora* warblers. The original resolution of each data source is noted in brackets under each source and all spatially explicit data were resampled to achieve a standardized resolution equal to the resolution of the geolocator data (~0.500°).

Risk factor (expected relationship)	Explanation	Citations	Data source [resolution]
Natural			
Forest and shrub cover (positive)	*Vermivora* warblers use areas with forest or shrub cover to rest and refuel during migration. I predicted that populations migrating through areas with greater amounts of forest and shrub cover would be more likely to be stationary or increasing if variation in the amount of forest and shrub cover is driving or contributing to population declines.	Rohrbaugh et al. 2016	U.S. Geological Survey (USGS) Global Land Cover Characterization (GLCC); USGS 1997 [0.008°]
Net increase in forest cover 2000-2015 (positive)	If declining populations of *Vermivora* warblers are limited by the availability of forest cover along population-specific migration routes, then I expect declining populations to migrate through areas having lost relatively more forest than stationary or increasing populations.	Rohrbaugh et al. 2016	HYDE 3.1; Goldewijk et al. 2010, 2011 [0.500°]
Tornados* (negative)	Tornados and the powerful storms that produce them are known to cause mortality in migrating birds. Although tornados usually represent an acute threat to migrating individuals, these storms could contribute to population-level declines if variation in space use during migration leads to variation in exposure to tornadic storms among populations of *Vermivora* warblers.	Weidenfeld and Weidenfeld 1995, Newton 2007	National Oceanic and Atmospheric Administration (NOAA) Severe Weather Database Files; NOAA 2018 [N/A; point data]

Risk factor (expected relationship)	Explanation	Citations	Data source [resolution]
Hurricanes (negative)	Hurricanes pose a risk to migratory birds, especially if encountered during overwater barrier crossing (i.e., trans-Gulf of Mexico flights). Additionally, hurricanes may destroy coastal forest cover that may be important to migrants after crossing the Gulf of Mexico.	Newton 2007, Dionne et al. 2008	Atlantic HURDAT2; Landsea and Franklin 2013 [N/A, point data]
Anthropogenic			
Agricultural cover (negative)	Landscapes dominated by agriculture are considered poor quality stopover sites for migrating, insectivorous songbirds including *Vermivora* warblers. Therefore, regions with more agricultural cover may force migrants to travel greater distances between suitable stopover sites. Additionally, rural areas with high amounts of agricultural cover may be associated with increased exposure to chemical pesticides, herbicides, and vehicle collisions.	Blake 1986, Faaborg et al. 2010, Loss et al. 2014.	USGS GLCC; USGS 1997 [0.008°]
Human footprint (negative)	I used human footprint as a proxy variable to account for several correlated aspects of urbanization and human development that are known or hypothesized to increase mortality rate in migrating birds. First, urban landscapes generally contain less forest cover that many species (like *Vermivora* warblers) use during migration. Additionally, human footprint is strongly associated with increased levels of artificial light at night (ALAN), which may confuse nocturnally migrating birds and draw them into urban centers where they may be at a greater risk of colliding with buildings and windows. Human footprint is also highly correlated with population density, which may be associated with greater levels of environmental pollution, increased	Klem 1989, Van Doren et al. 2017, Cabrera-Cruz et al. 2018, Loss et al. 2015.	Global Human Footprint Dataset; Wildlife Conservation Society 2005, National Aeronautics and Space Administration (NASA) Socioeconomic Data and Applications Center (CEDAC) [0.008°]

	threats from poaching or non-native invasive predators (e.g., feral cats), and other non-fatal stressors.		

Risk factor (expected relationship)	Explanation	Citations	Data source [resolution]
Wind energy development* (negative)	Wind energy development (i.e., wind turbines) can cause direct mortality in migrating birds.	Osborn et al. 2000, Smallwood 2007, Loss et al. 2013	United States Wind Turbine Database; Hoen et al. 2018 [N/A, point data]
Communications towers* (negative)	Communications towers (often lighted) pose a direct mortality threat to migrating birds via collisions with the tower structure or guy-wires.	Kerlinger 2000, Longcore et al. 2013, Loss et al. 2015	Federal Communications Commission (FCC) Geospatial Data; FCC 2012 [N/A, point data]

*Data for US only.

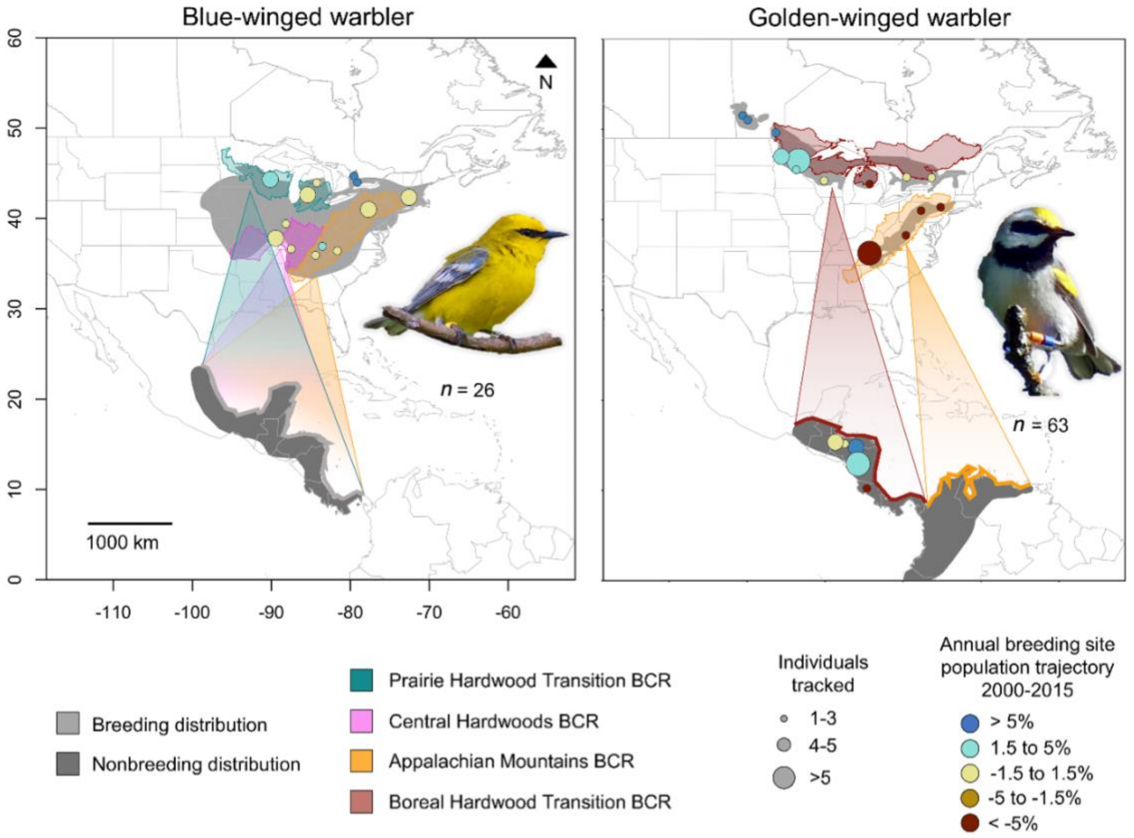

Figure 2 – 1: Breeding (light gray) and nonbreeding (dark gray) distributions of blue-winged warblers (*Vermivora cyanoptera*; left) and golden-winged warblers (*V. chrysoptera*; right). Sites where geolocators were deployed and recovered from *Vermivora* warblers are denoted by colored circles. The size of circles corresponds to the number of individuals tracked from that site. The color of circles indicates the population trajectory from 2000–2015 at breeding distribution sites or the average breeding population trajectory from 2000–2015 of individuals marked at nonbreeding distribution sites based on Breeding Bird Survey data (Sauer et al. 2017). Shaded polygons delineate Bird Conservation Regions (BCRs) that I used to aggregate sites into geographic populations. Shaded areas linking breeding and nonbreeding regions indicate the general migratory connectivity of populations but do not represent migratory routes. Geolocators from deployment sites in Central America are from Bennett et al. (2019b). Geolocators from deployment sites in the US and Canada are from Kramer et al. (2018b).

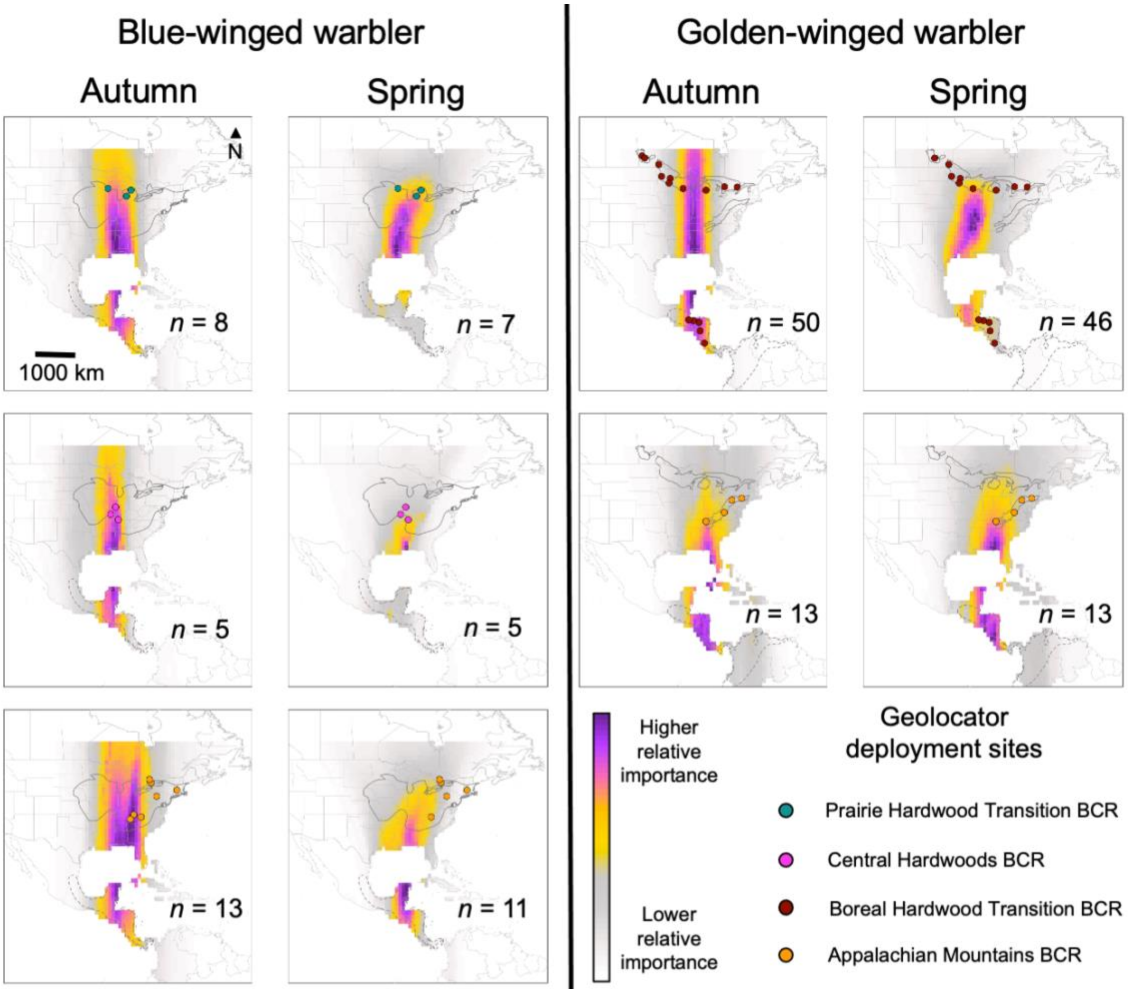

Figure 2 – 2: Average probability density functions for blue-winged warblers and golden-winged warbler populations (based on Bird Conservation Regions [BCRs]) during autumn and spring migrations. Darker purple cells represent areas of greater relative importance during migration (i.e., higher probability of use for greater durations by more individuals). I averaged the probability density functions of individual warblers derived from geolocator data spanning the duration of each warbler's seasonal migration period. Geolocator deployment sites are represented by open circles and colors correspond with Bird Conservation Regions (BCRs) of breeding sites. A solid gray line delineates the breeding distribution whereas a dashed line identifies the nonbreeding distribution (including a 100-km buffer).

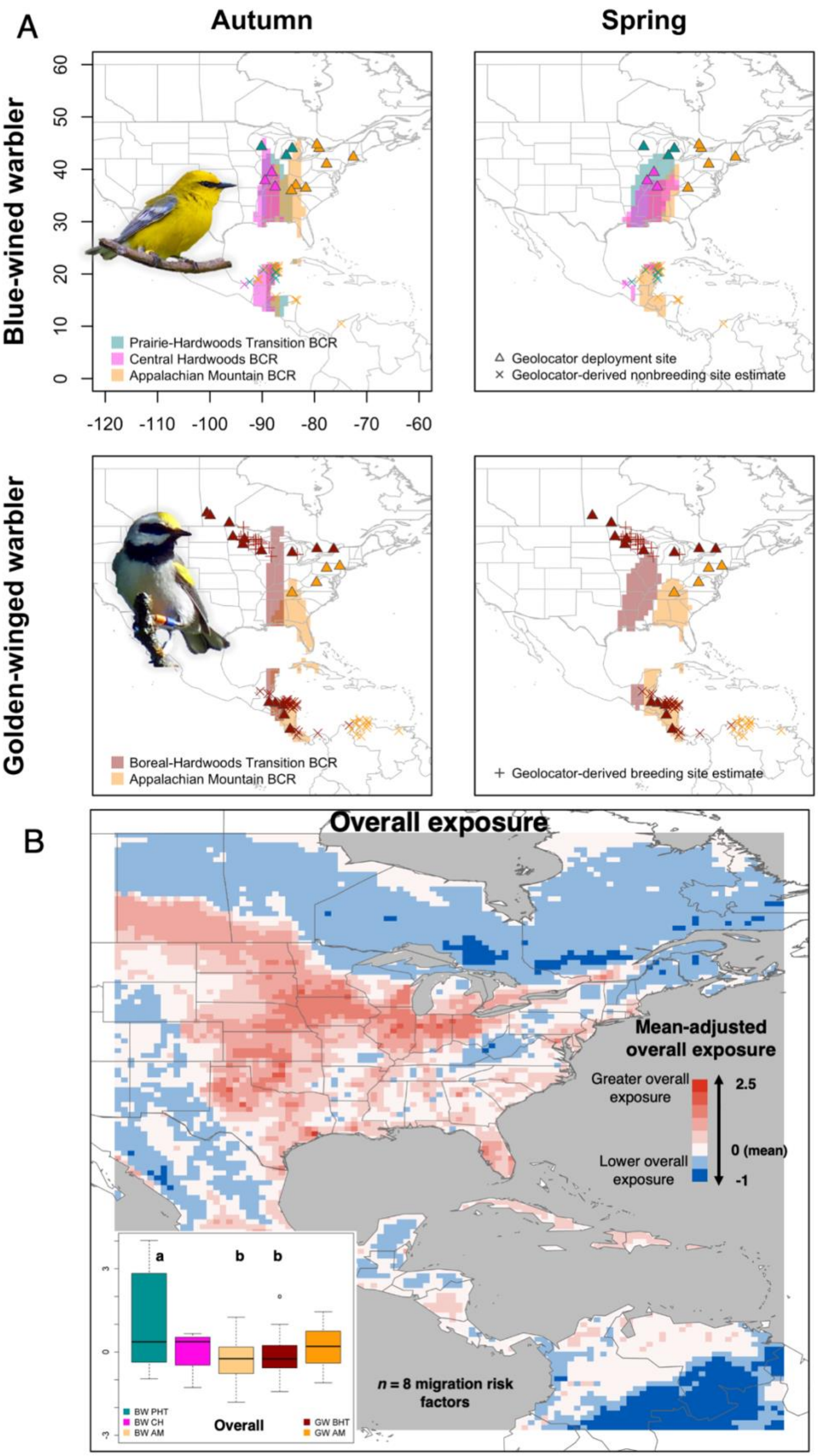
A
Autumn
Spring
Blue-winged warbler
60
50
40
30
20
10
0
-120
-110
-100
-90
-80
-70
-60
Prairie-Hardwoods Transition BCR
Central Hardwoods BCR
Appalachian Mountain BCR
△ Geolocator deployment site
× Geolocator-derived nonbreeding site estimate
Golden-winged warbler
Boreal-Hardwoods Transition BCR
Appalachian Mountain BCR
+ Geolocator-derived breeding site estimate
B
Overall exposure
Mean-adjusted overall exposure
Greater overall exposure
2.5
0 (mean)
Lower overall exposure
-1
a
b
b
3
0
-3
BW PHT
BW CH
BW AM
Overall
GW BHT
GW AM
n = 8 migration risk factors

Figure 2 – 3: Population-specific core-use areas (25th percentile; A) of *Vermivora* warblers during autumn and spring migration. Blue-winged warblers and golden-winged warblers from breeding sites (triangles) associated with different Bird Conservation Regions (BCRs) are represented by different colors. Geolocator-derived nonbreeding and breeding location estimates are identified by ×'s and +'s, respectively and colored according to breeding population (i.e., BCR). The spatial distribution of the mean-adjusted cumulative exposure to migration risk-factors (B) represents the sum of standardized rasters of eight migration risk-factors that I considered in my analyses. Red cells indicate areas with above-average exposure to migration risk-factors whereas blue cells are associated with below-average exposure. The spatial distribution of the individual migration risk-factors I considered ($n = 8$; C) are colored based on their expected association with population-trends (i.e., positive association = blue, negative association = red; see Table 2.1). Boxplots (D) show the scaled exposure of different populations (based on the exposure of individuals tracked within each population; colors correspond with the center panel) of *Vermivora* warblers to each migration risk-factor. Populations that experienced different levels of exposure (based on one-way ANOVA and Tukey HSD; $P < 0.05$) are denoted with letters. Populations are defined based on BCR and species (blue-winged warbler [BW] or golden-winged warbler [GW]) in boxplots: Prairie Hardwood Transition BCR (BW PHT, teal), Central Hardwoods BCR (BW CH, pink), Appalachian Mountains BCR (BW AM, light orange; GW AM, dark orange), and Boreal Hardwood Transition (GW BHT; maroon) BCR.

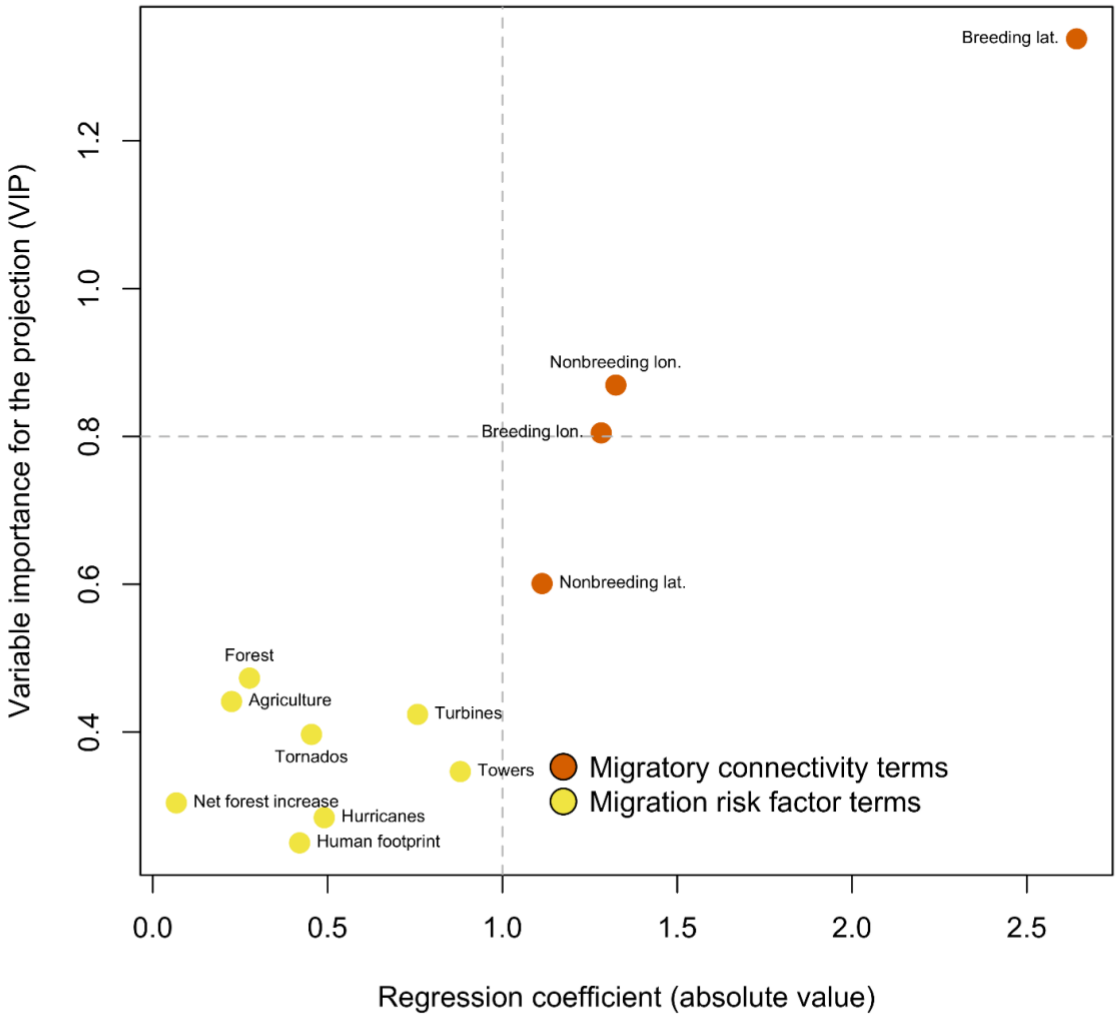

Figure 2 – 4: Comparison plot of the absolute value of regression coefficients and variable importance for the projection (VIP) of explanatory variables included in a partial least squares (PLS) regression model relating explanatory variables to variation in recent population trends of *Vermivora* warblers (i.e., since 2000). Explanatory variables fall into two categories: those associated with migration risk-factors experienced during migration (migration risk-factors terms; yellow circles) and those related to factors experienced during breeding and/or nonbreeding periods (migratory connectivity terms; orange circles). Gray dashed lines denote regression coefficients with absolute values > 1 and VIP > 0.8 which correspond with terms that are important in the PLS model.

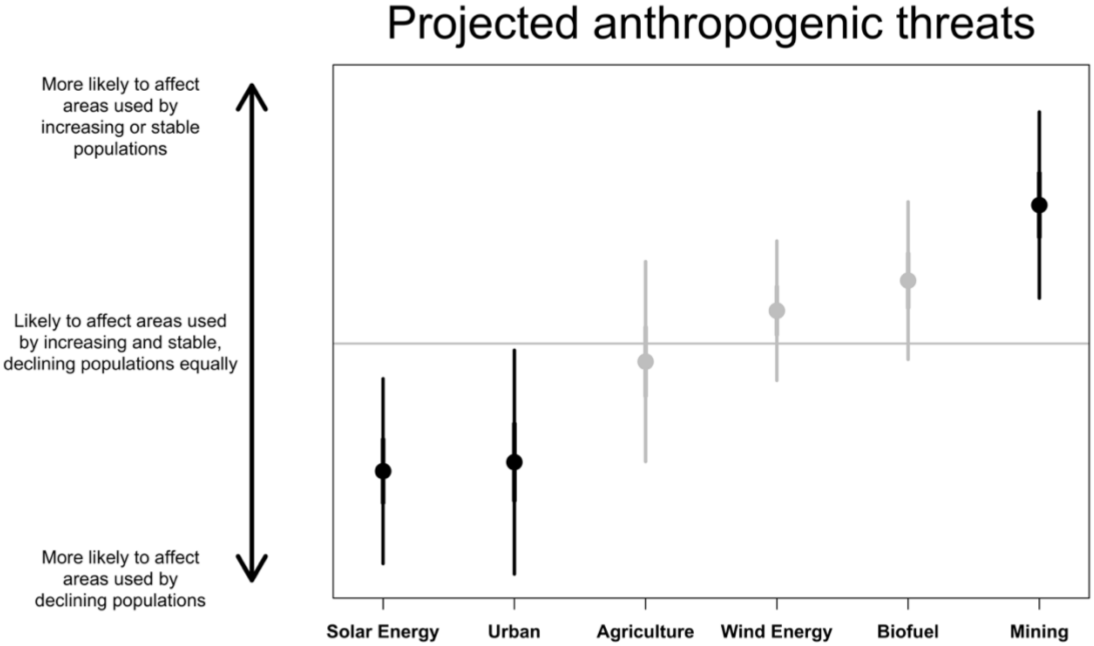

Figure 2 – 5: Results of multilevel logistic regression (point estimates with 95% CI) exploring the potential future exposure of declining and stationary or increasing populations of *Vermivora* warblers to anthropogenic migration risk-factors. Migration risk-factors with estimates above the horizontal line are more likely to occur in areas used by stationary or increasing populations of *Vermivora* warblers during migration. Factors with estimates below the horizontal line are more likely to occur in areas used by declining populations of *Vermivora* warblers. Factors with 95% CI estimates overlapping the gray line are equally likely to occur in areas used by declining and stationary and increasing populations of *Vermivora* warblers. Spatially explicit data for the future (i.e., 2030) migration risk-factors come from NASA Socioeconomic Data and Applications Center (SEDAC; Oakleaf et al. 2015, 2019).

Chapter 3

Migratory Connectivity and Barrier-crossing Flights of *Vermivora* Warblers are Affected by Synoptic Weather Conditions

3.1 Abstract

Migratory species are often required to navigate inhospitable barriers (e.g., oceans, deserts) during migration. Barrier-crossings are frequently associated with increased mortality rate and likely impose selective pressures on migratory species that shape their behavior and distribution. Therefore, understanding how exogenous conditions (i.e., weather) influence the crossing behavior of migratory birds at a major barrier can provide insight into the adaptive evolution of long-distance migrations involving barrier crossing and how changing climatic conditions might affect migratory species in the future. Here, I used light-level geolocator data collected from 95 individual *Vermivora* warblers to investigate the exogenous factors associated with individuals' departure across the Gulf of Mexico during both autumn and spring migrations. Exogenous factors associated with departure across the Gulf of Mexico differed between autumn and spring. In autumn, departure across the Gulf of Mexico was positively associated with favorable wind conditions and temperature, but negatively associated with relative humidity and 24-hr change in barometric pressure. During spring migration, departure across the Gulf of Mexico was associated with humidity and barometric

pressure, but not with wind conditions. Extrapolating these results, I found that geographic variation in favorable weather conditions coincided with the geographic distribution of individuals during autumn and spring such that more individuals used areas where conditions were favorable. This led to a breakdown of strong migratory connectivity between breeding and nonbreeding regions for golden-winged warblers (*V. chrysoptera*) in which populations that occurred in isolation from each other during breeding and nonbreeding periods exhibited weak migratory connectivity (i.e., co-occurred) during migration immediately prior to crossing the Gulf of Mexico. Breeding populations of blue-winged warblers (*V. cyanoptera*) co-occurred during both autumn and spring migrations and during the nonbreeding period (i.e., exhibited weak migratory connectivity). These results suggest weather conditions may shape the migratory connectivity and geographic distribution of small, long-distance migrants during migration. Based on projections of future climate conditions, increasing levels of humidity may decrease the favorability of conditions associated with crossing the Gulf of Mexico during spring migration for *Vermivora* warblers. Similarly, *Vermivora* warblers could experience less favorable conditions during autumn migration if hurricanes and other severe storms become more frequent and intense.

3.2 Introduction

Migration is a highly variable behavior that has evolved many times across taxa (Dingle 2014, Winger et al. 2014). Frequently, migratory species are required to navigate inhospitable landscapes or barriers (e.g., oceans, deserts) during migration (Dingle 2014). Because navigating migration barriers is often associated with an increased probability of mortality, these events likely impose significant selective pressures on migratory individuals that shape migratory strategies and routes (Strandberg et al. 2010, Hewson et al. 2016, Ward et al. 2018). Therefore, understanding how exogenous conditions (i.e., weather) are associated with migratory species' navigation of barriers can provide insight into the evolutionary origins and maintenance of migration and how changing climatic conditions might affect migratory species (Both et al. 2006, Gill et al. 2009, Iwamura et al. 2013).

One barrier to many Nearctic-Neotropical migrants is the Gulf of Mexico (Cooke 1904, Williams 1945, Deppe et al. 2015). Every year, billions of individual birds (~2/3 of all eastern North American species) navigate the Gulf of Mexico during autumn and spring migration (Rappole and Ramos 1994, Rappole 1995, Doktor et al. 2018) by undertaking one or more over-water flights (crossing) or circumventing the Gulf to the west using primarily over-land routes along the Mexican coast (circumventing; Rappole and Ramos 1994, Deppe et al. 2015). Crossing flights can consist of a ~10-24 hour non-stop, > 800 km, over-water flight (direct crossing) or two or more shorter over-water flights (~300-500 km each) with individuals stopping over in Cuba or other islands in the western Caribbean Sea (island-hopping; Lincoln 1935). The most direct route is often over-water across the Gulf of Mexico (Cooke 1904, Williams 1945). However, this route may be the most dangerous because terrestrial birds are unable to land and rest on water and therefore must complete the crossing in a single, non-stop flight (Smolinsky et al. 2013, Deppe et al. 2015). Both endogenous factors (e.g., fuel stores and muscle condition) and exogenous factors (e.g., wind speed and direction, precipitation, severe weather) can work independently or in concert to impede or facilitate the ability for migrants to complete the barrier crossing, thus affecting their probability of survival (Smolinsky et al. 2013, Deppe et al. 2015).

Despite these risks, that diverse species navigate the Gulf of Mexico up to twice a year suggests there may be context-dependent adaptive benefits to different strategies (i.e., direct crossing, island-hopping, or circumventing). Golden-winged warblers (*Vermivora chrysoptera*) exhibit individual, seasonal, and population-level variation in migratory behavior at the Gulf of Mexico during both autumn and spring (e.g., Kramer et al. 2017, Bennett et al. 2019b). However, little information exists on how exogenous factors (i.e., weather conditions) influence the initiation of trans-Gulf flights and whether favorable conditions vary seasonally, temporally, or spatially. Moreover, how exogenous conditions shape the migratory connectivity of small songbirds during migration is poorly understood. Migratory connectivity is a term frequently used to describe the strength of linkages among populations between distinct portions of the annual cycle (Webster et al. 2002). Species exhibiting strong migratory connectivity consist of populations that tend to occur together and in isolation from other populations throughout the annual cycle whereas species with weak connectivity consist of populations that mix during different periods of the annual cycle (Webster et al. 2002). Frequently, assessments of migratory connectivity consider the linkages of populations between the breeding and nonbreeding period during which individuals tend to be sedentary and populations may be especially vulnerable to limiting factors (e.g., Kramer et al. 2018a). However, population-specific limiting factors and bottlenecks can also occur if populations are isolated in time or space during migration (Hewson et al. 2016, Knight et al. 2021). Therefore, quantifying the strength of migratory connectivity of breeding populations during the nonbreeding period and during seasonal migrations can help identify the extent to which populations are isolated during different portions of the annual cycle and provide context to improve conservation efforts.

Here, I used geolocator data from 90 individual *Vermivora* warblers (golden-winged warblers, blue-winged warblers [*V. cyanoptera*], and phenotypic hybrids between these two very closely related species; Toews et al. [2016]) to test if weather conditions were associated with barrier-crossing behavior and if relationships between weather conditions and barrier crossing varied between autumn and spring migration periods. I also assessed the frequency of route-use by different populations and estimated the migratory connectivity of *Vermivora* warbler breeding populations during autumn and spring migrations to quantify spatial and temporal segregation of breeding populations (based on Bird Conservation Region [BCR]) prior to navigating a major migration barrier. Spatial segregation (i.e., strong migratory connectivity) among breeding populations of *Vermivora* warblers prior to crossing the Gulf of Mexico during autumn and/or spring migration could affect population dynamics if different regions are associated with different rates of survival (e.g., Hewson et al. 2016). I predicted that barrier-crossing behavior in golden-winged and blue-winged warblers would be similar between species and associated with factors previously described to influence barrier-crossing in other, larger species (e.g., generally favorable wind conditions, low relative humidity; Deppe et al. 2015). Based on previous evidence from golden-winged warblers, I expected *Vermivora* warbler populations to exhibit stronger migratory connectivity during autumn migration than spring migration when individuals may be under greater time constraints to reach the breeding grounds (Kramer et al. 2017). Understanding how a barrier shapes the migratory behavior of a small (<10 g) bird provides context for understanding how abiotic factors shape the evolution of diverse migratory strategies across taxa (Winger et al. 2019).

3.3 Methods

3.3.1 Geolocator Data Collection

I used published geolocator data from 90 individual *Vermivora* warblers (*n* = 96 geolocator tracks; 6 individuals were tracked for 2 years) collected from 2013–2017 (Kramer et al. 2018b, Bennett 2019). Geolocators are a relatively simple tracking technology that record the level of ambient light at regular intervals (typically 2-5 minutes, depending on model). These light data can then be used to estimate geographic location of the geolocator based on the seasonal variation in the timing and duration of sunlight across the globe (Hill and Braun 2001, Ekstrom 2004).

I analyzed data from 95 geolocators carried by 90 individual *Vermivora* warblers (Table C.1, C.2). Most of the geolocator data (75/95; 79%; Kramer et al. 2018b) were collected from 2013–2017 from *Vermivora* warblers at 26 sites spanning the breeding distribution of both golden- and blue-winged warblers (Kramer et al. 2018a). Previously, these data were used to identify population dispersion during the nonbreeding period (Chapter 1; Kramer et al. 2017, 2018a) and assess whether regional variation in space-use during migration was associated with exposure to natural and anthropogenic risk-factors (Chapter 2). These data were supplemented with geolocator data from 20 individual male golden-winged warblers collected by Bennett et al. (2019b) from five sites in Central America (Bennett 2019) in 2016. For individuals with two years of tracking data (i.e., two geolocator tracks; *n* = 6), I assumed that migration during the first year was independent of migration in the second year because golden-winged warblers are known to use different migration routes in different years and because weather conditions are likely independent among years (Stanley et al. 2012, Kramer et al. 2017).

I defined populations of *Vermivora* warblers based on the BCR of an individual's breeding location. However, several study areas occurred on the periphery of the species' distribution and I assigned individuals at those sites to the nearest BCR containing other study sites and containing a greater proportion of the species' distribution (Table C.1; Fig. 3 – 1, C – 1; Appendix C). Detailed descriptions of study sites and field methods are presented in Kramer et al. (2018a) and Bennett et al. (2019b). Both studies used the same model of geolocator (ML6240, 2-min light-sampling regime; Biotrak, Wareham, UK) and modified leg-loop harness to attach geolocators to *Vermivora* warblers (Rappole and Tipton 1991, Streby et al. 2015b). Peterson et al. (2015) found no evidence of any effects of geolocators on the migratory ecology or apparent survival rate of golden-winged warblers marked with geolocators using this harnessing method.

3.3.2 Geolocator Data Processing and Delineation of Migration Routes

I analyzed all geolocator data in R (v. 4.0.4; R Core Team 2021) using the template-fit method in 'FLightR' (v. 4.9: Rakhimberdiev et al. 2015, Rakhimberdiev and Saveliev 2019). The template-fit method derives location estimates from raw light data using the timing and slope of transition events (i.e., dawns and dusks; Ekstrom 2004, Rakhimberdiev et al. 2015). To prepare raw light-level data for analysis, I used the package 'BAStag' (Wotherspoon et al. 2016) to identify transition events using a threshold of 1.5 (Kramer et al. 2017, 2018b). I calibrated geolocator data in 'FLightR' using the period that individuals were known (or assumed) to be resident at breeding

(Kramer et al. 2018a, 2018b) or nonbreeding (Bennett et al. 2019b) deployment sites. I analyzed data from each geolocator using the movement model in ‘FLightR’ (optimized with one million particles) to derive seasonal migration tracks. I used a behavioral mask that allowed migrating *Vermivora* warblers to use over-water routes but prevented them from being stationary >25 km from land (Kramer et al. 2018a, Delancey et al. 2020). I also constrained the maximum distance between subsequent twilights to 1,200 km, which limited the effects of erroneous location estimates, and used the automatic outlier exclusion function of ‘FLightR’ to identify and eliminate extreme location estimates during the movement modeling process (Rakhimberdiev and Saveliev 2019). I used the function ‘*find.times.distribution*’ in FLightR to estimate commencement and termination of seasonal migrations (median date) from known (Kramer et al. 2018a) or estimated (Bennet et al. 2019b) breeding sites to known (Bennett et al. 2019b) or estimated (Kramer et al. 2018a) nonbreeding sites.

3.3.3 Identification of Full Light Pattern (FLP) Anomalies

Vermivora warblers, like most other Nearctic-Neotropical migrant songbirds, are widely thought to initiate and undertake migratory flights primarily at night and use daytime periods to rest and refuel (Scott 1881, Alerstam 2011). Light profiles recorded by geolocators when individuals are known to be present at breeding and nonbreeding sites consistently show that individuals experience some environmental shading (i.e., light-levels < 64 [arbitrary maximum light value]) during twilights (i.e., dawns and dusks) and during the daytime. Shading during twilights often results in extremely rapid transitions (i.e., < 6 min) between complete darkness (i.e., light level = 0) and full light (i.e., light-level = 64), or *vice versa*. Moreover, shading is also frequent during the daytime and can be substantial (i.e., very low [light level <10] or no light [light level = 0] recorded; Fig. 3 – 2; Fudickar et al. 2012). If *Vermivora* warblers undertake migratory flights that persist and/or proceed throughout the daytime (e.g., during flights across the Gulf of Mexico), those events would be readily identifiable as anomalies in the geolocator data because of their unique light profiles (i.e., little or no shade) compared to other days (Fig. 3 – 2; Adamík et al. 2016). Moreover, these anomalies should occur during autumn and spring migration periods and coincide with significant changes in location estimates indicating geographical displacement (i.e., movements > 500 km).

I used similar methods to those described by Adamík et al. (2016) to define full light pattern (FLP) anomalies in geolocator data from *Vermivora* warblers during autumn and spring migrations. I considered FLP anomalies to be consistent with prolonged migratory flight into daytime if (1) dawn was unshaded (i.e., exhibited increasing light levels from first light, to full light) and occurred not too rapidly (i.e., < 6 min) or too slowly (i.e., i.e., > 12 min; Appendix C Supplementary Methods), (2) if recorded light levels remained at maximum intensity (i.e., 64 for > 5 hrs after dawn), and (3) if the timing of dawn and dusk on the day of the FLP anomaly differed from the previous day in a manner consistent with a large magnitude (i.e., >500 km) shift in location in the expected direction (autumn = southward, spring = northward).

3.3.4 Filtering FLP Anomalies

To determine whether visually identified FLP anomalies differed from light profiles of non-FLP days, I randomly selected days from both autumn and spring migration periods (*n* = 50 for each period) and estimated the amount of shade during dawn, daytime, and dusk periods. To quantify shading during dawn and dusk periods, I fit a quadratic regression to the light data and calculated the summed absolute residuals (Adamík et al. 2016). To quantify shading during the daytime period, I calculated the sum of deviations from maximum light intensity (i.e., 64; Adamík et al. 2016). I also determined the duration (in minutes) of dawn, daytime, and dusk periods for all identified FLP anomalies (Appendix C Supplementary Methods).

I tested whether FLP anomalies differed in sum of absolute residuals (log scale) and duration of dawn (in seconds; log scale) compared to randomly selected (i.e., non-FLP anomaly) days using a two-way analysis of variance (ANOVA) and Tukey's Honest Significant Difference (Tukey's HSD) test to account for both FLP anomaly status (i.e., "yes" or "no") and period (i.e., "dawn", "daytime", "dusk") as independent variables. I predicted that days identified as FLP anomalies would have lower total absolute residuals during dawn and daytime periods compared to randomly selected days because migrating warblers crossing the Gulf of Mexico would experience virtually no shading during dawn and during the first ~5 hr of the daytime period. I did not expect total absolute residuals during dusk periods to differ between random days and days identified as FLP anomalies because warblers crossing the Gulf of Mexico would likely complete their journey prior to the following dusk (i.e., ~24 hr after departure) and could be expected to land and experience environmental or behavioral shading prior to dusk and the onset of total darkness (Adamík et al. 2016).

If individual *Vermivora* warblers had multiple FLP anomalies in the same seasonal migration period (i.e., autumn or spring), I used the function '*find.times.distribution*' in 'FLightR' to determine which FLP was associated with the estimated latitude of the individual crossing 24.5° (i.e., the approximate latitudinal midpoint of Gulf of Mexico). Multiple FLP anomalies from a single geolocator-marked *Vermivora* warbler may indicate variation in individual behavior, different migratory strategies, and/or multiple flights involving prolonged flight into daytime (Adamík et al. 2016; Table C.3).

3.3.5 Determining Take-off Sector

To understand the spatial dispersion of individuals from distinct breeding populations during migration but prior to navigating the Gulf of Mexico, I classified the take-off sector of geolocator-marked *Vermivora* warblers based on individuals' estimated location just before navigating (i.e., crossing or circumventing) the Gulf of Mexico. Geolocator-derived estimates of latitude have lower precision (~150–250 km) than estimates of longitude (~25–50 km; Fudickar et al. 2012). Therefore, I generally classified geolocator-marked *Vermivora* warblers into four groups based on whether they circumvented the Gulf of Mexico (circumvent), or based on their longitude prior to departing across the Gulf of Mexico (i.e., western, central, or eastern). I classified individuals as "circumventing" the Gulf of Mexico if they did not exhibit an FLP anomaly during the migration period of interest or if they exhibited an FLP anomaly, but a straight line connecting their location estimate immediately before and after the FLP anomaly was over land (i.e., west of the western coast of the Gulf of Mexico; < -97.5°). Individuals that exhibited an FLP anomaly and occurred in locations that required crossing the Gulf of Mexico to reach the estimated location following the FLP anomaly were classified into three sectors depending on their estimated longitude prior to departing to cross the Gulf of Mexico: the western sector included individuals occurring between -97.5° and -93°, the central sector included individuals occurring between -93°

and -87°, and the eastern sector included individuals occurring > -87° (Fig. 3 – 1). All individuals were assigned to a point in the center of each sector (Table C.4), which was also the location for which I extracted weather data (see below).

3.3.6 Selecting Weather Variables and Collecting Weather Data

To understand whether barrier crossing behavior in *Vermivora* warblers was associated with weather conditions, I considered synoptic (i.e., regional) weather variables known or suggested to be associated with the migratory behavior of Nearctic-Neotropical bird species near the Gulf of Mexico (Smolinksy et al. 2013, Deppe et al. 2015, Bolus et al. 2017). These included surface-level wind profit (i.e., wind speed multiplied by the directionality of the wind relative to north [0°; autumn] or south [180°; spring]; Appendix C Supplementary Methods), surface-level temperature (°C), surface-level relative humidity (%), surface-level barometric pressure (hPa), 24-hr change in surface-level wind profit (unitless), 24-hr change in surface-level temperature (°C), 24-hr change in surface-level relative humidity (%), and 24-hr change in surface-level barometric pressure (hPa). Additionally, I considered wind profit, temperature, and relative humidity at 850 hPa (~1,500 m above ground level). I obtained weather data from https://earth.nullschool.net (Beccario 2021). These weather data were derived from Global Forecasting System (GFS) models available from the US National Center for Environmental Prediction and had a spatial resolution of 25 km and temporal resolution of 3 hr. It was impossible to determine the exact time of day individuals initiated migratory flights across the Gulf of Mexico from geolocator data. However, data from radar and telemetry research indicate many birds initiate migration shortly after dusk (Deppe et al. 2015, Van Doren and Horton 2018). Therefore, I extracted weather data at the interval nearest local sunset (i.e., 20:00 local time) for each migration sector that was within 1.5 hrs of sunset during both autumn and spring migration periods due to both migrations occurring relatively near the equinoxes (Table C.4). I extracted weather data for each day in both autumn and spring migration periods. I tested for correlation (i.e., Pearson's correlation coefficient) among selected weather variables and excluded variables that were strongly correlated (i.e., $|r| \geq 0.6$ (Table C.3, C.4; Deppe et al. 2015) from my analyses. I also tested if weather conditions differed between days with ≥ 1 FLP anomaly vs. days without an FLP anomaly (Fig. C – 2). Last, I assessed whether the predicted favorability of weather conditions experienced during autumn and spring migration (separately and combined) differed among populations of *Vermivora* warblers (based on BCR) using one-way ANOVAs and Tukey's HSD tests.

3.3.7 Correlation Among Weather Variables

I excluded temperature at 850 hPa from analysis of autumn barrier crossing behavior because it was strongly correlated with surface-level temperature ($|r| = 0.61$, $P < 0.001$; Table C.5). Similarly, I excluded wind profit at 850 hPa, surface-level temperature, temperature at 850 hPa, and 24-hr change in temperature because they were strongly correlated with surface-level wind profit ($|r| = 0.64$, $P < 0.001$), surface-level relative humidity ($|r| = 0.83$, $P < 0.001$), surface-level barometric pressure ($|r| = 0.84$, $P < 0.001$), and 24-hr change in humidity ($|r| = 0.77$, $P < 0.001$), respectively (Table C.6). Consequently, I considered ten weather variables in analysis of autumn barrier crossing behavior and seven weather variables in analysis of spring barrier crossing in *Vermivora* warblers (Appendix C, Table C.5, C.6).

3.3.8 Modeling and Statistical Analyses

I built logistic regression models using the 'lme4' package in R (Bates et al. 2015) to test if weather variables were associated with which route *Vermivora* warblers used to cross the Gulf of Mexico during autumn and spring migrations. The dependent variable in my logistic regression models was whether an individual initiated a trans-Gulf flight ("1"; following day classified as an FLP anomaly), or did not initiate a trans-Gulf flight, but was assumed to be near the Gulf of Mexico ("0"; following day was not characterized as an FLP anomaly). Determining the period during which individual *Vermivora* warblers were near the Gulf of Mexico and did not initiate trans-Gulf flights (i.e., days classified as "0" in logistic regression models) was difficult given the timing of migration (near the equinoxes) and the coarseness of geolocator data (Fudickar et al. 2012). Therefore, I considered three different periods in my logistic regression models. First, I considered a seven-day period that included the departure day (i.e., day prior to observed FLP anomaly; "1"), and the six days leading up to the departure day (i.e., "0"). I also considered a four-day period (including the departure day ["1"] and the three previous days ["0"]), and a two-day period (including the departure day ["1"] and the previous day ["0"]). For each period, I assumed individual *Vermivora* warblers were present at, or near the Gulf of Mexico but did not initiate trans-Gulf flights until the dusk prior to the observed FLP anomaly.

Preliminary models indicated no differences among years or populations in the timing or probability of individuals exhibiting FLPs ($\Delta AIC_c > 2$ compared to intercept-only model; Table C.7). Therefore, I grouped data from all years and populations in subsequent analyses. I did not include ordinal day in models because it was confounded with my modeling approach of comparing weather conditions of departure days to the previous 1–6 days wherein I assumed the individual was stationary. The structure of the dataset therefore should be expected to produce an erroneous positive association with ordinal date because each 1 (i.e., FLP) necessarily occurred after one or more 0s (i.e., non-FLPs). Ordinal day may be a factor influencing the barrier-crossing behavior of *Vermivora* warblers and/or there may be meaningful interactions between ordinal day and weather conditions as reported in other migratory species (Deppe et al. 2015). However, those relationships may be better addressed with other technologies or analyses that require different assumptions than those used in this study (e.g., passive telemetry; Deppe et al. 2015).

I used a drop-one modeling approach that involved building a full model containing a suite of predictor variables associated with regional weather conditions (see above) for each season (i.e., autumn and spring) that are hypothesized to be associated with barrier-crossing behavior in migratory songbirds (Ward et al. 2018). I iteratively eliminated unimportant variables based on their contribution to model performance (i.e., AIC_c) using the stats::drop1() function in R, which compared the full model to models reduced by a single covariate. Final models included variables that that did not improve the model if dropped (Tredennick et al. 2021). I assessed final model performance using receiver operating characteristic (ROC) curves and transformed logit-scale model coefficients to log-odds ratios for interpretation. I extrapolated the final seasonal two-day model (i.e., based on departure day and the previous day) to predict the number of days during autumn and spring migration periods with favorable weather conditions for trans-Gulf flights (i.e., predicted probability of initiating trans-Gulf flight > 0.5) and used two-sample proportional tests to compare the proportion of individuals using different migration sectors during autumn and spring migration. Although largely exploratory, this analysis considered a limited suite of variables previously shown to influence the migratory behavior of songbirds. Therefore, observed associations may warrant future testing using different approaches (i.e., passive telemetry, global positioning system [GPS] tracking; Deppe et al. 2015). Weather variables identified as important in final models derived within the drop-one framework were similar to the those with statistically significant effects (i.e., 95% CIs around estimates of effect size did not overlap zero) to full models containing all potential weather variables in each season (Fig. C – 3). Predictive accuracy was also similar between full models and final models using a drop-one approach (Fig. C – 4, Table C.8).

3.3.9 Quantifying Migratory Connectivity Throughout Migration Periods

I used the estMC function in the 'MigConnectivity' package in R (Hostetler and Hallworth 2020) to estimate overall migratory connectivity of distinct breeding populations at three biologically relevant stages of the annual cycle: (1) prior to navigating the Gulf of Mexico during autumn migration, (2) during the nonbreeding period, and (3) prior to navigating the Gulf of Mexico during spring migration (Fig. 3 – 1). I estimated the strength of migratory connectivity by calculating two commonly used metrics: the Mantel correlation coefficient (r_M; Ambrosini et al. 2009) and the migratory connectivity metric (MC; Cohen et al. 2018). When sampling sites are broadly distributed (Vickers et al. 2021), both metrics are useful for quantifying the strength of migratory connectivity among populations by comparing the distances between individuals during different periods (Cohen et al. 2018). However, MC provides an estimate of migratory connectivity while accounting for incomplete sampling and inherent error in geolocator-derived location estimates (Cohen et al. 2018). I estimated r_M and MC among breeding populations (*n* = 2 golden-winged warbler breeding populations, *n* = 3 blue-winged warbler populations; Appendix C Supplementary Methods) at four autumn and spring departure sectors signifying general route type at the Gulf of Mexico (i.e., circumvent, western, central, and eastern), and two potential nonbreeding regions (i.e., Central America, South America). I excluded *Vermivora* warblers with hybrid plumage phenotypes (*n* = 5) from estimates of migratory connectivity of both parent species. For estimates of MC, I accounted for inherent uncertainty in geolocator-derived location estimates by including the measured error from ovenbirds (*Seiurus aurocapilla*) included in the 'MigConnectivity' package (Hostetler and Hallworth 2020). I also incorporated BCR-level estimates of *Vermivora* warbler abundance (Partners in Flight 2020) to account for unbalanced sampling effort relative to population abundance (Cohen et al. 2018). Mean r_M and MC estimates for each period were based on 1,000 resamples.

Estimates of r_M and MC near zero indicate that there is no relationship between breeding proximity and proximity during other portions of the annual cycle (i.e., weak migratory connectivity and extensive mixing of populations; Ambrosini et al. 2009, Cohen et al. 2018). Positive values of r_M and MC indicate that individuals from proximate breeding locations also occur near one another in subsequent periods of the annual cycle (i.e., strong migratory connectivity) and negative values indicate that individuals that occur closely together in one portion of the annual cycle occur farther apart from one another during subsequent periods (Ambrosini et al. 2009, Cohen et al. 2018). I visualized the general movements of populations throughout the annual cycle using the ‘ggforce’ package in R (Pedersen 2021) to create line plots. I created cumulative sum plots to visualize temporal variation in Gulf-crossing behavior among populations and calculated the ordinal date at which 50% of the population had crossed the Gulf of Mexico (50% passage date). I created simple linear models to test for associations between populations’ 50% passage date and average breeding latitude, and nonbreeding latitude and longitude to test for temporal connectivity.

3.4 Results

I identified 144 FLP anomalies during autumn migration (n = 94 geolocators, n = 89 individual *Vermivora* warblers) and 154 during spring migration (n = 87 geolocators, n = 85 individuals; Table C.3). One individual (1%) did not exhibit FLP anomalies during autumn migration, three individuals (3%) did not exhibit FLP anomalies during spring migration, and one individual (1%) did not exhibit FLP anomalies in either autumn or spring migration periods (Table C.3). Most individuals (n_{autumn} = 57 [61%]; n_{spring} = 52 [60%]) exhibited one FLP anomaly per migration season. Of individuals that exhibited multiple FLP anomalies in either autumn (n = 32 [34%]) or spring (n = 33 [38%]) migration periods, the average was 2.7 (0.3 SE) and 2.4 (0.4 SE) FLP anomalies for autumn and spring, respectively. Furthermore, 17 of those individuals exhibited consecutive FLP anomalies (i.e., two successive days of virtually no shading recorded) with the vast majority occurring during autumn (n = 15 [88%]) vs. spring (n = 2 [12%]). Compared to randomly selected days during both autumn (n = 50) and spring (n = 50) periods, FLP anomalies had lower absolute residual scores indicating less shading (log-scale; two-way ANOVA, $F_{2,1153}$ = 163.9, P <0.0001; Fig. C – 5) during dawn (P = 0.008, Tukey HSD) and daytime periods (P < 0.0001, Tukey HSD) but not during dusk (P =

0.34, Tukey HSD). Similarly, the duration of dawn and dusk periods was shorter during FLP anomalies compared to randomly selected days (log-scale; two-way ANOVA, $F_{2,1153} = 28.7$, $P < 0.0001$; $P < 0.0001$ for both comparisons, Tukey HSD).

The FLP anomalies indicated that the majority of *Vermivora* warblers used over-water flights to navigate the Gulf of Mexico during autumn (80%; 75/94) and spring (74%; 63/88) migration periods (Table C.3). However, 20% of individuals (19/94; $n = 8$ blue-winged warblers; $n = 9$ golden-winged warblers; $n = 2$ hybrids) circumvented the Gulf of Mexico during autumn migration and 26% (23/87; $n = 3$ blue-winged warblers; $n = 18$ golden-winged warblers; $n = 2$ hybrids) during spring migration based on the lack of an FLP anomaly or on the timing and location of individuals during observed FLP anomalies. Considering individuals with data for both autumn and spring migration, 12% (10/86; $n = 3$ blue-winged warblers, $n = 6$ golden-winged warblers, $n = 1$ hybrid) circumvented the Gulf of Mexico during both migration periods.

At the Gulf of Mexico, the frequency at which *Vermivora* warblers used different takeoff sectors varied between autumn and spring migration periods (Pearson's χ^2-test, $\chi^2 = 31.0$, df = 3, $P < 0.001$). This seasonal variation was driven by a greater frequency of *Vermivora* warblers using the eastern take-off sector during autumn (two-sample proportion test, $\chi^2 = 28.9$, df = 1, $P < 0.001$) compared to the spring migration period when more individuals initiated trans-Gulf flights from the central sector (two-sample proportion test, $\chi^2 = 10.5$, df = 1, $P = 0.001$). The frequency at which individuals initiated trans-Gulf flights from the western sector or circumvented the Gulf of Mexico did not differ between seasons (two-sample proportion test, $P > 0.05$ for both comparisons).

3.4.1 Effects of Weather Conditions on Departure Events

Weather conditions were associated with departure of *Vermivora* warblers during both autumn and spring migrations. The parameters included in final models differed slightly depending on which pre-departure interval (i.e., 7-day, 4-day, and 2-day intervals) I used. However, the direction and magnitude of the effect size (transformed from logit to log-odds ratio) remained consistent across models with different pre-departure intervals (Fig. 3 – 3) and final models adequately characterized departure events (all AUC values 0.65-0.80; Fig. C – 4).

Covariates included in final models differed between autumn and spring migration periods (Fig. 3 – 3). Compared to the previous day's weather conditions (i.e., 2-day model), the initiation of trans-Gulf flights was positively associated with wind profit at the surface and surface temperature and negatively associated with relative humidity at the surface and 24-hr change in barometric pressure (Fig. 3 – 3, Fig. 3 – 4). During spring migration, the initiation of trans-Gulf flight was positively associated with relative humidity at 850 hPa and negatively associated with relative humidity at the surface and barometric pressure compared to weather conditions the previous day (2-day model; Fig. 3 – 3, Fig. 3 – 4). Extrapolating from top-models (2-day) for both autumn and spring, I found that the proportion of days during autumn and spring migration periods with a predicted probability of initiating trans-Gulf flight ≥ 0.50 ("favorable days") varied annually (Fig. 3 – 5), but the average proportion of favorable days was 81% higher during autumn than spring ($\bar{x}_{\text{autumn}} = 0.29$, $\bar{x}_{\text{spring}} = 0.16$; two-sample *t*-test, $t_{1,22} = -2.1$, $P = 0.05$; Fig. 3 – 5). Moreover, the average proportion of days with favorable conditions varied among sectors and within seasons with conditions generally being more favorable in the central and eastern sectors during autumn (one-way ANOVA, $F_{2,9} = 5.3$, $P = 0.03$)

whereas the central sector had more favorable conditions during spring (one-way ANOVA, $F_{2,9} = 60.9$, $P < 0.001$).

3.4.2 Quantifying Migratory Connectivity Throughout Migration Periods

Migratory connectivity between golden-winged warbler breeding and nonbreeding regions was strong (MC = 0.84 [0.14 SE]; $r_M = 0.76$ [0.06 SE]). However, migratory connectivity was very weak prior to navigating the Gulf of Mexico during both autumn (MC = 0.05 [0.06 SE]; $r_M = 0.04$ [0.05 SE]) and spring (MC = 0.05 [0.04 SE]; $r_M = 0.06$ [0.05 SE]) migrations (Fig. 3 – 6). Overall migratory connectivity between blue-winged warbler breeding and nonbreeding regions was weak (MC = -0.10 [0.01 SE]; $r_M = 0.30$ [0.10 SE]) and remained weak during both autumn (MC = 0.12 [0.13 SE]; $r_M = 0.15$ [0.11 SE]) and spring migrations (MC = 0.09 [0.13 SE]; $r_M = 0.17$ [0.11 SE]; Fig. 3 – 6).

Vermivora warbler populations exhibited temporal variation in the date at which 50% of individuals had crossed the Gulf of Mexico (Fig. 3 – 7). During autumn, the 50% passage date was associated with average breeding latitude but not with average nonbreeding latitude or longitude (Fig. C – 6). Thus, the 50% passage date for golden-winged warblers from Appalachian Mountain BCR breeding sites was 33 days earlier than for golden-winged warblers from breeding sites in the Boreal Hardwood Transition BCR and 7–26 days earlier than blue-winged warbler populations (Fig. 3 – 7). During spring migration, the difference between the earliest and latest 50% passage date for *Vermivora* warbler populations was smaller (18 days vs. 33 days in autumn) and the timing of the 50% passage date was not associated with any population-specific spatial characteristics (i.e., average breeding latitude, average nonbreeding latitude, average nonbreeding longitude; Figs. 3 – 7, C – 3).

I found no evidence of differences in predicted favorability of conditions among populations of *Vermivora* warblers during autumn migration (one-way ANOVA; $F_{4,70} = 0.3$, $P = 0.62$), or overall (i.e., when considering both autumn and spring migration together; one-way ANOVA; $F_{4,134} = 1.2$; $P = 0.32$; Fig. C – 7). However, Golden-winged warblers from breeding populations in the Appalachian Mountains BCR experienced less favorable conditions ($\bar{x} = -0.13$; 95% CI = -0.26–0.01; $P = 0.05$) than individuals from breeding populations in the Boreal Hardwood Transition BCR during spring migration (one-way ANOVA; $F_{4,59} = 2.9$, $P = 0.03$)

3.5 Discussion

Most *Vermivora* warblers (88%) in my sample exhibited FLP anomalies that coincided with long-distance flights across the Gulf of Mexico during either autumn or spring. Thus, directly crossing the Gulf of Mexico is likely the most common migration strategy in this species complex. Moreover, a subset of individuals exhibited consecutive FLP anomalies, primarily during autumn migration, indicating the potential for *Vermivora* warblers to be undertaking prolonged, multi-day flights (Adamík et al. 2016). One possibility is that consecutive FLP anomalies during autumn migration indicate that individual warblers undertake longer, continuous migratory flights (i.e., ≥36 hr) potentially associated with crossing the Gulf of Mexico and Caribbean Sea to reach either Central America (~1,600 km south of the eastern departure sector) or even northern South America (~2,200 km south of the eastern departure sector) in a single, non-stop flight. These types of flights have been reported in larger migratory bird species using the

Gulf of Mexico region during migration (i.e., Gómez et al. 2017), and are similar to trans-Atlantic migratory flights described in other warbler species traveling from the eastern US to the Caribbean or northern South America during autumn (DeLuca et al. 2015, McKinnon et al. 2017). Interestingly, all *Vermivora* warblers that exhibited consecutive FLP anomalies were golden-winged warblers and most departed from the eastern sector during autumn migration. Notably, 42% (5/12) of individual golden-winged warblers from Appalachian Mountain BCR breeding sites exhibited consecutive FLP anomalies, including one individual that was tracked for two years, suggesting this strategy may be especially common for this population of golden-winged warblers migrating between eastern North America and northern South America (Kramer et al. 2018a). Conversely, 23% (11/47) of golden-winged warblers from Boreal Hardwood Transition BCR breeding sites exhibited consecutive FLP anomalies suggesting this strategy is less common for individuals migrating between central North America and Central America.

At the Gulf of Mexico, I found strong evidence that at the Gulf of Mexico, surface-level weather conditions, but not those aloft, influenced the barrier-crossing behavior of *Vermivora* warblers during both autumn and spring migration periods. During autumn migration, *Vermivora* warblers exhibited similar relationships with weather conditions (i.e., wind profit, relative humidity, and barometric pressure) as three larger species that cross the Gulf of Mexico: red-eyed vireos (*Vireo olivaceous*; 17 g) Swainson's thrush (*Catharus ustulatus*; 33 g), and wood thrush (*Hylocichla mustelina*; 46 g) tracked with automated telemetry (Deppe et al. 2015). That similar exogenous cues are associated with trans-Gulf departure of three distantly related species with different morphologies and migratory ecologies suggests that the evolutionary pressures shaping barrier-crossing behavior may be consistent among Nearctic-Neotropical migratory passerines. Historical and contemporary reports documenting the highly episodic nature of migration in Nearctic-Neotropical birds wherein large numbers of diverse migrant species arrive together in distinct waves at migratory stopover sites along the Gulf of Mexico provide additional support for this hypothesis (Paynter 1953, Van Doren and Horton 2018). It was not possible to infer the endogenous, physiological conditions (i.e., fat stores and/or pectoral muscle volume) of individual *Vermivora* warblers prior to initiating flight crossing the Gulf of Mexico. Endogenous factors are known to interact with weather variables to influence barrier-crossing departure in other migratory birds (e.g., Goyman et al. 2010, Deppe et al. 2015) and likely influence migratory behavior in *Vermivora* warblers. Defining the relationships between endogenous factors, exogenous conditions (i.e., weather), and migratory behavior of *Vermivora* warblers could provide additional context for interpreting the drivers and constraints of barrier navigation in small songbirds and may be better addressed with different technologies (e.g., rapidly expanding networks of passive telemetry stations; Taylor et al. 2017).

Compared to autumn migration, less is known about how weather conditions influence barrier-crossing in Nearctic-Neotropical migrants during spring migration (Lavallée et al. 2021). Importantly, I found that weather variables associated with spring migration differed from those associated with autumn migration. In spring, departure across the Gulf of Mexico was negatively associated with surface-level relative humidity and barometric pressure and positively associated with relative humidity aloft (at 850 hPa, ~1,500 m) but not associated with wind profit. Similarly, purple martins (*Progne subis*) did not exhibit a preference for favorable wind conditions during spring migration

(Abdulle and Fraser 2018, Lavallée et al. 2021). This may be related to timing constraints that *Vermivora* warblers and other Nearctic-Neotropical migrants face during spring migration when individuals must balance arriving at breeding sites early enough to secure mating opportunities and establish territories, but late enough to ensure weather conditions and the availability of resources are suitable for survival and reproduction (Pulido and Widmer 2005, Kramer et al. 2017, Shipley et al. 2020). During autumn migration, individuals may be less likely to cross the Gulf of Mexico under neutral or unfavorable wind conditions because there may be less of a fitness penalty associated with waiting for conditions to become more favorable than in spring. Alternatively, variation in the use of favorable weather conditions between spring and autumn could be associated with where the Gulf (or any other barrier) fits into the overall migration journey; waiting for favorable weather conditions may be more beneficial when the Gulf crossing occurs after traveling greater distances than when the crossing occurs earlier in the migratory route. Moreover, the proportion of days during the migration period with a predicted probability of initiating trans-Gulf flights > 0.50 was greater during autumn than during spring. Therefore, individuals experiencing unfavorable conditions at the Gulf of Mexico during autumn migration likely wait shorter periods before conditions become more favorable compared to spring migration.

The strength of migratory connectivity of *Vermivora* warblers was weak prior to crossing the Gulf of Mexico during both autumn and spring migration periods. Migratory connectivity of blue-winged warblers remained weak throughout the annual cycle, including during both seasonal migration periods. Conversely, strong breeding-nonbreeding migratory connectivity exhibited by golden-winged warblers broke down during migration. The weak migratory connectivity of *Vermivora* warblers during migration was similar to findings in common nighthawks (*Chordeiles minor*) in which spatial connectivity among 13 breeding populations was relatively weak (i.e., $r_M < 0.30$) during migration periods, especially at latitudes around the Gulf of Mexico ($r_M \sim 0.1$; Knight et al. 2021). Notably, autumn migration (i.e., breeding to first autumn stopover site) was the period of the annual cycle during which tree swallows (*Tachycineta bicolor*) exhibited the strongest migratory connectivity ($r_M = 0.75$; Knight et al. 2018). Relatively weak spatial migratory connectivity during migration suggests that variation in population trends of *Vermivora* warblers (and especially golden-winged warblers) are unlikely to be linked to limiting factors experienced during migration near the Gulf of Mexico and more likely to be associated with nonbreeding factors (Kramer et al. 2017, 2018a).

Populations of *Vermivora* warblers exhibited evidence of temporal connectivity at the Gulf of Mexico during autumn migration (based on 50% passage dates), which was associated with breeding site longitude. Despite low rates of spatial migratory connectivity during autumn migration, golden-winged warblers from Appalachian Mountain BCR breeding sites tend to cross the Gulf of Mexico earlier compared to other populations, which could result in those individuals experiencing different conditions (Knight et al. 2021) that could impact survival and affect population dynamics. Notably, golden-winged warblers from Appalachian Mountain BCR breeding sites crossed the Gulf of Mexico on days associated with lower predicted favorability of conditions compared to golden-winged warblers from breeding sites in the Boreal Hardwood Transition BCR (Fig. C – 7). If less favorable conditions are associated with reduced survival during migration, conditions experienced during migration could be contributing to ongoing population declines in golden-winged warblers breeding in the Appalachian Mountains. Further research is warranted to identify factors influencing survival during trans-Gulf flights compared to survival at stopover sites and whether differences in migratory behavior (e.g., higher frequency of multi-day flights) or timing are associated with mortality rates.

The breakdown in spatial migratory connectivity in migrating *Vermivora* warblers (especially golden-winged warblers) may be linked to geographic variation in the availability of favorable conditions for crossing the Gulf of Mexico. The favorability of conditions varied spatially during both autumn and spring and the proportion of birds using different sectors to initiate trans-Gulf flights generally aligned with the relative favorability of the weather conditions. For example, most *Vermivora* warblers departed from the central sector during spring migration where conditions were relatively favorable compared to the western and eastern sectors. If synoptic weather conditions tend to be more favorable for migration in specific areas, migratory individuals that use those areas may have greater survival and potentially experience greater fitness as a result of both direct (i.e., increased survival; Hewson et al. 2016) and indirect effects (i.e., carry-over effects; Legagneux et al. 2012). If the directionality of migratory movements is an innate and heritable trait in *Vermivora* warblers as it appears to be in some other species (Berthold and Helbig 1992) and individuals that use areas with more favorable conditions experience greater relative fitness, then natural selection (via historically consistent weather conditions) may have shaped the observed patterns of space use in *Vermivora* warblers around the Gulf of Mexico during migration. Thus, general weather patterns during migration periods may explain the breakdown of otherwise strong migratory connectivity in golden-winged warblers and the maintenance of weak migratory connectivity in blue-winged warblers during autumn and spring migration. Notably, a single gene is associated with differences in nonbreeding locations in *Vermivora* warblers (Toews et al 2019). Therefore, it is likely that other aspects of migratory behavior also may be under genetic control in *Vermivora* warblers and may underlie patterns in migratory distribution of individuals from this species complex. Which genes are associated with different migratory behaviors and whether those same genes are also associated with the apparently convergent strategies of other Nearctic-Neotropical migrants and/or other taxa remains unknown (Harringmeyer et al. 2021).

An alternative explanation for the patterns in connectivity that I observed is that *Vermivora* warblers migrate through all sectors of the Gulf of Mexico region in equal numbers but that survival is lower in areas with less favorable conditions and therefore I primarily retrieved data from individuals that used routes that also conferred favorable conditions. This alternative hypothesis may be less likely, however, because individual golden-winged warblers are known to use different routes in different years, suggesting that individuals may exhibit flexibility in response to temporally variable conditions (Kramer et al. 2017). Furthermore, the data from *Vermivora* warblers in this study were collected over four years and longer-term monitoring could quantify the consistency of the associations among weather conditions, space-use, and barrier-crossing behavior in this species complex. Further efforts to understand the fitness consequences of different migration routes, timing, and speed might provide insight into the evolutionary development and maintenance of diverse migratory behaviors.

Identifying the exogenous factors that are associated with migration in small songbirds like *Vermivora* warblers may help in predicting how climate change will affect migratory animals (Crick 2004). In the case of *Vermivora* warblers, predicted increases in relative humidity, especially over large expanses of water, may result in fewer favorable migration days during spring migration (Coffel et al. 2017). Conversely, warming temperatures and stronger winds predicted to occur in the future may improve the frequency of favorable days for crossing the Gulf of Mexico during autumn migration (Zeng et al. 2019, Chen 2020). A reduction in the number of favorable days during a migration period may lead to individuals stopping over for longer durations or needing to accumulate more energy reserves prior to barrier-crossing, which could lead to increased mortality during migration and/or carry-over effects in other portions of the annual cycle (Legagneux et al. 2012). Moreover, hurricanes are predicted to continue to become more frequent and more intense in the Gulf of Mexico and eastern Atlantic Ocean regions (Mann and Emanuel 2006), which could pose a substantial risk to migratory birds (e.g., Dionne et al. 2008). Hurricanes can cause mortality in migratory birds when they intercept migrating individuals over the Gulf of Mexico or Atlantic Ocean (Dionne et al. 2008). Hurricanes can also affect migratory birds indirectly by destroying or degrading coastal stopover habitat and reducing food availability (Dobbs et a. 2009, but see Lain et al. 2017). Thus, monitoring the extent to which migratory species' population dynamics are affected by increased frequency of severe weather is likely to be important for disentangling drivers of population trends, especially for species or populations that occur largely within hurricane-prone areas during migration (e.g., Cooper et al. 2017), or engage in prolonged, multi-day, barrier-crossing flights (e.g., blackpoll warblers

[*Setophaga striata*; DeLuca et al. 2015], Connecticut warblers [*Oporornis agilis*; McKinnon et al. 2017], golden-winged warblers from breeding sites in the Appalachian Mountains BCR [this chapter]).

Exactly how changing weather conditions interact to affect the barrier-crossing behavior of migrating animals and the effects of more frequent extreme weather conditions (e.g., storms) remains unknown (Newton 2007). Continued monitoring to document shifting relationships between weather conditions and migratory conditions may illuminate the flexibility of these behaviors and/or the adaptive potential of species and how a changing climate may shape the future migratory connectivity and distribution of species during migration. Similarly, wing morphology of some long-distance migrant birds appears to be changing in response to climate change (Weeks et al. 2020). Understanding how climate conditions experienced during migration shape the morphology of migratory birds could provide context for predicting shifts in the evolutionary trajectories of migratory species under future climate scenarios.

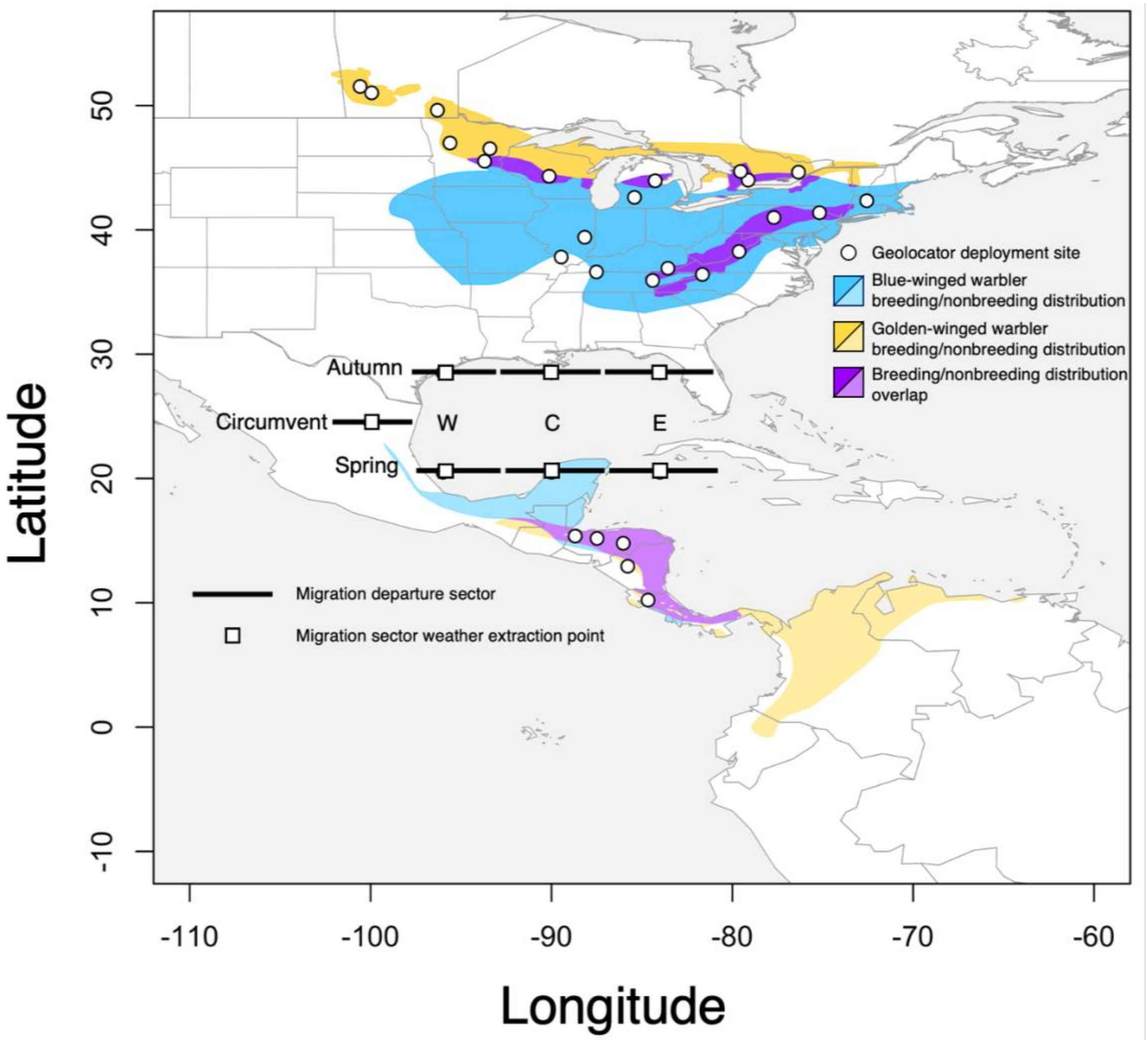

Figure 3 – 1: Map of breeding and nonbreeding distributions of blue-winged and golden-winged warblers. Sites where geolocators were recovered are indicated by white circles. Migration departure sectors (W = west, C = central, and E = east) and the points (white squares) from which weather data were extracted are depicted.

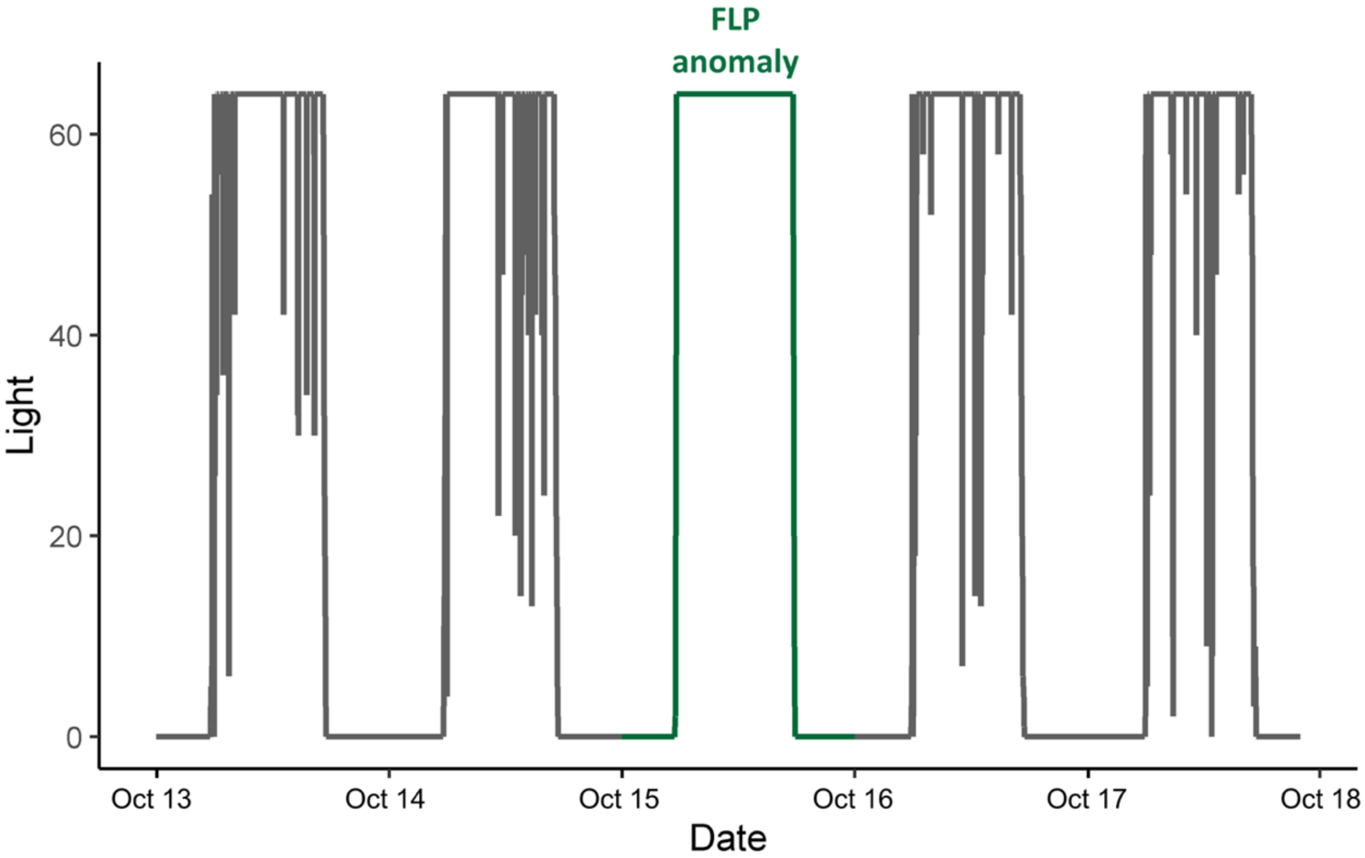

Figure 3 – 2: Example of full light pattern (FLP) anomaly (green) in geolocator-derived light data. Light curves show the maximum level of ambient light recorded by the geolocator every two minutes. Light levels were recorded on a scale from 0-64 in arbitrary units. This light curve is from a male golden-winged warbler (SLG18; Table C.2, C.3) during autumn migration in 2015. Shading in the geolocator-derived light data indicate this individual initiated a trans-Gulf of Mexico flight on the evening of 14 October 2015 and experienced virtually no shading during 15 October 2015 (FLP anomaly).

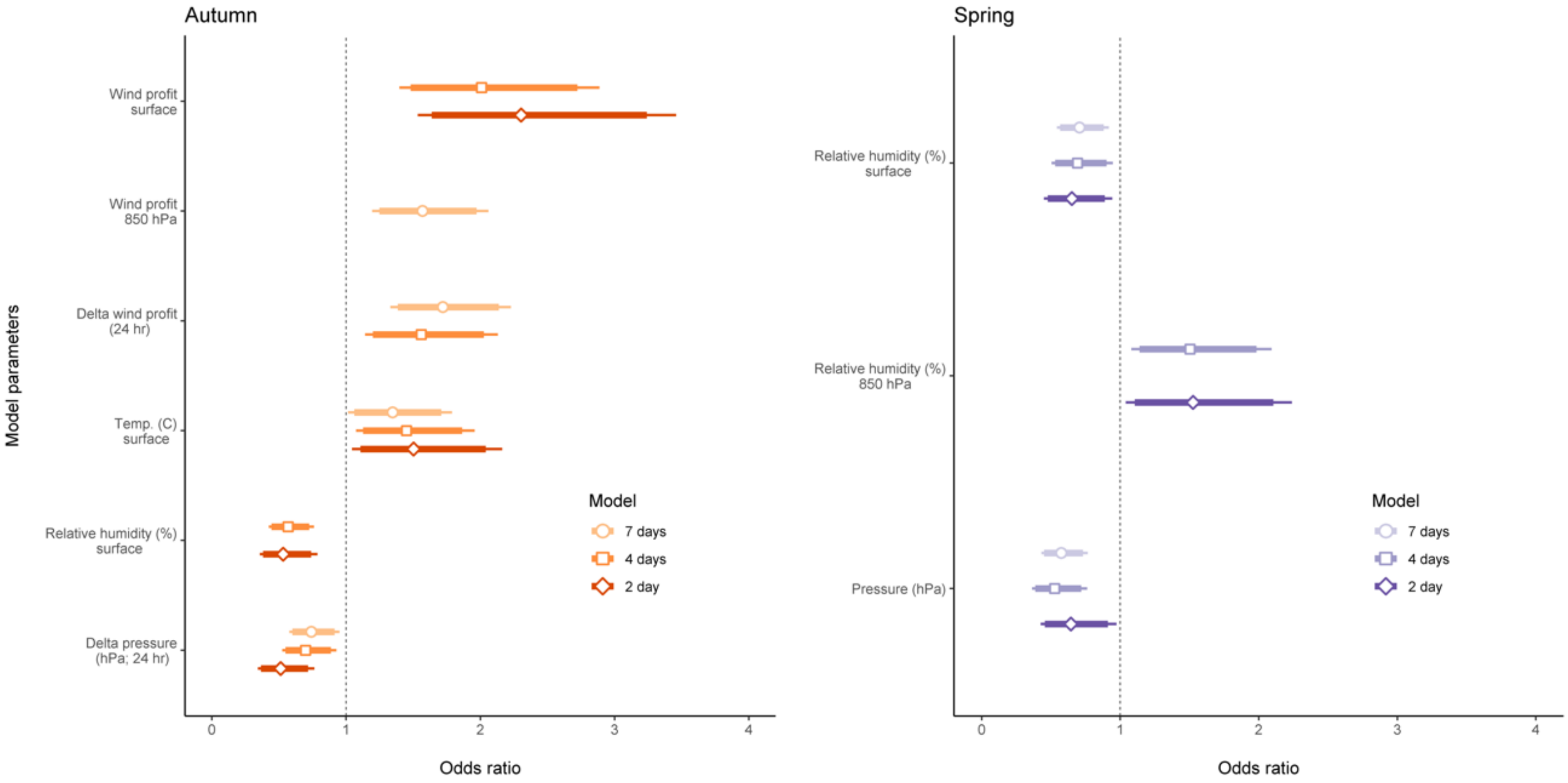

Figure 3 – 3: Coefficient plot for top multiple logistic regression models exploring the effects of weather conditions on the initiation of trans-Gulf of Mexico flights in *Vermivora* warblers. Top models selected using a drop-one modeling approach and final models included all terms that, if dropped, would reduce model performance (based on AIC_c). I considered models exploring the relationship between weather conditions on departure day and during the previous day (two-day model), departure day and the previous three days (four-day model), and departure day and the previous six days (seven-day model). In both panels, an odds ratio of 1 equates to equal odds and odds ratios > 1 or < 1 equate to increased or decreased odds of initiating trans-Gulf flights, respectively.

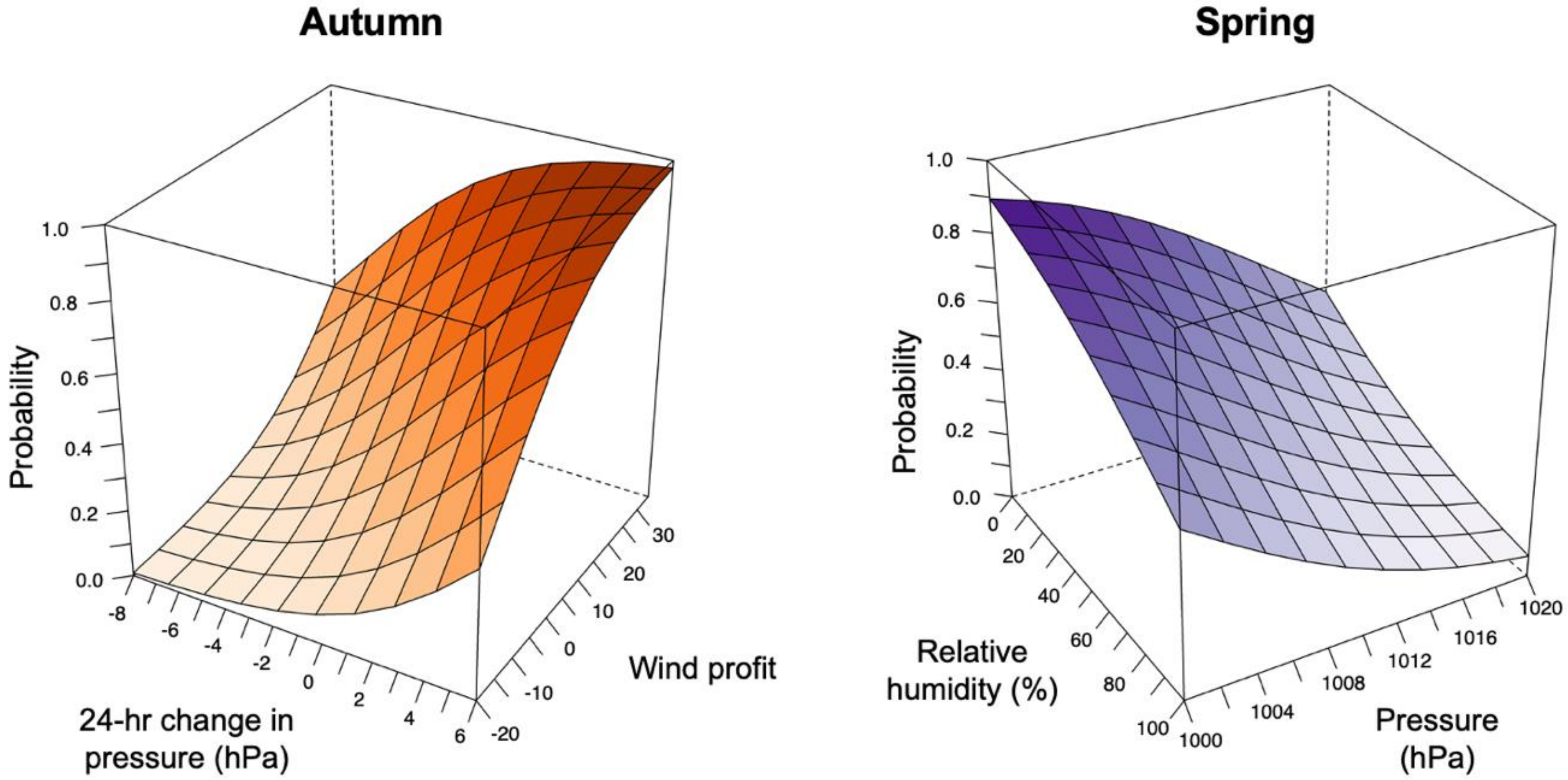

Figure 3 – 4: Predicted probability of *Vermivora* warblers initiating trans-Gulf flights as a function of 24-hr change in barometric pressure and wind profit during autumn (left) and surface-level relative humidity and barometric pressure during spring migration (right). Predicted probabilities were generated using the top two-day model (i.e., including departure day and previous day; see text for details) and holding all other variables at their estimated average values. Darker hues indicate higher probabilities.

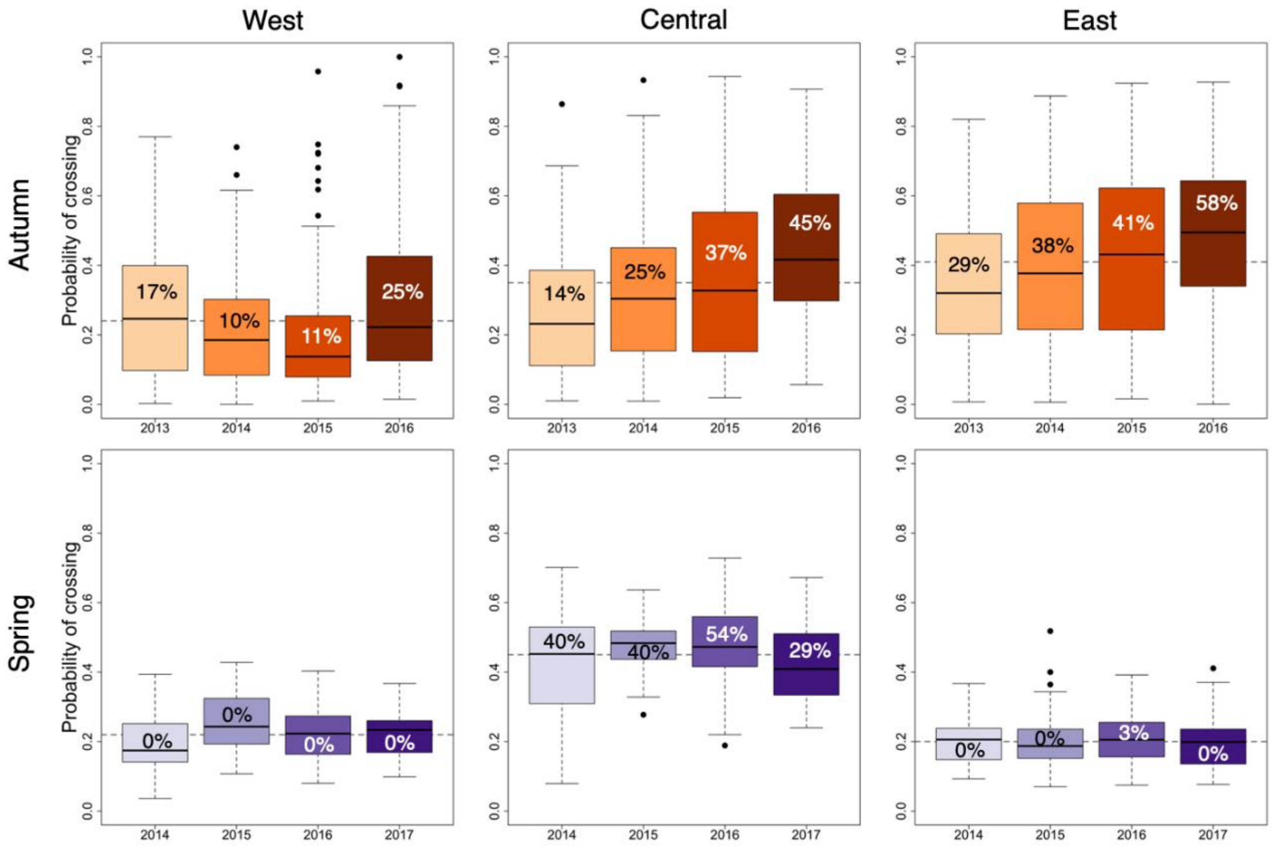

Figure 3 – 5: Boxplots summarizing the predicted probability of *Vermivora* warblers crossing the Gulf of Mexico by year, sector (west, central, and east), and season (autumn, top row; spring, bottom row). Probabilities estimated using the top-performing two-day model (i.e., departure day and previous day) and represent the favorability of weather conditions. Gray horizontal line indicates mean probability of each sector across all years. Values within boxes specify the percent of days with favorable conditions (i.e., probability of initiating trans-Gulf flight ≥ 0.50). Total duration of autumn and spring migration periods differed (n_{autumn} = 92 days, n_{spring} = 30 days).

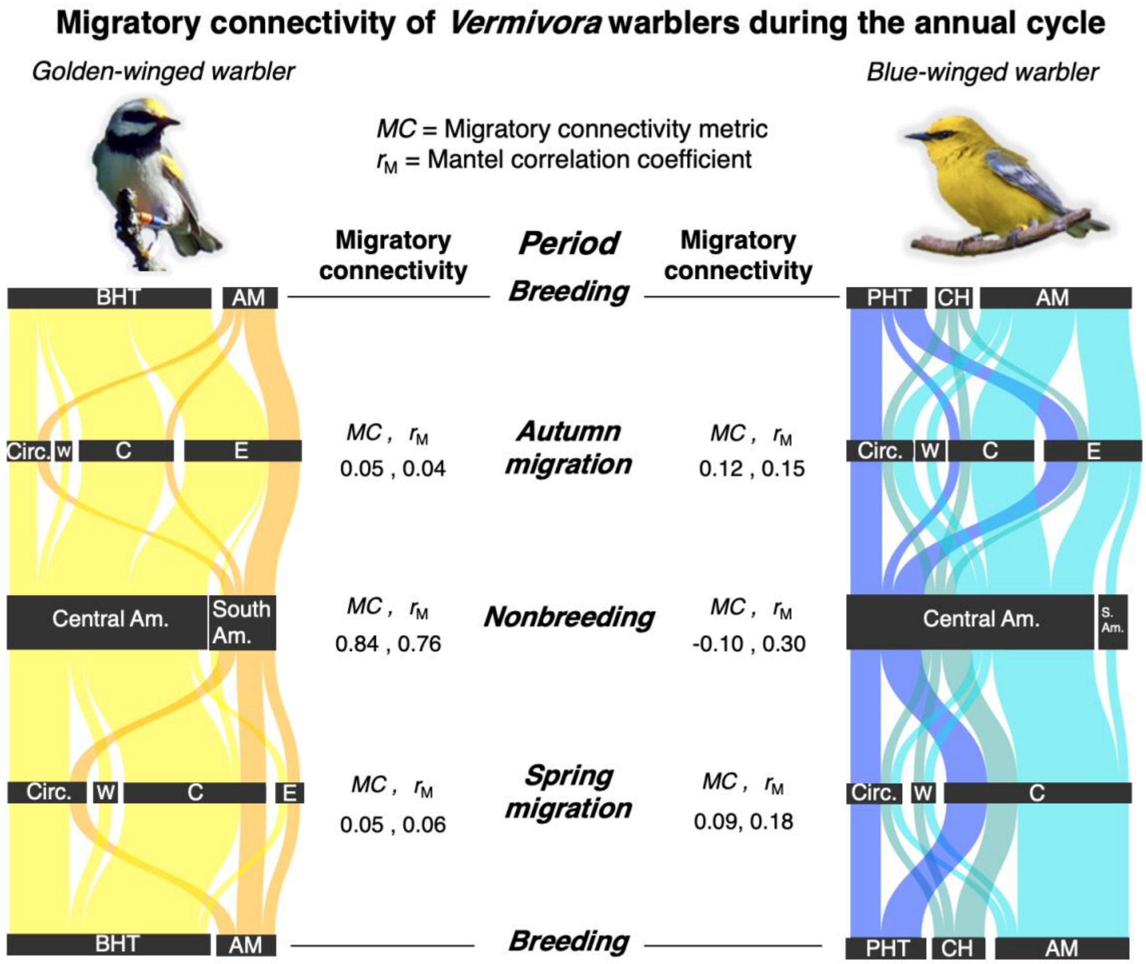

Figure 3 – 6: Seasonal distribution of blue-winged warblers and golden-winged warblers and sites where individuals were tracked with geolocators. Line plots show the proportion of individuals from distinct breeding populations using different autumn departure sectors, nonbreeding regions, and spring departure sectors. Migratory connectivity of breeding populations estimated with the MC metric, and Mantel correlation coefficient (r_M) are shown for each portion of the annual cycle. Populations were delimited based on Bird Conservation Region (BCR): Boreal Hardwood Transition BCR (BHT), Appalachian Mountain BCR (AM), Prairie Hardwood Transition BCR (PHT), and Central Hardwood BCR (CH). Migration sectors were classified as based on the departure longitude (west [W], central [C], or east [E]). Nonbreeding regions were classified as either occurring in Central America or South America.

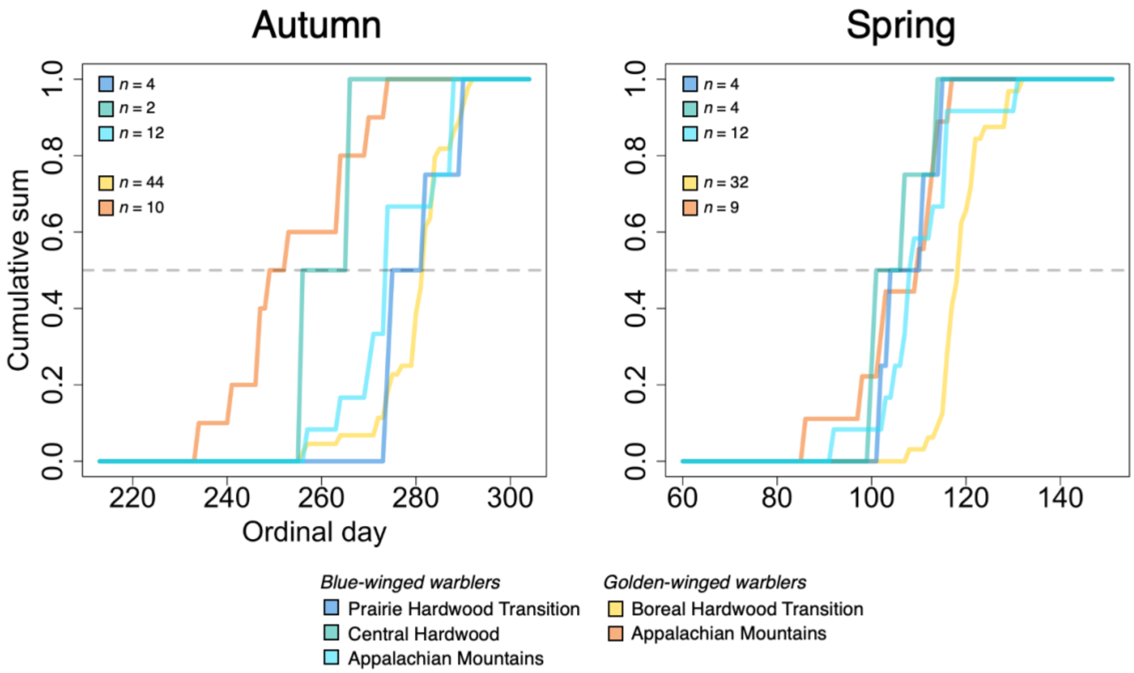

Figure 3 – 7: Cumulative sum plots illustrating the proportion of individuals that crossed the Gulf of Mexico by ordinal day and population. Colors indicate populations based on Bird Conservation Regions. The threshold at which 50% of individuals have crossed the Gulf of Mexico (50% passage rate) is indicated by the dashed gray line.

Chapter 4

The Evolution and Evolutionary Constraints of Strong Migratory Connectivity in the Anthropocene

4.1 Abstract

Migration is an adaptive behavior that involves the regular movements of individuals between distinct regions during different periods of the annual cycle. Migratory connectivity is the level of dispersion among distinct breeding populations during different portions of the annual cycle. Species with weak migratory connectivity are comprised of breeding populations that disperse broadly whereas species with strong migratory connectivity are comprised of populations with individuals that tend to co-occur throughout the annual cycle. The strength of migratory connectivity is important for understanding a species' ecology and population dynamics, and for developing effective conservation strategies. Ongoing efforts to document the strength of migratory connectivity of birds suggests that weak migratory connectivity is more common than strong migratory connectivity. However, the evolutionary processes and conditions under which strong migratory connectivity might evolve remain poorly understood. I used computer simulations to model the evolved strength of migratory connectivity under biologically plausible scenarios that I hypothesized could facilitate the evolution of strong migratory connectivity. Populations evolved strong migratory connectivity when

selection favored individuals that migrated between distinct breeding and nonbreeding sub-regions relative to individuals that migrated between other sub-regions. The evolved strength of migratory connectivity was weaker in scenarios where fitness penalties were imposed less frequently (i.e., not imposed every generation). Strong migratory connectivity evolved rapidly and remained strong in scenarios in which fitness penalties were imposed for fifty generations and then relaxed for fifty generations suggesting that strong migratory connectivity may constitute an evolutionary trap if previously adaptive relationships become disentangled from historical fitness outcomes. This type of evolutionary trap may become more prevalent and problematic for migratory species with strong migratory connectivity given the scale, speed, and intensity of ongoing anthropogenic change. Efforts to describe the evolutionary processes that shape the distribution of migratory animals will provide a more comprehensive understanding of the implications of diverse migratory strategies in the future.

4.2 Introduction

Migration is a relatively common strategy that has evolved many times across taxa. Populations of a migratory species exhibit varying levels of dispersion during different stages of their annual cycles (Webster et al. 2002). The dispersion of populations across space and time has important implications for understanding a species' ecology (Sherry and Holmes 1996), the evolutionary origins of these patterns (Winger et al. 2014), and for the development of meaningful conservation strategies (Reynolds et al. 2017). Similarly, understanding whether distinct populations remain spatially segregated from other populations during different portions of the annual cycle can have important consequences for identifying factors limiting population growth (Chapter 1; Kramer et al.

2018). Ultimately, the dispersion and behavior of migratory species throughout the annual cycle may represent a previously adaptive strategy associated with the availability of critically important resources often separated by large distances and/or the favorability of abiotic factors that shape animal movements (Alerstam and Enckell 1979, Cox 1985, Norevik et al. 2020).

Migratory connectivity is a term frequently used to describe the strength of linkages among populations throughout the annual cycle (Webster et al. 2002). Species exhibiting strong migratory connectivity consist of populations that tend to co-occur throughout different periods of the annual cycle whereas species with weak connectivity consist of populations that mix during different periods of the annual cycle (Webster et al. 2002). Often, migratory connectivity is described as a fixed trait that is inherent to a species (e.g., Webster et al. 2002, Kramer et al. 2018), whereas others view it as an emergent and dynamic property of a species that is constantly being shaped by natural selection (Winger et al. 2019).

The proliferation of miniaturized tracking devices has fueled efforts to describe and quantify the migratory connectivity of migratory bird species to better understand their ecology and improve conservation outcomes (e.g., McKinnon and Love 2018). These efforts have been validated through the documentation of diverse migration strategies including the discovery of previously unknown migration routes and nonbreeding regions for at-risk species (McKinnon et al. 2017), the identification of population bottlenecks (Hewson et al. 2016), and the development of more robust conservation strategies (Tonra et al. 2019). As data from tracking studies continue to accumulate, it has been proposed that weak migratory connectivity is common in migratory birds and strong migratory connectivity is quite rare (Finch et al. 2017). However, it remains unclear why such a pattern exists and under which conditions strong migratory connectivity may originate and be maintained.

Increasing evidence from genomic research supports the notion that migration is genetically controlled in birds and other taxa (e.g., Berthold 1991, Toews et al. 2019, Thompson et al. 2020). The theoretical framework within which strong migratory connectivity may be expected to evolve in species for which migration is genetically based has been proposed and discussed previously (Webster et al. 2002, Finch et al. 2017, Sherry 2018). Theory predicts that strong migratory connectivity might evolve under a variety of scenarios wherein fitness (i.e., reproduction and/or survival) is relatively greater among individuals migrating between distinct breeding and nonbreeding sub-regions within a species' broader distribution relative to other individuals that migrate between other sub-regions. This type of scenario could arise under several biologically plausible scenarios wherein a species has multiple breeding regions and multiple nonbreeding regions and individuals experience differences in fitness based on the pairing of breeding and nonbreeding regions that an individual inhabits (e.g., Fig. 4 – 1). Strong migratory connectivity could be expected to evolve if individuals with adaptations to local breeding conditions also experience relatively greater fitness if they occur in a nonbreeding region with similar conditions (i.e., niche tracking; Tingley et al. 2009, Bay et al. 2021) compared to individuals that occurred in a nonbreeding region with conditions that differed from those experienced during the breeding period.

Selective pressure leading to the evolution of strong migratory connectivity could arise through fitness consequences associated with reproduction, survival, or both reproduction and survival. For example, an individual that is locally adapted to the climatic conditions of its breeding region may be more likely to survive the nonbreeding period if it winters in a region with a climate that is similar to that experienced during the breeding period compared to an individual that breeds and winters in areas with substantially different climates (Zurell et al. 2018). Alternatively, strong migratory connectivity might be expected to evolve if individuals that breed and winter in specific regions produce more juveniles than individuals occurring in other regions. For example, an individual might have relatively greater fecundity if the pairing of breeding and nonbreeding regions is associated with less arduous or dangerous migration allowing the individual to invest more energy in reproduction (i.e., carry-over effects; Harrison et al. 2011) or if the specific pairing of the individual's breeding and nonbreeding regions confers relatively higher fecundity via timing reproduction to match the phenological availability of resources (Renfrew et al. 2013). It is unclear whether the evolved strength of migratory connectivity and the rate at which it evolves differs among scenarios in which natural selection imposes fitness consequences on reproduction, survival, or both reproduction and survival. Identifying the conditions under which strong migratory connectivity may evolve from weak connectivity, the rate at which a species can evolve strong migratory connectivity, the stability of strong migratory connectivity over time, and whether strong migratory connectivity may impose evolutionary constraints on migratory species in the Anthropocene is an important frontier in migration research.

Here, I used computer simulations to compare the strength of migratory connectivity that evolved under biologically plausible scenarios involving a species distributed across two distinct breeding regions and two distinct nonbreeding regions. In these scenarios, I imposed fitness penalties that simulated selection for individuals that occurred in specific pairings of breeding and nonbreeding regions (Fig. 4 – 1) and/or selection against individuals that occurred in those specific pairings of breeding and nonbreeding regions but in an area near the boundary between breeding and/or nonbreeding regions (i.e., along the periphery of the population's potential breeding and/or nonbreeding distribution). I tested whether fitness penalties imposed on different components of fitness (i.e., reproduction and/or survival) and at different frequencies (i.e., constant, every other generation, every fourth generation, every tenth generation, or every generation for fifty generations followed by fifty generations of no selection) affected the strength or timing of evolved migratory connectivity. I hypothesized that strong migratory connectivity could evolve under a variety of scenarios in which fitness penalties were imposed on either reproduction or survival but would evolve fastest and be strongest when selection acted on both reproduction and survival. I also expected that strong migratory connectivity would evolve fastest under constant selection and that increasingly infrequent selection would result in populations exhibiting weaker migratory connectivity.

4.3 Methods

4.3.1 General Methods and Model Background

I used a density-dependent population model to explore how the evolved strength of migratory connectivity varied under different scenarios. Each simulation began with a randomly generated starting population (N_0) of 2,000 individuals that were randomly assigned breeding and nonbreeding genotype scores between -1–1. Genotype scores represent an unspecified combination of alleles at causal genes that determine an individual's breeding and nonbreeding location along a two-dimensional axis (Fig. D – 1) and are heritable. I assigned individuals a breeding and nonbreeding phenotype based on their genotype scores (breeding genotype score < 0 = breeding region A, breeding genotype score > 0 = breeding region B; nonbreeding genotype score < 0 = nonbreeding region A, nonbreeding genotype score > 0 = nonbreeding region B; Fig. 4 – 1, D – 1). I considered individuals with the same breeding phenotype to be part of the same breeding population that reproduced in isolation from the other breeding population. Reproduction was a discrete event (i.e., a pulse) and was constrained by the abundance of individuals within a breeding population (i.e., negative density-dependence; Rodenhouse et al. 2003) to simulate a natural system with limited space and resources. I imposed mortality events that occurred during four periods of the annual cycle: individuals experienced mortality on the breeding grounds but prior to reproducing, during autumn and spring migrations, and during the nonbreeding period. The individuals remaining after reproduction and the four potential mortality events represented the next pre-breeding generation ($N_{B,t+1}$; Fig. 4 – 2). To estimate the strength of migratory connectivity at the end of each generation (i.e., after reproduction and four potential mortality events), I calculated the Mantel correlation coefficient (r_M) using individuals' breeding and nonbreeding genotype scores as proxies for geographic location with the 'mantel.test' function in the 'cultevo' package (Stadler 2018) in R (R Core Team 2020). Mantel correlation involves the comparison of two distance matrices containing the pairwise distances between individuals during periods of interest (Ambrosini et al. 2009). If individuals that are closer together during one period remain close together in a subsequent period (i.e., strong migratory connectivity), r_M will be strongly positive (i.e., ~1). If there is no relationship between the distribution of individuals during distinct seasons (weak migratory connectivity), then r_M will be ~0 (Ambrosini et al. 2009). I simulated how the strength of migratory connectivity evolved over 100 generations under 25 different scenarios and ran 1,000 replications for each scenario.

4.3.2 Starting Population

I randomly generated a starting population of 2,000 females for each simulation. Sex-ratios and sex-linked traits related to migration may influence the strength of migratory connectivity that evolves in some species (Mayr 1939, Toews et al. 2019, Fischer 2020) and this population model can be adapted to include males, variation in mate-choice, sex-specific survival, and other more complex scenarios. However, addressing my primary questions for this analysis did not require the inclusion of those parameters.

Individuals in the starting population were assigned a breeding, autumn migration, nonbreeding, and spring migration genotype score. I randomly drew numbers between -1–1 to represent each genotype score representing a period of the annual cycle. An individual's genotype scores were not linked (i.e., the nonbreeding genotype score had no relationship to any other genotype score). I assigned individuals to a phenotype based on their genotype scores. For breeding and nonbreeding phenotypes, breeding and nonbreeding genotype scores < 0 represented individuals occurring in breeding and nonbreeding region A (breeding or nonbreeding phenotype "A") whereas genotype scores > 0 represented individuals occurring in breeding and nonbreeding region B (breeding or nonbreeding phenotype "B"; Fig. 4 – 1, D – 1). Individuals were similarly assigned to one of three migration phenotypes based on whether their autumn or spring migration genotype was < -0.33 (migration phenotype “C”), ≥ -0.33 and ≤ 0.33 (migration phenotype “D”), or > 0.33 (migration phenotype “E”). I did not impose fitness penalties during migration periods (based on migration phenotype or genotype scores) but included migration in my population model to account for random regional variation in survival during migration and to potentially address questions in the future related to how selective pressure experienced during migration shapes the strength of migratory connectivity of a species.

4.3.3 Population Model

I used an agent-based, density-dependent population model to simulate how the strength of migratory connectivity evolved under different scenarios. Each simulation started with a randomly generated population of 2,000 females (e.g., Fig. D – 1) exhibiting weak migratory connectivity (i.e., $r_{\mathrm{M}} \sim 0.00$; Fig. D – 1). The global population size of the subsequent generation ($\mathrm{N}_{\mathrm{B},t+1}$) can be generalized as the number of females in the population after one generation (1 year) wherein new individuals entered the population during a discrete breeding period. Regionally specific mortality occurred immediately prior to reproduction within distinct breeding regions ($n = 2$) and during autumn migration ($n = 3$ regions), nonbreeding ($n = 2$ regions), and spring migration ($n = 3$ regions) periods (Fig. 4 – 2). I chose survival rates that generally corresponded with typical rates reported in studies of songbirds during different periods (Powell et al. 1999, Sillett and Holmes 20002, Streby et al. 2013; Table 4.1). Songbird survival rates tend to be higher during stationary breeding and nonbreeding periods and lower during migration (Sillett and Holmes 2002). I simulated pre-reproductive breeding-season mortality for each breeding population wherein the number of individuals from a distinct breeding population i in generation t surviving to reproduce ($N_{R,i,t}$) was the product of the pre-breeding population size at time t ($N_{B,i,t}$) multiplied by the population-specific pre-breeding period survival rate ($\varphi_{B,i,t}$):

$$\text{Eq. 1: } N_{R,i,t} = N_{B,i,t} \times \varphi_{B,i,t}$$

Where $\varphi_{B,i,t}$ is a randomly generated, generation- and breeding population-specific survival rate estimated by drawing 100 samples from a binomial distribution with a probability of 0.98 (Sillett and Holmes 2002, Streby et al. 2013) and dividing by 100:

$$\varphi_{B,i,t} \sim B(100, 0.98)/100$$

The number of juvenile females produced per generation (t) in population i ($J_{i,t}$) was the product of the generation- and population-specific rate of reproduction ($R_{i,t}$) and the number of reproducing females ($N_{R,i,t}$) and multiplied by a term for negative density dependence where the number of juveniles produced decreased as the abundance of reproducing females ($N_{R,i,t}$) approached the population-specific carrying capacity (K_i):

$$\text{Eq. 2: } J_{i,t} = (R_{i,t} \times N_{R,i,t})\left(\frac{K_i - N_{R,i,t}}{K_i}\right)$$

I selected a population-specific rate of reproduction ($R_{i,t}$) that was variable but generally corresponded with relative population stability and was biologically plausible for relatively short-lived songbirds (Powell et al. 1999). The population-specific rate of reproduction was drawn from a truncated normal distribution with a mean of 1.25 (Powell et al. 1999) and a standard deviation of 0.30:

$$R_{i,t} \sim N(1.25, 0.30)$$

If the population of reproductive females ($N_{R,i,t}$) exceeded the carrying capacity (K_i) and the density dependent factor $\left(\frac{K_i - N_{R,i,t}}{K_i}\right)$ became negative, I set the number of juveniles produced ($J_{i,t}$) to zero. I assigned breeding, migration, and nonbreeding genotype scores (GS) to juveniles by independently (i.e., breeding, migration, and nonbreeding genotype scores were not linked) drawing random samples from a normal distribution with a mean and standard deviation of the genotype scores (i.e., breeding, autumn migration, nonbreeding, spring migration) of each breeding population (*i*) for each generation (*t*; i.e., $N_{R,i,t}$):

$$\text{Juvenile genotype score} \sim N(\bar{x}_{GS,i,t}, \sigma_{GS,i,t})$$

I assigned juveniles phenotypes based on their genotype scores the same as adults (see above).

The number of individuals present at the end of the breeding season ($N_{A,i,t}$), prior to autumn migration in breeding population *i* at generation *t* was therefore:

$$\text{Eq. 3: } N_{A,i,t} = N_{R,i,t} + J_{i,t}$$

Mortality occurred during autumn migration when individuals transitioned between breeding and nonbreeding regions. Individuals were assigned to migrate through one of three autumn migration regions based on their autumn migration genotype score. The survival rate for autumn migration (φ_A) in region *j* at generation *t* was calculated by drawing 100 samples from a binomial distribution with a probability of 0.75 (e.g., Sillett and Holmes 2002) and dividing by 100:

$$\varphi_{A,j,t} \sim B(100, 0.75)/100$$

The population of individuals at nonbreeding region *m* during generation *t* was comprised of the sum of the products of the post-reproductive population that transitioned to nonbreeding region *m* through migration region *j* at generation *t* ($N_{R,m,j,t}$) and that region's autumn migration survival rate ($\varphi_{A,j,t}$):

$$\text{Eq. 4: } N_{NB,m,t} = \sum_{j=1}^{3} N_{R,m,j,t} \times \varphi_{A,j,t}$$

The number of individuals that survived the nonbreeding period and entered the spring migration period from nonbreeding region *m* ($N_{S,m,t}$) was the sum of the product of the number of individuals in nonbreeding region *m* at time *t* ($N_{NB,m,t}$) and the nonbreeding period survival rate for that region in generation *t* ($\varphi_{NB,m,t}$):

$$\text{Eq. 5: } N_{S,m,t} = N_{NB,m,t} \times \varphi_{NB,m,t}$$

where the regional nonbreeding period survival rate ($\varphi_{NB,m,t}$) was calculated by drawing 100 samples from a binomial distribution with a probability of 0.98 (e.g., Sillett and Holmes 2002, Streby et al. 2013) and dividing by 100:

$$\varphi_{NB,m,t} \sim B(100, 0.98)/100$$

I also simulated mortality during spring migration when individuals transitioned between nonbreeding and breeding regions. Individuals migrated through one of three spring migration regions based on their spring migration genotype score. The survival rate for spring migration (φ_S) in region *j* at generation *t* was calculated by drawing 100 samples from a binomial distribution with a probability of 0.75 (e.g., Sillett and Holmes 2002) and dividing by 100:

$$\varphi_{S,j,t} \sim B(100, 0.75)/100$$

Thus, the population of pre-breeding individuals returning to breeding region *i* in the next generation (i.e., generation t+1; $N_{B,i,t+1}$) was comprised of the sum of the products of the post-reproductive population migrating to breeding region *i* through migration region *j* at generation *t* ($N_{S,m,j,t}$) and that region's spring migration survival rate ($\varphi_{S,j,t}$):

$$\text{Eq. 6: } N_{B,i,t+1} = \sum_{j=1}^{3} N_{S,i,j,t} \times \varphi_{S,j,t}$$

The global pre-breeding population at generation t+1 ($N_{B,t+1}$) was the sum of both breeding populations:

$$\text{Eq. 7: } N_{B,t+1} = \sum_{i=1}^{2} N_{B,i,t+1}$$

My goal was to explore the evolution of the strength of migratory connectivity in this analysis. I was less interested in describing implications on population abundance or dynamics. However, this model is constructed such that future analyses could explore how the strength of migratory connectivity evolves under different numbers of breeding regions, migration regions, and nonbreeding regions, and combinations of vital rates, which may better describe other systems or species.

4.3.4 Modeling Different Scenarios

4.3.4.1 Modeling Background

I compared the outcomes of 25 scenarios selected *a priori* to explore how stronger migratory connectivity might evolve in a species with weak migratory connectivity (i.e., r_M ~0). In each scenario, I used the same set of initial populations but varied reproduction rate, survival rate, or both reproduction and survival rates to impose fitness penalties on individuals that occurred in specific pairings of breeding and nonbreeding regions. I considered individuals that had matching breeding and nonbreeding phenotypes (i.e., breeding region A and nonbreeding region A; breeding region B and nonbreeding region B) as being concordant. I classified individuals that had mismatched breeding and nonbreeding phenotypes (i.e., breeding region A and nonbreeding region B; breeding region B and nonbreeding region A) as discordant. My decision to select for individuals with “matching” breeding and nonbreeding region phenotypes was arbitrary and I would expect similar results if I had instead selected for individuals with “mismatched” breeding and nonbreeding phenotypes.

I also considered scenarios in which I imposed additional fitness penalties on individuals with concordant phenotypes, but intermediate genotype scores. In these scenarios, individuals with concordant breeding and nonbreeding phenotypes experienced intermediate survival and/or reproduction rates if they possessed breeding and/or nonbreeding genotype scores within a certain distance from the boundary between breeding and/or nonbreeding regions (i.e., genotype score = 0; Fig. D – 2). In these scenarios, larger intermediate genotype score ranges are associated with a greater spatial distance between breeding and/or nonbreeding sub-regions in which individuals occupying those landscapes experience reduced fitness, either through reduced reproduction or reduced nonbreeding survival rates (Fig. D – 2). Biologically, this scenario could occur when habitat loss or reduction in habitat quality occurs in a population’s periphery and is associated with reduced fitness for individuals occupying those regions (Hornseth et al. 2014). Alternatively, this scenario could represent changing climatic conditions that result in reduced fitness for individuals along a leading or trailing edge of a population (Chen et al. 2011, Wiens 2016). Across all simulations, individuals’ genotype scores were static and did not change over time. Thus, individuals were not allowed to switch phenotypes (i.e., exhibit phenotypic plasticity) during a simulation.

All simulations started with an initial population size of 2,000 females (Fig. D – 1). The carrying capacity of each breeding population was 5,000 individuals. No carrying capacity was imposed during the nonbreeding period. I did not include density-dependent effects on survival although future analyses could include those interactions in this model. Survival during autumn and spring migration varied randomly by region (n = 3 regions per season) and across generations but were drawn from the same distribution (~B[100, 0.75]/100). This model has the capacity to simulate numerous other scenarios including how selective pressures exerted during autumn and spring migration periods shape the strength of migratory connectivity of species, how age-specific survival may influence population structure, and how these processes affect the evolved strength of migratory connectivity over longer periods, although I did not explore those scenarios here.

4.3.4.2 Null Scenario

In the null scenario, there were no non-random fitness differences among individuals based on breeding and nonbreeding phenotype concordance. Survival and reproductive rates were population-specific but were drawn from distributions with the same mean and standard deviation ($\bar{x}_{\text{reproduction}}$ = 1.25, SD = 0.30) and with the same probability of success (0.98; Fig. 4 – 3).

4.3.4.3 Reproduction, Survival, and Reproduction and Survival Scenarios

In the remaining 24 scenarios, I simulated the evolved strength of migratory connectivity following selection against individuals with discordant breeding and nonbreeding phenotypes (i.e., breeding region A and nonbreeding region B, or *vice versa*) and/or individuals with concordant breeding and nonbreeding phenotypes but that occurred relatively near the boundary between breeding and/or nonbreeding regions (i.e., individuals with intermediate genotype scores). First, I imposed fitness penalties on individuals with discordant breeding and nonbreeding phenotypes by reducing the average rate of reproduction, survival, or both reproduction and survival by ~33%

(scenarios R1, S1, B1; Fig. 4 – 3). The severity of fitness penalties can be adjusted to test specific hypotheses. However, the fitness penalties I imposed were not as severe as those reported by Hewson et al. (2016) in common cuckoos (*Cuculus canorus*) using different migration routes to cross the Sahara (~49%). In scenarios R2-4, S2-4, and B2-4, I maintained the fitness penalty against individuals with discordant breeding and nonbreeding phenotypes and also imposed an intermediate fitness penalty (~16% reduction in reproduction, survival, or both reproduction and survival) for individuals with concordant breeding and nonbreeding phenotypes but intermediate genotype scores (Fig. 4 – 3, Fig. D – 2). This intermediate fitness penalty can also be adjusted. I chose to use a rate that was half of the penalty imposed on individuals with discordant breeding and nonbreeding phenotypes (i.e., ~33%) to reflect a scenario wherein individuals with concordant breeding and nonbreeding phenotypes that occur near the periphery of those distributions may have reduced fitness relative to individuals with concordant breeding and nonbreeding phenotypes that occur in the core of the range, but increased relative fitness compared to individuals with discordant breeding and nonbreeding phenotypes.

I considered different ranges of intermediate genotype scores to simulate how selection against individuals occupying regions close to the boundary between populations affected the strength of migratory connectivity. The different thresholds I used to classify intermediate genotype scores were -0.25–0.25 (R2, S2, B2), -0.50–0.50 (R3, S3, B3), and -0.75–0.75 (R4, S4, B4; Fig. D – 2). I also explored how the frequency of selective pressure shapes the evolution of strong migratory connectivity by imposing fitness penalties against individuals with discordant breeding and nonbreeding phenotypes and those with concordant phenotypes but intermediate genotype scores using an intermediate genotype score threshold -0.50–0.50 (as in scenarios R3, S3, B3; Fig. D – 2) every other generation (RF2, SF2, BF2), every fourth generation (RF4, SF4, BF4), every tenth generation (RF10, SF10, BF10), and constant selection for fifty generations followed by no selection pressure for fifty generations (RF50, SF50, BF50; Fig. 4 – 3).

4.3.5 Statistical Analysis

I estimated the mean Mantel correlation coefficient (r_M) of 300 randomly sampled individuals present at the end of each simulation (i.e., 100th generation) to quantify the strength of evolved migratory connectivity (r_{M100}). I also calculated the generation at which r_M exceeded 0.60 (i.e., strong migratory connectivity; T_{60}) for each simulation to determine the rate at which strong migratory connectivity evolved under different scenarios. I used ANOVAs to test for differences in the average evolved strength of migratory connectivity (r_{M100}) and the average rate at which a population attained strong migratory connectivity (T_{60}) among groups of simulations characterized by the vital rates on which I imposed fitness penalties (i.e., reproduction vs. survival vs. reproduction and survival) and the frequency of fitness penalties. I used *post-hoc* Tukey HSD test to determine significant differences among different groups of simulations. I also used simple linear regression models to test for differences in r_{M100} and T_{60} between constant selection scenarios (i.e., R1, S1, B1) and scenarios where constant selection was relaxed after 50 generations (i.e., RF50, SF50, BF50). I considered differences to be significant at $\alpha = 0.05$.

4.4 Results

Strong migratory connectivity did not evolve in the null scenario (average r_{M100} = 0.01 ± 0.02 SD; Fig. 4 – 4, Fig. D – 3). Under null scenario conditions (i.e., no selection pressure or fitness penalties) r_{M100} ranged from -0.05–0.13 and r_M never reached 0.60 during any simulation.

On average, strong migratory connectivity evolved in 18 (± 9 SD) generations under constant-selection scenarios (R1–4, S1–4, B1–4; Fig. 4 – 5). In these constant-selection scenarios, the mean strength of migratory connectivity after 100 generations was similar regardless of whether fitness penalties were imposed on reproduction, survival, or both reproduction and survival (overall mean $r_M = 0.72$; one-way ANOVA, $F_{2,9} = 2.50$, $P = 0.14$). However, it took longer to evolve strong migratory connectivity (i.e., $r_M \geq 0.60$) in constant-selection scenarios when fitness penalties were imposed on reproduction (i.e., scenarios R1–R4; one-way ANOVA, $F_{2,9} = 31.70$, $P < 0.001$) compared to scenarios in which constant selection was imposed via reduced survival (i.e., scenarios S1–4; Tukey HSD < 0.001) or reduced reproduction and survival (i.e., scenarios B1–B4; Tukey HSD < 0.001). The strength of migratory connectivity that evolved following 100 generations in constant selection scenarios did not differ among the intermediate genotype thresholds that I tested (one-way ANOVA, $F_{1,7} = 1.69$, $P = 0.24$).

Strong migratory connectivity evolved more slowly when selection and fitness consequences were not imposed every generation, compared to scenarios in which selective pressure was constant for all 100 generations or were imposed for 50 generations and then relaxed (43 generations vs. 17 generations, respectively; $F_{1,19} = 18.0$, $P < 0.01$; Fig. 4 – 5). Similarly, the average strength of migratory connectivity was 15% lower when selective pressure was not constant or when selection was constant for 50 generations before being relaxed for 50 generations (0.62 vs. 0.73, respectively; $F_{1,22}$

= 7.49, $P = 0.01$). In three simulations (RF4, RF10, and SF10), average r_M did not reach 0.60 after 100 generations (Fig. 4 – 5). However, selection on reproduction or survival every other generation (RF2, SF2) resulted in the evolution of strong migratory connectivity (mean $r_M = 0.69$ and 0.74, respectively; Fig. 4 – 5). Furthermore, strong migratory connectivity evolved in all three frequency scenarios when selection pressure was imposed on both survival and reproduction (i.e., BothF2, $r_M=0.73$; BothF4 $r_M=0.72$; BothF10, $r_M=0.66$; Fig. 4 – 5).

Strong migratory connectivity evolved and was maintained after 100 generations in all three scenarios in which selection pressure was imposed on individuals for 50 generations but then relaxed for 50 generations (RF50, SF50, BF50; Fig. 4 – 5). In these three scenarios the strength of migratory connectivity after 50 generations of selection and 50 generations of no selection was similar to the strength of migratory connectivity that evolved under scenarios of constant selection pressure with the same (-0.50–0.50; R3, S3, B3) genotype score threshold ($F_{1,4} = 1.2$, $P = 0.33$).

4.5 Discussion

Populations in my simulations evolved migratory connectivity that spanned the spectrum from weak to strong (Fig. 4 – 7; Fig. D – 3). However, I found that strong migratory connectivity evolved rapidly under a variety of scenarios wherein constant selection, imposed via fitness penalties on reproduction and/or survival rates, favored individuals that occurred in specific pairings of breeding and nonbreeding regions. Conversely, the strength of migratory connectivity remained weak (i.e., <0.30) when no selection pressures were imposed on individuals (i.e., null scenario). The selection pressures I imposed in these simulations represent biologically plausible scenarios (e.g., Sillett and Holmes 2002, Hewson et al. 2016) in which fitness consequences may be related to where an individual spends the breeding and nonbreeding periods (Robbins et al. 1989, Hallworth et al. 2021). Specifically, this could arise when populations become locally adapted to climatic conditions and/or the availability of resources during one period of the annual cycle and track those conditions across other portions of the annual cycle (Martínez-Meyer et al. 2004, Nakazawa et al. 2004, Thorup et al. 2017).

The evolved strength of migratory connectivity did not differ under scenarios in which fitness penalties were imposed on individuals with concordant breeding and nonbreeding phenotypes that occurred near the boundary between breeding and/or nonbreeding regions (i.e., intermediate genotype scores; Fig. D – 2). This suggests that strong migratory connectivity can evolve even between populations that are separated by relatively short geographic distances effectively forming a migratory divide. Migratory divides have been described in several species and can be very narrow (e.g., < 50 km for Swainson's thrush [*Catharus ustulatus*]; Delmore and Irwin 2014). Conversely, decreasing the frequency of selective pressure increased the variability of outcomes (i.e., evolved strength of migratory connectivity) and in some cases, reduced the average strength of migratory connectivity that I observed after 100 generations (Fig. 4 – 6). However, for simulations that did not evolve strong migratory connectivity within 100 generations (i.e., RF4, RF10, SF10; Fig.4 – 6), I expect that the strength of migratory connectivity would continue to increase if I allowed simulations to continue for additional generations suggesting that strong migratory connectivity could also evolve more gradually.

To date, examples of migratory birds exhibiting strong migratory connectivity remain rare in species for which adequate tracking data are available (Finch et al. 2017). However, my analyses suggest that strong migratory connectivity is the most likely outcome and can evolve relatively quickly (i.e., in < 10 generations) under a range of biologically realistic conditions if individuals experience differences in fitness based on the pairing of breeding and nonbreeding regions that they inhabit. The question remains as to why weak migratory connectivity is most commonly reported in investigations of the migratory connectivity of birds. One explanation could be that the conditions required to evolve strong migratory connectivity (e.g., heritable adaptation that leads to differences in relative fitness among individuals that use distinct areas during different portions of the annual cycle) may be relatively uncommon (Finch et al. 2017). Alternatively, if the direction of selective pressure oscillates, or is unpredictable (i.e., positive fitness consequences in one generation, but negative in another) as could be expected in systems with relatively variable breeding or nonbreeding conditions, or reliably cyclical conditions (e.g., El Niño-Southern Oscillation) then natural selection might favor the production of juveniles that disperse relative to one another throughout different portions of the annual cycle (Botero et al. 2015, Finch et al. 2017). Other scenarios could also explain why weak migratory connectivity is commonly observed in birds including species sampling biases or restricted geographic sampling (Vickers et al. 2021).

One alternative hypothesis that deserves additional attention is the possibility that the frequency of species exhibiting strong migratory connectivity has declined over the past ~100 years as a result of the extirpation of strongly linked populations from the effects of anthropogenic development and land-use change (*sensu* Sayol et al. 2020). If species with strong migratory connectivity lose a population segment that occurs in isolation from other populations during breeding and nonbreeding periods, then the strength of migratory connectivity in that species would likely decrease. For example, golden-winged warblers (*Vermivora chrysoptera*) are a Nearctic-Neotropical migrant that exhibits strong migratory connectivity with two distinct breeding populations remaining almost completely isolated during breeding and nonbreeding periods (Kramer et al. 2017, Kramer et al. 2018). Considered independently, each population segment exhibits weak migratory connectivity (Chapter 3). However, when considered together, the species exhibits strong migratory connectivity during breeding and nonbreeding periods (Kramer et al. 2018; Chapter 1, Chapter 3). Population trends for both populations of golden-winged warbler differ with the Boreal Hardwoods Transition population exhibiting numerically stable trends and the Appalachian Mountain population experiencing severe declines that have led to near-extirpation (Rosenberg et al. 2016, Kramer et al. 2018; Chapter 1). If the steeply declining Appalachian Mountain population of golden-winged warblers had been extirpated prior to efforts to delineate and describe the migratory connectivity of this species across its distribution, then it would have been concluded that the species exhibited weak migratory connectivity (Kramer et al. 2018, Vickers et al. 2021). Because migratory species are among the groups of birds experiencing the most dramatic population declines over the past 60 years (Robbins et al. 1989), it is possible that other species have already lost or are in the process of losing strongly linked populations in a similar fashion as golden-winged warblers (Kramer et al. 2018). It is possible that this phenomenon, driven primarily by a combination of extensive anthropogenic land-use changes (Kramer et al. 2018) and anthropogenic climate change (Walther et al. 2002), may help explain why observations of strong migratory connectivity are rare and observations of relatively weak migratory connectivity are common in assessments of migratory bird species (Finch et al. 2017). Perhaps some studies in which weak migratory connectivity has been reported have by chance, or by design, excluded peripheral, declining, low-density populations that may in fact be wintering in isolation. It is unclear how many species are currently in the process of losing, or have already lost strongly linked populations before they could be described. Therefore, future analyses would benefit from careful interpretation of assessments of migratory connectivity with the acknowledgement that the strength of migratory connectivity in any given species is an emergent trait (Winger et al. 2019) that can change rapidly and may be especially sensitive to rapid population declines brought about by anthropogenic change.

Interestingly, my analysis suggests that strong migratory connectivity can evolve more rapidly than it erodes. Specifically, strong migratory connectivity that evolved in 12–30 generations remained strong even after 50 years of relaxed selection (i.e., no selection against individuals with discordant phenotypes or concordant phenotypes but intermediate genotype scores; Fig. 4 – 6). This raises questions about the evolutionary constraints of strong migratory connectivity in the Anthropocene, a period characterized by rapid, expansive environmental change, and the unprecedented extinction of species (Otto 2018, Turvey and Crees 2019). Strong migratory connectivity has been described as potentially representing an evolutionary trap in the Anthropocene if anthropogenic land-use changes occur so broadly and quickly that strongly linked populations are unable to adapt due to a lack of underlying genetic variation and/or phenotypic plasticity (Kramer et al. 2018). Evolutionary traps occur when (1) individuals demonstrate a preference for a behavior or habitat type, or no preference (i.e., an equal-preference trap), (2) individuals experience differential fitness among behaviors or habitat types, and (3) fitness outcomes of individuals are lower for those using the preferred, or equally preferred habitat or exhibiting preferred, or equally preferred behavior relative to fitness attained by individuals using other available habitats or exhibiting other behaviors (Robertson and Hutto 2006). I propose that in scenarios under which natural selection on genetically determined migratory traits leads to strong migratory connectivity in a species, an evolutionary trap could develop if those previously adaptive associations become disentangled from historical fitness outcomes.

For example, the strong migratory connectivity observed in golden-winged warblers (Kramer et al. 2017, 2018; Fig. 4 – 8) is likely a signal of previously adaptive relationships between individuals and distinct breeding and nonbreeding areas and is likely genetically controlled (Toews et al. 2019). Changes in land-use patterns and deforestation in the Neotropics over the past 70 years have disproportionately affected regions in northern South America leading to the decline of populations of golden-winged warblers overwintering in that region whereas populations overwintering in Central America have remained numerically stable (Hansen et al. 2010, Kramer et al. 2018; Chapter 1). If land-use changes linked to anthropogenic activities occur across greater extents (e.g., across northern South America) and over shorter time-frames (i.e., in decades, not millennia) than would have been likely under natural disturbance regimes in the absence of anthropogenic change, it may not be possible for strongly linked populations to “escape” via the evolution of different migratory strategies or shifting distributions to more appropriate landscapes that would confer greater fitness. It may be useful to characterize this type of evolutionary trap (and all evolutionary traps) more generally within the context of ordinal habitat selection (Johnson 1980). In this case, the evolutionary trap exists because the previously adaptive cues associated with first order habitat selection (i.e., selection of the general region or location on Earth) become disentangled from past fitness outcomes due to expansive anthropogenic change wherein individuals using those preferred, and previously adaptive regions experience reduced fitness (Johnson 1980, Robertson and Hutto 2006).

To provide evidence that this type of evolutionary trap exists in natural populations, additional data need to be collected to determine whether individuals demonstrate a preference for one region, whether fitness outcomes differ among individuals using different regions, and if fitness outcomes are lower among individuals using the preferred region (Robertson and Hutto 2006). However, if this type of trap does exist, it is possible that species with strong migratory connectivity, as a group, may be more likely to experience population declines, extirpation, and extinction in the face of climate change and changing land-use practices. Moreover, because migratory behaviors are genetically linked in many migratory species (Berthold 1991), the trap-facilitated extinction of migratory populations with strong connectivity may not result in a loss of species (Runge et al. 2014), but would likely result in a hidden but significant human-facilitated loss of genetic diversity that may take millions of years to recover (Davis et al. 2018).

Under what conditions might selection favor the evolution of weak connectivity over strong connectivity? If low quality habitat is broadly distributed and does not support high abundances of individuals, then adults may experience greater fitness if they produce juveniles that disperse more broadly (Finch et al. 2017). In my analysis, even relatively infrequent selection led to the evolution of strong migratory connectivity. Therefore, neutral selection or selection for individuals that produce offspring that disperse from natal breeding sites and parental nonbreeding sites may be required to maintain weak migratory connectivity (Finch et al. 2017). However, many species are limited to occurring in relatively narrow niches or uncommon or spatially limited landscapes such that broadly dispersing juveniles may be unlikely to settle in appropriate regions. Efforts to explore the role of juvenile dispersal in the evolution of strong migratory connectivity could help explain species-specific distribution patterns and the strength of migratory connectivity in those systems (Sherry 2018, Taylor 2019).

Migration-related traits were not linked in this analysis. Whether migration-related traits are linked, either to other migration-related traits or to other non-migratory traits, on autosomes or on sex-chromosomes may have important implications for the patterns of heritability and the evolution of these traits (Mank et al. 2007). Considering scenarios in which breeding, nonbreeding, and/or migration traits are genetically linked could be assessed with different iterations of the model used in this analysis. Furthermore, many mammals and some birds develop migratory behaviors through social learning from conspecifics (Sawyer et al. 2009, Harrison et al. 2010). Recapitulating this model and applying it to species with learned migration behavior may be valuable for understanding how the evolution of migratory connectivity may differ between species with innate vs.

learned migratory behaviors. Lastly, this analysis assumed that species were obligate migrants (i.e., migrate every year; Newton 2012). However, understanding how evolution shapes the strength of migratory connectivity in species with different migration strategies (e.g., facultative migration, nomadism, altitudinal migration; Barçante et al. 2017, Pagel et al. 2020, Neumann et al. 2021) could provide meaningful context for understanding the implications and origins of migratory behavior. Ultimately, that migration is an adaptive strategy that manifests in a range of behaviors across diverse taxa suggests that the evolved strength of migratory connectivity may also be shaped by diverse processes in different species (Alerstam and Hedenström 1998, Winger et al. 2014, Somveille et al. 2021). Continuing to delineate and describe the migratory patterns and the strength of migratory connectivity of diverse species will deepen the collective understanding of the evolutionary processes and ramifications of different migratory strategies in animals.

Understanding the evolutionary processes that shape the distribution of animals is an area of ongoing research (Winger et al. 2019). The Anthropocene is characterized by fast and expansive environmental change that can impose selective pressure on organisms and facilitate rapid evolution (Campbell-Staton et al. 2017). Considering the origins and implications of species' distributions and seasonal migrations in evolutionary, ecological, and conservation frameworks will help illuminate how species will fare under future climatic conditions and will help inform effective conservation efforts for migratory species.

Table 4.1: Vital rates used in population models simulating the evolved strength of migratory connectivity. Point estimates (estimates), distributions used to generate generation- and region-specific rates (Distribution), and citations for references including the species from which estimates are derived (Species and citations) are presented. See main text for detailed description of vital rates.

Vital rate	Estimate	Distribution	Species and citation(s)
Breeding season survival rate	0.98	~*B*(100, 0.98)/100	Golden-winged warbler, Streby et al. (2013); Black-throated blue warbler (*Setophaga caerulescens*), Sillett and Holmes (2002)
Rate of reproduction	1.25	~*N*(1.25,0.30)	Wood thrush (*Hylocichla mustelina*), Powell et al. (1999)
Autumn migration survival rate	0.75	~*B*(100, 0.75)/100	Black-throated blue warbler (*Setophaga caerulescens*), Sillett and Holmes (2002)
Nonbreeding period survival rate	0.98	~*B*(100, 0.98)/100	Black-throated blue warbler (*Setophaga caerulescens*), Sillett and Holmes (2002)
Spring migration survival rate	0.75	~*B*(100, 0.75)/100	Black-throated blue warbler (*Setophaga caerulescens*), Sillett and Holmes (2002)

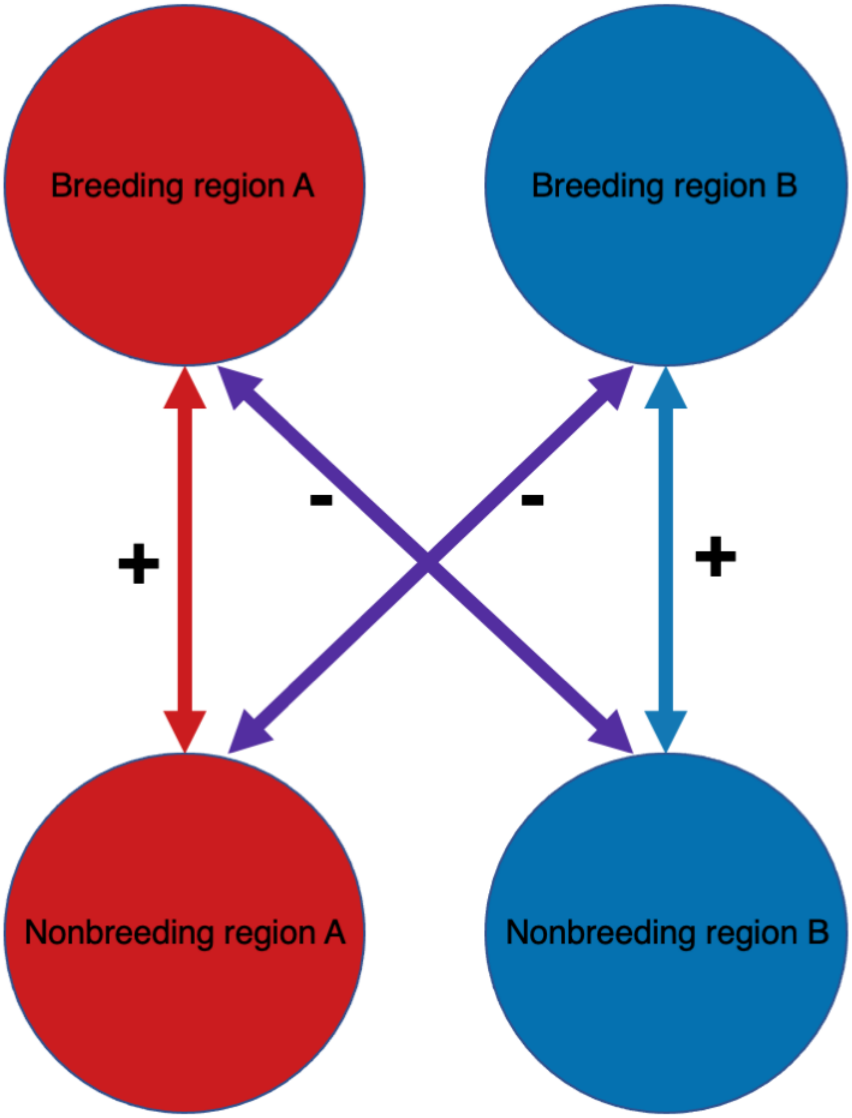

Figure 4 – 1: Schematic depicting a species with two breeding populations and two nonbreeding populations (circles). Arrows show possible combinations of breeding and nonbreeding region phenotypes that individuals could exhibit. In this analysis, I imposed selection pressure that favored individuals occurring in breeding region A and nonbreeding region A (red line) or breeding region B and nonbreeding region B (blue line). Individuals with these combinations of breeding and nonbreeding region phenotypes experienced higher relative fitness compared to individuals that exhibited other combinations of phenotypes (i.e., occurred in breeding region A and nonbreeding region B, or *vice versa*; purple lines)

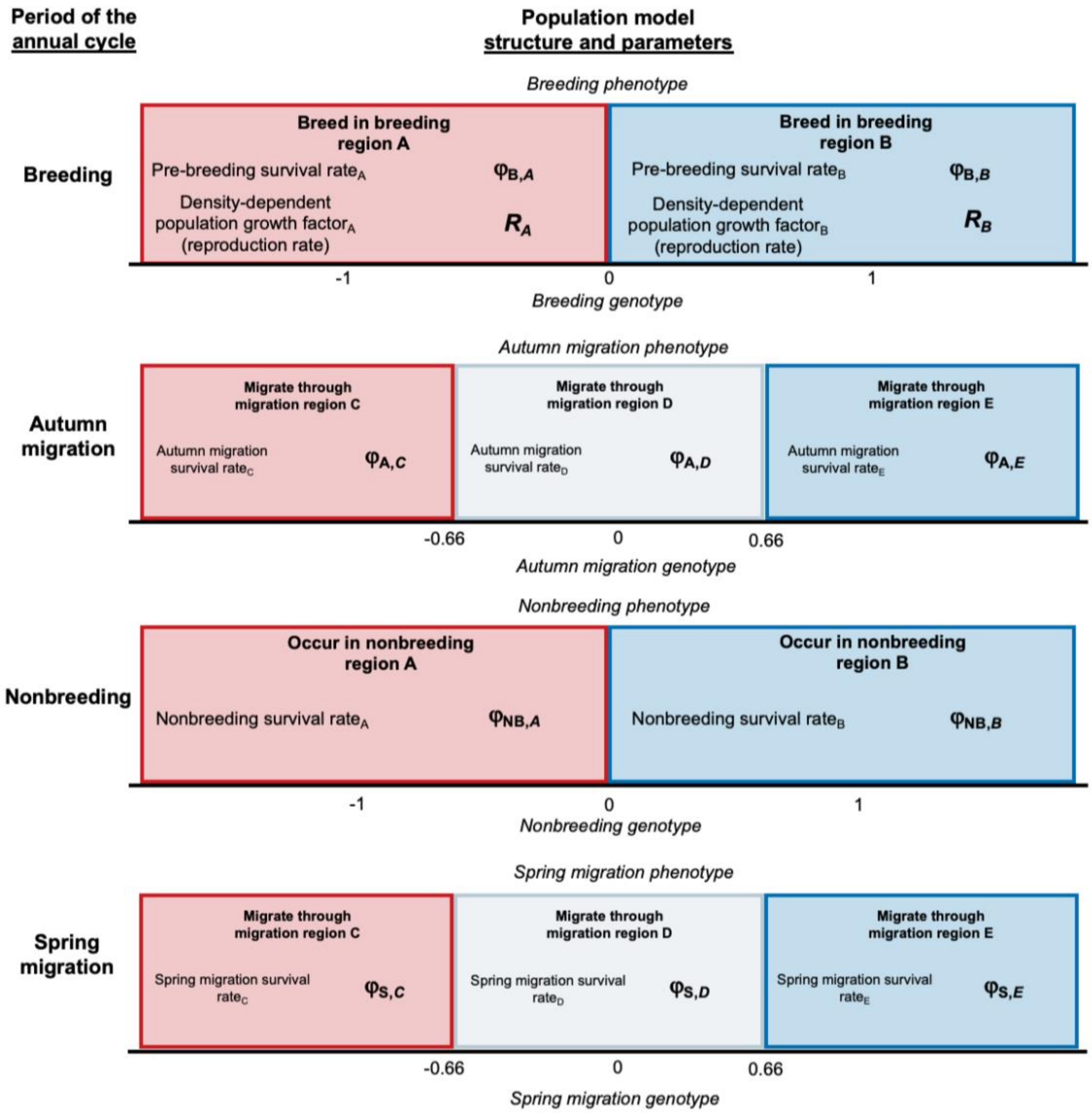

Figure 4– 2: Structure of population model used to simulate the evolved strength of migratory connectivity. Individuals were separated into groups based on their occurrence in different regions throughout the annual cycle (determined by genotype scores) where individuals experienced different rates of reproduction (breeding period) and/or survival (breeding period, autumn migration period, nonbreeding period, spring migration period).

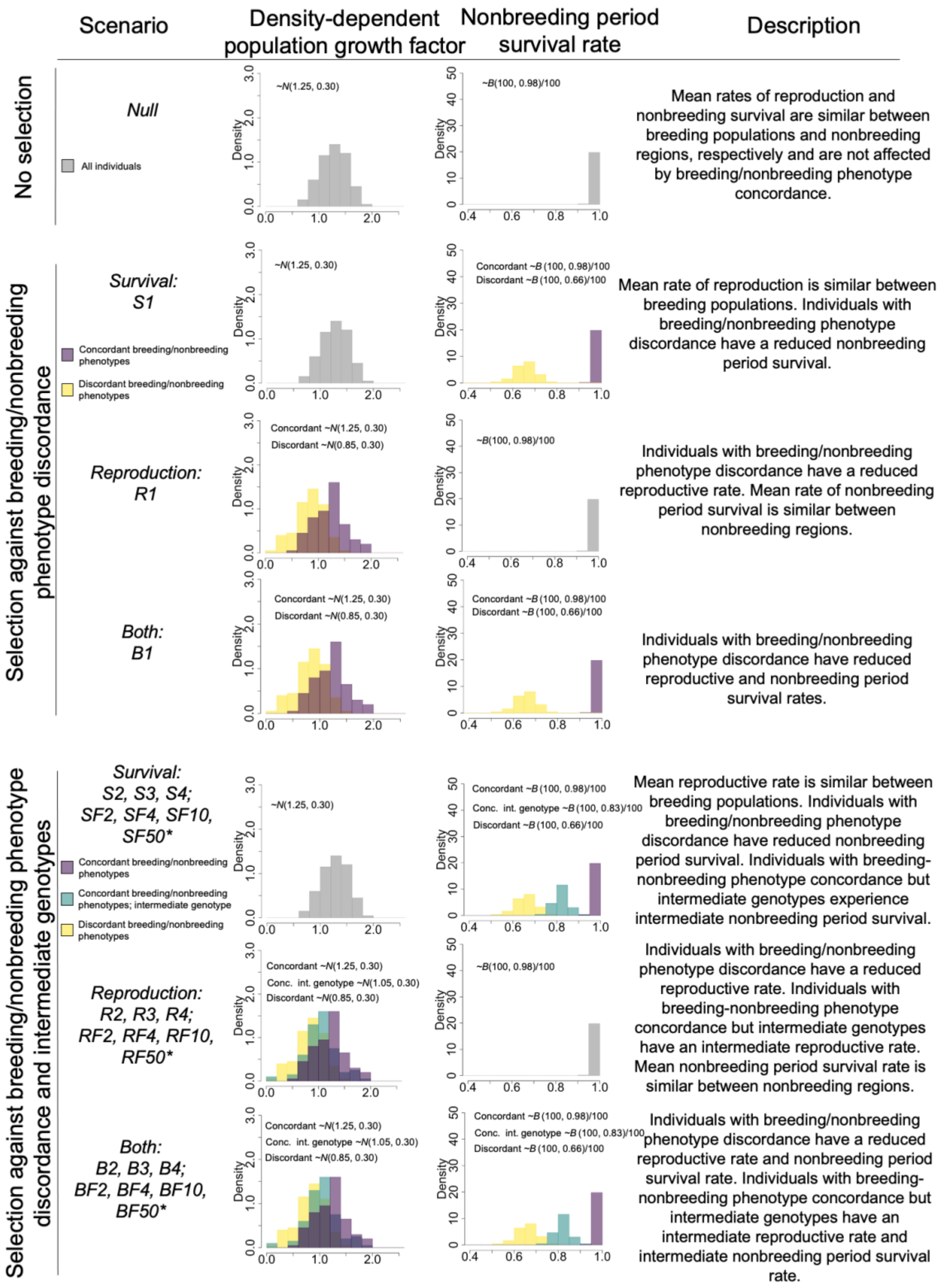

Mean rates of reproduction and nonbreeding survival are similar between breeding populations and nonbreeding regions, respectively and are not affected by breeding/nonbreeding phenotype concordance.

Mean rate of reproduction is similar between breeding populations. Individuals with breeding/nonbreeding phenotype discordance have a reduced nonbreeding period survival.

Individuals with breeding/nonbreeding phenotype discordance have a reduced reproductive rate. Mean rate of nonbreeding period survival is similar between nonbreeding regions.

Individuals with breeding/nonbreeding phenotype discordance have reduced reproductive and nonbreeding period survival rates.

Mean reproductive rate is similar between breeding populations. Individuals with breeding/nonbreeding phenotype discordance have reduced nonbreeding period survival. Individuals with breeding-nonbreeding phenotype concordance but intermediate genotypes experience intermediate nonbreeding period survival.

Individuals with breeding/nonbreeding phenotype discordance have a reduced reproductive rate. Individuals with breeding-nonbreeding phenotype concordance but intermediate genotypes have an intermediate reproductive rate. Mean nonbreeding period survival rate is similar between nonbreeding regions.

Individuals with breeding/nonbreeding phenotype discordance have a reduced reproductive rate and nonbreeding period survival rate. Individuals with breeding-nonbreeding phenotype concordance but intermediate genotypes have an intermediate reproductive rate and intermediate nonbreeding period survival rate.

Figure 4 – 3: Distributions of vital rates used to inform different parameters in population models that simulated the evolved strength of migratory connectivity. Vital rates were selected from the literature and

corresponded with estimated and theoretical rates of short-lived migratory songbirds. Scenario characterize whether fitness penalties were imposed on nonbreeding period survival rate (Survival), density-dependent population growth factor (Reproduction), both survival and reproduction (Both), or neither (Null). Selection was imposed on individuals wherein individuals experienced reduced fitness if they had discordant breeding and nonbreeding phenotypes (concordant = purple bars; discordant = yellow bars), or if they possessed concordant breeding and nonbreeding phenotypes, but intermediate genotype scores (concordant intermediate = green bars). In scenarios where fitness penalties were imposed on one vital rate (e.g., survival) the distribution of the other vital rate (e.g., reproduction) was the same as in the null scenario. A text description of each scenario is also presented.

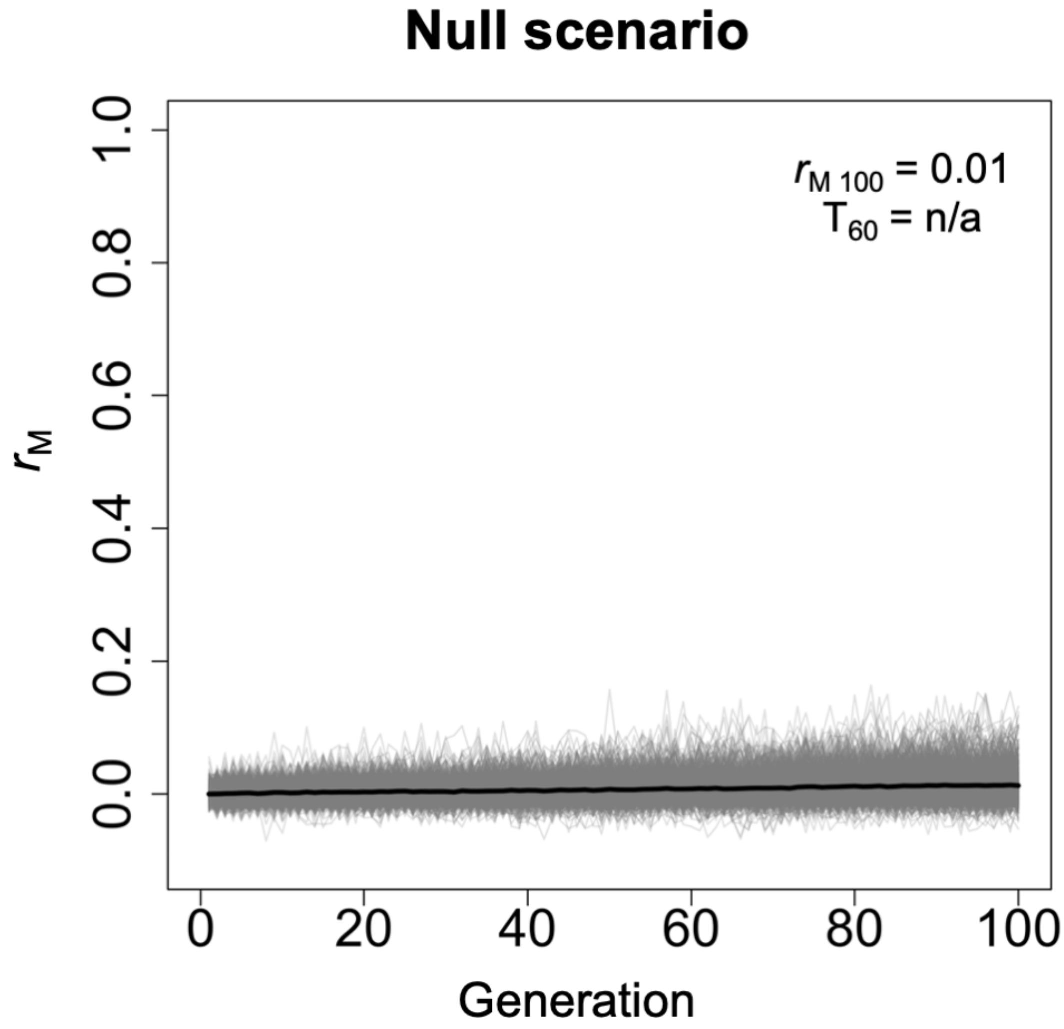

Figure 4 – 4: Outcomes of simulations (*n* = 1,000) of the evolution of migratory connectivity (Mantel correlation coefficient; r_M) under the null scenario in which no selection pressure was exerted on individuals based on the concordance of breeding and nonbreeding phenotypes. Gray lines represent individual simulations whereas the black line represents the mean r_M. The average strength of migratory connectivity (r_{M100}) and number of generations required to achieve strong migratory connectivity (i.e., $r_M \geq 0.60$; T_{60}) are presented.

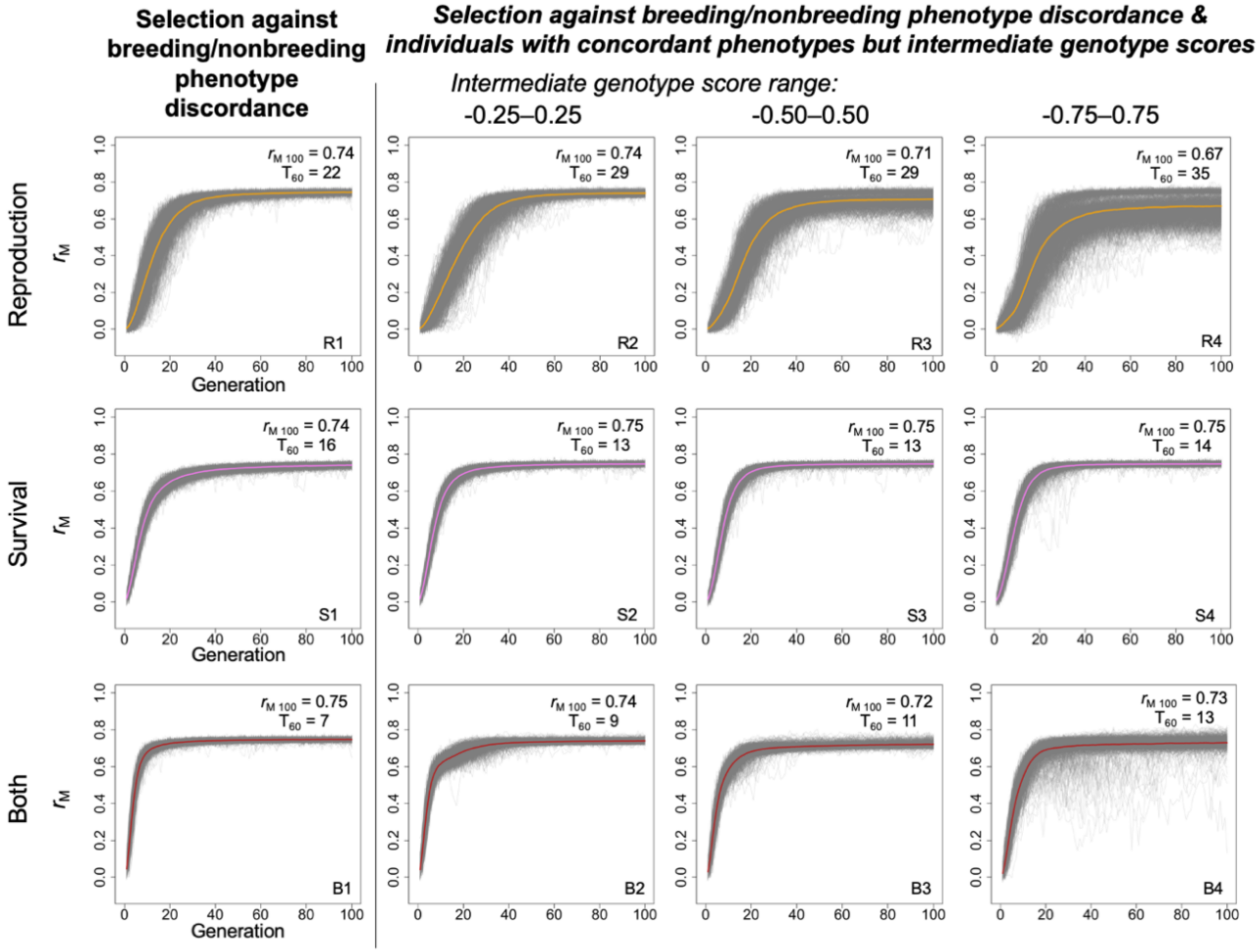

Figure 4 – 5: Outcomes of simulations of the evolution of migratory connectivity (Mantel correlation coefficient, r_M) under different scenarios in which selection pressure was constant across generations (n = 100). Individuals with discordant breeding and nonbreeding phenotypes experienced fitness penalties imposed on reproduction (density-dependent population

growth factor; R1–R4), survival (nonbreeding-period survival rate; S1–S4), or both reproduction and survival (B1–B4). Additionally, individuals with concordant breeding and nonbreeding phenotypes but intermediate genotypes experienced intermediate fitness in scenarios R2–R4, S2–S4, and B2–B4. For each panel, gray lines denote the estimated r_M of individual simulations (n = 1,000) for each generation (n = 100). The colored lines represent the mean r_M of each simulation. The simulation name is presented in the lower right corner and the average strength of migratory connectivity at the end of the 100-generation simulation (r_{M100}) is presented alongside the number of generations required to evolve strong migratory connectivity (i.e., $r_M \geq 0.60$; T_{60}).

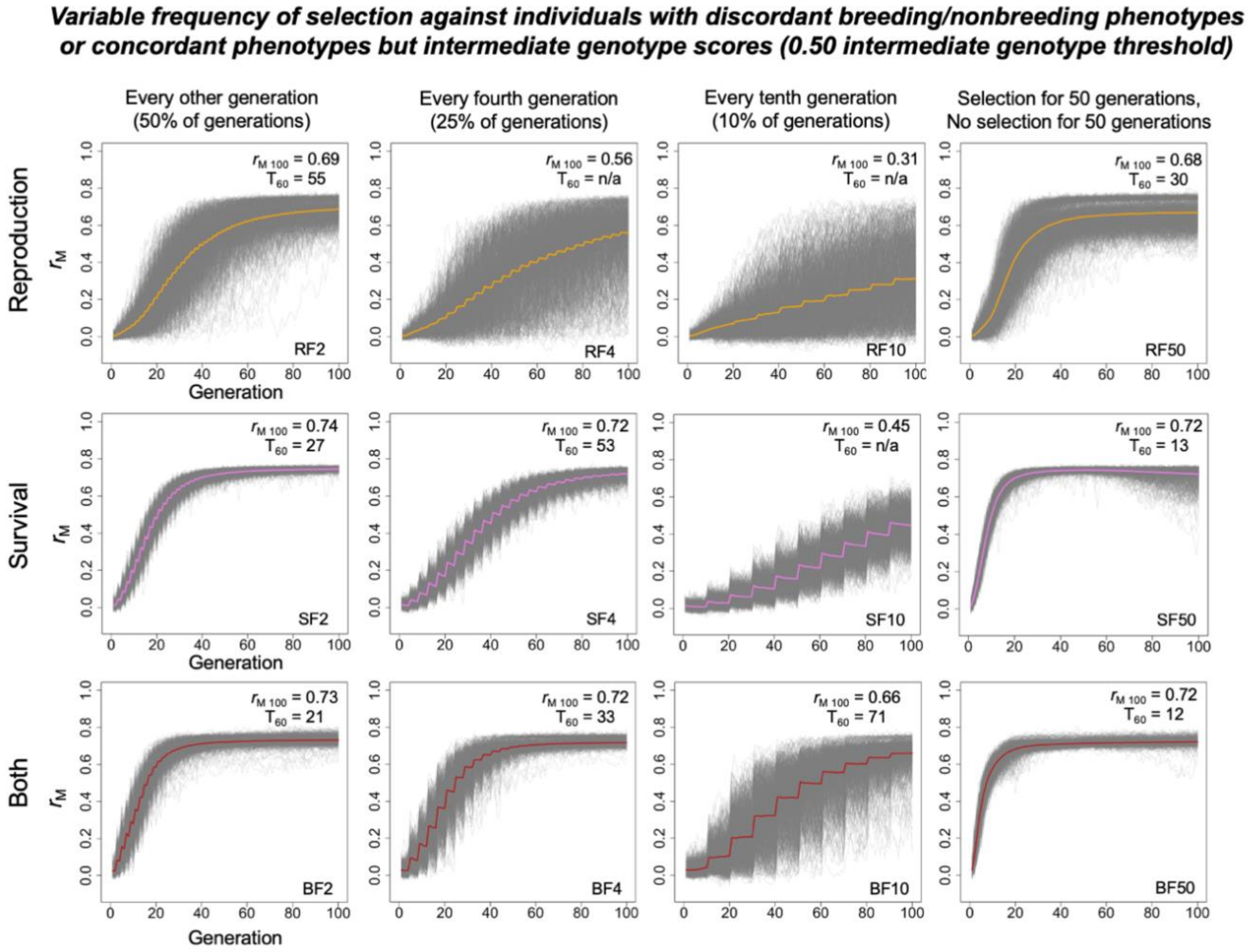

Figure 4 – 6: Outcomes of simulations of the evolution of migratory connectivity (Mantel correlation coefficient, r_M) under different scenarios in which selection pressure varied across generations (n = 100). Individuals with discordant breeding and nonbreeding phenotypes experienced fitness penalties imposed on reproduction (density-dependent population growth

factor), survival (nonbreeding-period survival rate), or both reproduction and survival and individuals with concordant breeding and nonbreeding phenotypes but intermediate genotypes experienced intermediate fitness (intermediate genotype score range = -0.50–0.50). Fitness penalties were imposed every other generation (RF2, SF2, BF2), every fourth generation (RF4, SF4, BF4), every tenth generation (RF10, SF10, BF10) and for fifty generations followed by fifty generations wherein no fitness penalties were imposed (RF50, SF50, BF50). For each panel, gray lines denote the estimated r_M of individual simulations (n = 1,000) for each generation (n = 100). The colored lines represent the mean r_M of each simulation. The simulation name is presented in the lower right corner and the average strength of migratory connectivity at the end of the 100-generation simulation (r_{M100}) is presented alongside the number of generations required to evolve strong migratory connectivity (i.e., $r_M \geq 0.60$; T_{60}).

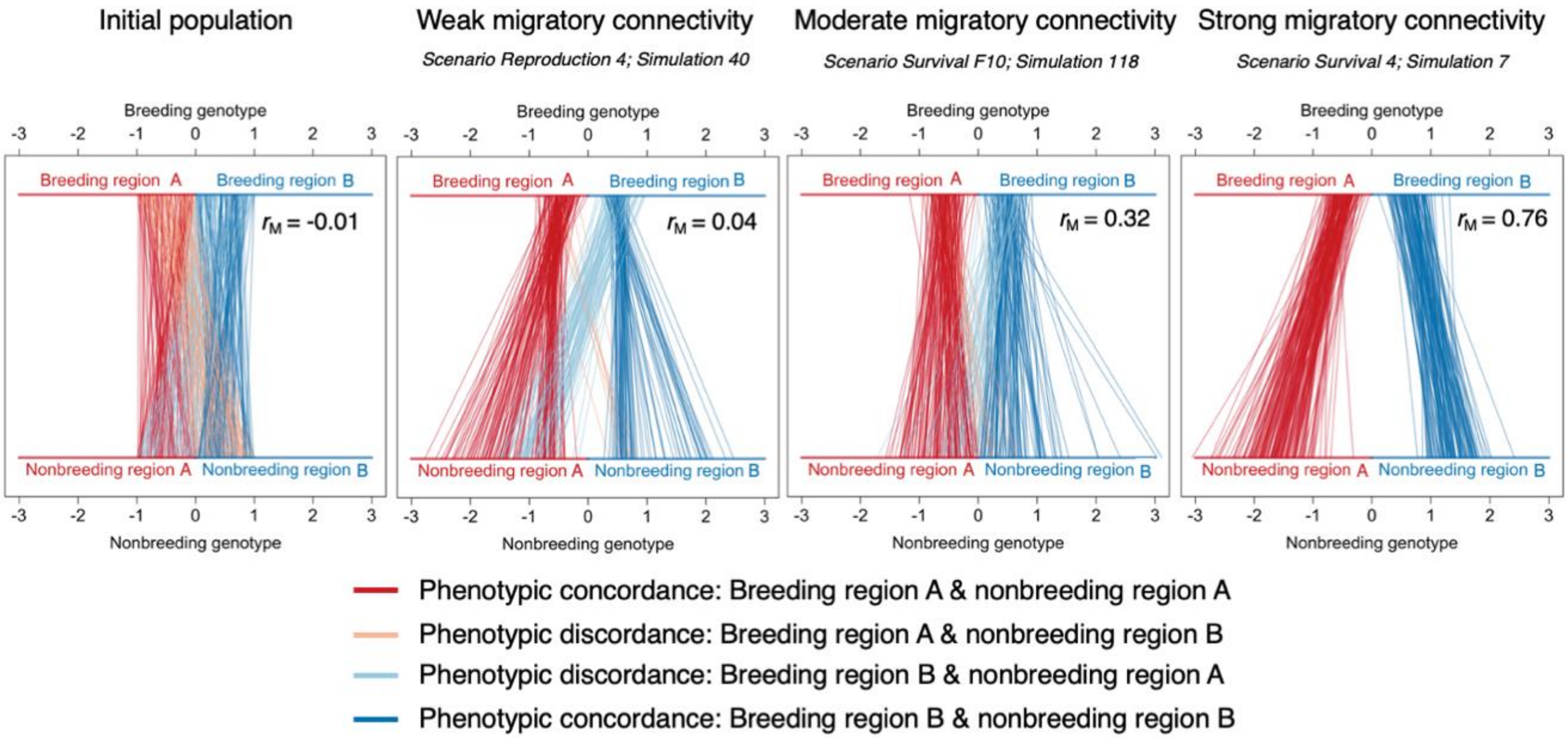

Figure 4 – 7: Examples of simulated populations exhibiting weak, moderate, and strong migratory connectivity after 100 generations under different scenarios in which fitness components (i.e., survival, reproduction, or both) were affected by imposed selection rules. Breeding and nonbreeding phenotypes are noted as horizontal lines spanning genotype values of -3–0 (breeding and nonbreeding region A) and 0–3 (breeding and nonbreeding region B). Slanting lines represent individuals (*n* = 300 per scenario) randomly sampled from the global simulated population and connect breeding and nonbreeding genotype values of individuals. The lines connecting individuals' breeding and nonbreeding genotypes are colored based on whether breeding and nonbreeding phenotypes match, or if they are mismatched. The strength of migratory connectivity of each scenario (after 100 generations) is indicated as the Mantel correlation coefficient (r_M).

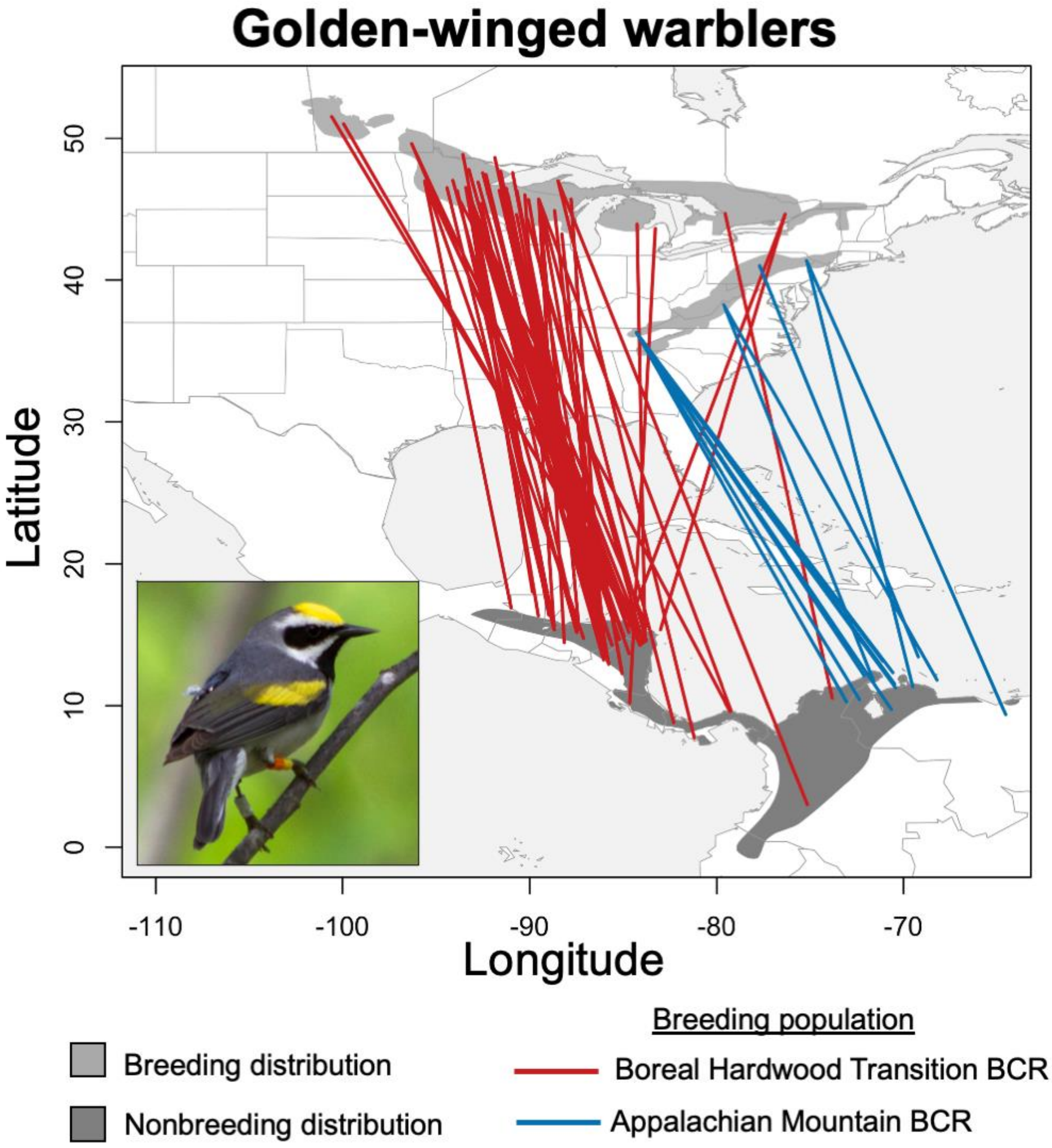

Figure 4 – 8: Migratory connectivity of golden-winged warblers (*n* = 79) tracked with light-level geolocators. Created using data from Kramer et al. (2017, 2018a), Bennett et al. (2019b), Buckardt-Thomas (2019), and Larkin et al. (2017). Lines connect breeding and nonbreeding sites of golden-winged warblers tracked with geolocators between 2013–2017 but are not migration routes of individuals. Colors indicate breeding population of individuals based on Bird Conservation Region (BCR). Breeding Bird Survey (BBS) Index data from Sauer et al. 2017.

References

Abdulle, S.A., and K.C. Fraser. 2018. Does wind speed and direction influence timing and route of a trans-hemispheric migratory songbird (purple martin) at a migration barrier? Animal Migration 5:49–58 https://doi.org/10.1515/ami-2018-0005.

Adamík, P., T. Emmenegger, M. Briedis, L. Gustafsson, I. Henshaw, M. Krist, T. Laaksonen, F. Liechti, P. Procházka, V. Salewski, and S. Hahn. 2016. Barrier crossing in small avian migrants: individual tracking reveals prolonged nocturnal flights into the day as a common migratory strategy. Scientific Reports 6:21560 https://doi.org/10.1038/srep21560.

Aldinger, K.R., T.M. Terhune II, P.B. Wood, D.A. Buehler, M.H. Bakermans, J.L. Confer, D.J. Flaspohler, J.L. Larkin, J.P. Loegering, K.L. Percy, A.M. Roth, and C.G. Smalling. 2015. Variables associated with nest survival of golden-winged warblers (*Vermivora chrysoptera*) among vegetation communities commonly used for nesting. Avian Conservation and Ecology 10:6 https://doi.org/10.5751/ACE-00748-100106.

Aldinger, K.R. 2018. Ecology and management of golden-winged warblers (*Vermivora chrysoptera*) and associated avian species in the Allegheny Mountains of West Virginia. PhD Dissertation. West Virginia University, Morgantown, WV. https://researchrepository.wvu.edu/etd/7152.

Alerstam, T. 2011. Optimal bird migration revisited. Journal of Ornithology 152:S5–S23. https://doi.org/10.1007/s10336-011-0694-1.

Alerstam, T., and A. Hedenström. 1998. The development of bird migration theory. Journal of Avian Biology 29:343–369 https://doi.org/10.2307/3677155.

Alerstam, T., and P.H. Enckell. 1979. Unpredictable habitats and evolution of bird migration. Oikos 33:228–232 https://doi.org/10.2307/3543999.

Ambrosini, R., A.P. Møller, and N. Saino. 2009. A quantitative measure of migratory connectivity. Journal of Theoretical Biology 257:203–211 https://doi.org/10.1016/j.jtbi.2008.11.019.

Arnold T.A., and Zink R.M.. 2011. Collision mortality has no discernible effect on population trends of North American birds. PLoS ONE 6:e24708 https://doi.org/10.1371/journal.pone.0024708.

Arnold T.A. 2010. Uninformative parameters and model selection using Akaike's Information Criterion. Journal of Wildlife Management 74:1175–1178 https://doi.org/10.1111/j.1937-2817.2010.tb01236.x.

Baiz, M.D., G.R. Kramer, H.M. Streby, S.A. Taylor, I.J. Lovette, and D.P.L. Toews. 2020. Genomic and plumage variation in *Vermivora* hybrids. Auk 137:ukaa027 https://doi.org/10.1093/auk/ukaa027.

Barçante, L. M.M. Vale, and M.A.S. Alves. 2017. Altitudinal migration by birds: A review of the literature and comprehensive list of species. Journal of Field Ornithology 88:321–335 https://doi.org/10.1111/jofo.12234.

Bates D., M. Maechler, B. Bolker, and S. Walker. 2015. Fitting linear mixed-effects models using lme4. Journal of Statistical Software 67:1–48 https://doi.org/10.18637/jss.v067.i01.

Bay, R.A., D.S. Karp, J.F. Saracco, W.R.L. Anderegg. L.O. Frishkoff, D. Wiedenfeld, T.B. Smith, and K. Ruegg. 2021. Genetic variation reveals individual-level climate tracking across the annual cycle of a migratory bird. Ecology Letters 24:819–828 https://doi.org/10.1111/ele.13706.

Beccario, C. 2021. earth. GitHub repository. https://github.com/cambecc/earth.

Bennett, R.E., A.D. Rodewald, K.V. Rosenberg. 2019a. Overlooked sexual segregation of habitats exposes female migratory landbirds to threats. Biological Conservation 240:108266 https://doi.org/10.1016/j.biocon.2019.108266.

Bennett, R.E., S.B. Swarthout, J.S. Bolsinger, A.D. Rodewald, K.V. Rosenberg, R.W. Rohrbaugh. 2017. Extreme genetic similarity does not predict non-breeding distribution of two closely related warblers. Journal of Field Ornithology 88:156–168 https://doi.org/10.1111/jofo.12195.

Bennett, R.E. 2019. GWWA geolocators. Retrieved from OSF repository https://doi.org/10.17605/OSF.IO/CEK45.

Bennett, R.E., A.D. Rodewald, K.V. Rosenberg, R. Chandler, L. Chavarria-Duriaux, J.A. Gerwin, D.I. King, and J.L. Larkin. 2019b. Drivers of variation in migration behavior for a linked population of long-distance migratory passerine. Auk 136:ukx051 https://doi.org/10.1093/auk/ukz051.

Berger, J. 2004. The last mile: How to sustain long-distance migration in mammals. Conservation Biology 18:320–331 https://doi.org/10.1111/j.1523-1739.2004.00548.x.

Berthold, P. 1991. Genetic control of migratory behavior in birds. Trends in Ecology and Evolution 6:254–257 https://doi.org/10.1016/0169-5347(91)90072-6.

Berthold, P., and A.J. Helbig. 1992. The genetics of bird migration: stimulus, timing, and direction. Ibis 134:35–40 https://doi.org/10.1111/j.1474-919X.1992.tb04731.x.

BirdLife International and Handbook of the Birds of the World. 2016 Bird species distribution maps of the world. Version 6.0. Available at http://datazone.birdlife.org/species/requestdis.

Blake, J.G. 1986. Species-area relationship of migrants in isolated woodlots in east-central Illinois. Wilson Bulletin 98:291–296 https://www.jstor.org/stable/4162234.

Bolus, R.T., R.H. Diehl, F.R. Moore, J.L. Deppe, M.P. Ward, J. Smolinsky, and T.J. Zenzal, Jr. 2017. Swainson's thrushes do not show strong wind selectivity prior to crossing the Gulf of Mexico. Scientific Reports 7:14280 https://doi.org/10.1038/s41598-017-14668-3.

Botero, C.A., F.J. Weissing, J. Wright, and D.R. Rubenstein. 2015. Evolutionary tipping points in the capacity to adapt to environmental change. Proceedings of the National Academy of Sciences 112:184–189 https://doi.org/10.1073/pnas.1408589111.

Both, C., S. Bouwhouis, C.M. Lessels, and M.E. Visser. 2006. Climate change and population declines in a long-distance migratory bird. Nature 441:81–83 https://doi.org/10.1038/nature04539.

Buckardt Thomas, A. 2019. Improving Conservation of Declining Young Forest Birds through Adaptive Management. M.S. Thesis. University of Maine.

Buehler, D.A., A.M. Roth, R. Vallender, T.C. Will, J.L. Confer, R.A. Canterbury, S.B. Swarthout, K.V. Rosenberg, and L.P. Bulluck. 2007. Status and conservation priorities of golden-winged warbler (*Vermivora chrysoptera*) in North America. Auk 124:1439–1445 https://doi.org/10.1093/auk/124.4.1439.

Bulluck, L., D. Buehler, R. Vallender, and R.J. Robertson. 2013. Demographic comparison of golden-winged warbler (*Vermivora chrysoptera*) populations in northern and southern extremes of their breeding range. Wilson Journal of Ornithology 125:479–490 https://doi.org/10.1676/12-154.1.

Burgio, K.R., C.J. Carlson, and M.W. Tingley. 2017. Lazarus ecology: Recovering the distribution and migratory patterns of the extinct Carolina parakeet. Ecology and Evolution 7:5467–5475 https://doi.org/10.1002/ece3.3135.

Campbell-Staton, S.C., Z.A. Cheviron, N. Rochette, J. Catchen, J.B. Losos, and S.V. Edwards. 2017. Winter storms drive rapid phenotypic, regulatory, and genomic shifts in the green anole lizard. Science. 357:495-498 https://doi.org/10.1126/science.aam5512.

Chandler, R.B., S. Tolfree, J. Gerwin, C. Smalling, L. Chavarría-Duriaux, G. Duriaux, and D.I. King. 2016. Conservation implications of golden-winged warbler social and foraging behaviors during the nonbreeding season. Pp. 175–192 *in* Streby, H.M., D.E. Andersen, and D.A. Buehler (editors). Golden-winged warbler ecology, conservation and habitat management. Studies in Avian Biology (no. 49), CRC Press, Boca Raton, FL. https://hdl.handle.net/11299/189700.

Chen, I.–C., J.K. Hill, R. Ohlemüller, D.B. Roy, and C.D. Thomas. 2011. Rapid range shifts of species associated with high levels of climate warming. Science 333:1024–1026 https://doi.org/10.1126/science.1206432.

Chen, L. 2020. Impacts of climate change on wind resources over North America based on NA-CORDEX. Renewable Energy 153:1428–1438 https://doi.org/10.1016/j.renene.2020.02.090.

Cohen, E.B., and D.A. Satterfield. 2020. 'Chancing on a spectacle': Co-occurring animal migrations and interspecific interactions. Ecography 43:1–15 https://doi.org/10.1111/ecog.04958.

Cohen, E.B., J.A. Hostetler, M.T. Hallworth, C.S. Rushing, T.S. Sillett, P.P. Marra. 2018. Quantifying the strength of migratory connectivity. Methods in Ecology and Evolution 9:513–524 https://doi.org/10.1111/2041-210X.12916.

Cooke, W. W. 1904. Distribution and migration of North American warblers. U.S. Department of Agriculture, Division of Biological Survey, Bulletin No. 18.

Cooper, N.W., M.T. Hallworth, and P.P. Marra. 2017. Light-level geolocation reveals wintering distribution, migration routes, and primary stopover locations of an endangered long-distance migratory songbird. Journal of Avian Biology 48:209–219 https://doi.org/10.1111/jav.01096.

Cox, G.W. 1985. The evolution of avian migration systems between temperate and tropical regions of the New World. American Naturalist 126:451–474 https://doi.org/10.1086/284432.

Crick, H.Q.P. 2004. The impact of climate change on birds. Ibis 146:48–56 https://doi.org/10.1111/j.1474-919X.2004.00327.x.

Dávalos, L.M., A.C. Bejarano, M.A. Hall, H.L. Correa, A. Corthals, and O. Espejo. 2011.

Forests and drugs: Coca-driven deforestation in tropical biodiversity hotspots. Environmental Science and Technology 45:1219–1227 https://doi.org/10.1021/es102373d.

Davis, M., S. Faurby, and J. Svenning. 2018. Mammal diversity will take millions of years to recover from the current biodiversity crisis. Proceedings of the National Academy of Sciences 115:11262–11267 https://doi.org/10.1073/pnas.1804906115.

Dawbin, W.H. 1956. The migrations of humpback whales which pass the New Zealand coast. Transactions and Proceedings of the Royal Society of New Zealand 84:147–196.

Delancey, C.D., K. Islam, G.R. Kramer, G.J. MacDonald, A.R. Sharp, and B.M. Connare. 2020. Geolocators reveal migration routes, stopover sites, and nonbreeding dispersion in a population of cerulean warblers. Animal Migration 7:19–26 https://doi.org/10.1515/ami-2020-0003.

Delmore, K.E., and D.E. Irwin. 2014. Hybrid songbirds employ intermediate routes in a migratory divide. Ecology Letters 17:1211–1218 https://doi.org/10.1111/ele.12326.

DeLuca, W.V., B.K. Woodworth, C.C. Rimmer, P.P. Marra, P.D. Taylor, K.P. McFarland, S.A. Mackenzie, and D.R. Norris. 2015. Transoceanic migration by a 12 g songbird. Biology Letters 11:20141045 https://doi.org/10.1098/rsbl.2014.1045.

Deppe, J.L., M.P. Ward, R.T. Bolus, R.H. Diehl, A. Celis-Murillo, T.J. Zenzal, Jr., F.R. Moore, T.J. Benson, J.A. Smolinsky, L.N. Schofield, D.A. Enstrom, E.H. Paxton, G. Bohrer, T.A. Beveroth, A. Raim, R.L. Obringer, D. Delaney, and W.W. Cochran. 2015. Fat, weather, and date affect migratory songbirds' departure decisions, routes, and time it takes to cross the Gulf of Mexico. Proceedings of the National Academy of Sciences 112:E6331–E6338 https://doi.org/10.1073/pnas.1503381112.

Dingle, H. 2014. Migration: the biology of life on the move, 2nd edn. Oxford University Press, Oxford.

Dionne, M., C. Maurice, J. Gauthier, and F. Shaffer. 2008. Impact of hurricane Wilma on migrating birds: the case of the chimney swift. Wilson Journal of Ornithology 120:784-792 https://www.jstor.org/stable/20456239.

Dobbs, R.C., W.C. Barrow, Jr., C.W. Jeske, J. DiMiceli, T.C. Michot, and J.W. Beck. 2009. Short-term effects of hurricane disturbance on food availability for migrant songbirds during autumn stopover. Wetlands 29:123–134 https://doi.org/10.1672/08-78.1.

Dokter, A.M., A. Farnsworth, D. Fink, V. Ruiz-Gutierrez, W.M. Hochachka, F.A. La Sorte, O.J. Robinson, K.V. Rosenberg, and S. Kelling. 2018. Seasonal abundance and survival of North America's migratory avifauna determined by weather radar. Nature Ecology & Evolution 2:1603–1609 https://doi.org/10.1038/s41559-018-0666-4.

Egevang, C., I.J. Stenhouse, R.A. Phillips, A. Petersen, J.W. Fox, and J.R.D. Silk. 2010.

Tracking of Arctic terns *Sterna paradisaea* reveals longest animal migration. Proceedings of the National Academy of Sciences 107:2078–2081 https://doi.org/10.1073/pnas.0909493107.

Ekstrom PA. 2004. An advance in geolocation by light. Memoirs of National Institute of Polar Research Special Issue 58:210–226.

Faaborg, J., R.T. Holmes, A.D. Anders, K.L. Bildstein, K.M. Dugger, S.A. Gauthreaux, Jr., P. Heglund, K.A. Hobson, A.E. Jahn, D.H. Johnson, S.C. Latta, D.J. Levey II, P.P. Marra, C.L. Merkord, E. Nol, S.I. Rothstein, T.W. Sherry, T.S. Sillett, F.R. Thompson III, and N. Warnock. 2010. Conserving migratory land birds in the New World: Do we know enough? Ecological Applications 20:398–418 https://doi.org/10.1890/09-0397.1.

Federal Communications Commission (FCC) Geospatial Data, United States. 2012. Federal Communications Commission (FCC) Media Bureau and Wireless Telecommunications Bureau. http://wireless.fcc.gov/geographic/index.htm?job=licensing_database_extracts.

Finch, T., P. Suanders, J.M. Avilés, A. Bermejo, I Catry, J. de la Puente, T. Emmenegger, I. Margeda, P. Mayet, D. Parejo, E. Račinskis, J. Rodríguez-Ruiz, P. Sackl, T. Schwartz, M. Tiefenbach, F. Valera, C. Hewson, A. Franco, and S.J. Butler. 2015. A pan-European, multipopulation assessment of migratory connectivity in a near-threatened migrant bird. Diversity and Distributions 21:1051–1062 https://doi.org/10.1111/ddi.12345.

Finch, T., S.J. Butler, A.M.A. Franco, and W. Cresswell. 2017. Low migratory connectivity is common in long-distance migrant birds. Journal of Animal Ecology 86:662–673 https://doi.org/10.1111/1365-2656.12635.

Fischer, S.E. 2020. Post-fledging and migration ecology of gray vireos (*Vireo vicinior*) and using ArtScience to explore gender and identity. Master's thesis. University of Toledo, Toledo, OH. http://rave.ohiolink.edu/etdc/view?acc_num=toledo158895774132047.

Flockhart, D.T.T., J.B. Pichancourt, D.R. Norris, and T.G. Martin. 2015. Unravelling the annual cycle in a migratory animal: breeding-season habitat loss drives population declines of monarch butterflies. Journal of Animal Ecology 84:155–165 https://doi.org/10.1111/1365-2656.12253.

Fraser, K.C., B.J.M. Stutchbury, C. Silverio, P.M. Kramer, J. Barrow, D. Newstead, N. Mickle, B.F. Cousens, J.C. Lee, D.M. Morrison, T. Shaheen, P. Mammenga, K. Applegate, and J. Tautin. 2012. Continent-wide tracking to determine migratory connectivity and tropical habitat associations of a declining aerial insectivore. Proceedings of the Royal Society of London: Series B 297:rspb20122207 https://doi.org/10.1098/rspb.2012.2207.

Fudickar, A.M., M. Wikelski, and J. Partecke. 2012. Tracking migratory songbirds: accuracy of light-level loggers (geolocators) in forest habitats. Methods in Ecology and Evolution 3:47–52 https://doi.org/10.1111/j.2041-210X.2011.00136.x.

Fuller, R.A. 2016. Dispersion explains declines. Nature 531:451–452 https://doi.org/10.1038/531451a.

Gandini, P., P.D. Boersma, E. Frere, M. Gandini, T. Holik, and V. Lichtschein. 1994. Magellanic penguins (*Sphieniscus magellanicus*) affected by chronic petroleum pollution along coast of Chubut, Argentina. Auk 111:20–27 https://doi.org/10.2307/4088501.

Gill, R.E., T.L. Tibbits, D.C. Douglas, C.M. Handel, D.M. Mulcahy, J.C. Gottschalck, N. Warnock, B.J. McCaffery, P.F. Battley, and T. Piersma. 2009. Extreme endurance flights by landbirds crossing the Pacific Ocean: ecological corridor rather than barrier? Proceedings of the Royal Society of London: Series B 276:447–457 https://doi.org/10.1098/rspb.2008.1142.

Gilroy, J.J., J.A. Gill, S.H.M. Butchart, V.R. Jones, and A.M.A. Franco. 2016. Migratory diversity predicts population declines in birds. Ecology Letters 19:308–317 https://doi.org/10.1111/ele.12569.

Global Forecast System (GFS) [0.5 Deg.]. 2021. DOC/NOAA/NWS/NCEP/EMC Environmental Modeling Center, National Centers for Environmental Prediction, National Weather Service, NOAA, U.S. Department of Commerce. https://www.ncei.noaa.gov/access/metadata/landing-page/bin/iso?id=gov.noaa.ncdc:C00634.

Gómez, C., N.J. Bayly, D.R. Norris, S.A. Mackenzie, K.V. Rosenberg, P.D. Taylor, K.A. Hobson, and C.D. Cadena. 2017. Fuel loads acquired at stopover site influence the pace of intercontinental migration in a boreal songbird. Scientific Reports 7:3405 https://doi.org/10.1038/s41598-017-03503-4.

Goymann, W., F. Spina, A. Ferri, and L. Fusani. 2010. Body fat influences departure from stopover sites in migratory birds: evidence from whole-island telemetry. Biology Letters 6:478–481 https://doi.org/10.1098/rsbl.2009.1028.

Hahn, S., V. Amrhein, P. Zehtindijev, and F. Liechti. 2013. Strong migratory connectivity and seasonally shifting isotopic niches in geographically separated populations of a long-distance migrating songbird. Oecologia 173:1217–1225 https://doi.org/10.1007/s00442-013-2726-4.

Hallworth, M.T., T.S. Sillett, S.L. Van Wilgenburg, K.A. Hobson, and P.P. Marra. 2015. Migratory connectivity of a Neotropical migratory songbird revealed by archival light-level geolocators. Ecological Applications 25:336–347 https://doi.org/10.1890/14-0195.1.

Hallworth, M.T., E. Bayne, E. McKinnon, O. Love, J.A. Tremblay, B. Drolet, J. Ibarzabal, S. Van Wilgenburg, and P.P. Marra. 2021. Habitat loss on the breeding grounds is a major contributor to population declines in a long-distance migratory songbird. Proceedings of the Royal Society of London: Series B 228:20203164 https://doi.org/10.1098/rspb.2020.3164.

Hansen, M.C., S.V. Stehman, and P.V. Potapov. 2010. Quantification of global gross forest loss. Proceedings of the National Academy of Sciences 107:8650–8655 https://doi.org/10.1073/pnas.0912668107.

Hanson, H.C., and R.H. Smith, 1950. Canada geese of the Mississippi Flyway with special reference to an Illinois flock. Illinois Natural History Survey Bulletin 25:67–210.

Hansson, M., and J. Pettersson. 1989. Competition and fat deposition in goldcrests (*Regulus regulus*) at a migration stop-over site. Die Vogelwarte 35:21–31.

Harringmeyer, O.S., M.L. Woolfolk, and H.E. Hoekstra. 2021. Fishing for the genetic basis of migratory behavior. Cell 184:303–305 https://doi.org/10.1016/j.cell.2020.12.037.

Harrison, X.A., J.D. Blount, R. Inger, D.R. Norris, and S. Bearhop. 2011. Carry-over effects as drivers of fitness differences in animals. Journal of Animal Ecology 80:4–18 https://doi.org/10.1111/j.1365-2656.2010.01740.x.

Harrison, X.A., T. Tregenza, R. Inger, K. Colhoun, D.A. Dawson, G.A. Gudmundsson, D.J. Hodgson, G.J. Hosrburgh, G. McElwaine, and S. Bearhop. 2010. Cultural inheritance drives site fidelity and migratory connectivity in a long-distance migrant. Molecular Ecology 19:5484–5496 https://doi.org/10.1111/j.1365-294X.2010.04852.x.

Hebblewhite, M., and E.H. Merrill. 2007. Multiscale wolf predation risk for elk: does migration reduce risk? Oecologia 152:377–387 https://doi.org/10.1007/s00442-007-0661-y.

Heinsohn, R., M. Webb, R. Lacy, A. Terauds, R. Alderman, and D. Stojanovic. 2015. A severe predator-induced population decline predicted for endangered, migratory swift parrots (*Lathamus discolor*). Biological Conservation 186:75–82 https://doi.org/10.1016/j.biocon.2015.03.006.

Hewson, C. M., K. Thorup, J. W. Pearce-Higgins, and P. W. Atkinson. 2016. Population decline is linked to migration route in the common cuckoo. Nature Communications 7:12296 https://doi.org/10.1038/ncomms12296.

Hijmans, R.J. 2020. raster: Geographic data analysis and modeling. R package version 3.0-12 https://CRAN.R-project.org/package=raster.

Hill, J.M., and R.B. Renfrew. 2019. Migratory patterns and connectivity of two North American grassland bird species. Ecology and Evolution 9:680–692 https://doi.org/10.1002/ece3.4795.

Hill, R.D., and M.J. Bruan. 2001. Geolocation by light-level–next step: Latitude. Pp. 315–330 *in* Sibert JR, Nielsen J (editors) Electronic Tagging and Tracking in Marine Fisheries. Kluwer Academic Publishers, Dordrecht, The Netherlands.

Hobson, K.A. 1999. Tracing origins and migration of wildlife using stable isotopes: a review. Oecologia 120:314–326 https://doi.org/10.1007/s004420050865.

Hobson, K.A., K.J. Kardynal, S.L. Van Wilgenburg, G. Albrecht, A. Salvadori, M.D. Cadman, F. Liechti, and J.W. Fox. 2015. A continent-wide migratory divide in North American breeding barn swallows (*Hirundo rustica*). PLoS ONE 10:e0129340 https://doi.org/10.1371/journal.pone.0129340.

Hobson, K.A., S.L. Van Wilgenburg, A.M. Roth, R.E. Bennett, N.J. Bayly, L. Chavarría-Duriaux, G.J. Colorado, P. Elizondo, C.G. Rengifo, and J.D. Ritterson. 2016. Golden-winged Warbler migratory connectivity derived from stable isotopes. Pp. 193–203 *in* Streby, H.M., D.E. Andersen, and D.A. Buehler (editors). Golden-winged warbler ecology, conservation and habitat management. Studies in Avian Biology (no. 49), CRC Press, Boca Raton, FL. https://hdl.handle.net/11299/189700.

Hoen, B.D., J.E. Diffendorfer, J.T. Rand, L.A. Kramer, C.P. Garrity, H.E. Hunt. 2018. United States Wind Turbine Database (ver. 2.3, January 2020): U.S. Geological Survey, American Wind Energy Association, and Lawrence Berkeley National Laboratory data release, https://doi.org/10.5066/F7TX3DN0.

Holland, R.A., M. Wikelski, and D.S. Wilcove. 2006. How and why do insects migrate? Science 313:794–796 https://doi.org/10.1126/science.1127272.

Hopcraft, J.G.C., J.M. Morales, H.L. Beyer, M. Borner, E. Mwangomo, A.R.E. Sinclair, H. Olff, and D.T. Haydon. 2014. Competition, predation, and migration: Individual choice patterns of Serengeti migrants captured by hierarchical models. Ecological Monographs 84:355–372 https://doi.org/10.1890/13-1446.1.

Hornseth, M.L., A.A. Walpole, L.R. Walton, J. Bowman, J.C. Ray, M.-J. Fortin, and D.L. Murray. 2014. Habitat loss, not fragmentation, drives occurrence patterns of Canada lynx at the southern range periphery. PLoS ONE 9:e113511 https://doi.org/10.1371/journal.pone.0113511.

Hostetler, J.A., and M.T. Hallworth. 2020. MigConnectivity: Estimating strength of migratory connectivity for migratory animals. R package version 0.3.1.

Iwamura, T., H.P. Possingham, I. Chadès, C. Minton, N.J. Murray, D. Rogers, E. Treml, and R.A. Fuller. 2013. Migratory connectivity magnifies the consequences of habitat loss from sea-level rise for shorebird populations. Proceedings of the Royal Society of London: Series B 280:20130325 https://doi.org/10.1098/rspb.2013.0325.

Jameson, J.W., and C.K.R. Willis. 2014. Activity of tree bats at anthropogenic tall structures: Implications for mortality of bats at wind turbines. Animal Behaviour 97:145–152 https://doi.org/10.1016/j.anbehav.2014.09.003.

Johnson, D.H. 1980. The comparison of usage and availability measurements for evaluating resource preference. Ecology 61:65–71 https://doi.org/10.2307/1937156.

Jones, T., and W. Cresswell. 2010. The phenological mismatch hypothesis: Are declines of migrant birds linked to uneven global climate change? Journal of Animal Ecology 79:98–108 https://doi.org/10.1111/j.1365-2656.2009.01610.x.

Kassambara, A., and F. Mundt. 2019. factoextra: extract and visualize the results of multivariate data analyses. R package version 1.0.6 https://CRAN.R-project.org/package=factoextra.

Kays, R., M.C. Crofoot, W. Jetz, and M. Wikelski. 2015. Terrestrial animal tracking as an eye on life and planet. Science 348:aaa2478 https://doi.org/10.1126/science.aaa2478.

Kerlinger, P. 2000. Avian mortality at communication towers: a review of recent literature, research, and methodology. US Fish & Wildlife Publications 162 https://digitalcommons.unl.edu/usfwspubs/162.

Goldewijk, K., A. Beusen, M. de Vos, and G. van Drecht. 2011. The HYDE 3.1 spatially explicit database of human induced land use change over the past 12,000 years. Global Ecology and Biogeography 20:73–86 https://doi.org/10.1111/j.1466-8238.2010.00587.x.

Goldewijk, K., A. Beusen, and P. Janssen. 2010. Long term dynamic modeling of global population and built-up area in a spatially explicit way, HYDE 3 .1. The Holocene 20:565-573 http://dx.doi.org/10.1177/0959683609356587.

Knight, S.M., G.M. Pitman, D.T.T. Flockhart, and D.R. Norris. 2019. Radio-tracking reveals how wind and temperature influence the pace of daytime insect migration. Biology Letters 15:20190327 https://doi.org/10.1098/rsbl.2019.0327.

Knight, E.C., A. Harrison, A.L. Scarpignato, S.L. Van Wilgenburg, E.M. Bayne, J.W. Ng, E. Angell, R. Bowman, R.M. Brigham, B. Drolet, W.E. Easton, T.R. Forrester, J.T. Foster, S. Haché, K.C. Hannah, K.G. Hick, J. Ibarzabal, T.L. Imlay, S.A. Mackenzie, A. Marsh, L.P. McGuire, G.N. Newberry, D. Newstead, A. Sidler, P.H. Sinclair, J.L. Stephens, D.L. Swanson, J.A. Tremblay, and P.P.

Marra. 2021. Comprehensive estimation of spatial and temporal migratory connectivity across the annual cycle to direct conservation efforts. Ecography 44:665-679 https://doi.org/10.1111/ecog.05111.

Knight, S.M., D.W. Bradley, R.G. Clark, E.A. Gow, M. Bélisle, L.L. Berzins, T. Blake, E.S. Bridge, L. Burke, R.D. Dawson, P.O. Dunn, D. Garant, G.L. Holroyd, D.J. Hussell, O. Lansdorp, A.J. Laughlin, M.L. Leonard, F. Peltier, D. Shutler, L. Siefferman, C.M. Taylor, H.E. Trefry, C.M. Vleck, D. Vleck, D.W. Winkler, L.A. Whittingham, and D.R. Norris. 2018. Constructing and evaluating a continent-wide migratory songbird network across the annual cycle. Ecological Monographs 88:445–460 https://doi.org/10.1002/ecm.1298.

Kramer, G.R., D.E. Andersen, D.A. Buehler, P.B. Wood, S.M. Peterson, J.A. Lehman, K.R. Aldinger, L.P. Bulluck, S. Harding, J.A. Jones, J.P. Loegering, C. Smalling, R. Vallender, and H.M. Streby. 2018b. Data from range-wide study of migratory connectivity of *Vermivora* warblers. Retrieved from the University of Minnesota Digital Conservancy, http://hdl.handle.net/:70968.

Kramer, G.R., D.E. Andersen, D.A. Buehler, P.B. Wood, S.M. Peterson, J.A. Lehman, K.R. Aldinger, L.P. Bulluck, S. Harding, J.A. Jones, J.P. Loegering, C. Smalling, R. Vallender, and H.M. Streby. 2018a. Population trends in *Vermivora* warblers are linked to strong migratory connectivity. Proceedings of the National Academy of Sciences 115:E3192–2300 https://doi.org/10.1073/pnas.1718985115.

Kramer, G.R., H.M. Streby, S.M. Peterson, J.A. Lehman, D.A. Buehler, P.B. Wood, D.J. McNeil, J.L. Larkin, and D.E. Andersen. 2016. Raw light-level geolocator data from golden-winged warblers breeding at three sites in North America. Retrieved from the Data Repository for the University of Minnesota, http://doi.org/10.13020/D6R59C.

Kramer, G.R., H.M. Streby, S.M. Peterson, J.A. Lehman, D.A. Buehler, P.B. Wood, D.J. McNeil, J.L. Larkin, and D.E. Andersen. 2017. Nonbreeding isolation and population-specific migration patterns among three populations of golden-winged warblers. Condor 119:108–121 https://doi.org/10.1650/CONDOR-16-143.1.

Kramer, G.R., R.K. Pagel, K. Maley, C. Ziegler, S.M. Peterson, D.E. Andersen, D.A. Buehler, and H.M. Streby. 2020. Say what? Bivalent singing in *Vermivora* warblers. Ecology 101:e02881.

Kramer, G.R., S.M. Peterson, K.O. Daly, H.M. Streby, and D.E. Andersen. 2019. Left out in the rain: Comparing productivity of two associated species exposes a leak in the umbrella species concept. Biological Conservation 233:276–288. https://doi.org/10.1016/j.biocon.2019.02.039.

Lain, E.J., T.J. Zenzal, Jr., F.R. Moore, W.C. Barrow, Jr., and R.H. Diehl. 2017. Songbirds are resilient to hurricane disturbed habitats during spring migration. Journal of Avian Biology 48:815–826 https://doi.org/10.1111/jav.01215.

Landsea, C.W., and J.L. Franklin. 2013. Atlantic Hurricane Database uncertainty and presentation of a new database format. Monthly Weather Review 141:3576–3592 https://doi.org/10.1175/MWR-D-12-00254.1.

Larkin, J.L., D. Raybuck, A. Roth, L. Chavarría-Duriaux, G. Duiraux, M. Siles, and C. Smalling. 2017. Geolocators reveal migratory connectivity between wintering and breeding areas of Golden-winged Warblers. Journal of Field Ornithology 88:288–298. https://doi.org/10.1111/jofo.12210.

Lavallée, C.D., S.B. Assadi, A.M. Korpach, J.D. Ray, J.D. Fischer, J. Siegrist, and K.C. Fraser. 2021. The use of nocturnal flights for barrier crossing in a diurnally migrating songbird. Movement Ecology 9:21 https://doi.org/10.1186/s40462-021-00257-7.

Legagneux, P., P.L.F. Fast, G. Gauthier, and J. Bêty. 2012. Manipulating individual state during migration provides evidence for carry-over effects modulated by environmental conditions. Proceedings of the Royal Society of London: Series B 279:876–883 https://doi.org/10.1098/rspb.2011.1351.

Lehman, J.A. 2017. Survival and habitat selection of golden-winged warblers (*Vermivora chrysoptera*) during nesting and post-fledging periods at North Cumberland Wildlife Management Area, Tennessee. Master's thesis. University of Tennessee, Knoxville, TN. https://trace.tennessee.edu/utk_gradthes/4953.

Levin, S.A. 1992. The problem of pattern and scale in ecology. Ecology 73:1943–1967 https://doi.org/10.2307/1941447.

Lincoln, F.C. 1921. The history and purposes of bird banding. Auk 38:217–218 https://doi.org/10.2307/4073884.

Lincoln, F.C. 1935. Migration of birds. Circular 363. U.S. Department of Agriculture, Washington D.C., USA.

Lindström, Å. 1989. Finch flock size and risk of hawk predation at a migratory stopover site. Auk 106:225–232 https://www.jstor.org/stable/4087716.

Lisovski, S., S. Wotherspoon, and M. Sumner. 2016. TwGeos: basic data processing for light-level geolocation archival tags. R package version 0.1.2.

Lloyd, P., T.E. Martin, R.L. Redmond, U. Langner, and M.M. Hart. 2005. Linking demographic effects of habitat fragmentation across landscapes to continental source-sink dynamics. Ecological Applications 15:1504–1514 https://doi.org/10.1890/04-1243.

Longcore, T., C. Rich, P. Mineau, B. MacDonald, D.G. Bert, L.M. Sullivan, E. Mutrie, S.A. Gauthreaux, Jr., M.L. Avery, R.L. Crawford, A.M. Manville II, E.R. Travis, and D. Drake. 2013. Avian mortality at communications towers in the United States and Canada: which species, how many, and where? Biological Conservation 158:410–419 https://doi.org/10.1016/j.biocon.2012.09.019.

Loss, S.R., T. Will, S.S. Loss, and P.P. Marra. 2014. Bird-building collisions in the United States: Estimates of annual mortality and species vulnerability. Condor 116:8–23 https://doi.org/10.1650/CONDOR-13-090.1.

Loss, S.R., T. Will, and P.P. Marra. 2013. Estimates of bird collision mortality at wind facilities in the contiguous United States. Biological Conservation 168:201–209 https://doi.org/10.1016/j.biocon.2013.10.007.

Loss, S.R., T. Will, and P.P. Marra. 2015. Direct mortality of birds from anthropogenic causes. Annual Review of Ecology, Evolution, and Systematics 46:99–120 https://doi.org/10.1146/annurev-ecolsys-112414-054133.

Malcolm, S.B. 2018. Anthropogenic impacts on mortality and population viability of the monarch butterfly. Annual Review of Entomology 63:277–302 https://doi.org/10.1146/annurev-ento-020117-043241.

Mandel, J.T., K.L. Bildstein, G. Bohrer, and D.W. Winkler. 2008. Movement ecology of migration in turkey vultures. Proceedings of the National Academy of Sciences 105:19102–19107 https://doi.org/10.1073/pnas.0801789105.

Mank, J.E., E. Axelsson, and H. Ellegren. 2007. Fast-X on the Z: Rapid evolution of sex-linked genes in birds. Genome Research 17:618–624 http://www.genome.org/cgi/doi/10.1101/gr.6031907.

Mann, M.E., and K.A. Emanuel. 2006. Atlantic hurricane trends linked to climate change. Eos 87:233–244 https://doi.org/10.1029/2006EO240001.

Marra, P.P., E.B. Cohen, S.R. Loss, J.E. Rutter, and C.M. Tonra. 2015. A call for full annual cycle research in animal ecology. Biology Letters 11:20150552 https://doi.org/10.1098/rsbl.2015.0552.

Marra, P.P., K.A. Hobson, and R.T. Holmes RT. 1998. Linking winter and summer events in a migratory bird by using stable-carbon isotopes. Science 282:1884–1886 https://doi.org/10.1126/science.282.5395.1884.

Martínez-Meyer, E., A.T. Peterson, and A.G. Navarro-Sigüenza. 2004. Evolution of seasonal ecological niches in the *Passerina* buntings (Aves: Cardinalidae). Proceedings of the Royal Society of London: Series B 271:1151–1157 https://doi.org/10.1098/rspb.2003.2564.

Maury, M.F. 1851. The winds and currents of the sea. National Observatory, Washington.

Mayr, E. 1939. The sex ratio in wild birds. American Naturalist 73:156–179 https://www.journals.uchicago.edu/doi/abs/10.1086/280824.

McKinnon, E.A., and O.P. Love. 2018. Ten years tracking the migration of small landbirds: Lessons learned in the golden-age of bio-logging. Auk 135:834–856 https://doi.org/10.1642/AUK-17-202.1.

McKinnon, E.A., C. Artuso, and O.P. Love. 2017. The mystery of the missing warbler. Ecology 98:1970–1972 https://doi.org/10.1002/ecy.1844.

McNeil, D.J. 2019. Population dynamics of species recovery: Multiscale demography in restored habitats. PhD Dissertation. Cornell University, Ithaca, NY. https://doi.org/10.7298/S2VW-CS78.

Meiyappan, P., and A.K. Jain AK. 2012. Three distinct global estimates of historical land-cover change and land-use conversions for over 200 years. Frontiers of Earth Science 6:122–139 https://doi.org/10.1007/s11707-012-0314-2.

Mihoub, J.B., O. Gimenez, P. Pilard, and F. Sarrazin. 2010. Challenging conservation of migratory species: Sahelian rainfalls drive first-year survival of the vulnerable lesser kestrel *Falco naumanni*. Biological Conservation 143:839–847 https://doi.org/10.1016/j.biocon.2009.12.026.

Milner-Gulland, E.J., O.M. Bukreeva, T. Coulson, A.A. Lushchekina, M.V. Kholodova, A.B. Bekenov, and I.A. Grachev. 2003. Reproductive collapse in saiga antelope harems. Nature 422:135 https://doi.org/10.1038/422135a.

Nakazawa, Y., A.T. Peterson, E. Martínez-Meyer, and A.G. Navarro-Sigüenza. 2004. Seasonal niches of Nearctic-Neotropical migratory birds: Implications for the evolution of migration. Auk 121:610–618 https://doi.org/10.2307/4090425.

National Oceanic and Atmospheric Administration. 2018. Severe Weather Database Files (1950–2017). https://www.spc.noaa.gov/wcm/#data.

Negret, P.J., J. Allan, A. Braczkowski, M. Maron, J.E.M Watson. 2017. Need for conservation planning in postconflict Colombia. Conservation Biology 31:499–500 https://doi.org/10.1111/cobi.12935.

Neumann, L.K., A.E. Higdon, E.A. Flaherty, B.J. Bumgardner, A.B. Wilms, K.D. Gavenda, C.D. Delancey, and J.B. Dunning, Jr. 2021. Delineating the origin of migratory northern saw-whet owls (*Aegolius acadicus*) in Indiana using stable isotope analysis. Wilson Journal of Ornithology 132:967–977 https://doi.org/10.1676/19-00036.

Neville, K.J., R. Vallender, and R.J. Robertson. 2008. Nestling sex ratio of golden-winged warblers *Vermivora chrysoptera* in an introgressed population. Journal of Avian Biology 39:599–604 https://www.jstor.org/stable/30243857.

Newton, I. 2006. Can conditions experienced during migration limit the population levels of birds? Journal of Ornithology 147:146–166 https://doi.org/10.1007/s10336-006-0058-4.

Newton, I. 2007. Weather-related mass-mortality events in migrants. Ibis 149:453–467 https://doi.org/10.1111/j.1474-919X.2007.00704.x.

Newton, I. 2012. Obligate and facultative migration in birds: ecological aspects. Journal of Ornithology 153:171–180 https://doi.org/10.1007/s10336-011-0765-3.

Nicholson, M.C., R.T. Bowyer, and J.G. Kie. 1997. Habitat selection and survival of mule deer: tradeoffs associated with migration. Journal of Mammalogy 78:483–504 https://doi.org/10.2307/1382900.

Norevik, G., S. Åkesson, T. Artois, N. Beenaerts, G. Conway, B. Cresswell, R. Evens, I. Henderson, F. Jiguet, A. Hedenström. 2020. Wind-associated detours promote seasonal migratory connectivity in a flapping flying long-distance avian migrant. Journal of Animal Ecology 89:635–646 https://doi.org/10.1111/1365-2656.13112.

O'Shea, T.J., P.M. Cryan, D.T.S. Hayman, R.K. Plowright, and D.G. Streicker. 2016. Multiple mortality events in bats: A global review. Mammal Review 46:175–190 https://doi.org/10.1111/mam.12064.

Oakleaf, J. R., C. M. Kennedy, S. Baruch-Mordo, P. C. West, J. S. Gerber, L. Jarvis, and J. Kiesecker. 2019. Development Threat Index. Palisades, NY: NASA Socioeconomic Data and Applications Center (SEDAC). https://doi.org/10.7927/61jv-th84. Accessed 02 February 2020.

Oakleaf, J. R., C. M. Kennedy, S. Baruch-Mordo, P. C. West, J. S. Gerber, L. Jarvis, and J. Kiesecker. 2015. A world at risk: Aggregating development trends to forecast global habitat conversion. PLoS ONE 10: e0138334 https://doi.org/10.1371/journal.pone.0138334.

Otto, S.P. 2018. Adaptation, speciation and extinction in the Anthropocene. Proceedings of the Royal Society of London: Series B 285:20182047 https://doi.org/10.1098/rspb.2018.2047.

Ouwehand, J., M.P. Ahola, A.N.M.A. Ausems, E.S. Bridge, M. Burgess, S. Hahn, C. Hewson, R.H.G. Klaassen, T. Laaksonen, H.M. Lampe, W. Velmala, and C. Both. 2016. Light-level geolocators reveal migratory connectivity in European populations of pied flycatchers *Ficedula hypoleuca*. Journal of Avian Biology 47:69–83. https://doi.org/10.1111/jav.00721.

Pagel, R.K., E.H. West, A.W. Jones, and H.M. Streby. 2020. Variation in individual autumn migration and winter paths of Great Lakes red-headed woodpeckers (*Melenerpes erythrocephalus*). Animal Migration 7:9–18 https://doi.org/10.1515/ami-2020-0002.

Pardieck, K.L., D.J. Ziolkowski, Jr, M. Lutmerding, K. Campbell, and M.A.R. Hudson.

2016. North American Breeding Bird Survey Dataset 1966-2016, version 2016.0. U.S. Geological Survey, Patuxent Wildlife Research Center. www.pwrcusgs.gove/BBS/RawData. Accessed 1 Aug 2016.

Parkes, K.C. 1951. The genetics of the golden-winged X blue-winged warbler complex. Wilson Bulletin 63:5–15.

Partners in Flight. 2020. Population Estimates Database, version 3.1. Available at http://pif.birdconservancy.org/PopEstimates. Accessed on 14 March 2021.

Paynter, R.A., Jr. 1953. Autumnal migrants on the Campeche Bank. Auk 70:338–349 https://doi.org/10.2307/4081323.

Pedersen, T.L. 2021. ggforce: Accelerating ‘ggplot2’. R package version 0.3.3. https://CRAN.R-project.org/package=ggforce.

Peterson, S.M., H.M. Streby, G.R. Kramer, J.A. Lehman, D.A. Buehler, and D.E. Andersen. 2015. Geolocators on golden-winged warblers do not affect migratory ecology. Condor 117:256–261 https://doi.org/10.1650/CONDOR-14-200.1.

Probst, J.R. 1986. A review of factors limiting the Kirtland’s warbler on its breeding grounds. American Midland Naturalist 116:87–100 https://www.jstor.org/stable/2425940.

Prop, J., J.M. Black, and P. Shimmings. 2003. Travel schedules to the High Arctic: Barnacle geese trade-off the timing of migration with accumulation of fat deposits. Oikos 103:403–414 http://www.jstor.org/stable/3548173.

Pulido, F., and M. Widmer. 2005. Are long-distance migrants constrained in their evolutionary response to environmental change? Causes of variation in the timing of autumn migration in a blackcap (*S. atricapilla*) and two garden warbler (*Sylvia borin*) populations. Annals of the New York Academy of Sciences 1046:228–241 https://doi.org/10.1196/annals.1343.020.

R Core Team. 2016. R: A language and environment for statistical computing. R Foundation for Statistical Computing, Vienna, Austria. https://www.R-project.org/.

R Core Team. 2019. R: A language and environment for statistical computing. R Foundation for Statistical Computing, Vienna, Austria. https://www.R-project.org/.

R Core Team. 2020. R: A language and environment for statistical computing. R Foundation for Statistical Computing. Vienna, Austria. https://www.R-project.org/.

R Core Team. 2021. R: A language and environment for statistical computing. R Foundation for Statistical Computing, Vienna, Austria. https://www.R-project.org/.

Rakhimberdiev, E., A. Saveliev, T. Piersma, and J. Karagicheva. 2017. FLightR: an R package for reconstructing animal paths from solar geolocation loggers. Methods for Ecology and Evolution. https://doi.org/doi:10.1111/2041-210X.12765.

Rakhimberdiev, E., and A. Saveliev. 2019. FLightR: SSM for solar geolocation. R package version 0.4.9 http://github.com/eldarrak/FLightR.

Rakhimberdiev, E., N.R. Senner, M.A. Verhoeven, D.W. Winkler, W. Bouten, and T. Piersma. 2016. Comparing inferences of solar geolocation data against high-precision GPS data: annual movements of a double-tagged black-tailed godwit. Journal of Avian Biology 47:589–596 https://doi.org/10.1111/jav.00891.

Rakhimberdiev, E., D. Winkler, E. Bridge, N. Seavy, D. Sheldon, T. Piersma, and D. Saveliev. 2015. A hidden Markov model for reconstructing animal paths from solar geolocation loggers using templates for light intensity. Movement Ecology 3:25 https://doi.org/10.1186/s40462-015-0062-5.

Rappole, J.H. 1995. Ecology of Migrant Birds: A Neotropical Perspective. Smithsonian Institutional Press, Washington, DC.

Rappole, J.H., and A.R. Tipton. 1991. New harness design for attachment of radio transmitters to small passerines. Journal of Field Ornithology 62:335–337 https://www.jstor.org/stable/20065798.

Rappole, J.H., M.A. Ramos. 1994. Factors affecting migratory bird routes over the Gulf of Mexico. Bird Conservation International 4:251–262 https://doi.org/doi:10.1017/S095927090000280X.

Renfrew, R., D. Kim, N. Perlut, and M.D. Cadman. 2019. Migration tactics of a long-distance migratory songbird from across a continental breeding range. Wilson

Journal of Ornithology 131:735–749 https://doi.org/10.1676/1559-4491-131.4.735.

Reynolds, M.D., B.L. Sullivan, E. Hallstein, S. Matsumoto, S. Kelling, M. Merrifield, D. Fink, A. Johsnston, W.M. Hochachka, N.E. Bruns, M.E. Reiter, S. Veloz, C. Hickey, N. Elliott, L. Martin, J.W. Fitzpatrick, P. Spraycar, G.H. Golet, C.McColl, C. Low, and S.A. Morrison. 2017. Dynamic conservation for migratory species. Science Advances 3:e1700707 http://www.doi.org/10.1126/sciadv.1700707.

Richardson, D.E., K.E. Marancik, J.R. Guyon, M.E. Lutcavage, B. Galuardi, C.H. Lam, H.J. Walsh, S. Wildes, D.A. Yates, and J.A. Hare. 2016. Discovery of a spawning ground reveals diverse migration strategies in Atlantic bluefin tuna (*Thunnus thynnus*). Proceedings of the National Academy of Sciences 113:3299–3304 https://doi.org/10.1073/pnas.1525636113.

Robbins, C.S., J.R. Sauer, R.S. Greenberg, S. and Droege. 1989. Population declines in North American birds that migrate to the Neotropics. Proceedings of the National Academy of Sciences, USA 86:7658–7662 https://doi.org/10.1073/pnas.86.19.7658.

Robertson, B.A., and R.L. Hutto. 2006. A framework for understanding ecological traps and an evaluation of existing evidence. Ecology 87:1075–1085 https://doi.org/10.1890/0012-9658(2006)87[1075:AFFUET]2.0.CO;2.

Robinson, R.A., H.Q.P. Crick, J.A. Learmonth, I.M.D. Maclean, C.D. Thomas, F. Beirlein, M.C. Forchhammer, C.M. Francis, J.A. Gill, B.J. Godley, J. Harwood, G.C. Hays, B. Huntly, A.M. Hutson, G.J. Pierce, M.M. Rehfisch, D.W. Sims, B.M. Santos, T.H. Sparks, D.A. Stroud, and M.E. Visser. 2009. Travelling through a warming world: climate change and migratory species. Endangered Species Research 7:87–99 https://doi.org/10.3354/esr00095.

Rodenhouse, N.L., T.S. Sillett, P.J. Doran, and R.T. Holmes. 2003. Multiple density-dependence mechanisms regulate a migratory bird population during the breeding season. Proceedings of the Royal Society of London: Series B 270:2105–2110 https://doi.org/10.1098/rspb.2003.2438.

Rohrbaugh, R.W., D.A. Buehler, S.B. Swarthout, D.I. King, J.L. Larkin, K.V. Rosenberg, A.M. Roth, R. Vallender, and T. Will. 2016. Conservation perspectives: Review of new science and primary threats to golden-winged warblers. Pp. 207–215 *in* Streby, H.M., D.E. Andersen, and D.A. Buehler (editors). Golden-winged warbler ecology, conservation and habitat management. Studies in Avian Biology (no. 49), CRC Press, Boca Raton, FL. https://hdl.handle.net/11299/189700.

Rosenberg, K.V., T. Will, D.A. Buehler, S.B. Swarthout, W.E. Thogmartin, R.E. Bennett, and R.B. Chandler. 2016. Dynamic distributions and population declines of golden-winged warblers. Pp. 3–28 *in* Streby, H.M., D.E. Andersen, and D.A. Buehler (editors). Golden-winged warbler ecology, conservation and habitat management. Studies in Avian Biology (no. 49), CRC Press, Boca Raton, FL. https://hdl.handle.net/11299/189700.

Runge, C.A., J.E.M. Watson, S.H.M. Butchart, J.O. Hanson, H.P. Possingham, and R.A. Fuller. 2015. Protected areas and global conservation of migratory birds. Science. 350:1255–1258 https://doi.org/0.1126/science.aac9180.

Runge, C.A., J.E.M. Watson, S.H.M. Butchart, J.O. Hanson, H.P. Possingham, S.G. Willis, and R.A. Fuller. 2014. Conserving mobile species. Frontiers in Ecology and the Environment 12:395–402 https://doi.org/10.1890/130237.

Rushing, C.S., A.M. Van Tatenhove, A.J. Sharp, V. Ruiz-Gutierrez, M.C. Freeman, P.W. Sykes, A.M. Given, and T.S. Sillett. 2020. Integrating tracking and resight data enables unbiased inferences about migratory connectivity and winter range survival from archival tags. Ornithological Applications 123:duab010 https://doi.org/10.1093/ornithapp/duab010.

Sanderson, F.J., P.F. Donald, D.J. Pain, I.J. Burfield, and F.P.J. van Brommel. 2006. Long-term population declines in Afro-Palearctic migrant birds. Biological Conservation 131:93–105 https://doi.org/10.1016/j.biocon.2006.02.008.

Sauer, J.R., D.K. Niven, J.E. Hines, D.J. Ziolkowski, K.L. Pardieck, J.E. Fallon, and W.A. Link. 2017. The North American Breeding Bird Survey, Results and Analysis 1966–2015. Version 2.07.2017 USGS Patuxent Wildlife Research Center, Laurel, MD.

Sauer, J.R., G.W. Pendleton, and B.G. Peterjohn. 1996. Evaluating causes of population change in North American insectivorous songbirds. Conservation Biology 10:465-478 https://doi.org/10.1046/j.1523-1739.1996.10020465.x.

Sawyer, H., M.J. Kauffman, R.M. Nielson, and J.S. Horne. 2009. Identifying and prioritizing ungulate migration routes for landscape-level conservation. Ecological Applications 8:2016–2025 https://doi.org/10.1890/08-2034.1.

Sayol, F., M.J. Steinbauer, T.M. Blackburn, A. Antonelli, and S. Faurby. 2020. Anthropogenic extinctions conceal widespread evolution of flightlessness in birds. Science Advances 6:eabb6095 https://doi.org/10.1126/sciadv.abb6095.

Schlaepfer, M.A., M.C. Runge, and P.W. Sherman. 2002. Ecological and evolutionary traps. Trends in Ecology and Evolution 17:474-480 https://doi.org/10.1016/S0169-5347(02)02580-6.

Scott, W.E.D. 1881. Some observations on the migration of birds. Bulletin of the Nuttall Ornithological Club 6:97–100.

Seidler, R.G., R.A. Long, J. Berger, S. Bergen, J.P. Beckmann. 2015. Identifying impediments to long-distance mammal migrations. Conservation Biology 29:99–109 https://doi.org/10.1111/cobi.12376.

Sherry, T.W. 2018. Identifying migratory birds' population bottlenecks in time and space. Proceedings of the National Academy of Sciences 115:3515–3517 https://doi.org/10.1073/pnas.1802174115.

Sherry, T.W., and R.T. Holmes. 1996. Winter habitat quality, population limitation, and conservation of Neotropical-Nearctic migrant birds. Ecology 77:36–48 https://doi.org/10.2307/2265652.

Shipley, J.R., C.W. Twining, C.C. Taff, M.N. Vitousek, A. Flack, D.W. Winkler. 2020. Birds advancing laying dates with warming springs face greater risk of chick mortality. Proceedings of the National Academy of Sciences 117:25590–25594 https://doi.org/10.1073/pnas.2009864117.

Sillett, T.S., and R.T. Holmes. 2002. Variation in survivorship of a migratory songbird throughout its annual cycle. Journal of Animal Ecology 71:296–308 https://www.jstor.org/stable/2693447.

Smallwood, K.S. 2013. Comparing bird and bat fatality-rate estimates among North-American wind-energy projects. Wildlife Society Bulletin 37:19–33 https://doi.org/10.1002/wsb.260.

Smolinsky, J.A., R.H. Diehl, T.A. Radzio, D.K. Delaney, F.R. Moore. 2013. Factors influencing the movement biology of migrant songbirds confronted with an ecological barrier. Behavioral Ecology and Sociobiology 67:2041–2051 https://doi.org/10.1007/s00265-013-1614-6.

Somveille, M., R.A. Bay, T.B. Smith, P.P. Marra, and K.C. Ruegg. 2021. A general theory of avian migratory connectivity. Ecology Letters 24:1848–1858 https://doi.org/10.1111/ele.13817.

Stadler, K. 2018. cultevo: Tools, measures, and statistical tests for cultural evolution. R package version 1.0.2. https://kevinstadler.github.io/cultevo/.

Stanley, C.Q., E.A. McKinnon, K.C. Fraser, M.P. Macpherson, G. Casbourn, L. Friesen, P.P. Marra, C. Studds, T.B. Ryder, N.E. Diggs, B.J.M. Stutchbury. 2014.

Connectivity of wood thrush breeding, wintering, and migration sites based on range-wide tracking. Conservation Biology 29:164–174 https://doi.org/10.1111/cobi.12352.

Stanley, C.Q., M.M. MacPherson, K.C. Fraser, E.A. McKinnon, and B.J.M. Stutchbury. 2012. Repeat tracking of individual songbirds reveal consistent migration timing but flexibility in route. PLoS ONE 7:e40688 https://doi.org/10.1371/journal.pone.0040688.

Strandberg, R., R.H.G. Klaassen, M. Hake, and T. Alerstam. 2010. How hazardous is the Sahara Desert crossing for migratory birds? Indications from satellite tracking of raptors. Biology Letters 6:297–300 https://doi.org/10.1098/rsbl.2009.0785.

Streby, H.M., and D.E. Andersen. 2011. Seasonal productivity in a population of migratory songbirds: Why nest data are not enough. Ecosphere 2:1–15 https://doi.org/10.1890/ES10-00187.1.

Streby, H.M., G.R. Kramer, S.M. Peterson, and D.E. Andersen. 2018. Evaluating outcomes of young forest management on a target species of conservation concern. *PeerJ* 6:e4319 https://doi.org/10.7717/peerj.4319.

Streby, H.M., G.R. Kramer, S.M. Peterson, J.A. Lehman, D.A. Buehler, and D.E. Andersen. 2015a. Tornadic storm avoidance behavior in breeding songbirds. Current Biology 25:98–102 https://doi.org/10.1016/j.cub.2014.10.079.

Streby, H.M., R.W. Rohrbaugh, D.A. Buehler, D.E. Andersen, R. Vallender, D.I. King, and T. Will. 2016a. Research on golden-winged warblers: Recent progress and current needs. Golden-winged Warbler Ecology, Conservation, and Habitat Management. Pp. 217–227 *in* Streby, H.M., D.E. Andersen, and D.A. Buehler (editors). Golden-winged warbler ecology, conservation and habitat management. Studies in Avian Biology (no. 49), CRC Press, Boca Raton, FL. https://hdl.handle.net/11299/189700.

Streby, H.M., S.M. Peterson, and D.E. Andersen. 2016b. Survival and habitat use of fledgling golden-winged warblers in the western Great Lakes region. Pp. 127–140 *in* Streby, H.M., D.E. Andersen, and D.A. Buehler (editors). Golden-winged warbler ecology, conservation and habitat management. Studies in Avian Biology (no. 49), CRC Press, Boca Raton, FL. https://hdl.handle.net/11299/189700.

Streby, H.M., T.L. McAllister, S.M. Peterson, G.R. Kramer, J.A. Lehman, and D.E. Andersen. 2015b. Minimizing marker mass and handling time when attaching radio-transmitters and geolocators to small songbirds. Condor 117:249–255 https://doi.org/10.1650/CONDOR-14-182.1.

Studds, C.E., B.E. Kendall, N.J. Murray, H.B. Wilson, D.I. Rogers, R.S. Clemens, K. Gosbell, C.J. Hassell, R. Jessop, D.S. Melville, D.A. Milton, C.D.T. Minton, H.P. Possingham, A.C. Riegen, P. Straw, E.J. Woehler, and R.A. Fuller. 2017. Rapid population decline in migratory shorebirds relying on Yellow Sea tidal mudflats as stopover sites. Nature Communications 8:14895 https://doi.org/10.1038/ncomms14895.

Stutchbury, B.J.M., S.A. Tarof, T. Done, E. Gow, P.M. Kramer, J. Tautin, J.W. Fox, V. Afanasyev. 2009. Tracking long-distance songbird migration by using geolocators. Science 323:896 https://doi.org/10.1126/science.1166664.

Taylor, C.M., and B.J.M. Stutchbury. 2017. Effects of breeding versus winter habitat loss and fragmentation on the population dynamics of a migratory songbird. Ecological Applications 26:424-437 https://doi.org/10.1890/14-1410.

Taylor, C.M. 2019. Effects of natal dispersal and density-dependence on connectivity patterns and population dynamics in a migratory network. Frontiers in Ecology and Evolution 7:354 https://doi.org/10.3389/fevo.2019.00354.

Taylor, P.D., T.L. Crewe, S.A. Mackenzie, D. Lepage, Y. Aubry, Z. Crysler, G. Finney, C.M. Francis, C.G. Gugliemo, D.J. Hamilton, R.L. Holberton, P.H. Loring, G.W. Mitchell, D.R. Norris, J. Paquet, R.A. Roncini, J.R. Smetzer, P.A. Smith, L.J. Welch, and B.K. Woodworth. 2017. The Motus Wildlife Tracking System: A collaborative research network to enhance the understanding of wildlife movement. Avian Conservation and Ecology 12:8 https://doi.org/10.5751/ACE-00953-120108.

Thorup, K. A.P. Tøttrup, M. Willemoes, R.H.G. Klaassen, R. Strandberg, M.L. Vega, H.P. Dasari, M.B. Araújo, M. Wikelski, and C. Rahbek. 2017. Resource tracking within and across continents in long-distance bird migrants. Science Advances 3:e1601360 https://doi.org/10.1126/sciadv.1601360.

Toews, D.P.L. 2017. Habitat suitability and the constraints of migration in New World warblers. Journal of Avian Biology https://doi.org/10.1111/jav.0115.

Toews, D.P.L., M.D. Baiz, G.R. Kramer, I.J. Lovette, H.M. Streby, and Scott A. Taylor. 2021. Extensive historical and contemporary hybridization suggests premating isolation in *Vermivora* warblers is not strong: A reply to Confer et al. Ecology and Evolution 11:10720–10723 https://doi.org/10.1002/ece3.7327.

Toews, D.P.L., S.A. Taylor, H.M. Streby, G.R. Kramer, and I.J. Lovette. 2019. Selection on *VPS13A* linked to migration in a songbird. Proceedings of the National Academy of Sciences 116:18272–18274 https://doi.org/10.1073/pnas.1909186116.

Toews, D.P.L., S.A. Taylor, R. Vallender, A. Brelsford, B.G. Butcher, P.W. Messer, and I.J. Lovette. 2016. Plumage genes and little else distinguish the genomes of hybridizing warblers. Current Biology 26:2313–2318 https://doi.org/10.1016/j.cub.2016.06.034.

Tonra, C.M., M.T. Hallworth, T.J. Boves, J. Reese, L.P. Bulluck, M. Johnson, C. Viverette, K. Percy, E.M. Ames, A. Matthews, M.C. Slevin, R.R. Wilson, and E.I. Johsnon. 2019. Concentration of a widespread breeding population in a few critically important nonbreeding areas: Migratory connectivity in the prothonotary warbler. Condor 121:duz019 https://doi.org/10.1093/condor/duz019.

Tredennick, A.T., G. Hooker, S.P. Ellner, and P.B. Adler. 2021. A practical guide to selecting models for exploration, inference, and prediction in ecology. Ecology 102:e03336 https://doi.org/10.1002/ecy.3336.

Turvey, S.T., and J.J. Crees. 2019. Extinction in the Anthropocene. Current Biology 29:R942–R995 https://doi.org/10.1016/j.cub.2019.07.040.

U.S. Geological Survey. 1997. Global Land Cover Characterization Program. Version 1.2. Archived by National Aeronautics and Space Administration, U.S. Government, USGS. http://landcover.usgs.gov/glcc/.

Vallender, R., V.L. Friesen, and R.J. Robertson. 2007a. Paternity and performance of golden-winged warblers (*Vermivora chrysoptera*) and golden-winged x blue-winged warbler (*V. pinus*) hybrids at the leading edge of a hybrid zone. Behavioral Ecology and Sociobiology 61:1797–1807 https://doi.org/10.1007/s00265-007-0413-3.

Vallender, R., R.J. Robertson, V.L. Friesen, and I.J. Lovette. 2007b. Complex hybridization dynamics between golden-winged warblers and blue-winged warblers (*Vermivora chrysoptera* and *Vermivora pinus*) revealed by AFLP, microsatellite, intron, and mtDNA markers. Molecular Ecology 16:2017–2029 https://doi.org/10.1111/j.1365-294X.2007.03282.x.

Van Doren, B.M., and K.G. Horton. 2018. A continental system for forecasting bird migration. Science 361:1115–1118 https://doi.org/10.1126/science.aat7526.

Vansteelant, W.M.G., J. Kekkonen, P. Byholm. 2017. Wind conditions and geography shape the first outbound migration of juvenile honey buzzards and their distribution across sub-Saharan Africa. Proceedings of the Royal Society of London: Series B 284:20170387 https://doi.org/10.1098/rspb.2017.0387.

Venter, O., E.W. Sanderson, A. Magrach, J.R. Allan, J. Beher, K.R. Jones, H.P. Possingham, W.F. Laurance, P. Wood, B.M. Fekete, M.A. Levy, and J.E. Watson. 2018. Last of the Wild Project v. 3 (LWP-3): 2009 Human Footprint, 2018 Release. Palisades, NY: NASA Socioeconomic Data and Applications Center (SEDAC). https://doi.org/10.7927/H46T0JQ4. Accessed 14 January 2020.

Venter, O., E.W. Sanderson, A. Magrach, J.R. Allan, J. Beher, K.R. Jones, H.P. Possingham, W.F. Laurance, P. Wood, B.M. Fekete, M.A. Levy, and J.E. Watson. 2016. Global terrestrial human footprint maps for 1993 and 2009. Scientific Data 3:160067 https://doi.org/10.1038/sdata.2016.67.

Vickers, S.H., A.M.A. Franco, and J.J. Gilroy. 2021. Sensitivity of migratory connectivity estimates to spatial sampling design. Movement Ecology 9:16 https://doi.org/10.1186/s40462-021-00254-w.

Walther, G.-R., E. Post, P. Convey, A. Menzel, C. Parmesan, T.J.C. Beebee, J.-M. Fromentin, O. Hoegh-Guldberg, and F. Bairlein. 2002. Ecological responses to recent climate change. Nature 416:389–395 https://doi.org/10.1038/416389a.

Ward, M.P., T.J. Benson, J. Deppe, T.J. Zenzal, Jr., R.H. Diehl, A. Celis-Murillo, R. Bolus, and F.R. Moore. 2018. Estimating apparent survival of songbirds crossing the Gulf of Mexico during autumn migration. Proceedings of the Royal Society of London: Series B 285:20181747 https://doi.org/10.1098/rspb.2018.1747.

Weber, T.P., A.I. Houston, and B.J. Ens. 1999. Consequences of habitat loss at migratory stopover sites: a theoretical investigation. Journal of Avian Biology 30:416–426 http://doi.org/10.2307/3677014.

Webster, M.S., P.P. Marra, S.M. Haig, S. Bensch, and R.T. Holmes. 2002. Links between worlds: Unraveling migratory connectivity. Trends in Ecology and Evolution 17:76–83 https://doi.org/10.1016/S0169-5347(01)02380-1.

Weeks, B.C., D.E. Willard, M. Zimova, A.A. Ellis, M. L. Witynski, M. Hennen, and B.M. Winger. 2020. Shared morphological consequences of global warming in North American migratory birds. Ecology Letters 23:316–325 https://doi.org/10.1111/ele.13434.

Weins, J.J. 2016. Climate-related local extinctions are already widespread among plant and animal species. PLoS Biology 14:e2001104 https://doi.org/10.1371/journal.pbio.2001104.

Wiedenfeld, D.A., and M.G. Wiedenfeld. 1993. Large kill of Neotropical migrants by tornado and storm in Louisiana, April 1993. Journal of Field Ornithology 66:70–80.

Wilcove, D.S., and M. Wikelski. 2008. Going, going, gone: Is animal migration disappearing? PLoS Biology 6:e188 https://doi.org/10.1371/journal.pbio.0060188.

Wildlife Conservation Society - WCS, and Center for International Earth Science Information Network - CIESIN - Columbia University. 2005. Last of the Wild

Project, Version 2, 2005 (LWP-2): Global Human Footprint Dataset (Geographic). Palisades, NY: NASA Socioeconomic Data and Applications Center (SEDAC). https://doi.org/10.7927/H4M61H5F. Accessed 11 November 2019.

Wilkes, C. 1845. Narrative of the United States exploring expedition during the years 1838, 1839, 1840, 1841 and 1842. Vol. 5. London and Philadelphia.

Williams, G.G. 1945. Do birds cross the Gulf of Mexico in spring? Auk 62:98–111 https://www.jstor.org/stable/4079964.

Wilson, S., J.F. Saracco, R. Krikun, D.T.T. Flockhart, C.M. Godwin, and K.R. Foster. 2018. Drivers of demographic decline across the annual cycle of a threatened migratory bird. Scientific Reports 8:7316 https://doi.org/10.1038/s41598-018-25633-z.

Winger, B.M., F.K. Barker, and R.H. Ree. 2014. Temperate origins of long-distance seasonal migration in New World songbirds. Proceedings of the National Academy of Sciences 111:12115–12120 https://doi.org/10.1073/pnas.1405000111.

Winger, B.M., G.G. Auteri, T.M. Pegan, and B.C. Weeks. 2019. A long winter for the Red Queen: Rethinking the evolution of seasonal migration. Biological Reviews 94:737–752 https://doi.org/10.1111/brv.12476.

Wolfson, D., J. Fieberg, J.S. Lawrence, T.R. Cooper, and D.E. Andersen. 2017. Range overlap between Mid-continent and Eastern sandhill cranes revealed by GPS-tracking. Wildlife Society Bulletin 41:489–498 https://doi.org/10.1002/wsb.799.

Wotherspoon, S., M. Sumner, and S. Lisovski. 2016. BAStag: Basic data processing for light based geolocation archival tags. R package version 0.1.3.

Xie, Y. 2013. animation: An R package for creating animations and demonstrating statistical methods. Journal of Statistical Software 53:1–27 http://www.jstatsoft.org/v53/i01/.

Xie, Y., C. Mueller, L. Yu, and W. Zhu. 2018. animation: A gallery of animations in statistics and utilities to create animations. R package version 2.6.

Yang, D., A. Yang, J. Yang, R. Xu, and H. Qiu. 2021. Unprecedented migratory bird die-off: A citizen-based analysis on the spatiotemporal patterns of mass mortality events in the western United States. GeoHealth 5:e2021GH000395 https://doi.org/10.1029/2021GH000395.

Zeng, Z., A.D. Ziegler, T. Searchinger, L. Yang, A. Chen, K. Ju, S. Piao, L.Z.X. Li, P. Ciais, D. Chen, J. Liu, C. Azorin-Molina, A. Chappell, D. Medvigy, and E.F. Wood. 2019. A reversal in global terrestrial stilling and its implications for wind energy production. Nature Climate Change 9:979–985 https://doi.org/10.1038/s41558-019-0622-6.

Appendix A

Supplementary Information for Chapter 1: Population Trends in *Vermivora* Warblers are Linked to Strong Migratory Connectivity

Supplementary Methods:

Basic background on light-level geolocators –

Light-level geolocators (geolocators) are a simple, yet powerful tool used to estimate location based on seasonal and locational differences in the timing of day and night. Simply, geolocators record the amount of ambient light using a light sensor at a regular interval throughout the life of the unit. A measure of the amount of light is stored with a timestamp such that the full light regime experienced by a geolocator can be recreated upon its recovery. Two primary methods exist for analyzing geolocator data: the threshold method, and the template-fit method. Both methods have been used to identify movements of migratory species and both methods have their advantages (Stutchbury et al. 2009, Kramer et al. 2017). The threshold method is simpler, uses less information, and has been shown to be less accurate when compared directly to the template-fit method (Rakhimberdiev et al. 2016). The template-fit method uses the entire curve of light intensity during twilight periods (i.e., dawn and dusks) to estimate a likelihood surface that can be combined with other likelihood surfaces from previous or subsequent twilights to provide a location estimate (Rakhimberdiev et al. 2017). The template-fit method also provides the user with an understanding of variability or error around the location estimate as it produces a spatially-explicit likelihood surface where the likelihood of the geolocator being in any given cell is relative to the likelihood of it being in the rest of the cells. I chose to use the template-fit method because it allowed me to create spatially-explicit estimates of nonbreeding location that I could standardize for each individual and compare among individuals and populations. For further details, see Kramer et al. (2017).

Assigning species status to individuals –

The plumage of typical, phenotypically pure golden-winged warblers and blue-winged warblers is strikingly different and easily differentiable. Golden-winged warblers are mostly gray with a gold crown, gold patch on the wing (wing-bar), and a black mask and throat patch (Fig. 1 – 1: A, Fig. 1 – 2: A). Blue-winged warblers are mostly yellow often with separate white wing-bars, and a black eye-line without any black mask or throat patch (Fig. 1 – 1: B, 1 – 2: F). Hybrids occur in two recognized phenotypes representing crosses between pure parental types (i.e., F1 hybrid, “Brewster’s warbler”; Fig. 1 – 1: H) and the rare homozygous-recessive offspring produced from an F1-cross (i.e., “Lawrence’s warbler”). Intermediate phenotypes with combinations of plumage traits commonly occur in individuals with complex ancestral lineages. I assigned species status in the field following capture and took standardized, diagnostic photographs of each individual for confirmation. Upon capture individuals were classified as hybrids or phenotypically pure species based on their plumage. I classified individuals with at least one obviously incongruous plumage character (i.e., mostly blue-winged warbler characters: yellow body plumage, no throat patch, and eye-stripe but with one yellow wing-bar instead of two white wing-bars) as hybrids. All hybrids referenced in this study possessed plumage characters typical of F1 hybrids (i.e., gray body plumage, black eye-line, no black throat patch).

Methods for interpreting changes in historical land-use data –

I generally quantified the modeled changes in land use across broad geographical regions that corresponded with three groups of *Vermivora* warblers based on their nonbreeding distributions. I used the HYDE 3.1 database (Goldewijk et al. 2010, Goldewijk et al. 2011, Meiyappan and Jain 2012) to quantify modeled changes in land use in cells (0.5° x 0.5°) containing land from 200–2,400 masl. This elevational range generally contains the humid, mid-elevation forests that *Vermivora* warblers occupy during the nonbreeding period (Rosenberg et al. 2016, Chandler et al. 2016). The HYDE 3.1 database provides model-generated estimates of historical land use based on a variety of factors. Although it provides estimates of the area of different land-cover types, due to the coarseness and uncertainty of the models, I chose to measure the proportion of forest-dominated cells that fell in population masks for each group (i.e., southern Mexico, Central America, and northern South America). As such, I did not attempt to measure the true amount of any land-cover types; instead, I only measured the number of cells for which native forest was the dominant land-cover type (i.e., >50%). In this way, the data accomplish the goal of providing large-scale, regional, and general information about the predicted changes in land-use patterns in the northern Neotropics from 1940–2010.

Observations of site-level differences in population trends explained by nonbreeding site affinity –

I found additional evidence for this relationship at the site-level. The only golden-winged warbler from the historically stable Great Lakes breeding population that occurred in northern South America during the nonbreeding period was from a site in western Ontario, Canada that has experienced declines at a rate of > -2.5%/year (Pardieck et al. 2016) similar to populations in the Appalachian Mountains. Populations of golden-winged warblers to the east and west of this historically declining population are numerically stable or increasing (Sauer et al. 2017; Fig. A – 7) and individuals tracked from these populations occurred exclusively in Central America during the nonbreeding period (Fig. 1 – 2, Fig. A – 7). Despite the limited sample size in this portion of the breeding distribution, this finding highlights the importance of defining conservation strategies based on biologically meaningful populations instead of relying solely on arbitrary boundaries (e.g., state lines) or general ecoregions (e.g., BCRs) especially in migratory species.

Table A.1: Transition windows and total numbers of transitions (i.e., sunrises and sunsets) used to create nonbreeding probability density functions for *Vermivora* warblers. Deployment year is the year the specific geolocator was attached to an individual. Some tags failed before recovery and therefore did not record a full track of those individuals. Species reference the apparent species (based on plumage phenotype) with "GW" representing golden-winged warbler, "BW" representing blue-winged warbler, and "H" representing phenotypic hybrid (based on plumage characteristics). The longitude and latitude where individuals were marked with geolocators is provided along with the extracted longitude and latitude of the highest probability cell in the nonbreeding probability density function. The highest probability of the nonbreeding probability density function is presented and values may be compared for a relative measure of error around latitude and longitude estimates. Briefly, higher probabilities are associated with spatially constrained (i.e., tighter) probability density functions. All individuals are males unless otherwise noted.

ID	Year	Transition span	Total # of transitions used	Full track	Species	Deployment site latitude	Deployment site longitude	Nonbreeding latitude	Nonbreeding longitude	Probability
DMG03	2015	1 Dec to 15 Jan	82	N	GW	51.535	-100.581	15.9893	-85.386	0.005575
ILB04	2015	1 Jan to 29 Feb	110	Y	BW	37.816	-89.463	21.4972	-87.8896	0.005323
ILB06	2015	1 Jan to 29 Feb	110	Y	BW	37.816	-89.463	21.4972	-87.3889	0.005114
ILB08	2015	1 Jan to 29 Feb	114	Y	BW	37.816	-89.463	17.9922	-93.3976	0.006060
ILB18	2015	1 Jan to 29 Feb	115	Y	BW	39.407	-88.161	21.4972	-87.8896	0.005246
KYB14	2015	20 Sep to 23 Oct	65	N	BW	36.913	-83.562	20.9965	-87.3889	0.004951
MAB05	2015	1 Jan to 29 Feb	112	Y	BW	42.343	-72.568	10.4814	-74.8709	0.004974
MAB06	2015	1 Jan to 29 Feb	114	Y	BW	42.343	-72.568	14.9879	-83.3831	0.009560
MAB09	2015	1 Jan to 29 Feb	117	Y	BW	42.343	-72.568	20.9965	-86.8882	0.006007
MAB12	2015	1 Jan to 29 Feb	116	Y	BW	42.343	-72.568	14.9879	-83.3831	0.008518
MIB02	2015	1 Jan to 29 Feb	112	Y	BW	43.948	-84.267	20.9965	-86.8882	0.006974
MIB05	2015	11 Feb to 18 Mar	70	N	BW	42.615	-85.41	21.1235	-86.9527	0.005591
MIB12	2015	1 Jan to 29 Feb	110	Y	BW	42.615	-85.41	21.4972	-87.3889	0.006442
MIB14	2015	1 Jan to 29 Feb	96	Y	BW	42.615	-85.41	20.9965	-89.3918	0.005409
MIG01	2015	1 Jan to 29 Feb	105	Y	GW	43.948	-84.267	14.9879	-83.3831	0.005125
MIH02	2015	1 Jan to 29 Feb	113	Y	H	43.948	-84.267	20.9965	-88.3904	0.004580

ID	Year	Transition span	Total # of transitions used	Full track	Species	Deployment site latitude	Deployment site longitude	Nonbreeding latitude	Nonbreeding longitude	Probability
MN03 [a]	2013	14 Sep to 28 Sep	28	Y	GW	46.533	-93.407	14.4871	-85.386	0.004360
MN05 [a]	2013	1 Jan to 28 Feb	110	Y	GW	46.533	-93.407	15.4886	-84.3846	0.004582
MN06 [a]	2013	1 Jan to 28 Feb	107	Y	GW	46.533	-93.407	15.4886	-84.3846	0.003474
MN11 [a]	2013	1 Jan to 28 Feb	113	Y	GW	46.533	-93.407	15.9893	-85.386	0.007540
MN12 [a]	2013	1 Jan to 28 Feb	109	Y	GW	46.533	-93.407	16.9907	-88.8911	0.005720
MN14 [a]	2013	1 Jan to 26 Feb	94	Y	GW	46.533	-93.407	14.9879	-83.3831	0.005082
MN14	2015	6 Nov to 10 Jan	122	Y	GW	46.533	-93.407	15.4886	-84.3846	0.004282
MN15 [a]	2013	27 Dec to 6 Jan	20	N	GW	46.533	-93.407	15.9893	-85.3860	0.003221
MN16 [a]	2013	1 Jan to 28 Feb	100	Y	GW	46.533	-93.407	14.9879	-83.8839	0.005006
MN20 [a]	2013	1 Jan to 28 Feb	109	Y	GW	46.533	-93.407	15.9893	-85.3860	0.006177
MN25[a]	2014	1 Jan to 28 Feb	133	Y	GW	46.533	-93.407	15.4886	-84.3846	0.005637
MN29 [a]	2014	1 Jan to 28 Feb	112	Y	GW	46.533	-93.407	14.9879	-83.3831	0.005051
MN29	2015	1 Nov to 28 Dec	113	N	GW	46.533	-93.407	14.9879	-83.3831	0.004626
MN36 [a]	2014	1 Jan to 28 Feb	115	Y	GW	46.533	-93.407	17.4915	-90.3932	0.008099
MN36	2015	1 Jan to 29 Feb	118	Y	GW	46.533	-93.407	16.9907	-88.3904	0.005714
NCB01	2015	1 Jan to 29 Feb	115	Y	BW	36.412	-81.655	20.9965	-86.8882	0.005368
ONB02	2015	1 Jan to 29 Feb	104	Y	BW	44.003	-79.123	21.4972	-87.3889	0.006879
ONB05	2015	1 Jan to 29 Feb	117	Y	BW	44.7	-79.545	20.9965	-86.8882	0.006027
ONG03	2015	1 Jan to 29 Feb	107	Y	GW	44.641	-76.343	14.9879	-83.3831	0.007138
ONG05	2015	1 Jan to 29 Feb	112	Y	GW	44.641	-76.343	14.9879	-83.3831	0.006794
ONG10	2015	1 Jan to 29 Feb	105	Y	GW	44.7	-79.545	10.9821	-73.3687	0.004923
PA05 [a]	2014	1 Jan to 28 Feb	108	Y	GW	41.38	-75.18	11.9835	-69.8637	0.005327
PA11 [a]	2014	1 Jan to 28 Feb	115	Y	GW	41.38	-75.18	9.9806	-63.8550	0.006809
PAB01	2015	1 Jan to 29 Feb	118	Y	BW	40.995	-77.701	20.9965	-89.3918	0.005524
PAB03	2015	1 Jan to 29 Feb	115	Y	BW	40.995	-77.701	20.9965	-86.8882	0.006134

ID	Year	Transition span	Total # of transitions used	Full track	Species	Deployment site latitude	Deployment site longitude	Nonbreeding latitude	Nonbreeding longitude	Probability
PAB05	2015	1 Jan to 29 Feb	111	Y	BW	40.995	-77.701	21.4972	-87.3889	0.005295
PAB07	2015	1 Jan to 29 Feb	111	Y	BW	40.995	-77.701	18.9936	-90.8940	0.005835
PAG12	2015	1 Jan to 29 Feb	105	Y	GW	40.995	-77.701	11.9835	-69.8637	0.005171
PAH01	2015	1 Jan to 29 Feb	119	Y	H	40.995	-77.701	10.9821	-73.8694	0.004082
PAH06	2015	1 Jan to 29 Feb	110	Y	H	40.995	-77.701	11.9835	-71.8665	0.004909
RLG16	2015	1 Jan to 11 Feb	80	N	GW	46.533	-93.407	15.9893	-85.3860	0.002996
RLG23	2015	1 Jan to 29 Feb	112	Y	GW	46.533	-93.407	15.9893	-85.3860	0.004066
RLGF15[b]	2015	1 Jan to 29 Feb	112	Y	GW	46.533	-93.407	14.4871	-83.8839	0.006869
RMG02	2015	1 Jan to 29 Feb	111	Y	GW	51.024	-99.941	15.4886	-84.3846	0.005192
SHG07	2015	1 Jan to 29 Feb	117	Y	GW	45.517	-93.699	9.4799	-79.3774	0.004460
SLG12	2015	1 Jan to 29 Feb	114	Y	GW	49.624	-96.307	15.9893	-85.3860	0.005836
SLG18	2015	1 Jan to 29 Feb	108	Y	GW	49.624	-96.307	14.9879	-83.8839	0.006849
TAG07	2015	1 Jan to 29 Feb	114	Y	GW	46.987	-95.611	17.4915	-90.3932	0.006745
TAG09	2015	1 Jan to 29 Feb	113	Y	GW	46.987	-95.611	15.4886	-86.3875	0.004290
TAG14	2015	1 Jan to 29 Feb	115	Y	GW	46.987	-95.611	14.9879	-83.3831	0.004864
TN05[a]	2013	1 Jan to 28 Feb	116	Y	GW	36.291	-84.302	11.4828	-72.3673	0.005868
TN06[a]	2013	1 Jan to 28 Feb	115	Y	GW	36.291	-84.302	10.0423	-70.5386	0.005575
TN09[a]	2013	1 Jan to 28 Feb	113	Y	GW	36.291	-84.302	11.9835	-69.8637	0.005270
TN10[a]	2013	1 Jan to 28 Feb	115	Y	GW	36.291	-84.302	11.9835	-71.3658	0.004930
TN13[a]	2013	1 Jan to 28 Feb	105	Y	GW	36.291	-84.302	11.9835	-69.8637	0.004946
TN13[a]	2014	1 Jan to 28 Feb	111	Y	GW	36.291	-84.302	11.9835	-71.3658	0.005333
TN16[a]	2013	1 Jan to 28 Feb	116	Y	GW	36.291	-84.302	11.9835	-71.8665	0.005747
TNB03	2015	1 Jan to 29 Feb	111	Y	BW	35.927	-84.404	18.9936	-90.894	0.004836
TNB09	2015	1 Jan to 29 Feb	111	Y	BW	36.62	-87.515	21.4972	-87.8896	0.006032
TNG13	2015	1 Jan to 29 Feb	107	Y	GW	36.291	-84.302	11.9835	-71.3658	0.005063

ID	Year	Transition span	Total # of transitions used	Full track	Species	Deployment site latitude	Deployment site longitude	Nonbreeding latitude	Nonbreeding longitude	Probability
VAG01	2015	1 Jan to 29 Feb	117	Y	GW	38.26	-79.627	11.9835	-71.3658	0.005735
VAG02	2015	1 Jan to 29 Feb	113	Y	GW	38.26	-79.627	11.9835	-69.8637	0.005708
WIB05	2015	1 Jan to 29 Feb	113	Y	BW	44.319	-90.131	20.9965	-86.8882	0.006157
WIB11	2015	2 Feb to 24 Feb	40	Y	BW	44.319	-90.131	20.9965	-89.8925	0.004362
WIB11	2016	1 Jan to 28 Feb	91	Y	BW	44.319	-90.131	18.4929	-92.3961	0.004500
WIB19	2016	30 Jan to 9 Mar	70	Y	BW	44.319	-90.131	21.4972	-87.3889	0.005115
WIG01	2015	1 Jan to 29 Feb	119	Y	GW	44.319	-90.131	14.9879	-83.3831	0.005170
WIG02	2015	1 Jan to 29 Feb	114	Y	GW	44.319	-90.131	14.9879	-83.3832	0.006351
WIH03	2015	1 Jan to 29 Feb	87	Y	H	44.319	-90.131	18.9936	-90.8940	0.003502
WIH03	2016	1 Jan to 28 Feb	111	Y	H	44.319	-90.131	15.9893	-85.3860	0.005575

[a] Data reanalyzed from Kramer et al. (29, 68)

[b] Female golden-winged warbler

Table A.2: Common name, species name, and distribution and trend data for Nearctic-Neotropical migratory bird species (Passeriformes). Information on nonbreeding distribution was gathered from BirdLife International (44). Trend data were retrieved from the Breeding Bird Survey database (42, 43). Orange-highlighted entries represent species I predict may exhibit strong migratory connectivity as described in golden-winged warblers in this study based on characteristics of population trends and geographical distributions described in detail in Materials and Methods.

Species name (common)	Species name *(Latin)*	Nonbreeding range includes South America	Nonbreeding range includes Central America	Nonbreeding range includes Central and South America	Regional variation in breeding population trends?	Survey-wide trend 1966-1990	Survey-wide trend 1991-2015
Olive-sided flycatcher	*Contopus cooperi*	X	X	X	No		
Western wood-pewee	*Contopus sordidulus*	X	X	X	Yes; N declining, S increasing	Declining	Stable after 2000
Eastern wood-pewee	*Contopus virens*	X	X	X	Yes; E declining, W increasing	Declining	Declining
Yellow-bellied flycatcher	*Empidonax flaviventris*		X				
Acadian flycatcher	*Empidonax virescens*	X	X	X	Yes; E declining, W, increasing	Stable	Stable
Willow flycatcher	*Empidonax traillii*		X				
Alder flycatcher	*Empidonax alnorum*	X					
Least flycatcher	*Empidonax minimus*		X				
Hammond's flycatcher	*Empidonax hammondii*		X				
Gray flycatcher	*Empidonax wrightii*		X				
Dusky flycatcher	*Empidonax oberholseri*		X				

Species name (common)	Species name *(Latin)*	Nonbreeding range includes South America	Nonbreeding range includes Central America	Nonbreeding range includes Central and South America	Regional variation in breeding population trends?	Survey-wide trend 1966-1990	Survey-wide trend 1991-2015
Pacific-slope flycatcher	*Empidonax occident*		X				
Cordilleran flycatcher	*Empidonax difficilis*		X				
Ash-throated flycatcher	*Myiarchus cinerascens*		X				
Great-crested flycatcher	*Myiarchus crinitus*	X	X	X	Complicated; E stable, W declining, but smaller scale differences	Stable	Stable
Western kingbird	*Tyrannus verticalis*		X				
Eastern kingbird	*Tyrannus tyrannus*	X					
Scissor-tailed flycatcher	*Tyrannus forficatus*		X				
Black-capped vireo	*Vireo atricapilla*		X				
White-eyed vireo	*Vireo griseus*		X				
Bell’s vireo	*Vireo bellii*		X				
Gray vireo	*Vireo vicinior*		X				
Yellow-throated vireo	*Vireo flavifrons*	X	X	X	Yes; E declining, W increasing	Increasing	Increasing
Cassin’s vireo	*Vireo cassinii*		X				
Blue-headed vireo	*Vireo solitarius*		X				
Plumbeous vireo	*Vireo plumbeus*		X				
Philadelphia vireo	*Vireo philadelphicus*		X				

Species name (common)	Species name *(Latin)*	Nonbreeding range includes South America	Nonbreeding range includes Central America	Nonbreeding range includes Central and South America	Regional variation in breeding population trends?	Survey-wide trend 1966-1990	Survey-wide trend 1991-2015
Warbling vireo	*Vireo gilvus*		X				
Red-eyed vireo	*Vireo olivaceus*	X					
Northern rough-winged swallow	*Stelgidopteryx serripennis*		X				
Purple martin	*Progne subis*	X					
Tree swallow	*Tachycineta bicolor*		X				
Violet-green swallow	*Tachycineta thalassina*		X				
Barn swallow	*Hirundo rustica*	X	X	X	Yes; N declining, S increasing	Declining	Declining
Bank swallow	*Riparia riparia*	X					
Cliff Swallow	*Petrochelidon pyrrhonota*	X					
Veery	*Catharus fuscescens*	X					
Gray-cheeked thrush	*Catharus minimus*	X					
Swainson's thrush	*Catharus ustulatus*	X	X	X	Whole range not accounted for; complex; NW declining, central increasing, NE declining.	Declining	Stable
Hermit thrush	*Catharus guttatus*		X				

Species name (common)	Species name *(Latin)*	Nonbreeding range includes South America	Nonbreeding range includes Central America	Nonbreeding range includes Central and South America	Regional variation in breeding population trends?	Survey-wide trend 1966-1990	Survey-wide trend 1991-2015
Wood thrush	*Hyloichla mustelina*		X				
Gray catbird	*Dumetella carlinensis*		X				
Ovenbird	*Seiurus aurocapilla*		X				
Worm-eating warbler	*Helmitheros vermivorum*		X				
Louisiana waterthrush	*Parkesia motacilla*	X	X	X	Yes; E decreasing, W increasing	Stable	Increasing
Northern waterthrush	*Parkesia noveboracensis*	X	X	X	Full range not accounted for	Stable	Increasing
Golden-winged warbler	*Vermivora chrysoptera*	X	X	X	Yes; E declining, W increasing	Declining	Stable
Blue-winged warbler	*Vermivora cyanoptera*		X				
Black-and-white warbler	*Mniotilta varia*	X	X	X	Yes; E declining, W increasing/stable	Declining	Declining
Prothonotary warbler	*Protonotaria citrea*	X	X	X	Complex; declining SW and SE, increasing N and central	Declining	Stable
Swainson's warbler	*Limnothlypis swainsonii*		X				
Tennessee warbler	*Oreothlypis peregrina*	X	X	X	Full range not accounted for	Stable	Stable
Orange-crowned warbler	*Oreothlypis celata*		X				

Species name (common)	Species name *(Latin)*	Nonbreeding range includes South America	Nonbreeding range includes Central America	Nonbreeding range includes Central and South America	Regional variation in breeding population trends?	Survey-wide trend 1966-1990	Survey-wide trend 1991-2015
Lucy’s warbler	*Oreothlypis luciae*		X				
Nashville warbler	*Oreothlypis ruficapilla*		X				
Virginia’s warbler	*Oreothlypis virginiae*		X				
Connecticut warbler	*Oporornis agilis*	X					
MacGillivray’s warbler	*Geothlypis tolmiei*		X				
Mourning warbler	*Geothlypis philadelphia*	X	X	X	Complex; S increasing, N declining	Declining	Stable after 2000
Kentucky warbler	*Geothlypis formosa*	X	X	X	Yes; NE declines, S increases	Declining	Stable
Common yellowthroat	*Geothlypis trichas*		X				
Hooded warbler	*Setophaga citrina*		X				
American redstart	*Setophaga ruticilla*	X	X	X	Complex; central = stable/increasing, E and W declining	Declining	Stable after 2000
Cape May warbler	*Setophaga tigrina*		X				
Cerulean warbler	*Setophaga cerulean*	X					
Northern parula	*Setophaga americana*		X				
Magnolia warbler	*Setophaga magnolia*		X				

Species name (common)	Species name *(Latin)*	Nonbreeding range includes South America	Nonbreeding range includes Central America	Nonbreeding range includes Central and South America	Regional variation in breeding population trends?	Survey-wide trend 1966-1990	Survey-wide trend 1991-2015
Bay-breasted warbler	*Setophaga castanea*	X	X	X	Range not fully accounted for	Stable	Stable
Blackburnian warbler	*Setophaga fusca*	X	X	X	Yes; S declines, N increasing	Stable	Increasing
Yellow warbler	*Setophaga petechia*	X	X	X	Complex; declining E and W, stable central	Declining	Declining
Chestnut-sided warbler	*Setophaga pensylvanica*		X				
Blackpoll warbler	*Setophaga striata*	X					
Black-throated blue warbler	*Setophaga caerulescens*		X				
Palm warbler	*Setophaga palmarum*		X				
Audubon’s warbler	*Setophaga coronata auduboni*		X				
Myrtle’s warbler	*Setophaga coronata coronata*		X				
Yellow-throated warbler	*Setophaga dominica*		X				
Prairie warbler	*Setophaga discolor*		X				
Black-throated gray warbler	*Setophaga nigrescens*		X				
Townsend’s warbler	*Setophaga townsendi*		X				

Species name (common)	Species name *(Latin)*	Nonbreeding range includes South America	Nonbreeding range includes Central America	Nonbreeding range includes Central and South America	Regional variation in breeding population trends?	Survey-wide trend 1966-1990	Survey-wide trend 1991-2015
Hermit warbler	*Setophaga occidentalis*		X				
Golden-cheeked warbler	*Setophaga chrysoparia*		X				
Black-throated green warbler	*Setophaga virens*	X	X	X	No		
Canada warbler	*Cardellina canadensis*	X					
Wilson’s warbler	*Cardellina pusilla*		X				
Yellow-breasted chat	*Icteria virens*		X				
Summer tanager	*Piranga rubra*	X	X	X	No		
Scarlet tanager	*Piranga olivacea*	X					
Western tanager	*Piranga ludoviciana*		X				
Rose-breasted grosbeak	*Pheucticus ludovicianus*	X	X	X	Yes; E declining, W stable	Declining	Stable
Black-headed grosbeak	*Pheucticus melanocephalus*		X				
Blue grosbeak	*Passerina caerulea*		X				
Lazuli bunting	*Passerina amoena*		X				
Indigo bunting	*Passerina cyanea*		X				
Painted bunting	*Passerina ciris*		X				
Dickcissel	*Spiza Americana*	X	X	X	No		

Species name (common)	Species name *(Latin)*	Nonbreeding range includes South America	Nonbreeding range includes Central America	Nonbreeding range includes Central and South America	Regional variation in breeding population trends?	Survey-wide trend 1966-1990	Survey-wide trend 1991-2015
Bobolink	*Dolichonyx oryzivorous*	X					
Orchard oriole	*Icterus spurius*	X	X	X	Yes; N stable/increasing, S declining	Declining	Stable
Bulluck's oriole	*Icterus bullockii*		X				
Baltimore oriole	*Icterus galbula*	X	X	X	Yes; S stable, N declining	Declining	Declining

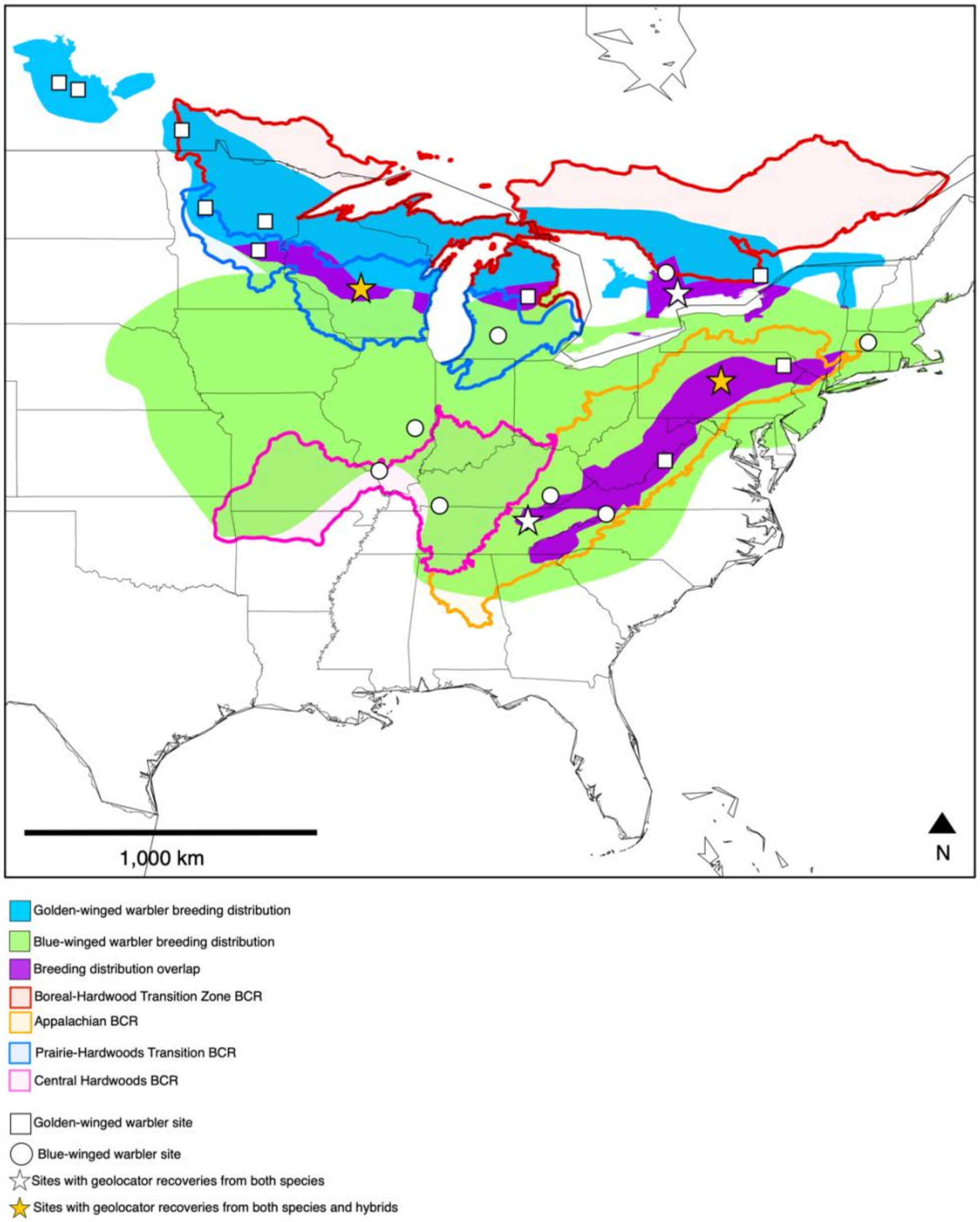

Figure A – 1: Detailed map of study sites in relation to Bird Conservation Regions (BCRs) and breeding distributions of *Vermivora* warblers. Distribution data adapted from BirdLife International (2016).

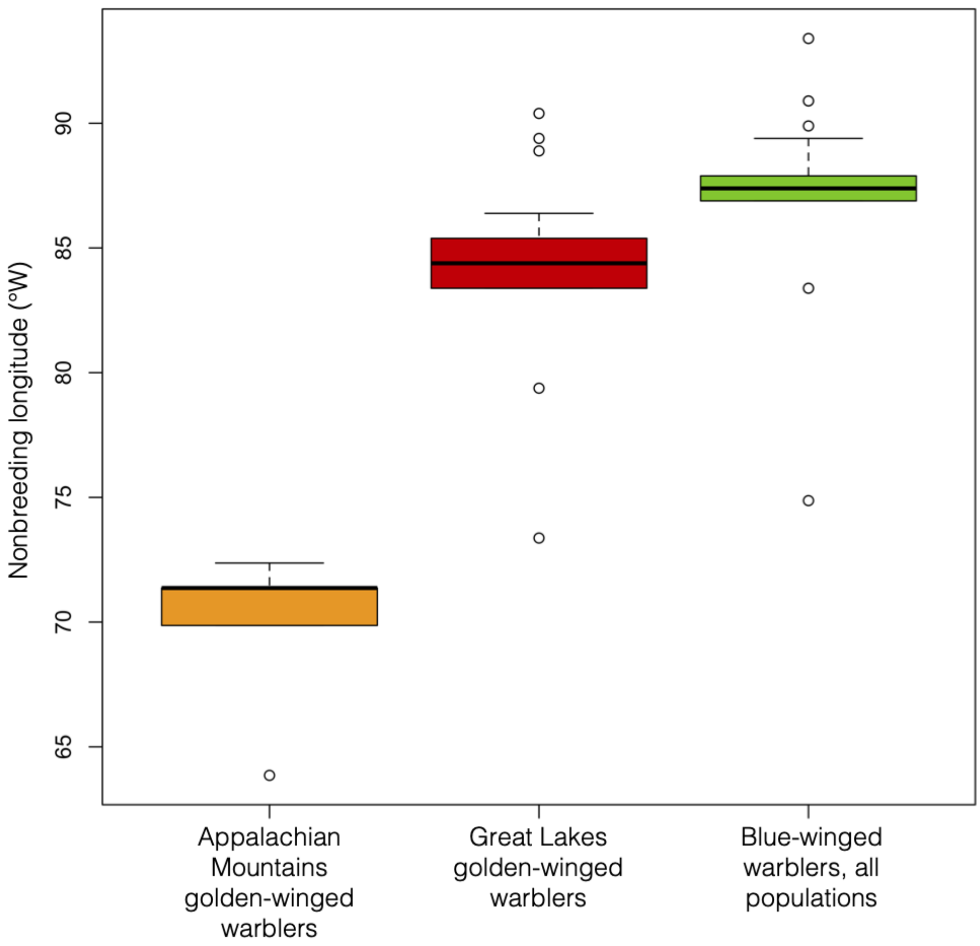

Figure A – 2: Boxplot of nonbreeding longitude in golden-winged warblers from Appalachian Mountain (orange) and Great Lakes (red) breeding sites and blue-winged warblers from throughout their breeding range (green). Blue-winged warblers and golden-winged warblers breeding in the Great Lakes region exhibit historically stable population trends, whereas golden-winged warbler breeding in the Appalachian Mountains region have experienced declines.

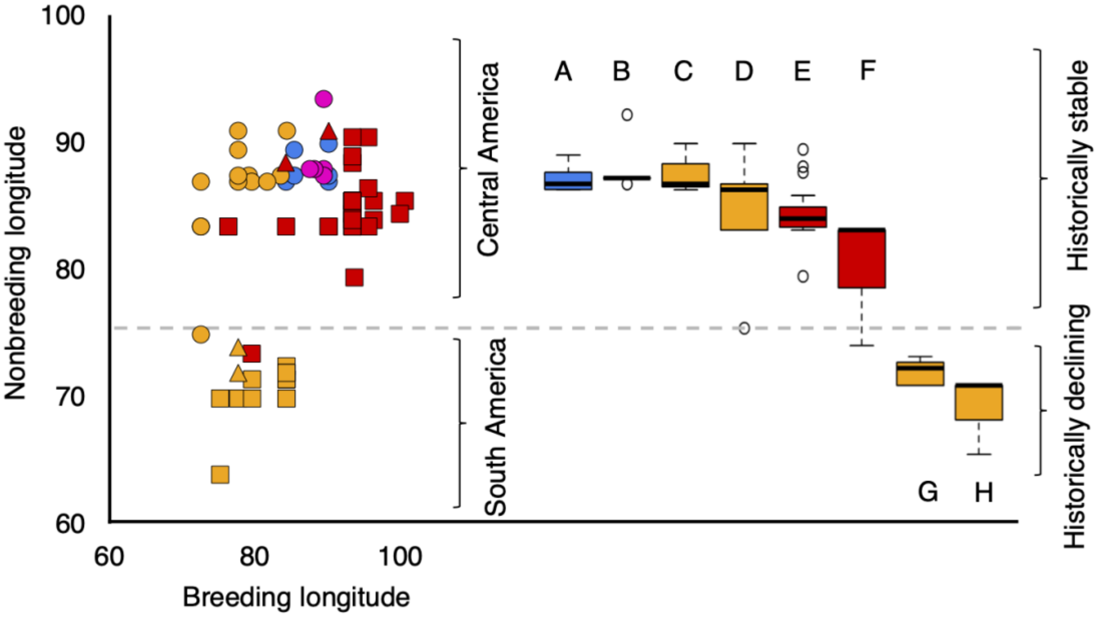

Figure A – 3: Nonbreeding longitude as a function of breeding longitude among individual blue-winged warblers, golden-winged warblers, and hybrids (left) and average nonbreeding longitude by population (right). Individuals are identified as golden-winged warblers (squares), blue-winged warblers (circles), or hybrids (triangles) from breeding sites in Bird Conservation Regions (BCRs; identified in Fig. 1 – 1, colors correspond to those in Fig. 1 – 1; orange, Appalachian Mountains BCR [C–D, G–H]; blue, Prairie-Hardwoods Transition BCR [A]; pink, Central Hardwoods BCR [B]; red, Boreal-Hardwoods Transition BCR [E–F]). The boxplot shows average nonbreeding longitude of blue-winged warbler populations (A–D) and golden-winged warbler populations (E–H) with the dashed gray line representing the longitude separating Central America and South America (75° W). I considered southern and northern Appalachian Mountains populations of blue-winged warblers (C, southern; D, northern) and golden-winged warblers (G, southern; H northern) separately. I also considered western and eastern populations of Great Lakes golden-winged warblers separately (E, western; F, eastern).

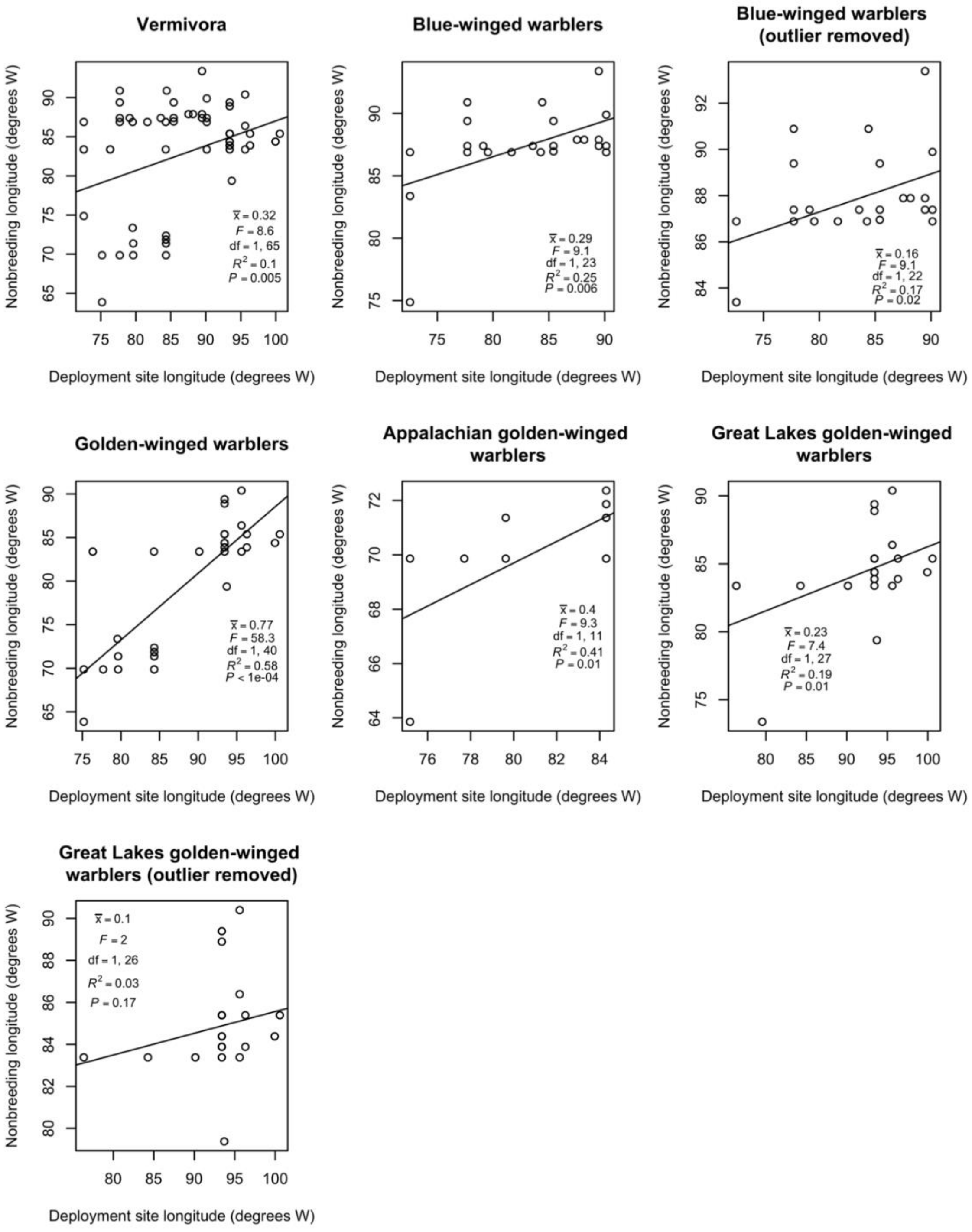

Figure A – 4: Relationships between deployment site longitude (°W) and nonbreeding longitude (°W) derived from the longitude of the highest probability cell in the nonbreeding probability density functions of individual *Vermivora* warblers (phenotypic hybrids not included). See Fig. 1 – 1 and Materials and Methods (Section 1.5) for descriptions of populations.

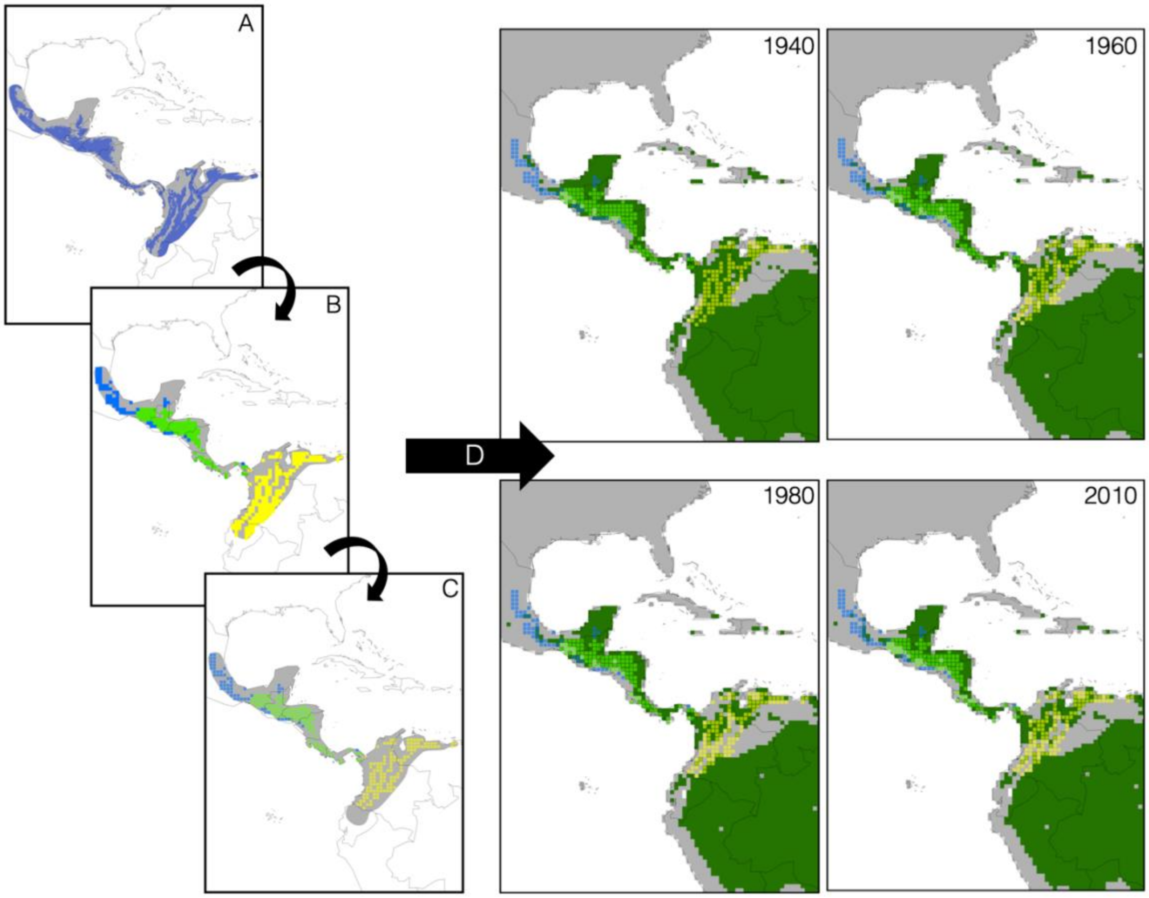

Figure A – 5: Conceptual model of estimating changes in land-use patterns using the HYDE 3.1 database. First, I identified cells (0.5° x 0.5°) in the nonbreeding distribution of *Vermivora* warblers containing land 200–2,400 masl (A). Then I characterized cells (B) based on their geographic location and an understanding of the nonbreeding distribution of *Vermivora* warblers as being likely to affect blue-winged warblers (blue cells + lime green cells), Great Lakes breeding populations of golden-winged warblers (lime green cells), or Appalachian Mountain breeding populations of golden-winged warblers (yellow cells). I then eliminated cells (C) that were outside the known historical nonbreeding distribution of *Vermivora* (40). Finally, I extracted modeled land-use characteristics from each cell that overlapped with the mask (C) in 5-year increments from 1940–2010 (D). Here, I show only forest-dominated cells (dark green cells) in 1940, 1960, 1980, and 2010 overlaid with a partially transparent mask (C) representing the nonbreeding distribution of different groups of *Vermivora* warblers.

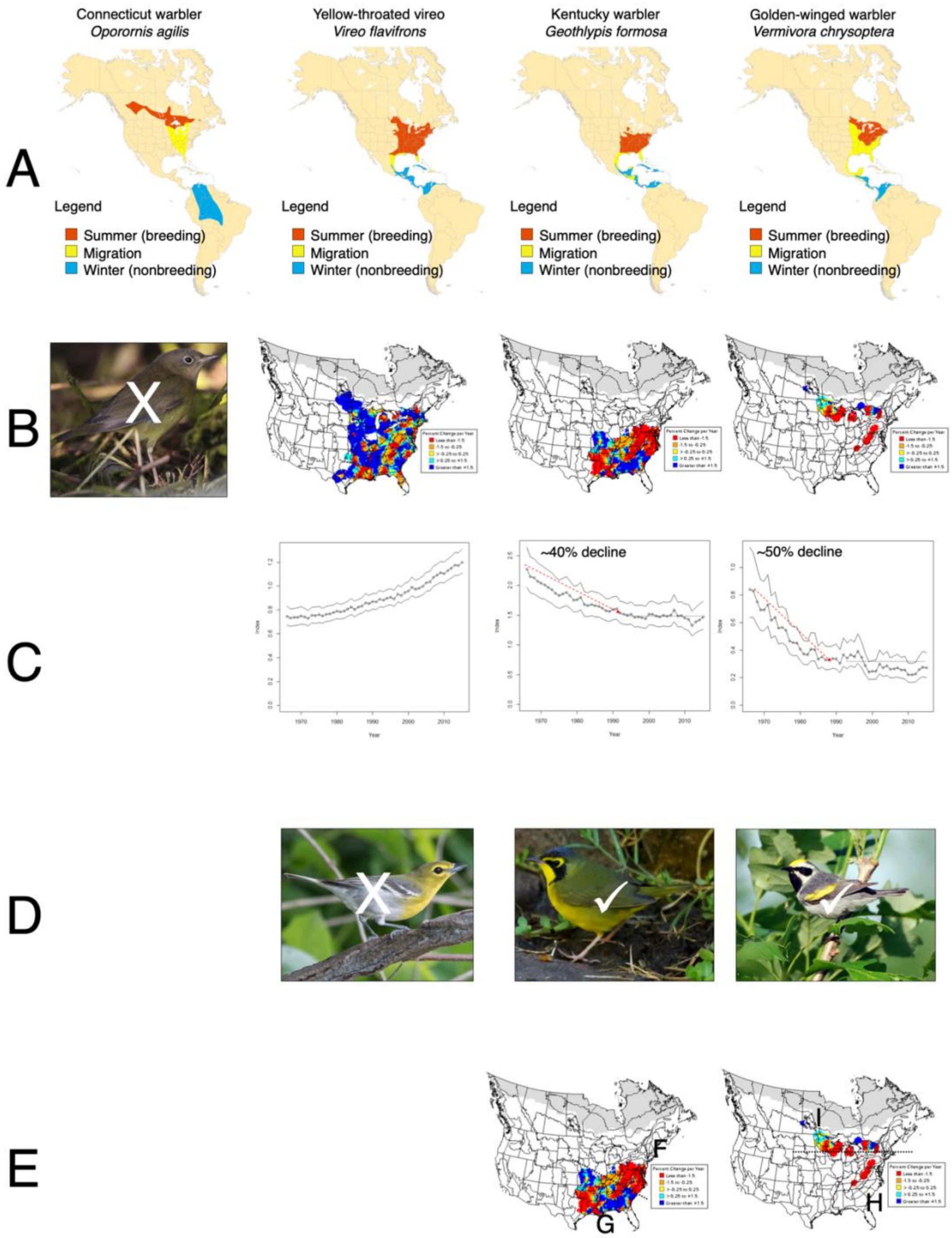

Figure A – 6: Conceptual model used to identify other species (Table A.2) that may experience similar limiting factors as golden-winged warblers due to strong migratory connectivity. I (A) visually inspected the annual distribution of Nearctic-Neotropical migrant songbird species and identified those that had relatively broadly dispersed breeding distributions, and nonbreeding distributions in Central America and South

America (similar to golden-winged warblers). I visually inspected the Breeding Bird Survey trend maps (B) for the species meeting the criteria in (A) and selected species that exhibited regionally-specific population trends. Using the survey-wide population trends (C) estimated by the Breeding Bird Survey, I identified species that showed declines from the beginning of monitoring (~1966) to ~1990 before stabilizing (similar to golden-winged warblers). In this example, Connecticut warblers (*Oporornis agilis*) did not occur in Central America during the nonbreeding period, so were eliminated from consideration as a species that may exhibit similar nonbreeding population structure and migratory connectivity as golden-winged warblers. Yellow-throated vireos (*Vireo flavifrons*) wintered in both Central America and South America, exhibited regional patterns in breeding population trends, but were eliminated from consideration as a species that I would predict to have strong migratory connectivity similar to golden-winged warblers because the range-wide population trend was stable until ~1985 when it began to increase. Kentucky warblers (*Geothylipis formosa*) wintered in both Central America and South America, exhibited regional patterns in breeding population trends, and showed range-wide patterns of declines from 1966–1990 with stable trends thereafter. Kentucky warblers show many of the same signals of strong migratory connectivity as golden-winged warblers (D). Therefore, I predict a migratory divide in Kentucky warblers with individuals in declining, northeastern populations (F) occurring in South America and stable/increasing southwestern populations (G) occurring in Central America during the nonbreeding period reflecting the nonbreeding structure of declining (H), and numerically stable (I) populations of golden-winged warblers. Range maps adapted from BirdLife International (2016). Photos of Connecticut warbler (A Maizlish), yellow-throated vireo (M Stratmoen), and Kentucky warbler (budgora) retrieved from Flickr Creative Commons. Golden-winged warbler photo by H Streby.

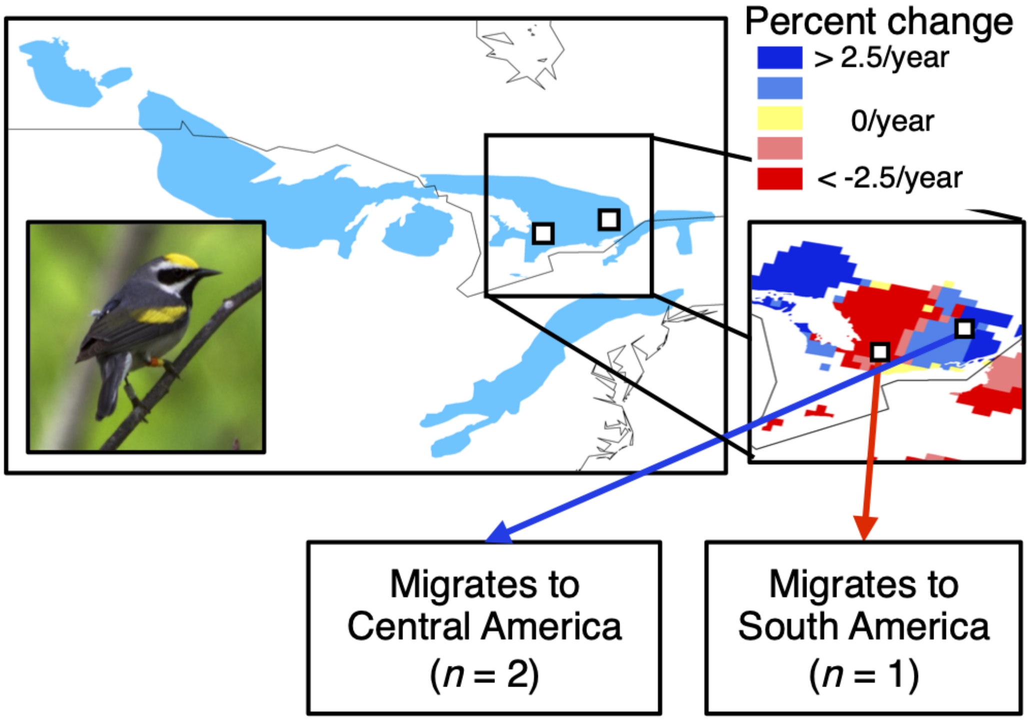

Figure A – 7: Breeding distribution of golden-winged warblers (blue) with detail of the eastern portion of the Great Lakes (BCR 12) population (inset) showing more detailed population trends. Sites with geolocator data are denoted with white squares. Range maps adapted from BirdLife International (2016).

Appendix B

Supplementary Information for Chapter 2: Exposure to Risk Factors Experienced During Migration is not Associated with Recent *Vermivora* warbler population trends

Supplementary Methods:

Processing hurricane and tornado data—

I downloaded datasets containing spatially explicit historical hurricane (Best Track Data HURDAT2, National Hurricane Center; https://www.nhc.noaa.gov/data/) and tornado (Storm Events Database; https://www.ncdc.noaa.gov/stormevents/) data. Historical hurricane data spanned 1851–2013 and historical tornado data spanned 1950–2019. I selected tornado and hurricane tracks that occurred during migration periods (April–May, August–November) from 2000 to the most recent year available for each dataset. I transformed track data for hurricanes and tornados into point data and rasterized each layer in R using a standardized extent (i.e., y = 0, 60; x = -120, -60) and resolution (~0.5° × 0.5°).

Hierarchical modeling—

Population trends in *Vermivora* warblers are strongly associated with both breeding and nonbreeding regions (Buehler et al. 2007, Kramer et al. 2018). To determine whether individual migration risk-factors explained additional variation in recent *Vermivora* warbler population trends while controlling for breeding and nonbreeding factors, I used an information-theoretic approach in which I added singular migration risk-factor variables to a base model comprised of breeding and nonbreeding locations of *Vermivora* warblers. I considered more complex models (i.e., base model with an additional migration risk-factor variable) to be uninformative if they were < 2 ΔAIC_c from the base model (Table B.6, B.7, B.8, B.10; Arnold 2010).

I tested for associations between *Vermivora* warbler population trends and the overall (annual) exposure to migration risk-factors and seasonal (i.e., autumn and spring) exposure to migration risk-factors in stopover regions prior to crossing the Gulf of Mexico. For models exploring the associations between annual exposure to migration risk-factors and population trends, I omitted individuals with incomplete geolocator tracks (i.e., geolocator stopped collecting data prior to completion of a full annual cycle). In models exploring associations between seasonal exposure to migration risk-factors, I included individuals with geolocators that collected data during individual migration period (autumn or spring) regardless of if they collected a data for the entire annual cycle. To test for potential associations between population trends and the amount of migration risk-factors in population-specific areas used prior to crossing a major migration barrier (Gulf of Mexico), I summed the amount of each migration risk-factor within an individual's 25th percentile core-use area cropped between latitudes corresponding with regions containing likely stopover sites where individuals rest and refuel prior to initiating trans-Gulf flights during both autumn and spring migration periods (Kramer et al. 2017). Specifically, I cropped 25th percentile core-use areas between 25–35° latitude during autumn migration and between 15–23.5° latitude during spring migration.

Table B.1: Metadata of geolocator-marked *Vermivora* warblers. Individual identification code (ID), U.S. Geological Survey band number (Band #), geolocator deployment year (Dep. year), species (Sp.; GW=golden-winged warbler, BW=blue-winged warbler, HY=hybrid), start and end of seasonal migrations (Aut. start, Aut. end, Spr. start, Spr. end), breeding and nonbreeding coordinates (Br. Lat., Br. Lon., NB Lat., NB Lon.). Cells for which geolocator data were not collected, or for which data were not available are denoted by "n/a".

ID	Band #	Dep. year	Sp.	BCR	Aut. start	Aut. end	Spr. start	Spr. end	Br. Lat.	Br. Lon.	NB Lat.	NB Lon.
DMG03	2840-78903	2015	GW	BHT	9/10/15	10/25/15	n/a	n/a	51.535	-100.581	15.989	-85.386
ILB04	2750-63504	2015	BW	CH	9/24/15	10/23/15	2/14/16	4/8/16	37.816	-89.463	21.497	-87.890
ILB06	2750-63506	2015	BW	CH	8/1/15	9/27/15	4/20/16	5/4/16	37.816	-89.463	21.497	-87.389
ILB08	2750-63508	2015	BW	CH	9/21/15	11/16/15	4/17/16	5/5/16	37.816	-89.463	17.992	-93.398
ILB18	2750-63523	2015	BW	CH	9/6/15	11/9/15	4/17/16	5/16/16	39.407	-88.161	21.497	-87.890
KYB14	2690-98096	2015	BW	AM	9/7/15	10/3/15	n/a	n/a	36.913	-83.562	20.997	-87.389
MAB05	2750-63237	2015	BW	AM	8/23/15	10/24/15	3/29/16	5/2/16	42.343	-72.568	10.481	-74.871
MAB06	2750-63238	2015	BW	AM	8/5/15	11/1/15	4/12/16	5/16/16	42.343	-72.568	14.988	-83.383
MAB09	2750-63243	2015	BW	AM	10/10/15	10/23/15	4/11/16	4/27/16	42.343	-72.568	20.997	-86.888
MAB12	2770-39353	2015	BW	AM	9/8/15	11/7/15	3/28/16	4/25/16	42.343	-72.568	14.988	-83.383
MIB02	2750-63335	2015	BW	PHT	9/3/15	11/19/15	4/11/16	5/2/16	43.948	-84.267	20.997	-86.888
MIB05	2750-63353	2015	BW	PHT	8/15/15	9/3/15	n/a	n/a	42.615	-85.410	21.124	-86.953

ID	Band #	Dep. year	Sp.	BCR	Aut. start	Aut. end	Spr. start	Spr. end	Br. Lat.	Br. Lon.	NB Lat.	NB Lon.
MIB12	2750-63360	2015	BW	PHT	9/20/15	9/29/15	4/11/16	4/15/16	42.615	-85.410	21.497	-87.389
MIB14	2750-63362	2015	BW	PHT	10/10/15	10/17/15	4/29/16	5/18/16	42.615	-85.410	20.997	-89.392
MIG01	2750-63331	2015	GW	BHT	9/8/15	11/12/15	4/20/16	5/6/16	43.948	-84.267	14.988	-83.383
MIH02[a]	2750-63351	2015	HY	BHT	9/19/15	11/25/15	4/15/16	5/4/16	43.948	-84.267	20.997	-88.390
RLG12	2690-98282	2015	GW	BHT	8/29/15	10/14/15	4/29/16	5/9/16	46.533	-93.407	15.489	-84.385
RLG19	2690-98043	2015	GW	BHT	9/2/15	10/12/15	n/a	n/a	46.533	-93.407	14.988	-83.383
RLG18	2690-98276	2015	GW	BHT	9/9/15	11/18/15	4/19/16	5/8/16	46.533	-93.407	16.991	-88.390
NCB01	2700-29578	2015	BW	AM	9/16/15	10/10/15	4/2/16	4/19/16	36.412	-81.655	20.997	-86.888
ONB02	2740-78971	2015	BW	AM	9/21/15	11/4/15	4/22/16	5/26/16	44.003	-79.123	21.497	-87.389
ONB05	2740-78972	2015	BW	AM	9/7/15	10/22/15	4/3/16	5/2/16	44.700	-79.545	20.997	-86.888
ONG03	2740-78953	2015	GW	BHT	9/5/15	10/14/15	4/23/16	5/10/16	44.641	-76.343	14.988	-83.383
ONG05	2740-78955	2015	GW	BHT	9/1/15	10/31/15	4/24/16	5/19/16	44.641	-76.343	14.988	-83.383
ONG10	2740-78968	2015	GW	BHT	9/6/15	10/29/15	4/10/16	5/11/16	44.700	-79.545	10.982	-73.369
PAB01	2750-63202	2015	BW	AM	9/27/15	10/17/15	3/11/16	4/23/16	40.995	-77.701	20.997	-89.392
PAB03	2750-63206	2015	BW	AM	8/26/15	11/3/15	4/18/16	4/26/16	40.995	-77.701	20.997	-86.888
PAB05	2750-63211	2015	BW	AM	8/26/15	10/26/15	4/17/16	4/25/16	40.995	-77.701	21.497	-87.389
PAB07	2750-63225	2015	BW	AM	9/12/15	10/19/15	4/17/16	4/25/16	40.995	-77.701	18.994	-90.894

ID	Band #	Dep. year	Sp.	BCR	Aut. start	Aut. end	Spr. start	Spr. end	Br. Lat.	Br. Lon.	NB Lat.	NB Lon.
PAG12	2750-63222	2015	GW	AM	8/8/15	11/14/15	4/7/16	5/15/16	40.995	-77.701	11.984	-69.864
PAH01[a]	2750-63210	2015	HY	AM	9/14/15	11/16/15	3/27/16	4/26/16	40.995	-77.701	10.982	-73.869
PAH06[a]	2750-63228	2015	HY	AM	8/13/15	9/25/15	3/5/16	4/19/16	40.995	-77.701	11.984	-71.867
RLG16	2750-63373	2015	GW	BHT	8/25/15	10/26/15	n/a	n/a	46.533	-93.407	15.989	-85.386
RLG23	2750-63256	2015	GW	BHT	9/4/15	11/1/15	4/17/16	5/12/16	46.533	-93.407	15.989	-85.386
RLGF15	2750-63255	2015	GW	BHT	9/6/15	10/19/15	4/9/16	5/8/16	46.533	-93.407	14.487	-83.884
RMG02	2840-78914	2015	GW	BHT	9/7/15	11/7/15	4/15/16	5/20/16	51.024	-99.941	15.489	-84.385
SHG07	2750-63448	2015	GW	BHT	8/20/15	11/21/15	3/30/16	5/15/16	45.517	-93.699	9.480	-79.377
SLG12	2740-84922	2015	GW	BHT	9/4/15	10/25/15	4/22/16	5/25/16	49.624	-96.307	15.989	-85.386
SLG18	2740-84929	2015	GW	BHT	9/15/15	10/25/15	4/17/16	5/23/16	49.624	-96.307	14.988	-83.884
TAG07	2750-63418	2015	GW	BHT	8/24/15	10/28/15	4/17/16	5/8/16	46.987	-95.611	17.492	-90.393
TAG09	2750-63410	2015	GW	BHT	9/17/15	10/24/15	4/24/16	5/15/16	46.987	-95.611	15.489	-86.388
TAG14	2750-63416	2015	GW	BHT	8/12/15	10/6/15	4/9/16	5/23/16	46.987	-95.611	14.988	-83.383
TNB03	2560-53231	2015	BW	AM	9/4/15	10/28/15	n/a	n/a	35.927	-84.404	18.994	-90.894
TNB09	2560-53254	2015	BW	CH	9/15/15	10/11/15	4/4/16	5/2/16	36.620	-87.515	21.497	-87.890
TNG13	2560-53206	2015	GW	AM	8/20/15	9/12/15	3/31/16	5/11/16	36.291	-84.302	11.984	-71.366
VAG01	2770-39700	2015	GW	AM	9/16/15	10/23/15	3/25/16	4/27/16	38.260	-79.627	11.984	-71.366

ID	Band #	Dep. year	Sp.	BCR	Aut. start	Aut. end	Spr. start	Spr. end	Br. Lat.	Br. Lon.	NB Lat.	NB Lon.
VAG02	2770-39698	2015	GW	AM	9/12/15	11/20/15	3/23/16	4/25/16	38.260	-79.627	11.984	-69.864
WIB05	2750-63537	2015	BW	PHT	9/3/15	11/28/15	3/28/16	5/18/16	44.319	-90.131	20.997	-86.888
WIB11	2750-63550	2015	BW	PHT	9/2/15	11/11/15	4/16/16	5/6/16	44.319	-90.131	20.997	-89.893
WIB11	2750-63550	2016	BW	PHT	9/23/16	11/10/16	3/28/17	5/12/17	44.319	-90.131	18.493	-92.396
WIB19	2750-63464	2016	BW	PHT	9/11/16	11/23/16	4/26/17	5/9/17	44.319	-90.131	21.497	-87.389
WIG01	2750-63528	2015	GW	BHT	8/30/15	10/28/15	4/17/16	5/7/16	44.319	-90.131	14.988	-83.383
WIG02	2750-63529	2015	GW	BHT	8/15/15	10/2/15	4/4/16	5/7/16	44.319	-90.131	14.988	-83.383
WIH03[a]	2750-63553	2015	HY	BHT	8/20/15	11/15/15	4/23/16	5/5/16	44.319	-90.131	18.994	-90.894
WIH03[a]	2750-63553	2016	HY	BHT	9/20/16	10/27/16	4/22/17	5/7/17	44.319	-90.131	15.989	-85.386
MN03[a]	2660-29638	2013	GW	BHT	n/a	n/a	n/a	n/a	46.533	-93.407	14.487	-85.386
MN05	2660-29468	2013	GW	BHT	9/9/13	11/5/13	4/8/14	5/17/14	46.533	-93.407	15.489	-84.385
MN06	2660-29468	2013	GW	BHT	9/10/13	11/25/13	4/16/14	5/15/14	46.533	-93.407	15.489	-84.385
MN11	2660-29675	2013	GW	BHT	9/12/13	11/1/13	4/12/14	5/21/14	46.533	-93.407	15.989	-85.386
MN12	2690-98293	2013	GW	BHT	9/10/13	11/11/13	4/25/14	5/28/14	46.533	-93.407	16.991	-88.891
MN14	2660-29420	2013	GW	BHT	9/18/13	10/26/13	n/a	n/a	46.533	-93.407	14.988	-83.383
MN15	2660-29451	2013	GW	BHT	8/29/13	11/24/13	n/a	n/a	46.533	-93.407	15.989	-85.386
MN16	2690-98294	2013	GW	BHT	9/22/13	10/13/13	4/25/14	5/17/14	46.533	-93.407	14.988	-83.884

ID	Band #	Dep. year	Sp.	BCR	Aut. start	Aut. end	Spr. start	Spr. end	Br. Lat.	Br. Lon.	NB Lat.	NB Lon.
MN20	2690-98300	2013	GW	BHT	9/15/13	10/19/13	3/31/14	5/19/14	46.533	-93.407	15.989	-85.386
MN25	2690-98039	2014	GW	BHT	8/24/14	11/5/14	4/8/15	5/7/15	46.533	-93.407	15.489	-84.385
MN29	2690-98043	2014	GW	BHT	8/24/14	11/28/14	4/23/15	5/16/15	46.533	-93.407	14.988	-83.383
MN36	2690-98276	2014	GW	BHT	9/1/14	10/28/14	4/22/15	5/6/15	46.533	-93.407	17.492	-90.393
PA05	2520-97749	2014	GW	AM	9/3/14	10/25/14	3/18/15	5/10/15	41.380	-75.180	11.984	-69.864
PA11	2670-48410	2014	GW	AM	9/14/14	10/26/14	3/25/15	5/8/15	41.380	-75.180	9.981	-63.855
TN05	2550-08479	2013	GW	AM	8/14/13	9/10/13	3/21/14	4/11/14	36.291	-84.302	11.483	-72.367
TN06	2470-16207	2013	GW	AM	9/13/13	11/8/13	3/18/14	4/29/14	36.291	-84.302	10.042	-70.539
TN09	2560-53002	2013	GW	AM	8/30/13	9/27/13	3/24/14	4/27/14	36.291	-84.302	11.984	-69.864
TN10	2470-16213	2013	GW	AM	9/8/13	10/10/13	3/19/14	4/19/14	36.291	-84.302	11.984	-71.366
TN13	2560-53004	2013	GW	AM	8/17/13	9/13/13	3/27/14	4/30/14	36.291	-84.302	11.984	-71.366
TN13	2560-53004	2014	GW	AM	8/14/14	9/11/14	3/19/15	4/16/15	36.291	-84.302	11.984	-71.366
TN16	2560-53009	2013	GW	AM	9/10/13	10/3/13	3/8/14	4/17/14	36.291	-84.302	11.984	-71.867
B1	n/a	2016	GW	BHT	9/11/16	10/24/16	4/15/16	5/15/16	44.650	-91.260	14.786	-86.029
B2	n/a	2016	GW	BHT	9/3/16	10/20/16	4/27/16	5/20/16	46.920	-92.760	14.784	-86.032
B3	n/a	2016	GW	BHT	9/17/16	10/26/16	5/1/16	5/22/16	46.340	-91.630	14.786	-86.033
B4	n/a	2016	GW	BHT	8/27/16	11/21/16	4/14/16	5/10/16	46.500	-91.260	14.787	-86.025
B5	n/a	2016	GW	BHT	9/5/16	10/13/16	4/17/16	5/27/16	43.640	-83.290	10.215	-84.659
B6	n/a	2016	GW	BHT	9/15/16	11/8/16	4/29/16	5/16/16	45.690	-90.070	12.945	-85.778
B7	n/a	2016	GW	BHT	9/5/16	11/12/16	4/28/16	5/25/16	46.050	-91.170	12.937	-85.782

ID	Band #	Dep. year	Sp.	BCR	Aut. start	Aut. end	Spr. start	Spr. end	Br. Lat.	Br. Lon.	NB Lat.	NB Lon.
B8	n/a	2016	GW	BHT	9/2/16	10/28/16	4/16/16	5/12/16	47.570	-92.510	12.928	-85.780
B9	n/a	2016	GW	BHT	9/17/16	10/24/16	4/20/16	5/18/16	45.570	-91.200	13.234	-86.050
B10	n/a	2016	GW	BHT	9/5/16	10/17/16	4/29/16	5/9/16	46.460	-93.280	13.236	-86.054
B11	n/a	2016	GW	BHT	9/17/16	10/19/16	4/18/16	5/10/16	44.890	-88.670	13.242	-86.055
B12	n/a	2016	GW	BHT	8/29/16	10/26/16	3/25/16	5/16/16	44.620	-90.700	13.240	-86.052
B13	n/a	2016	GW	BHT	8/30/16	11/10/16	4/23/16	5/29/16	45.400	-92.600	15.178	-87.480
B14	n/a	2016	GW	BHT	9/11/16	10/9/16	4/20/16	5/11/16	46.020	-90.260	15.364	-88.690
B15	n/a	2016	GW	BHT	8/29/16	10/26/16	4/6/16	5/9/16	46.520	-94.420	15.377	-88.702
B16	n/a	2016	GW	BHT	8/24/16	11/9/16	4/28/16	5/17/16	46.310	-93.870	15.671	-88.684
B17	n/a	2016	GW	BHT	8/28/16	10/23/16	4/30/16	5/17/16	48.860	-93.570	15.364	-88.677
B18	n/a	2016	GW	BHT	9/10/16	10/11/16	4/11/16	5/3/16	43.250	-88.280	14.787	-86.025
B19	n/a	2016	GW	BHT	n/a	n/a	4/22/16	5/11/16	46.320	-90.690	12.941	-85.780
B20	n/a	2016	GW	BHT	8/27/16	10/31/16	4/15/16	5/16/16	47.040	-94.110	15.208	-87.505

[a] Individual omitted from analysis.

Table B.2: Summary table of the geolocators used in this analysis and collected from *Vermivora* warblers at 26 sites across the North American breeding distribution and 5 sites within the Central America nonbreeding distribution. Breeding sites are stratified by Bird Conservation Region (BCR).

	Autumn migration					Spring migration				
Breeding Bird Conservation Region	2013	2014	2015	2016	**Total**	2014	2015	2016	2017	**Total**
Golden-winged warblers										
Boreal Hardwood Transition	8	3	20[a]	19	**50**	6	3	37[a]	0	**46**
Appalachian Mountains	6	3[b]	4	0	**13**	6	3[b]	4	0	**13**
Blue-winged warblers										
Appalachian Mountains	0	0	13	0	**13**	0	0	11	0	**11**
Prairie Hardwood Transition	0	0	6	2[c]	**8**	0	0	5	2[c]	**7**
Central Hardwoods	0	0	5	0	**5**	0	0	5	0	**5**
Total	14	6	48	21	**89**	12	6	62	2	**82**

[a] Includes one female golden-winged warbler and two male golden-winged warblers that were also tracked in autumn 2014 and spring 2015.

[b] Includes one male golden-winged warbler also tracked in autumn 2013 and spring 2014.

[c] Includes one male blue-winged warbler also tracked in autumn 2015 and spring 2016.

Table B.3: Summary of a power analysis of multiple linear regression models with five parameters (not including the intercept) corresponding with multiple linear regression models with migratory connectivity terms (BrLat, BrLon, NBLat, NBLon) and an additional migration risk-factor term. Small, medium, and large effect sizes are generally considered to correspond with f^2-values of 0.02, 0.15, and 0.35, respectively.

Number of coefficients (u)[a]	Number of observations (v)[b]	Model R^2	Effect size (f^2)[c]	Significance level	Power
5	75	0.05	0.05	0.05	0.29
5	75	0.20	0.25	0.05	0.94
5	75	0.40	0.67	0.05	0.99
5	75	0.60	1.50	0.05	1.00
5	75	0.63*	1.68	0.05	1.00

[a] Number of coefficients that are being estimated in the model (not including intercept)

[b] Number of observations minus the number of coefficients minus one: effectively the degrees of freedom

[c] Effect size is calculated as $R^2/(1- R^2)$

* Actual R^2 of multiple linear regression model including migratory connectivity terms (Br Lat, Br Lon, NB Lat, NB Lon, and Forest and Shrub Cover.

Table B.4: Summary of a power analysis of simple linear regression models of the relationship between individual migration risk-factors and site-level population trend since 2000. Small, medium, and large effect sizes are generally considered to correspond with f^2-values of 0.02, 0.15, and 0.35, respectively.

Number of coefficients (u)[a]	Number of observations (v)[b]	Model R^2	Effect size (f^2)[c]	Significance level	Power
1	79	0.01	0.01	0.05	0.15
1	79	0.03	0.03	0.05	0.35
1	79	0.05	0.05	0.05	0.53
1	79	0.07	0.08	0.05	0.68
1	79	0.10	0.11	0.05	0.84
1	79	0.13	0.15	0.05	0.93
1	79	0.26	0.35	0.05	0.99

[a] Number of coefficients that are being estimated in the model (not including intercept)

[b] Number of observations minus the number of coefficients minus one: effectively the degrees of freedom

[c] Effect size is calculated as $R^2/(1- R^2)$

Table B.5: Variable inflation factors (VIF) used to assess the multicollinearity of terms used in the partial least squares (PLS) regression analysis. The PLS analysis modeled the relative importance of migration risk-factors (experienced during migration; 25th percentile core-use area) and migratory connectivity factors (experienced on breeding or nonbreeding sites) in explaining recent population trends in *Vermivora* warblers. VIF scores > 5 denote moderate to strong multicollinearity and are bold.

Variable category	Variable name	Variable inflation factor (VIF)
Migratory connectivity	Breeding latitude	2.6
Migratory connectivity	Breeding longitude	2.5
Migratory connectivity	Nonbreeding latitude	3.6
Migratory connectivity	Nonbreeding longitude	**5.9**
Migration risk-factor	Wind turbines	**5.8**
Migration risk-factor	Communications towers	2.6
Migration risk-factor	Hurricanes	3.2
Migration risk-factor	Tornados	**5.6**
Migration risk-factor	Agriculture	**9.6**
Migration risk-factor	Forest and shrub cover	**8.9**
Migration risk-factor	Human footprint	**17.0**
Migration risk-factor	Net increase in forest cover 2000-2015	2.4

Table B.6: Performance of generalized linear models considered in an information-theoretic, hierarchical regression analysis exploring whether the addition of individual migration risk-factor variables (sum of autumn and spring migration periods) explains additional variation relative to a base model of migratory connectivity terms (breeding location, nonbreeding location) with previously described associations with *Vermivora* warbler population trends. Model name (Model), the number of variables in each model (*k*), difference between Akaike's Information Criterion adjusted for sample size of top-performing model (ΔAIC_c), and model deviance (-2*log-likelihood) are provided. Base model (Base) included five estimated parameters: intercept, breeding latitude, breeding longitude, nonbreeding latitude, nonbreeding longitude. The variable "overall" was calculated by summing standardizing individual migration risk-factor rasters ($n = 8$; assigning equal weight to all risk factors).

Model	*k*	ΔAIC_c	-2*log-likelihood
Base + Communications towers*	7	0.00	424.33
Base	6	0.44	427.17
Base + Wind energy	7	1.78	426.11
Base + Agricultural cover	7	1.82	426.15
Base + Tornados	7	2.09	426.42
Base + Hurricanes	7	2.14	426.47
Base + Forest and shrub cover	7	2.23	426.56
Base + Overall	7	2.69	427.02
Base + Net change in forest cover 2000–2010	7	2.79	427.12
Base + Human footprint	7	2.84	427.15

*AIC_c of top model = 439.86

Table B.7: Model performance of factors considered in an information-theoretic, hierarchical regression analysis exploring whether the addition of individual migration risk-factor variables experienced before crossing the Gulf of Mexico in both autumn and spring (Fig. B – 2) explains additional variation relative to a base model of migratory connectivity terms (breeding location, nonbreeding location) with previously described associations with *Vermivora* warbler population trends. Model name (Model), the number of variables in each model (*k*), difference between Akaike's Information Criterion adjusted for sample size of top-performing model (ΔAIC_c), and model deviance (-2*log-likelihood) are provided. Base model (Base) included five estimated parameters: intercept, breeding latitude, breeding longitude, nonbreeding latitude, nonbreeding longitude. The variable "overall" was calculated by summing standardizing individual migration risk-factor rasters (*n* = 8; assigning equal weight to all risk factors).

Autumn	*k*	ΔAIC_c	-2*log-likelihood
Base[a]	6	0.00	466.78
Base + Wind energy	7	0.32	464.73
Base + Net change in forest cover 2000–2010	7	0.68	465.09
Base + Communications towers	7	1.35	465.76
Base + Hurricanes	7	1.93	466.34
Base + Forest and shrub cover	7	2.14	466.55
Base + Agricultural cover	7	2.25	466.66
Base + Human footprint	7	2.27	466.67
Base + Overall	7	2.29	466.70
Base + Tornados	7	2.34	466.75
Spring*	*k*	ΔAIC_c	-2*log-likelihood
Base[b]	6	0.00	349.64
Base + Forest and shrub cover	7	0.87	347.99
Base + Overall	7	1.78	348.90
Base + Human footprint	7	2.04	349.16
Base + Net change in forest cover 2000–2010	7	2.31	349.43
Base + Agricultural cover	7	2.35	349.47

[a] AIC_c of top model = 493.66

[b] AIC_c of top model = 363.08

*Data for wind energy, communications towers, hurricanes, and tornados not available for area considered during spring migration (i.e., only available for United States).

Table B.8: Performance of linear regression models assessing the relationship between individual migration risk-factor variables (sum of autumn and spring migration periods) and site-level *Vermivora* warbler population trends. I used migration risk-factor data extracted from 10%, 25%, and 50% core-use areas. Model name (Model), the number of variables in each model (k), difference between Akaike's Information Criterion adjusted for sample size of top-performing model (ΔAIC_c), and model deviance (-2*log-likelihood) are provided. Models in bold are >2 AIC_c from the intercept-only model.

Model	*k*	ΔAIC_c	-2*log-likelihood
10% core-use area			
Agriculture	3	0.0	502.3
Wind energy	3	0.8	503.1
Null (intercept-only)	2	1.7	506.1
Tornados	3	3.0	505.3
Forest and shrub cover	3	3.5	505.7
Communications towers	3	3.5	505.8
Human footprint	3	3.6	505.8
Net change in forest cover 2000–2010	3	3.6	505.9
Hurricanes	3	3.8	506.1
25% core-use area			
Agriculture	**3**	**0.0**	**501.6**
Tornados	3	1.5	503.1
Forest and shrub cover	3	1.7	503.3
Net change in forest cover 2000–2010	3	2.1	503.7
Wind energy	3	2.2	503.7
Null (intercept-only)	2	2.4	506.1
Communications towers	3	3.6	505.2
Human footprint	3	4.0	505.6
Hurricanes	3	4.1	505.7
50% core-use area			
Wind energy	**3**	**0.0**	**498.1**
Tornados	**3**	**0.6**	**498.7**
Forest and shrub cover	**3**	**0.8**	**498.9**
Agriculture	**3**	**2.8**	**500.9**
Human footprint	3	5.1	503.2
Net change in forest cover 2000–2010	3	5.4	503.5
Null (intercept-only)	2	5.9	506.1
Hurricanes	3	5.9	504.0
Communications towers	3	7.9	505.9

Table B.9: Coefficient estimates of linear regression models assessing the relationship between individual migration risk-factor variables (sum of autumn and spring migration periods) and site-level *Vermivora* warbler population trends. I used migration risk-factor data extracted from 10%, 25%, and 50% core-use areas. Shown are models from Table BX that were >2 AIC$_c$ from the intercept-only model. Coefficient being estimated (Parameter), the standard error of the coefficient estimate (Std. Error), P-value, and whether the direction of the relationship was congruent with expectations are provided.

Parameter*	Estimate	Std. Error	*P*-value	Direction of effect congruent with expectations?
10% core-use area				
N/A				
25% core-use area				
Agriculture	1.29	0.61	0.04	No, expected negative relationship
50% core-use area				
Wind energy	1.70	0.59	0.005	No, expected negative relationship
Tornados	1.64	0.60	0.007	No, expected negative relationship
Forest and shrub cover	-1.38	0.60	0.02	No, expected positive relationship
Agriculture	1.62	0.60	0.008	No, expected negative relationship

*All parameters are scaled (mean-centered)

Table B.10: Performance of generalized linear models considered in an information-theoretic, hierarchical regression analysis exploring whether the addition of individual migration risk-factor variables (sum of autumn and spring migration periods) explains additional variation relative to a base model of migratory connectivity terms (breeding location, nonbreeding location) with previously described associations with *Vermivora* warbler population trends. Model name (Model), the number of variables in each model (k), difference between Akaike's Information Criterion adjusted for sample size of top-performing model (ΔAIC_c), and model deviance (-2*log-likelihood) are provided. Base model (Base) included five estimated parameters: intercept, breeding latitude, breeding longitude, nonbreeding latitude, nonbreeding longitude.

Model	*k*	ΔAIC_c	-2*log-likelihood
10% core-use area			
Base + Forest and shrub cover	7	0.0	424.5
Base	6	0.3	427.2
Base + Tornados	7	0.3	424.8
Base + Agriculture	7	0.6	425.0
Base + Net change in forest cover 2000-2010	7	1.0	425.5
Base + Hurricanes	7	1.7	426.2
Base + Communications towers	7	2.2	426.7
Base + Wind energy	7	2.3	426.8
Base + Human footprint	7	2.3	426.8
Full model	14	10.7	416.4
25% core-use area			
Base + Communications towers	7	0.0	424.3
Base	6	0.4	427.2
Base + Wind energy	7	1.8	426.1
Base + Agriculture	7	1.8	426.1
Base + Tornados	7	2.1	426.4
Base + Hurricanes	7	2.1	426.5
Base + Forest and shrub cover	7	2.2	426.6
Base + Net change in forest cover 2000-2010	7	2.8	427.1
Base + Human footprint	7	2.8	427.2
Full model	14	9.9	415.4
50% core-use area			
Base	6	0.0	427.2
Base + Communications towers	7	1.8	426.5
Base + Hurricanes	7	2.1	426.9
Base + Agriculture	7	2.3	427.1
Base + Forest and shrub cover	7	2.4	427.2
Base + Tornados	7	2.4	427.2
Base + Wind energy	7	2.4	427.2
Base + Net change in forest cover 2000-2010	7	2.4	427.2
Base + Human footprint	7	2.4	427.2
Full model	14	18.4	424.4

Fig. B – 1: Predicted power vs. sample size of one-way analysis of variance (ANOVA) given the scaled mean, within-group, and among-group variances of the "Overall" migration risk-factor variable calculated for 81 *Vermivora* warblers. Warblers were classified into five groups based on Bird Conservation Region (BCR) and species. Sample size increments in the plot below are not constant: 2–10, by 1; 12–20, by 2; 22–50, by 5. I estimated the among-group variance without blue-winged warblers from breeding populations in the Prairie Harwood Transition Bird Conservation Region (i.e., n = 4 groups) because the rate of within-group variance was an order of magnitude greater than any of the other groups.

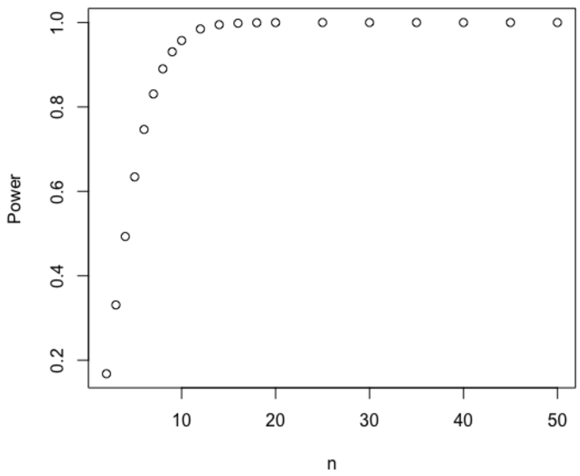

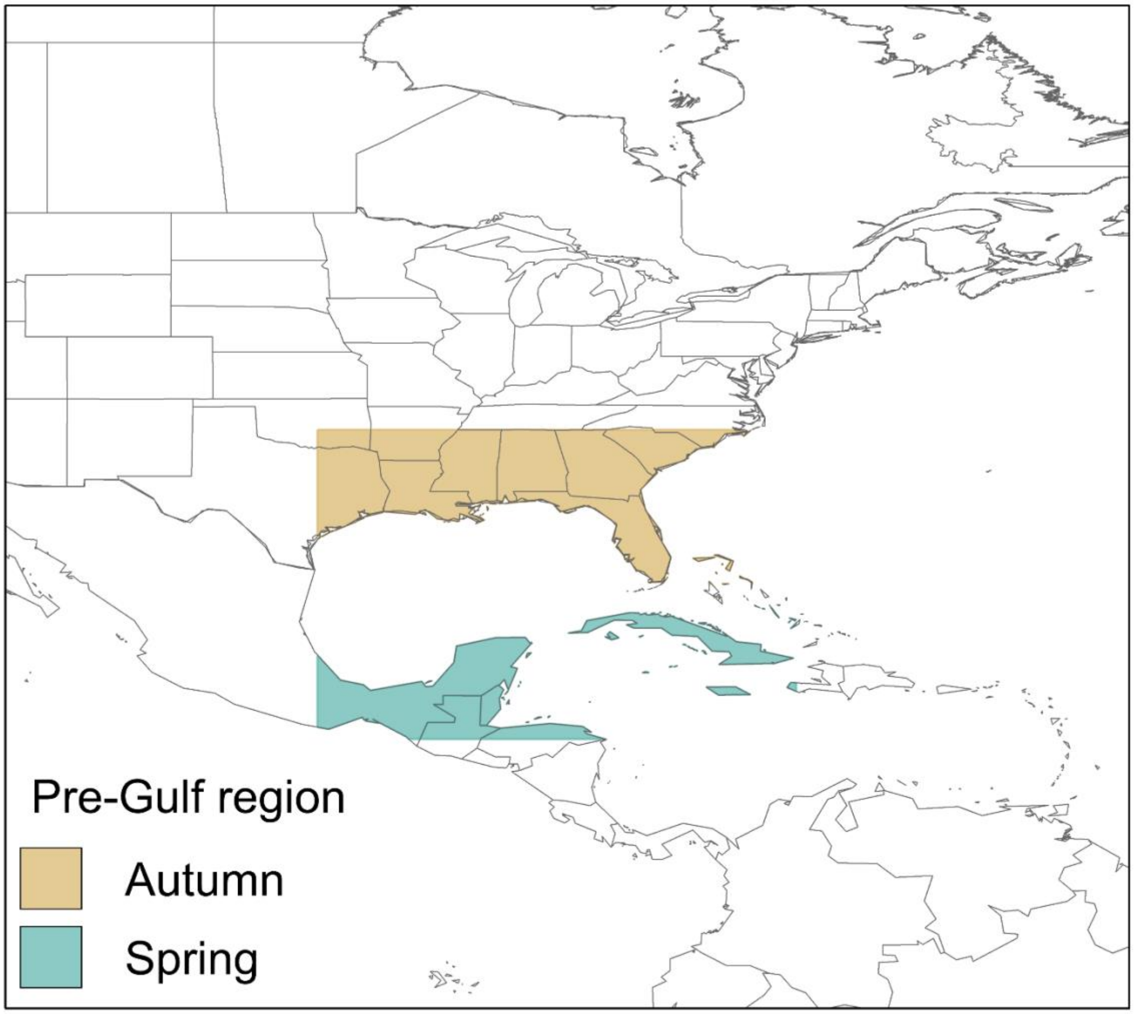

Figure B – 2: Map of region used to test for associations between *Vermivora* warbler population trends and migration risk-factors experienced in stopover regions before crossing the Gulf of Mexico during autumn (25–35°; tan) and spring (15–23.5°; blue) migration periods.

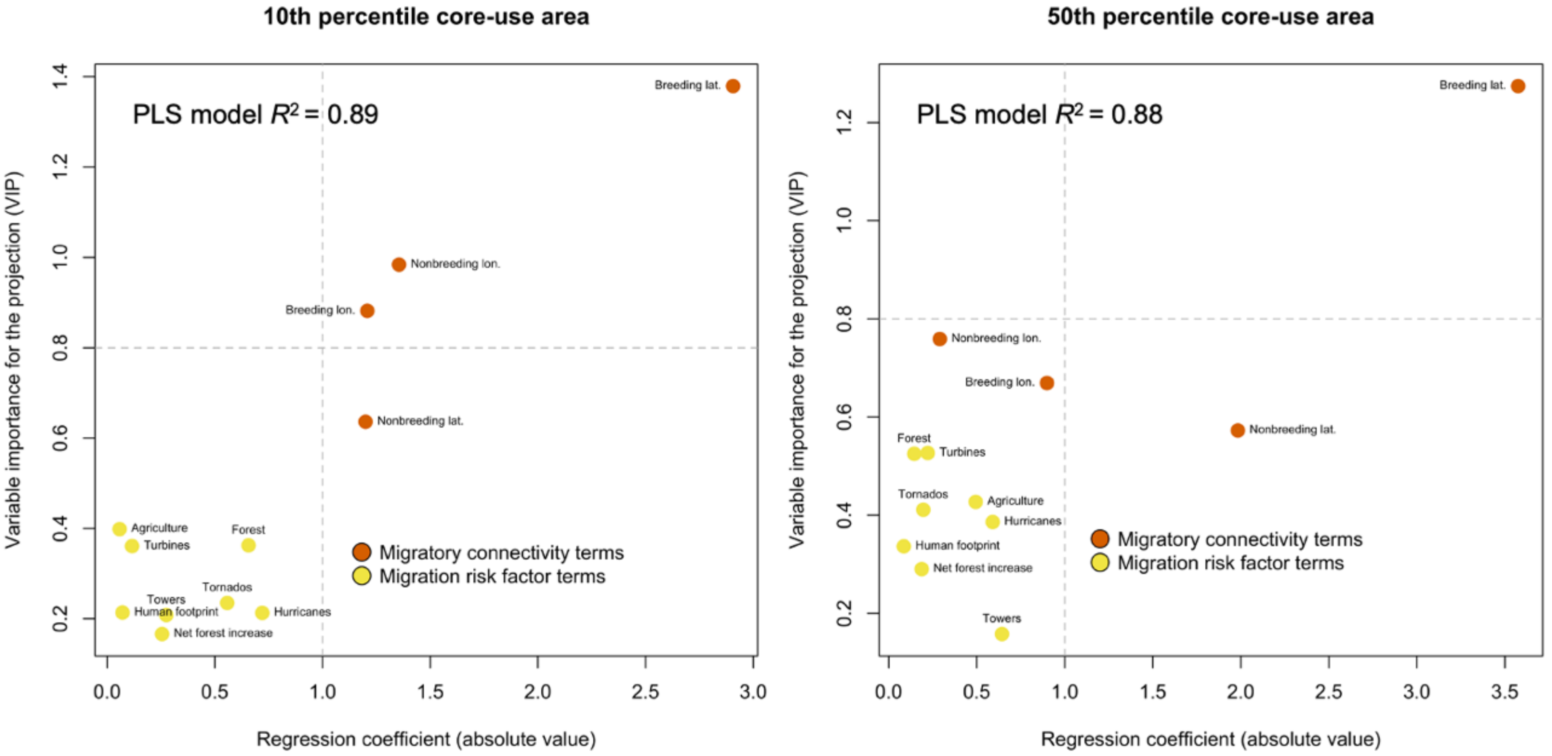

Figure B – 3: Comparison plots of the absolute value of regression coefficients and variable importance for the projection (VIP) of explanatory variables included in a partial least squares (PLS) regression model relating explanatory variables to variation in recent population trends of *Vermivora* warblers (i.e., since 2000) at two different core-use area scales (10th percentile, 50th percentile). Explanatory variables fall into two categories: those associated with migration risk-factors (migration risk-factors terms; yellow circles) and those related to factors experienced during breeding and/or nonbreeding periods (migratory connectivity terms; orange circles). Gray dashed lines denote regression coefficients with absolute values > 1 and VIP > 0.8, which correspond with terms that are important in the PLS model. Test set validation of PLS model performance is presented (R^2).

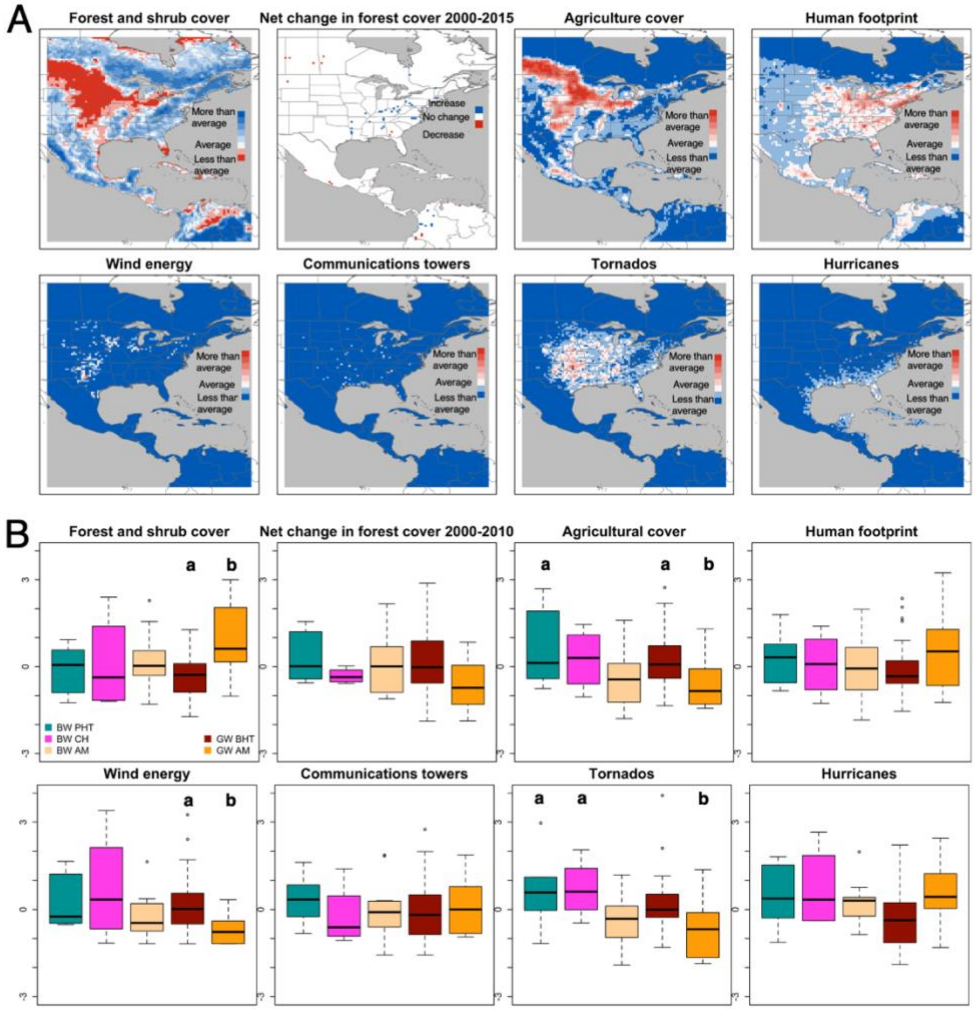

Figure B – 4: The spatial distribution of mean-adjusted individual migration risk-factors I considered (*n* = 8; A) are displayed using color schemes corresponding with their expected association with population-trends (i.e., positive association = blue for higher-than-average values, negative association = red for higher-than-average values; see Table 2 – 1). Boxplots (B) show the scaled exposure of different populations (based on the exposure of individuals tracked within each population; colors correspond with the center panel) of *Vermivora* warblers to each migration risk-factor. Populations that experienced different levels of exposure (based on one-way ANOVA and Tukey HSD; $P < 0.05$) are denoted with letters. Populations are defined based on BCR and species (blue-winged warbler [BW] or golden-winged warbler [GW]) in boxplots: Prairie Hardwood Transition BCR (BW PHT, teal), Central Hardwoods BCR (BW CH, pink), Appalachian Mountains BCR (BW AM, light orange; GW AM, dark orange), and Boreal Hardwood Transition (GW BHT; maroon) BCR.

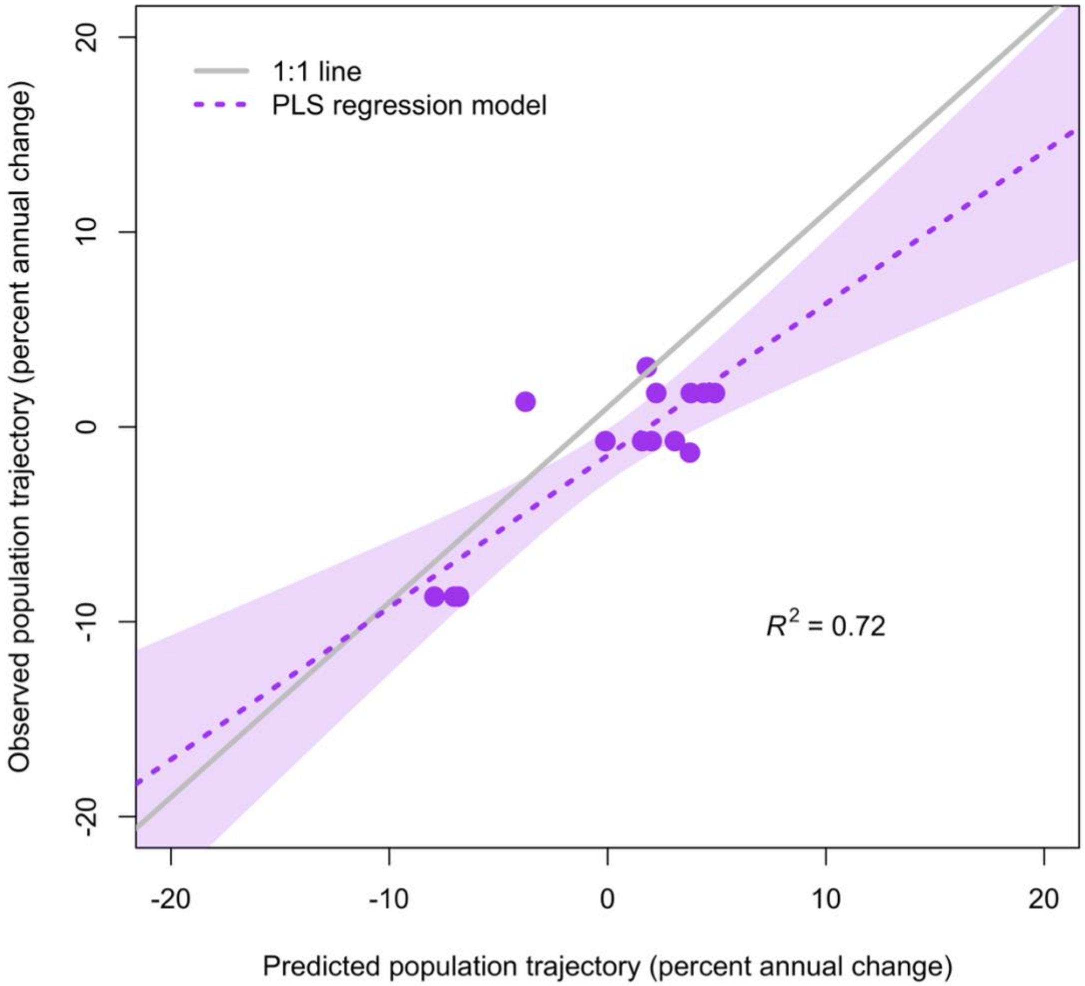

Figure B – 5: Test set validation of partial least squares (PLS) regression model (predicted vs. observed population trends). I trained a PLS regression model using 80% of the data and predicted the withheld (test) data to assess model accuracy. Predicted points are shown in purple and the fitted model is represented by a dashed purple line (shaded area = 95% CI).

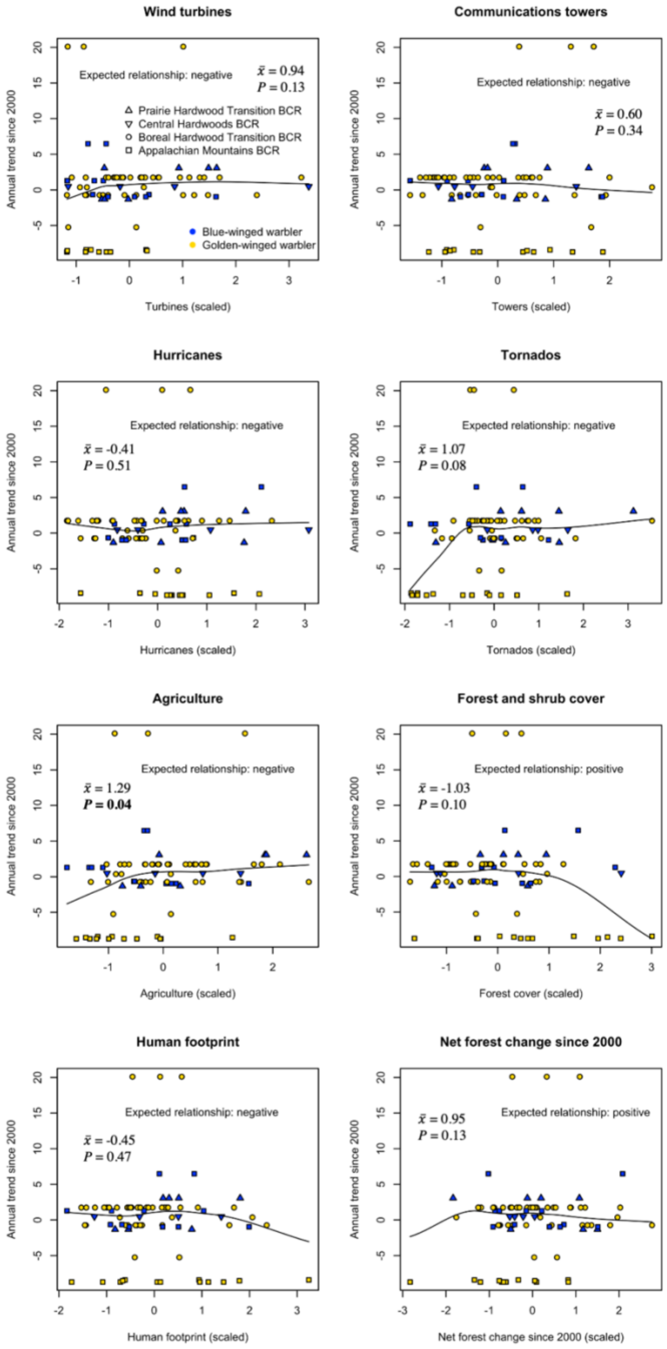

Figure B – 6: Scatterplots of the association (loess curve; black line) between recent annual population trend (since 2000) and exposure of individual *Vermivora* warblers to migration risk-factors. Blue-winged warblers (blue) and golden-winged warblers (gold) from different Bird Conservation regions are presented with different shapes. Statistical relationships (slope and *P*-value) between individual risk factors and site-level population trends assessed with simple linear regression are also presented with statistically significant relationships appearing in bold.

Appendix C

Supplementary Information for Chapter 3: Migratory Connectivity and Barrier-crossing Flights of *Vermivora* Warblers are Affected by Synoptic Weather Conditions

Supplementary Methods:

Defining populations of Vermivora *warblers*—

I defined populations of *Vermivora* warblers based on the Bird Conservation Region (BCR) of an individual's breeding location. However, several study areas occurred on the periphery of the species' distribution and I assigned individuals at those sites to the nearest BCR containing other study sites and containing a greater proportion of the species' distribution (Table C.1, C.2, Fig. C – 1). Specifically, I assigned blue-winged warblers breeding at two sites in southern Ontario, Canada (n = 2 individuals) and one site in Massachusetts, USA (n = 4 individuals) to the Appalachian Mountain BCR and golden-winged warblers breeding at two sites in western Manitoba, Canada (n = 2) to the Boreal Hardwood Transition BCR (Table C.1, Fig. C – 1). Thus, I classified golden-winged warblers into two populations: Boreal Hardwood Transition BCR and Appalachian Mountain BCR (Table C.1). I classified blue-winged warblers into three populations: Prairie Hardwood Transition BCR, Central Hardwood BCR, and Appalachian Mountain BCR (Table C.1).

Identification of full light pattern (FLP) anomalies—

I visually searched for FLP anomalies in geolocator-derived light data in both autumn (15 Aug – 15 Nov) and spring (15 Mar – 15 May) migration periods (Kramer et al. 2018b) using the preprocessLight function in the TwGeos package (Lisovski et al. 2016). I visually inspected the light curve (i.e., dawn, daytime, and dusk periods) for each day during autumn and spring periods and selected all days that met the three requirements listed in the Methods. I defined dawn as the period between the first recorded light (i.e., transition from no light [0] to ≥ 1; period includes the last measured instance of no light) and the first recorded instance of maximum light (i.e., 64; including the first measured instance of full light) for a given day. I defined dusk as the period between the last recorded instance of full light (i.e., 64) and the last recorded instance of light (i.e., transition from light levels ≥ 1 to 0) for each day. I defined daytime as the period between the end of dawn (i.e., first recorded instance of maximum light) and the beginning of dusk (i.e., last recorded instance of maximum light). For days that met the requirements, I estimated the amount of shade during dawn, daytime, and dusk periods. To quantify shading during dawn and dusk periods, I fit a quadratic regression to the light data and calculated the summed absolute residuals (Adamík et al. 2016). To quantify shading during the daytime period, I calculated the sum of deviations from maximum light intensity (i.e., 64; Adamík et al. 2016). I also determined the duration (in minutes) of dawn, daytime, and dusk periods for all identified FLP anomalies.

Calculating wind profit—

I calculated wind profit to determine the favorability of wind conditions for *Vermivora* warblers navigating the Gulf of Mexico. I calculated wind profit as the product of wind speed (m/s) and wind direction (°) relative to north or south depending on the season:

Autumn wind profit = wind speed × cos(wind direction)

Spring wind profit = wind speed × (1-cos(wind direction))

Differences between mean weather conditions on FLP vs. non-FLP days—

I tested if individual weather conditions differed on days that had a FLP anomaly compared to days with no observed FLP anomaly using simple linear regression. I tested conditions during autumn and spring separately and considered differences to be statistically significant at $P = 0.05$ (Fig. C – 2).

Table C.1: Summary table of geolocator data collected from individual *Vermivora* warblers at 26 sites across the North American breeding distribution and 5 sites within the Central America nonbreeding distribution. Breeding sites are stratified by Bird Conservation Region (BCR) based on occurrence each site within, or proximity to BCRs containing meaningful populations of *Vermivora* warblers (see Methods for details).

	Autumn migration					Spring migration				
Bird Conservation Region	2013	2014	2015	2016	**Total**	2014	2015	2016	2017	**Total**
Golden-winged warblers										
Boreal Hardwood Transition	8	3	20[a]	19	**50**	6	3	37[a]	0	**46**
Appalachian Mountain	6	3[b]	4	0	**13**	6	3[b]	4	0	**13**
Blue-winged warblers										
Appalachian Mountain	0	0	13	0	**13**	0	0	11	0	**11**
Prairie Hardwood Transition	0	0	6	2[c]	**8**	0	0	5	2[c]	**7**
Central Hardwoods	0	0	5	0	**5**	0	0	5	0	**5**
Hybrids										
Boreal Hardwood Transition	0	0	2	1[d]	**3**	0	0	2	1[d]	**3**
Appalachian Mountain	0	0	2	0	**2**	0	0	2	0	**2**
Total	14	6	50	23	**94**	12	6	66	3	**87**

[a] Includes one female golden-winged warbler and two male golden-winged warblers that were also tracked in autumn 2014 and spring 2015.

[b] Includes one male golden-winged warbler also tracked in autumn 2013 and spring 2014.

[c] Includes one male blue-winged warbler also tracked in autumn 2015 and spring 2016.

[d] Male hybrid also tracked in autumn 2015 and spring 2016.

Table C.2: Metadata of geolocator-marked *Vermivora* warblers including individual identification code (ID), U.S. Geological Survey band number (Band number), geolocator deployment year (Year), species (Species; GW=golden-winged warbler, BW=blue-winged warbler, H = hybrid), corresponding Bird Conservation Region (BCR) of breeding location, breeding and nonbreeding coordinates (Breeding latitude, Breeding longitude, Nonbreeding latitude, Nonbreeding longitude). Cells for which geolocator data were not collected, or for which data were not available are denoted by "n/a".

ID	Band #	Year*	Species	BCR	Breeding latitude	Breeding longitude	Nonbreeding latitude	Nonbreeding longitude
DMG03	2840-78903	2015	GW	BHT	51.535	-100.581	15.9893	-85.386
ILB04	2750-63504	2015	BW	CH	37.816	-89.463	21.4972	-87.8896
ILB06	2750-63506	2015	BW	CH	37.816	-89.463	21.4972	-87.3889
ILB08	2750-63508	2015	BW	CH	37.816	-89.463	17.9922	-93.3976
ILB18	2750-63523	2015	BW	CH	39.407	-88.161	21.4972	-87.8896
KYB14	2690-98096	2015	BW	AM	36.913	-83.562	20.9965	-87.3889
MAB05	2750-63237	2015	BW	AM	42.343	-72.568	10.4814	-74.8709
MAB06	2750-63238	2015	BW	AM	42.343	-72.568	14.9879	-83.3831
MAB09	2750-63243	2015	BW	AM	42.343	-72.568	20.9965	-86.8882
MAB12	2770-39353	2015	BW	AM	42.343	-72.568	14.9879	-83.3831
MIB02	2750-63335	2015	BW	PHT	43.948	-84.267	20.9965	-86.8882
MIB05	2750-63353	2015	BW	PHT	42.615	-85.41	21.1235	-86.9527
MIB12	2750-63360	2015	BW	PHT	42.615	-85.41	21.4972	-87.3889
MIB14	2750-63362	2015	BW	PHT	42.615	-85.41	20.9965	-89.3918
MIG01	2750-63331	2015	GW	BHT	43.948	-84.267	14.9879	-83.3831
MIH02	2750-63351	2015	H	BHT	43.948	-84.267	20.9965	-88.3904
MN14	2690-98282	2015	GW	BHT	46.533	-93.407	15.4886	-84.3846
MN 29	2690-98043	2015	GW	BHT	46.533	-93.407	14.9879	-83.3831
MN 36	2690-98276	2015	GW	BHT	46.533	-93.407	16.9907	-88.3904

ID	Band #	Year*	Species	BCR	Breeding latitude	Breeding longitude	Nonbreeding latitude	Nonbreeding longitude
NCB01	2700-29578	2015	BW	AM	36.412	-81.655	20.9965	-86.8882
ONB02	2740-78971	2015	BW	AM	44.003	-79.123	21.4972	-87.3889
ONB05	2740-78972	2015	BW	AM	44.7	-79.545	20.9965	-86.8882
ONG03	2740-78953	2015	GW	BHT	44.641	-76.343	14.9879	-83.3831
ONG05	2740-78955	2015	GW	BHT	44.641	-76.343	14.9879	-83.3831
ONG10	2740-78968	2015	GW	BHT	44.7	-79.545	10.9821	-73.3687
PAB01	2750-63202	2015	BW	AM	40.995	-77.701	20.9965	-89.3918
PAB03	2750-63206	2015	BW	AM	40.995	-77.701	20.9965	-86.8882
PAB05	2750-63211	2015	BW	AM	40.995	-77.701	21.4972	-87.3889
PAB07	2750-63225	2015	BW	AM	40.995	-77.701	18.9936	-90.894
PAG12	2750-63222	2015	GW	AM	40.995	-77.701	11.9835	-69.8637
PAH01	2750-63210	2015	H	AM	40.995	-77.701	10.9821	-73.8694
PAH06	2750-63228	2015	H	AM	40.995	-77.701	11.9835	-71.8665
RLG16	2750-63373	2015	GW	BHT	46.533	-93.407	15.9893	-85.386
RLG23	2750-63256	2015	GW	BHT	46.533	-93.407	15.9893	-85.386
RLGF15[a]	2750-63255	2015	GW	BHT	46.533	-93.407	14.4871	-83.8839
RMG02	2840-78914	2015	GW	BHT	51.024	-99.941	15.4886	-84.3846
SHG07	2750-63448	2015	GW	BHT	45.517	-93.699	9.4799	-79.3774
SLG12	2740-84922	2015	GW	BHT	49.624	-96.307	15.9893	-85.386
SLG18	2740-84929	2015	GW	BHT	49.624	-96.307	14.9879	-83.8839
TAG07	2750-63418	2015	GW	BHT	46.987	-95.611	17.4915	-90.3932
TAG09	2750-63410	2015	GW	BHT	46.987	-95.611	15.4886	-86.3875
TAG14	2750-63416	2015	GW	BHT	46.987	-95.611	14.9879	-83.3831
TNB03	2560-53231	2015	BW	AM	35.927	-84.404	18.9936	-90.894
TNB09	2560-53254	2015	BW	CH	36.62	-87.515	21.4972	-87.8896

ID	Band #	Year*	Species	BCR	Breeding latitude	Breeding longitude	Nonbreeding latitude	Nonbreeding longitude
TNG13	2560-53206	2015	GW	AM	36.291	-84.302	11.9835	-71.3658
VAG01	2770-39700	2015	GW	AM	38.26	-79.627	11.9835	-71.3658
VAG02	2770-39698	2015	GW	AM	38.26	-79.627	11.9835	-69.8637
WIB05	2750-63537	2015	BW	PHT	44.319	-90.131	20.9965	-86.8882
WIB11	2750-63550	2015	BW	PHT	44.319	-90.131	20.9965	-89.8925
WIB11	2750-63550	2016	BW	PHT	44.319	-90.131	18.4929	-92.3961
WIB19	2750-63464	2016	BW	PHT	44.319	-90.131	21.4972	-87.3889
WIG01	2750-63528	2015	GW	BHT	44.319	-90.131	14.9879	-83.3831
WIG02	2750-63529	2015	GW	BHT	44.319	-90.131	14.9879	-83.3832
WIH03	2750-63553	2015	H	BHT	44.319	-90.131	18.9936	-90.894
WIH03	2750-63553	2016	H	BHT	44.319	-90.131	15.9893	-85.386
MN03[b]	2660-29638	2013	GW	BHT	46.533	-93.407	14.4871	-85.386
MN05	2660-29468	2013	GW	BHT	46.533	-93.407	15.4886	-84.3846
MN06	2690-29281	2013	GW	BHT	46.533	-93.407	15.4886	-84.3846
MN11	2660-29675	2013	GW	BHT	46.533	-93.407	15.9893	-85.386
MN12	2690-98293	2013	GW	BHT	46.533	-93.407	16.9907	-88.8911
MN14	2690-98282	2013	GW	BHT	46.533	-93.407	14.9879	-83.3831
MN15	2660-29451	2013	GW	BHT	46.533	-93.407	15.9893	-85.386
MN16	2690-98294	2013	GW	BHT	46.533	-93.407	14.9879	-83.8839
MN20	2690-98300	2013	GW	BHT	46.533	-93.407	15.9893	-85.386
MN25	2690-98039	2014	GW	BHT	46.533	-93.407	15.4886	-84.3846
MN29	2690-98043	2014	GW	BHT	46.533	-93.407	14.9879	-83.3831
MN36	2690-98276	2014	GW	BHT	46.533	-93.407	17.4915	-90.3932
PA05	2520-97749	2014	GW	AM	41.38	-75.18	11.9835	-69.8637
PA11	2670-48410	2014	GW	AM	41.38	-75.18	9.9806	-63.855

ID	Band #	Year*	Species	BCR	Breeding latitude	Breeding longitude	Nonbreeding latitude	Nonbreeding longitude
TN05	2550-08479	2013	GW	AM	36.291	-84.302	11.4828	-72.3673
TN06	2470-16207	2013	GW	AM	36.291	-84.302	10.0423	-70.5386
TN09	2560-53002	2013	GW	AM	36.291	-84.302	11.9835	-69.8637
TN10	2470-16213	2013	GW	AM	36.291	-84.302	11.9835	-71.3658
TN13	2560-53004	2013	GW	AM	36.291	-84.302	11.9835	-71.3658
TN13	2560-53004	2014	GW	AM	36.291	-84.302	11.9835	-71.3658
TN16	2560-53009	2013	GW	AM	36.291	-84.302	11.9835	-71.8665
B1	n/a	2016	GW	BHT	44.65	-91.26	14.78623	-86.02944
B2	n/a	2016	GW	BHT	46.92	-92.76	14.78441	-86.03207
B3	n/a	2016	GW	BHT	46.34	-91.63	14.78613	-86.03323
B4	n/a	2016	GW	BHT	46.5	-91.26	14.78725	-86.02464
B5	n/a	2016	GW	BHT	43.64	-83.29	10.21512	-84.65889
B6	n/a	2016	GW	BHT	45.69	-90.07	12.94511	-85.77831
B7	n/a	2016	GW	BHT	46.05	-91.17	12.93735	-85.78214
B8	n/a	2016	GW	BHT	47.57	-92.51	12.92843	-85.78031
B9	n/a	2016	GW	BHT	45.57	-91.2	13.234	-86.05
B10	n/a	2016	GW	BHT	46.46	-93.28	13.23639	-86.05356
B11	n/a	2016	GW	BHT	44.89	-88.67	13.24183	-86.05484
B12	n/a	2016	GW	BHT	44.62	-90.7	13.2399	-86.05153
B13	n/a	2016	GW	BHT	45.4	-92.6	15.1775667	-87.4796
B14	n/a	2016	GW	BHT	46.02	-90.26	15.36432	-88.68967
B15	n/a	2016	GW	BHT	46.52	-94.42	15.3771	-88.702
B16	n/a	2016	GW	BHT	46.31	-93.87	15.67136	-88.68349
B17	n/a	2016	GW	BHT	48.86	-93.57	15.36437	-88.67723
B18	n/a	2016	GW	BHT	43.25	-88.28	14.7872	-86.02464

ID	Band #	Year*	Species	BCR	Breeding latitude	Breeding longitude	Nonbreeding latitude	Nonbreeding longitude
B19	n/a	2016	GW	BHT	46.32	-90.69	12.94104	-85.78009
B20	n/a	2016	GW	BHT	47.04	-94.11	15.2084	-87.504917

* Deployment year

[a] Female

[b] Mud caked over light sensor; omitted from analysis

Table C.3: Metadata of geolocator-marked *Vermivora* warblers including number and timing of full-light period (FLP) anomalies. Individual identification code (ID), U.S. Geological Survey band number (Band number), geolocator deployment year (Deployment year), species (Species; GW=golden-winged warbler, BW=blue-winged warbler, H = hybrid), corresponding Bird Conservation Region (BCR) of breeding location, start and end of seasonal migrations (Autumn start, Autumn end, Spring start, Spring end), number of autumn and spring FLPs identified (Number autumn FLPs, Number Spring FLPs), date of FLP associated with crossing the Gulf of Mexico (Date trans-Gulf FLP), breeding and nonbreeding coordinates (Breeding latitude, Breeding longitude, Nonbreeding latitude, Nonbreeding longitude). Individuals that circumvented the Gulf of Mexico are denoted by "Circ.". Cells for which geolocator data were not collected, or for which data were not available are denoted by "n/a".

ID	Year*	Species	BCR	Number aut. FLPs	Date aut. trans-Gulf FLP	Aut. departure sector	Number spr. FLPs	Date spr. trans-Gulf FLP	Spr. departure sector
DMG03	2015	GW	BHT	1	10/11/15	C	n/a	n/a	n/a
ILB04	2015	BW	CH	1	9/23/15	C	1	4/10/16	C
ILB06	2015	BW	CH	1	9/13/15	E	1	4/23/16	C
ILB08	2015	BW	CH	0	Circ.	Circ.	1	4/16/16	W
ILB18	2015	BW	CH	1	Circ.	Circ.	1	4/9/16	C
KYB14	2015	BW	AM	1	10/1/15	C	n/a	n/a	n/a
MAB05	2015	BW	AM	1	9/14/15	E	2	5/10/16	C
MAB06	2015	BW	AM	3	11/1/15	C	6	5/16/16	C
MAB09	2015	BW	AM	3	10/15/15	E	1	4/17/16	C
MAB12	2015	BW	AM	1	9/28/15	E	3	4/16/16	C
MIB02	2015	BW	PHT	1	10/1/15	E	1	4/13/16	C
MIB05	2015	BW	PHT	1	10/2/15	E	n/a	n/a	n/a
MIB12	2015	BW	PHT	1	Circ.	Circ.	1	4/11/16	C
MIB14	2015	BW	PHT	1	10/17/15	E	1	4/20/16	C
MIG01	2015	GW	BHT	1	9/13/15	C	1	5/8/16	E

ID	Year*	Species	BCR	Number aut. FLPs	Date aut. trans-Gulf FLP	Aut. departure sector	Number spr. FLPs	Date spr. trans-Gulf FLP	Spr. departure sector
MIH02	2015	H	BHT	1	10/3/15	C	1	4/27/16	C
MN14	2015	GW	BHT	1	10/11/15	C	1	5/1/16	C
MN29	2015	GW	BHT	1	10/1/15	E	n/a	n/a	n/a
MN36	2015	GW	BHT	2	10/11/15	C	0	Circ.	Circ.
NCB01	2015	BW	AM	1	10/1/15	C	1	4/1/16	C
ONB02	2015	BW	AM	1	10/15/15	C	1	4/22/16	C
ONB05	2015	BW	AM	1	10/11/15	E	1	4/25/16	C
ONG03	2015	GW	BHT	2	10/7/15	E	8	4/28/16	C
ONG05	2015	GW	BHT	1	10/8/15	E	2	4/25/16	C
ONG10	2015	GW	BHT	11	10/11/15	E	4	5/1/16	C
PAB01	2015	BW	AM	1	Circ.	Circ.	1	4/12/15	W
PAB03	2015	BW	AM	1	9/27/15	C	1	4/25/16	C
PAB05	2015	BW	AM	1	10/1/15	W	3	4/25/16	C
PAB07	2015	BW	AM	2	9/21/15	E	1	4/17/16	C
PAG12	2015	GW	AM	0	Circ.	Circ.	1	4/26/16	C
PAH01	2015	H	AM	1	9/5/15	C	0	Circ.	Circ.
PAH06	2015	H	AM	2	9/4/15	E	2	3/20/16	C
RLG16	2015	GW	BHT	1	10/16/15	E	n/a	n/a	n/a
RLG23	2015	GW	BHT	1	10/17/15	C	1	4/30/16	W
RLGF15[a]	2015	GW	BHT	2	10/11/15	E	2	4/26/16	C
RMG02	2015	GW	BHT	1	10/2/15	C	1	4/27/16	C
SHG07	2015	GW	BHT	2	Circ.	Circ.	2	4/21/16	E
SLG12	2015	GW	BHT	2	10/11/15	C	2	Circ.	Circ.
SLG18	2015	GW	BHT	1	10/15/15	E	4	Circ.	Circ.
TAG07	2015	GW	BHT	2	Circ.	Circ.	1	Circ.	Circ.

ID	Year*	Species	BCR	Number aut. FLPs	Date aut. trans-Gulf FLP	Aut. departure sector	Number spr. FLPs	Date spr. trans-Gulf FLP	Spr. departure sector
TAG09	2015	GW	BHT	1	10/11/15	E	1	Circ.	Circ.
TAG14	2015	GW	BHT	0	Circ.	Circ.	0	Circ.	Circ.
TNB03	2015	BW	AM	1	Circ.	Circ.	n/a	n/a	n/a
TNB09	2015	BW	CH	1	10/1/15	C	1	4/18/16	C
TNG13	2015	GW	AM	1	Circ.	Circ.	1	Circ.	Circ.
VAG01	2015	GW	AM	4	9/27/15	E	2	4/21/16	C
VAG02	2015	GW	AM	1	10/1/15	E	0	Circ.	Circ.
WIB05	2015	BW	PHT	1	Circ.	Circ.	1	Circ.	Circ.
WIB11	2015	BW	PHT	1	Circ.	Circ.	1	Circ.	Circ.
WIB11	2016	BW	PHT	0	Circ.	Circ.	1	Circ.	Circ.
WIB19	2016	BW	PHT	1	10/8/16	C	1	4/25/17	C
WIG01	2015	GW	BHT	3	10/1/15	C	5	4/28/16	C
WIG02	2015	GW	BHT	4	10/18/15	E	2	Circ.	Circ.
WIH03	2015	H	BHT	1	Circ.	Circ.	1	4/22/16	C
WIH03	2016	H	BHT	0	Circ.	Circ.	1	Circ.	Circ.
MN03[b]	2013	GW	BHT	n/a	n/a	n/a	n/a	n/a	n/a
MN05	2013	GW	BHT	1	10/7/13	C	5	4/18/14	C
MN06	2013	GW	BHT	1	Circ.	Circ.	1	Circ.	Circ.
MN11	2013	GW	BHT	2	10/8/13	E	1	4/25/14	C
MN12	2013	GW	BHT	2	10/7/13	C	1	4/24/14	C
MN14	2013	GW	BHT	4	10/7/13	E	n/a	n/a	n/a
MN15	2013	GW	BHT	1	10/7/13	C	n/a	n/a	n/a
MN16	2013	GW	BHT	1	Circ.	Circ.	4	Circ.	Circ.
MN20	2013	GW	BHT	1	10/8/13	E	1	5/4/14	C
MN25	2014	GW	BHT	2	10/17/14	E	2	4/26/15	C

ID	Year*	Species	BCR	Number aut. FLPs	Date aut. trans-Gulf FLP	Aut. departure sector	Number spr. FLPs	Date spr. trans-Gulf FLP	Spr. departure sector
MN29	2014	GW	BHT	1	Circ.	Circ.	2	Circ.	Circ.
MN36	2014	GW	BHT	1	10/4/14	C	1	4/27/15	C
PA05	2014	GW	AM	2	9/21/14	E	1	Circ.	Circ.
PA11	2014	GW	AM	1	9/21/14	E	1	4/23/15	C
TN05	2013	GW	AM	1	9/10/13	C	2	Circ.	Circ.
TN06	2013	GW	AM	1	Circ.	Circ.	1	4/24/14	C
TN09	2013	GW	AM	3	9/4/13	E	3	3/27/14	E
TN10	2013	GW	AM	1	9/6/13	E	1	4/20/14	E
TN13	2013	GW	AM	2	8/29/13	E	5	4/13/14	C
TN13	2014	GW	AM	3	8/22/14	E	2	4/12/15	C
TN16	2013	GW	AM	4	9/4/13	C	11	4/8/14	E
B1	2016	GW	BHT	1	9/13/16	E	1	4/29/16	W
B2	2016	GW	BHT	2	10/8/16	E	1	4/28/16	C
B3	2016	GW	BHT	1	10/17/16	E	2	Circ.	Circ.
B4	2016	GW	BHT	1	9/28/16	C	2	4/25/16	C
B5	2016	GW	BHT	2	10/1/16	E	1	5/11/16	C
B6	2016	GW	BHT	2	10/8/16	C	1	Circ.	Circ.
B7	2016	GW	BHT	3	10/14/16	C	1	5/8/16	C
B8	2016	GW	BHT	4	10/11/16	E	2	4/30/16	C
B9	2016	GW	BHT	1	10/9/16	C	2	4/25/16	C
B10	2016	GW	BHT	2	9/28/16	E	1	4/28/16	W
B11	2016	GW	BHT	2	9/30/16	C	1	4/26/16	C
B12	2016	GW	BHT	1	10/8/16	W	1	4/27/16	C
B13	2016	GW	BHT	1	10/8/16	E	0	Circ.	Circ.
B14	2016	GW	BHT	1	10/6/16	E	2	4/28/16	W

ID	Year*	Species	BCR	Number aut. FLPs	Date aut. trans-Gulf FLP	Aut. departure sector	Number spr. FLPs	Date spr. trans-Gulf FLP	Spr. departure sector
B15	2016	GW	BHT	1	10/18/16	C	2	4/25/16	C
B16	2016	GW	BHT	1	10/8/16	W	1	5/8/16	C
B17	2016	GW	BHT	1	10/8/16	C	1	5/1/16	C
B18	2016	GW	BHT	1	9/20/16	C	1	Circ.	Circ.
B19	2016	GW	BHT	n/a	n/a	n/a	3	5/1/16	C
B20	2016	GW	BHT	1	10/8/16	C	2	4/26/16	C

* Deployment year

[a] Female

[b] Mud caked over light sensor; omitted from analysis

Table C.4. Geographic coordinates of departure sectors used to characterize the location of *Vermivora* warblers before crossing the Gulf of Mexico and extract weather data.

	Season			
	Autumn		Spring	
Sector	Longitude	Latitude	Longitude	Latitude
Circumvent	-100°	24.5°	-100°	24.5°
West	-96°	28.5°	-96°	20.5°
Central	-90°	28.5°	-90°	20.5°
East	-84°	28.5°	-84°	20.5°

Table C.5: Correlation matrix among autumn weather variables used in logistic regression modeling of departure events in *Vermivora* warblers.

Variable	Wind profit (850 hPa)	Delta wind profit	Temp. (sfc)	Temp. (850 hPa)	Delta temp.	Humidity (sfc)	Humidity (850 hPa)	Delta humidity	Baro. pressure (sfc; hPa)	Delta baro. pressure
Wind profit (sfc)	r = 0.54 P < 0.001	r = 0.47 P < 0.001	r =-0.34 P < 0.001	r = -0.36 P < 0.001	r = -0.07 P = 0.10	r=-0.03 P=0.51	r=-0.01 P=0.78	r=-0.04 P=0.30	r = -0.14 P < 0.001	r = 0.07 P = 0.10
Wind profit (850 hPa)		r = 0.29 P < 0.001	r = -0.23 P < 0.001	r = -0.19 P < 0.001	r = 0.05 P = 0.24	r = -0.15 P < 0.001	r = -0.16 P < 0.001	r = -0.11 P = 0.01	r = -0.11 P = 0.006	r = 0.21 P < 0.001
Delta wind profit			r = 0.04 P = 0.31	r = -0.01 P = 0.81	r = -0.09 P = 0.03	r = -0.01 P = 0.73	r = -0.11 P = 0.006	r = -0.04 P = 0.30	r = -0.04 P = 0.29	r = -0.05 P = 0.27
Temp. (sfc)				**r = 0.61** **P < 0.001**	r = 0.33 P < 0.001	r = -0.08 P = 0.05	r = 0.00 P = 0.97	r = -0.02 P = 0.61	r = 0.12 P = 0.003	r = -0.09 P = 0.03
Temp. (850 hPa)					r = 0.19 P < 0.001	r = 0.10 P = 0.02	r = -0.43 P < 0.001	r = -0.08 P = 0.06	r = 0.09 P = 0.030	r = -0.04 P = 0.37
Delta temp.						r = -0.02 P = 0.70	r = -0.02 P = 0.59	r = -0.06 P = 0.14	r = 0.04 P = 0.34	r = 0.12 P = 0.003
Humidity (sfc)							r = 0.38 P < 0.001	r = 0.52 P < 0.001	r = -0.27 P < 0.001	r = -0.18 P < 0.001
Humidity (850 hPa)								r = 0.29 P < 0.001	r = -0.28 P < 0.001	r = -0.21 P < 0.001
Delta humidity									r = -0.02 P = 0.68	r = -0.19 P < 0.001
Baro. pressure (sfc; hPa)										r = 0.29 P < 0.001

Table C.6: Correlation matrix among spring weather variables used in logistic regression modeling of departure events in *Vermivora* warblers.

Variable	Wind profit (850 hPa)	Delta wind profit	Temperature (sfc)	Temperature (850 hPa)	Delta temperature	Humidity (sfc)	Humidity (850 hPa)	Delta humidity	Barometric pressure (sfc; hPa)	Delta barometric pressure
Wind profit (sfc)	**$r = 0.64$** **$P < 0.001$**	$r = 0.51$ $P < 0.001$	$r = 0.27$ $P < 0.001$	$r = 0.37$ $P < 0.001$	$r = 0.04$ $P = 0.38$	$r = -0.05$ $P = 0.27$	$r = -0.36$ $P < 0.001$	$r = 0.04$ $P = 0.31$	$r = -0.28$ $P < 0.001$	$r = -0.51$ $P < 0.001$
Wind profit (850 hPa)		$r = 0.30$ $P < 0.001$	$r = 0.30$ $P < 0.001$	$r = 0.41$ $P < 0.001$	$r = 0.11$ $P = 0.01$	$r = -0.13$ $P = 0.002$	$r = -0.18$ $P < 0.001$	$r = 0.01$ $P = 0.85$	$r = -0.37$ $P < 0.001$	$r = -0.42$ $P < 0.001$
Delta wind profit			$r = 0.09$ $P = 0.04$	$r = 0.09$ $P = 0.05$	$r = 0.17$ $P < 0.001$	$r = -0.10$ $P = 0.03$	$r = -0.11$ $P = 0.008$	$r = -0.12$ $P = 0.005$	$r = -0.06$ $P = 0.18$	$r = -0.25$ $P < 0.001$
Temp. (sfc)				$r = 0.57$ $P < 0.001$	$r = 0.35$ $P < 0.001$	**$r = -0.83$** **$P < 0.001$**	$r = -0.08$ $P = 0..07$	$r = -0.24$ $P < 0.001$	$r = -0.47$ $P < 0.001$	$r = -0.12$ $P = 0.007$
Temp. (850 hPa)					$r = 0.25$ $P < 0.001$	$r = -0.24$ $P < 0.001$	$r = -0.53$ $P < 0.001$	$r = -0.12$ $P = 0.004$	**$r = -0.84$** **$P < 0.001$**	$r = -0.30$ $P < 0.001$
Delta temp.						$r = -0.30$ $P < 0.001$	$r = -0.23$ $P < 0.001$	**$r = -0.77$** **$P < 0.001$**	$r = -0.15$ $P < 0.001$	$r = -0.32$ $P < 0.001$
Humidity (sfc)							$r = 0.05$ $P =0.23$	$r = 0.34$ $P < 0.001$	$r = 0.15$ $P < 0.001$	$r = 0.10$ $P = 0.02$
Humidity (850 hPa)								$r = 0.33$ $P < 0.001$	$r = 0.31$ $P < 0.001$	$r = 0.24$ $P < 0.001$
Delta humidity									$r = 0.01$ $P = 0.73$	$r = 0.14$ $P = 0.001$
Baro. pressure (sfc; hPa)										$r = 0.40$ $P < 0.001$

Table C.7: Performance of generalized linear models considered in a drop-one regression analysis modeling framework exploring whether the probability of exhibiting full light pattern (FLP) anomalies was associated with year, population, or both variables' interactions ordinal day. Top-performing models (based on Akaike's Information Criterion adjusted for sample size; AIC$_c$) are bold. Model name (Model), the number of estimated parameters (*k*), difference between AIC$_c$ of top-performing model (ΔAIC$_c$), model deviance (-2*log-likelihood), and migration period (Period) are presented.

Model	*k*	ΔAIC$_c$	-2*log-likelihood	Period
Seven-day window				
Intercept only[1]	1	0.0	447.0	Autumn
Population*Ordinal Day	10	2.7	431.3	Autumn
Year	4	5.7	446.6	Autumn
Year*Ordinal Day	8	6.5	439.3	Autumn
Population	5	7.2	446.1	Autumn
Year*Ordinal Day + Population*Ordinal Day	16	12.8	428.9	Autumn
Four-day window				
Intercept only[2]	1	0.0	354.8	Autumn
Year	4	5.7	354.4	Autumn
Population	5	7.2	348.3	Autumn
Year*Ordinal Day	8	11.9	352.2	Autumn
Population*Ordinal Day	10	12.4	348.5	Autumn
Year*Ordinal Day + Population*Ordinal Day	16	24.2	347.3	Autumn
Two-day window				
Intercept only[3]	1	0.0	228.6	Autumn
Year	4	5.7	228.0	Autumn
Population	5	7.1	227.3	Autumn
Year*Ordinal Day	8	13.8	227.5	Autumn
Population*Ordinal Day	10	15.7	224.9	Autumn
Year*Ordinal Day + Population*Ordinal Day	16	28.9	223.9	Autumn
Seven-day window				
Intercept only[4]	1	0.0	389.2	Spring
Population*Ordinal Day	10	3.5	374.3	Spring
Year*Ordinal Day	8	4.1	379.0	Spring
Year	4	4.4	387.5	Spring
Population	5	7.1	388.2	Spring
Year*Ordinal Day + Population*Ordinal Day	16	11.8	369.9	Spring

Model	*k*	ΔAIC_c	-2*log-likelihood	Period
Four-day window				
Intercept only[5]	1	0.0	311.0	Spring
Year	4	4.3	309.2	Spring
Population	5	7.0	309.8	Spring
Year*Ordinal Day	8	9.2	305.7	Spring
Population*Ordinal Day	10	12.7	305.0	Spring
Year*Ordinal Day + Population*Ordinal Day	16	22.6	301.7	Spring
Two-day window				
Intercept only[6]	1	0.0	204.7	Spring
Year	4	3.9	202.4	Spring
Population	5	6.8	203.1	Spring
Year*Ordinal Day	8	10.6	200.3	Spring
Population*Ordinal Day	10	16.0	201.1	Spring
Year*Ordinal Day + Population*Ordinal Day	16	27.6	198.3	Spring

[1] AIC_c of top model = 449.0
[2] AIC_c of top model = 356.8
[3] AIC_c of top model = 230.6
[4] AIC_c of top model = 391.2
[5] AIC_c of top model = 313.0
[6] AIC_c of top model = 206.7

Table C.8: Performance of generalized linear models exploring the relationship between weather conditions and departure of *Vermivora* warblers across the Gulf of Mexico. Models were parameterized using a drop-one modeling approach (Drop-one) or contained variables for all weather conditions considered (Full). Null (intercept-only) models are also presented. Top-performing models (based on Akaike's Information Criterion adjusted for sample size; AIC_c) are bold. Model name (Model), the number of estimated parameters (*k*), difference between AIC_c of top-performing model (ΔAIC_c), model deviance (-2*log-likelihood), and migration period (Period) are presented.

Model	*k*	ΔAIC_c	-2*log-likelihood	Period
Seven-day window				
Drop-one[1]	**6**	**0**	**391.2**	**Autumn**
Full	11	5.1	386	Autumn
Null	1	45.7	447	Autumn
Four-day window				
Drop-one[2]	**6**	**0**	**301.7**	**Autumn**
Full	11	8.3	299.4	Autumn
Null	1	42.8	354.8	Autumn
Two-day window				
Drop-one[3]	**5**	**0**	**192.8**	**Autumn**
Full	11	9	188.5	Autumn
Null	1	27.4	228.6	Autumn
Seven-day window				
Drop-one[4]	**3**	**0**	**363.7**	**Spring**
Full	8	1.9	355.5	Spring
Null	1	21.4	389.2	Spring
Four-day window				
Drop-one[5]	**4**	**0**	**287.7**	**Spring**
Full	8	5.3	284.6	Spring
Null	1	17.2	311	Spring
Two-day window				
Drop-one[6]	**4**	**0**	**189.4**	**Spring**
Full	8	8	188.7	Spring
Null	1	9	204.7	Spring

[1] AIC_c of top model = 403.3
[2] AIC_c of top model = 314.0
[3] AIC_c of top model = 203.2
[4] AIC_c of top model = 369.8
[5] AIC_c of top model = 295.8
[6] AIC_c of top model = 197.7

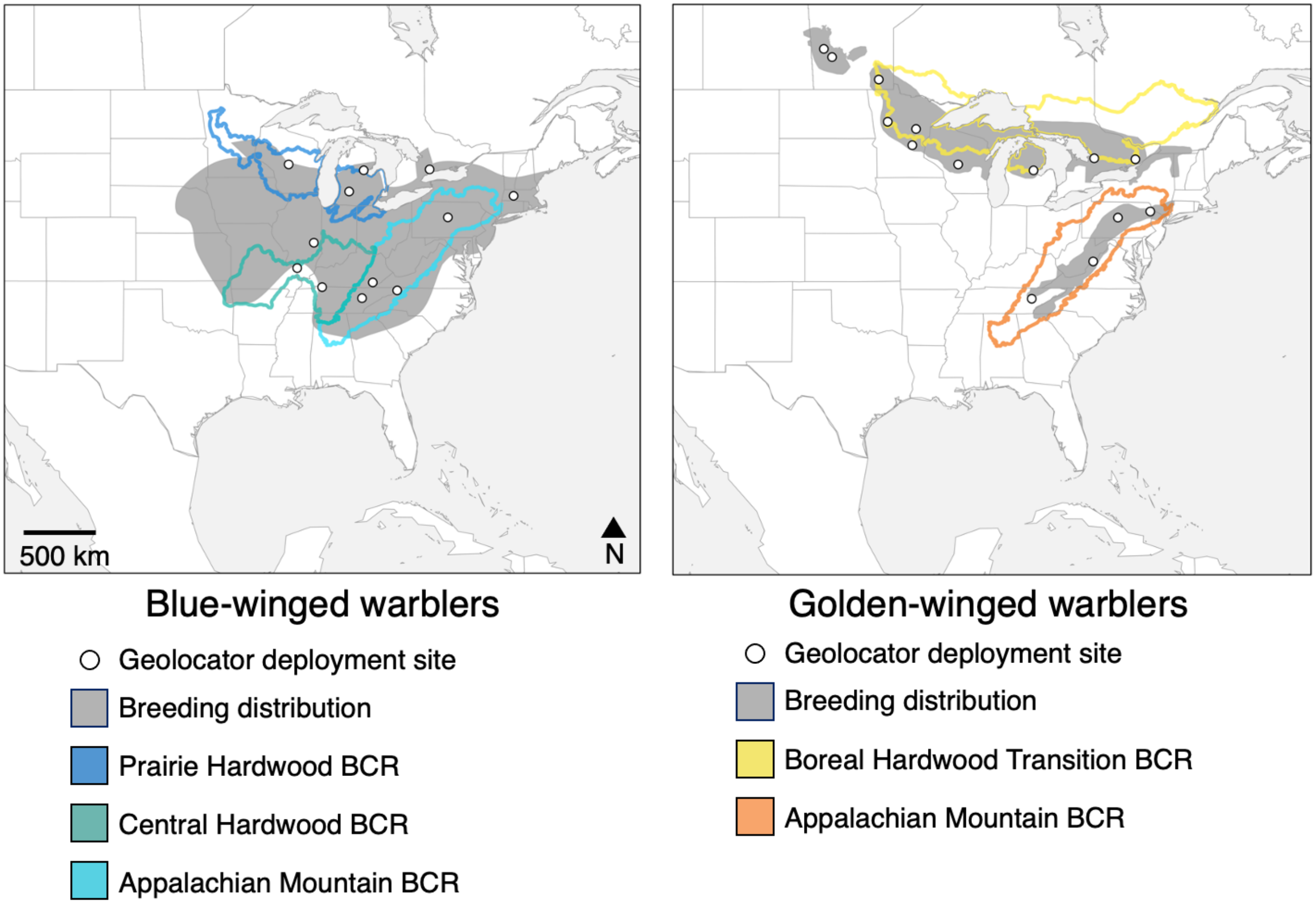

Figure C – 1: Map of breeding distributions, geolocator deployment sites, and Bird Conservation Regions relevant to blue-winged warblers (left) and golden-winged warblers (right).

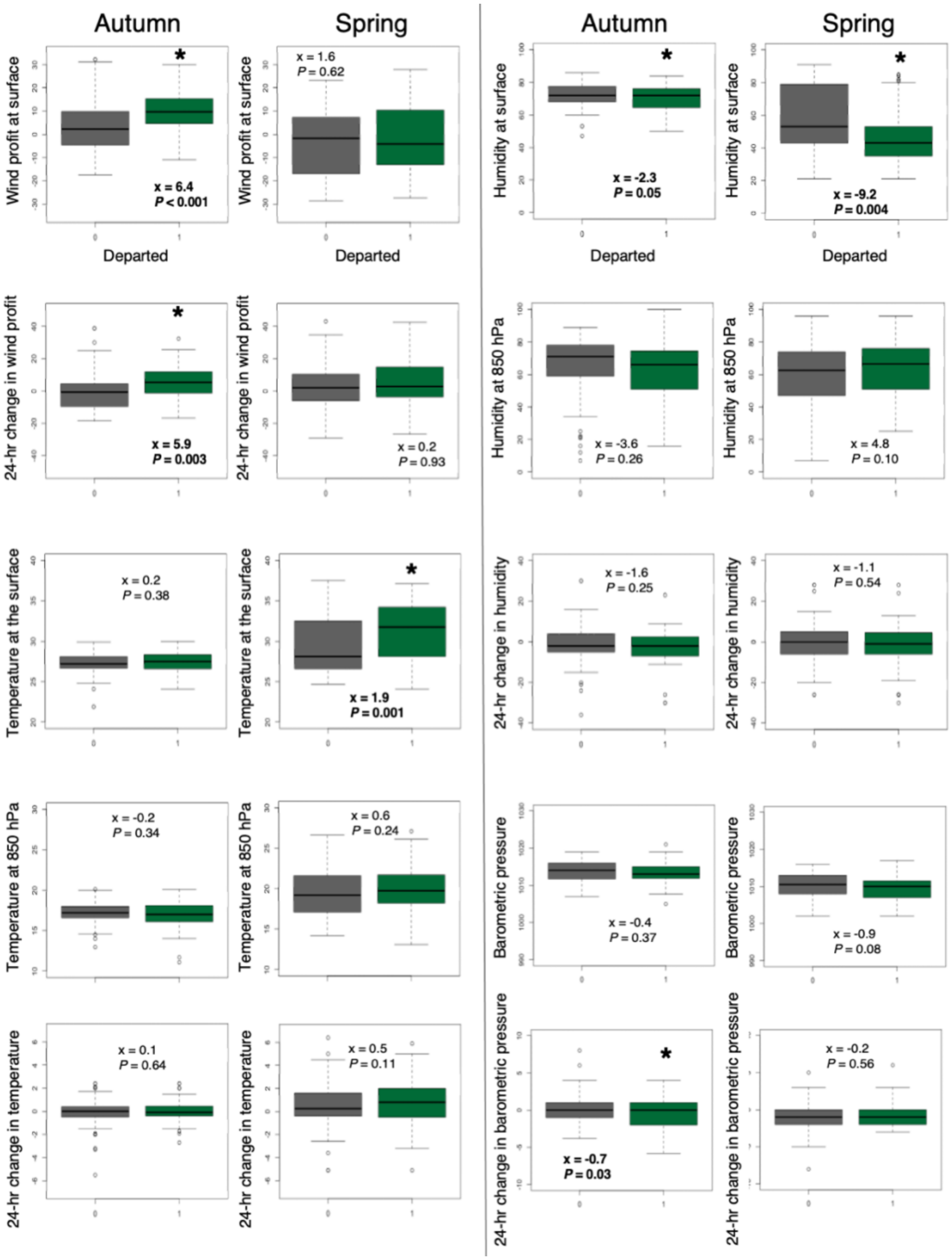

Fig. C – 2: Boxplots comparing weather conditions on days that *Vermivora* warblers departed across the Gulf of Mexico (green) vs. days with no observed departure (gray) based on the absence of full light period (FLP) anomalies in light-level geolocator data. I tested for differences in conditions on days with departures vs. those without during both autumn and spring migration periods using linear models and presented the results (mean difference and associated *P*-value) in each graph. Conditions that differed significantly between seasons (i.e., $P < 0.05$) are bold and noted with an asterisk. See main text for detailed descriptions of weather variables.

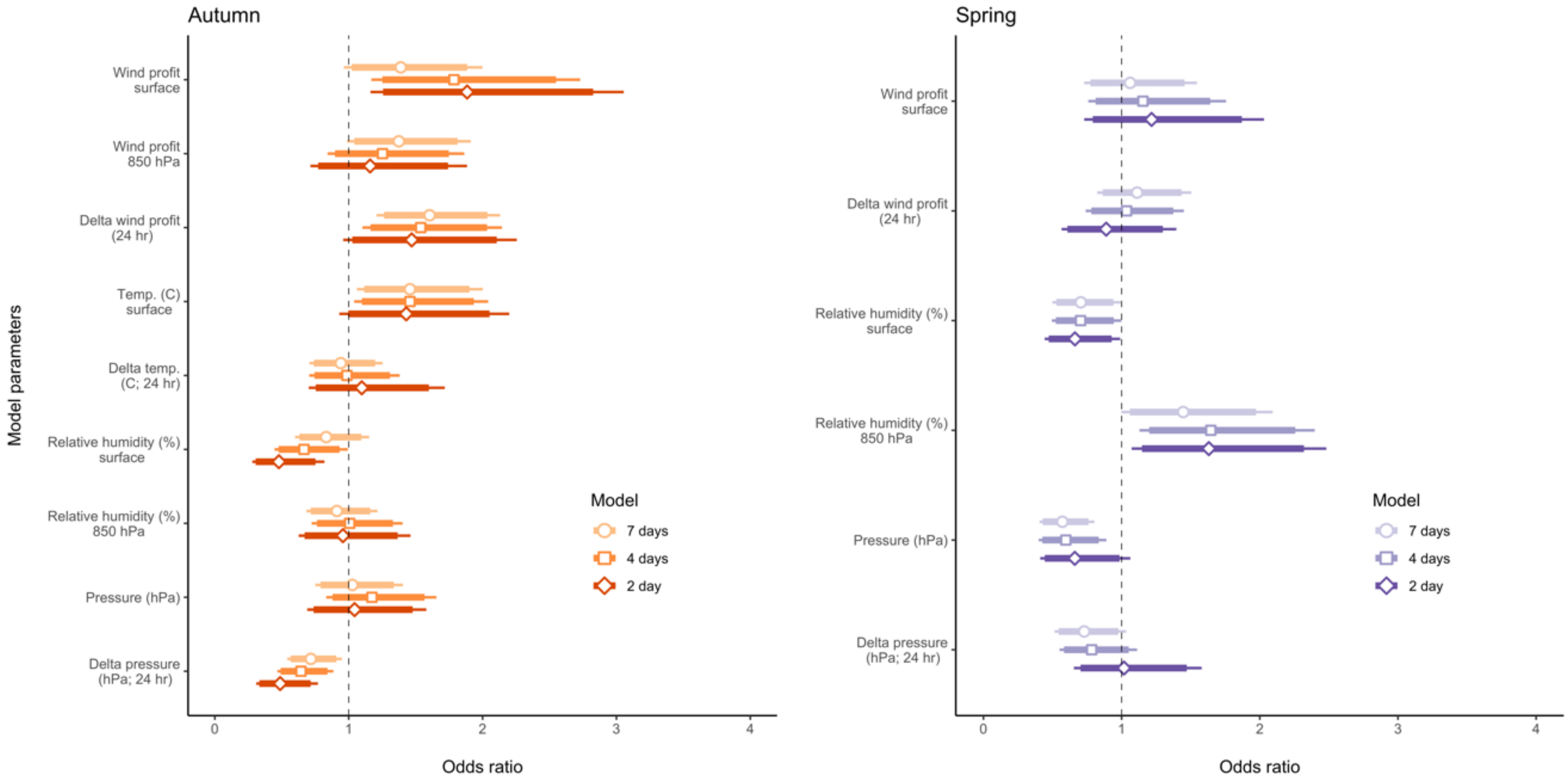

Figure C – 3: Coefficient plot for fully parameterized logistic regression models exploring the effects of weather conditions on the initiation of trans-Gulf of Mexico flights in *Vermivora* warblers. Models contain all weather terms considered in each migration season. I considered models exploring the relationship between weather conditions on departure day and during the previous day (two-day model), departure day and the previous three days (four-day model), and departure day and the previous six days (seven-day model).

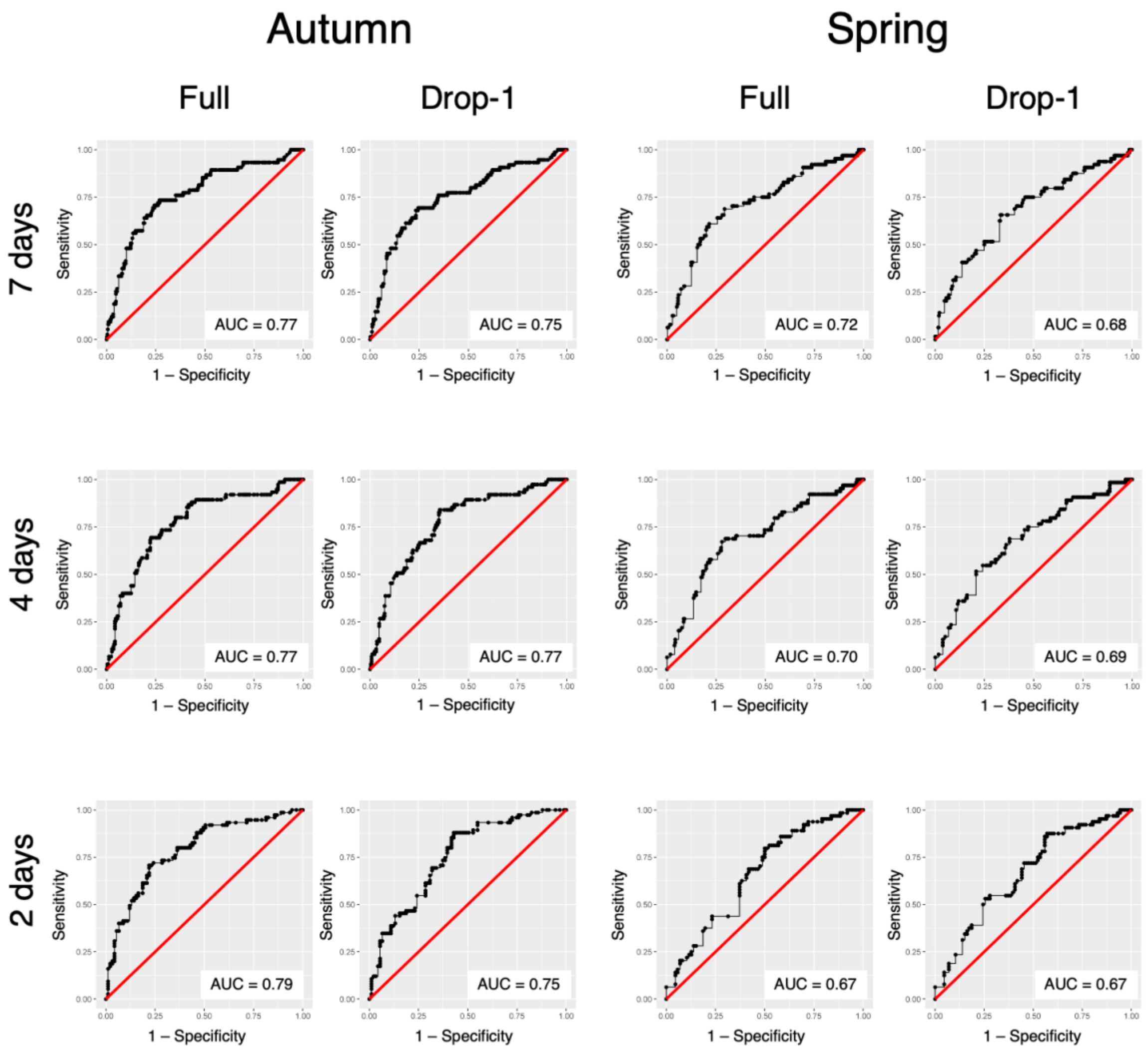

Figure C – 4: Receiver operating characteristic (ROC) curves of logistic regression models containing all weather variables considered (Full) and final models selected using a drop-one modeling approach (Drop-1) that included all terms that, if dropped, would reduce model performance (based on AIC$_c$). I considered models exploring the relationship between weather conditions on departure day and during the previous day (two-day model), departure day and the previous three days (four-day model), and departure day and the previous six days (seven-day model).

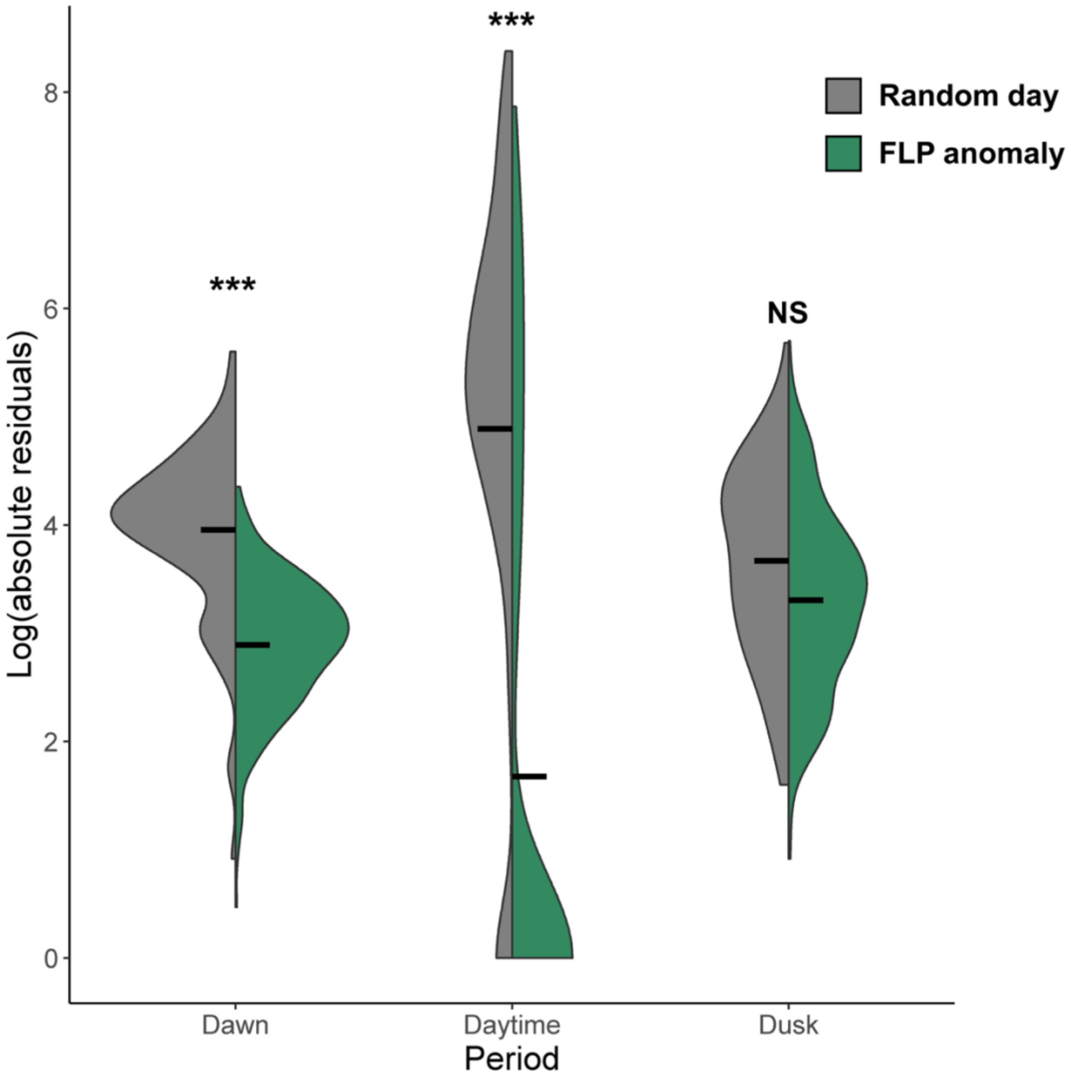

Figure C – 5: Violin plots of the absolute value of residuals (log-scale) of geolocator-derived light data during three periods on randomly selected days (gray) and on full light pattern (FLP)-anomaly days (green). Residuals calculated as the sum of absolute value of deviations from a quadratic equation fit to light data (dawn, dusk) or deviations from maximum light (daytime). Black lines are group means. Asterisks denote significant differences between light conditions on random days vs. FLP-days for a given period based on a two-way ANOVA and subsequent Tukey post-hoc test at $P < 0.05$. The lack of evidence for statistical differences is denoted by "NS".

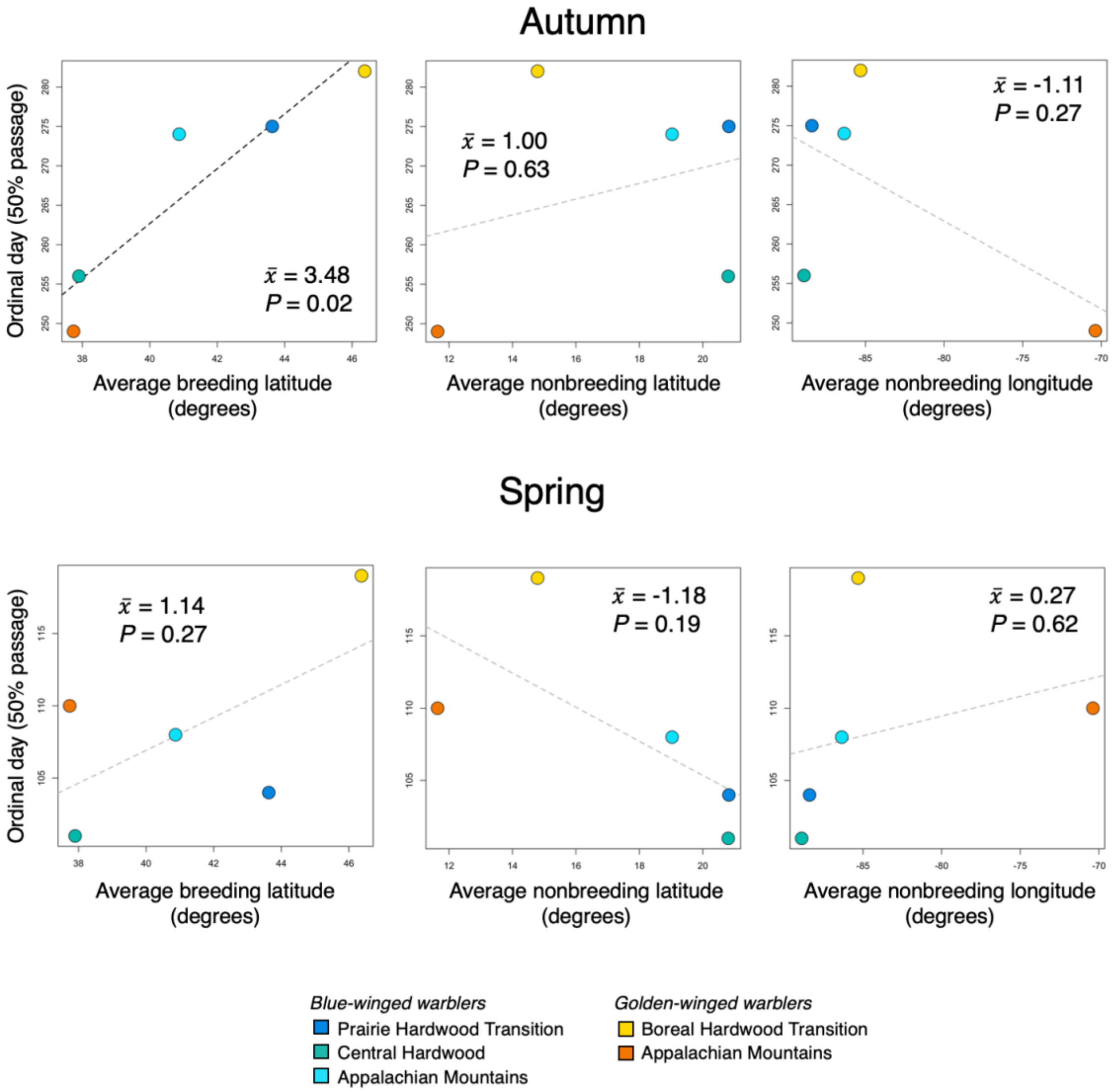

Figure C – 6: Regression plots displaying the seasonal relationship between the 50% passage date (i.e., ordinal day by which 50% of individuals crossed the Gulf of Mexico) and three population-specific spatial factors: average breeding latitude, average nonbreeding latitude, and average nonbreeding longitude. Colored points represent individual populations of *Vermivora* warblers and population-level metrics used for explanatory variables were derived as an average of individuals within a given population. Dashed lines show the results of linear regressions with gray lines indicating no statistically significant relationship (i.e., $P > 0.05$) and black lines indicating a statistically significant association between predictor variables and 50% passage date.

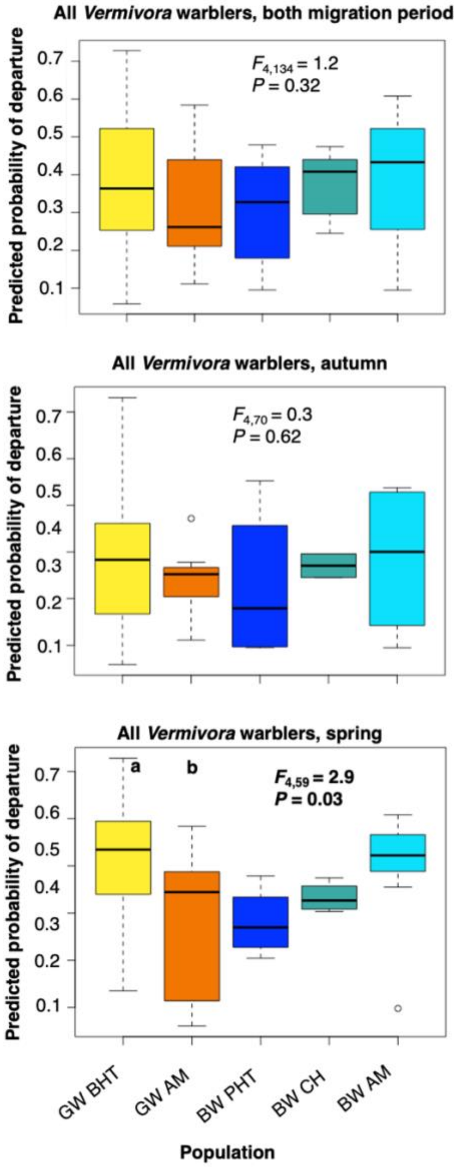

Fig. C – 7: Boxplots of predicted favorability of weather conditions (predicted probability of departure) by population (based on Bird Conservation Regions [BCR]). I tested for differences among groups using one-way ANOVAs and Tukey HSD ($P < 0.05$). Bold text indicates significant differences among groups based on ANOVAs and letters over bars indicate specific differences. Golden-winged warblers from breeding sites in the Boreal Hardwood Transition BCR (GW BHT), Appalachian Mountain BCR (GW AM) are represented with yellow and orange shades, respectively. Blue-winged warblers from breeding populations in the Prairie Hardwood Transition BCR (BW PHT), Central Hardwoods BCR (BW CH), or Appalachian Mountain BCR (BW AM) are represented by different shades of blue.

Appendix D

Supplementary Information for Chapter 4: The Evolution and Evolutionary Constraints of Strong Migratory Connectivity in the Anthropocene

Supplementary Methods:

Animating the evolution of migratory connectivity simulations— To visualize the evolution of migratory connectivity through time (Fig. D –3), I used the 'animation' package in R (Xie 2013, Xie et al. 2018). The animation depicts the breeding and nonbreeding genotype scores of individuals in the population at the end of each generation. Colors of points (representing individuals) indicate phenotype.

Plotting golden-winged warbler migratory connectivity— I plotted the breeding and nonbreeding coordinates of individual golden-winged warblers (*n* = 79) tracked with geolocators (Fig. 4 – 8). I aggregated data form published sources (Kramer et al. 2017, 2018a; Larkin et al. 2017; Bennett et al. 2019b) and a thesis (Buckardt Thomas 2019). All geolocator data were collected from 2013–2017.

Table D.1: Simulation scenario details describing the fitness penalties imposed on individuals in simulation. If penalty is "none", then vital rate was drawn from the distribution(s) used in the Null scenario (Fig. 4 – 2). Fitness penalties are relative to mean vital rate used in Null scenarios. For example, a fitness penalty of -33% on survival means that the nonbreeding period survival rate for individuals with discordant breeding (Br) and nonbreeding (NB) phenotypes is drawn from a distribution with a mean that is 33% lower than the null distribution. Constant penalties are imposed every generation of a simulation.

Scenario	Reproduction penalty for discordant Br/NB phenotype	Survival penalty discordant for Br/NB phenotype	Penalty for individuals with concordant Br/NB phenotypes but intermediate genotypes?	Intermediate genotype range	Generational frequency of penalty (percent of generations in simulation)
Null					
Null	None	None	None	N/A	N/A
Reproduction					
R1	-33%	None	None	N/A	Constant (100%)
R2	-33%	None	Yes; -16%	-0.25 – 0.25	Constant (100%)
R3	-33%	None	Yes; -16%	-0.50 – 0.50	Constant (100%)
R4	-33%	None	Yes; -16%	-0.75 – 0.75	Constant (100%)
RF2	-33%	None	Yes; -16%	-0.50 – 0.50	Every other generation (50%)
RF4	-33%	None	Yes; -16%	-0.50 – 0.50	Every fourth generation (25%)
RF10	-33%	None	Yes; -16%	-0.50 – 0.50	Every tenth generation (10%)
RF50	-33%	None	Yes; -16%	-0.50 – 0.50	Penalty for 50 generations, relaxed penalty for 50 generations (50%)
Survival					
S1	None	-33%	None	N/A	Constant (100%)
S2	None	-33%	Yes; -16%	-0.25 – 0.25	Constant (100%)
S3	None	-33%	Yes; -16%	-0.50 – 0.50	Constant (100%)
S4	None	-33%	Yes; -16%	-0.75 – 0.75	Constant (100%)
SF2	None	-33%	Yes; -16%	-0.50 – 0.50	Every other generation (50%)
SF4	None	-33%	Yes; -16%	-0.50 – 0.50	Every fourth generation (25%)
SF10	None	-33%	Yes; -16%	-0.50 – 0.50	Every tenth generation (10%)
SF50	None	-33%	Yes; -16%	-0.50 – 0.50	Penalty for 50 generations, relaxed penalty for 50 generations (50%)

Scenario	Reproduction penalty for discordant Br/NB phenotype	Survival penalty discordant for Br/NB phenotype	Penalty for individuals with concordant Br/NB phenotypes but intermediate genotypes?	Intermediate genotype range	Generational frequency of penalty (percent of generations in simulation)
Survival and Reproduction (Both)					
B1	-33%	-33%	None	N/A	Constant (100%)
B2	-33%	-33%	Yes; -16%	-0.25 – 0.25	Constant (100%)
B3	-33%	-33%	Yes; -16%	-0.50 – 0.50	Constant (100%)
B4	-33%	-33%	Yes; -16%	-0.75 – 0.75	Constant (100%)
BF2	-33%	-33%	Yes; -16%	-0.50 – 0.50	Every other generation (50%)
BF4	-33%	-33%	Yes; -16%	-0.50 – 0.50	Every fourth generation (25%)
BF10	-33%	-33%	Yes; -16%	-0.50 – 0.50	Every tenth generation (10%)
BF50	-33%	-33%	Yes; -16%	-0.50 – 0.50	Penalty for 50 generations, relaxed penalty for 50 generations (50%)

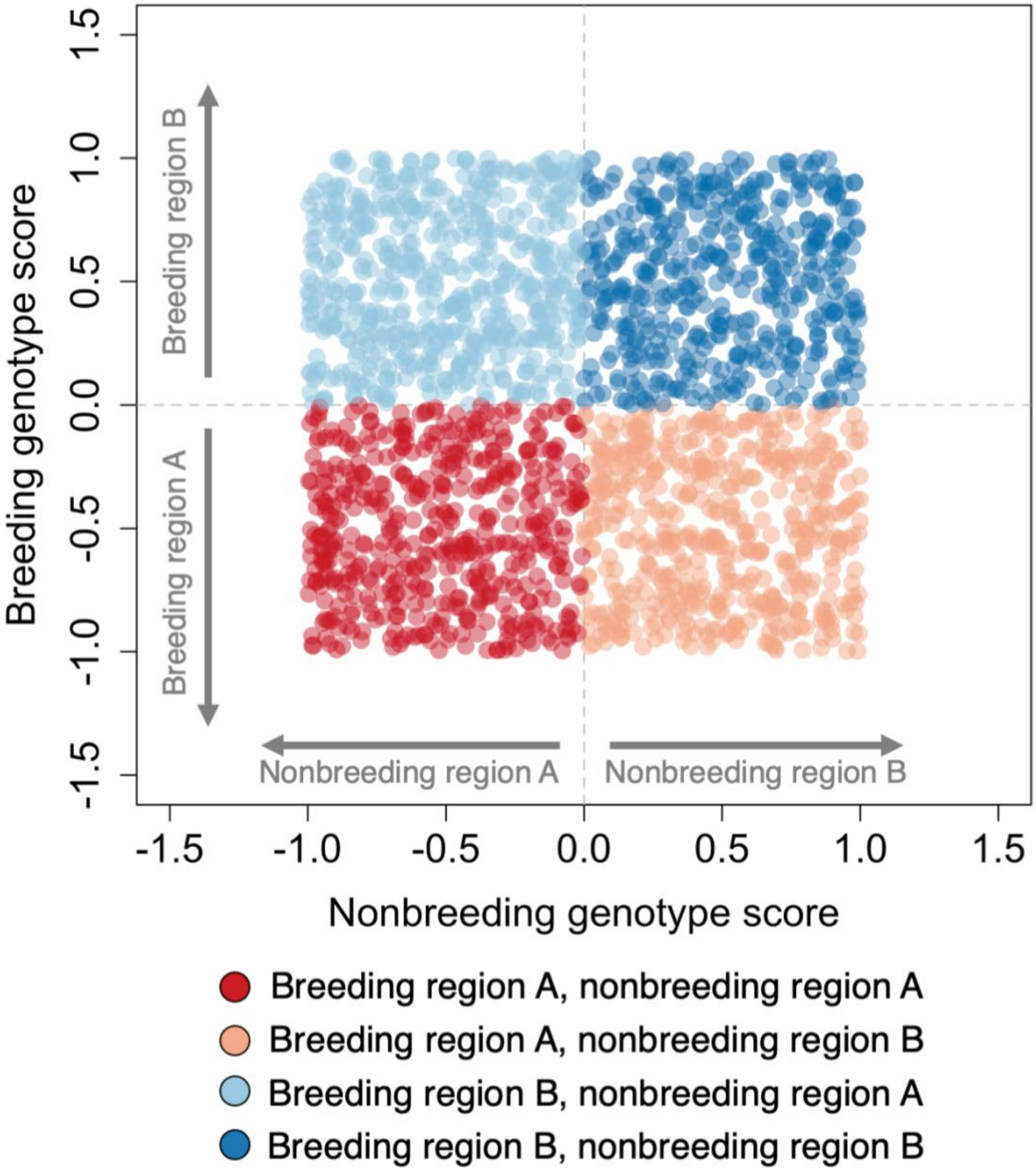

Figure D – 1: Plot of randomly generated breeding and nonbreeding genotype scores of a starting population used in simulations of the evolution of migratory connectivity. Phenotypes associated with underlying breeding and nonbreeding genotype scores are indicated by different colored points.

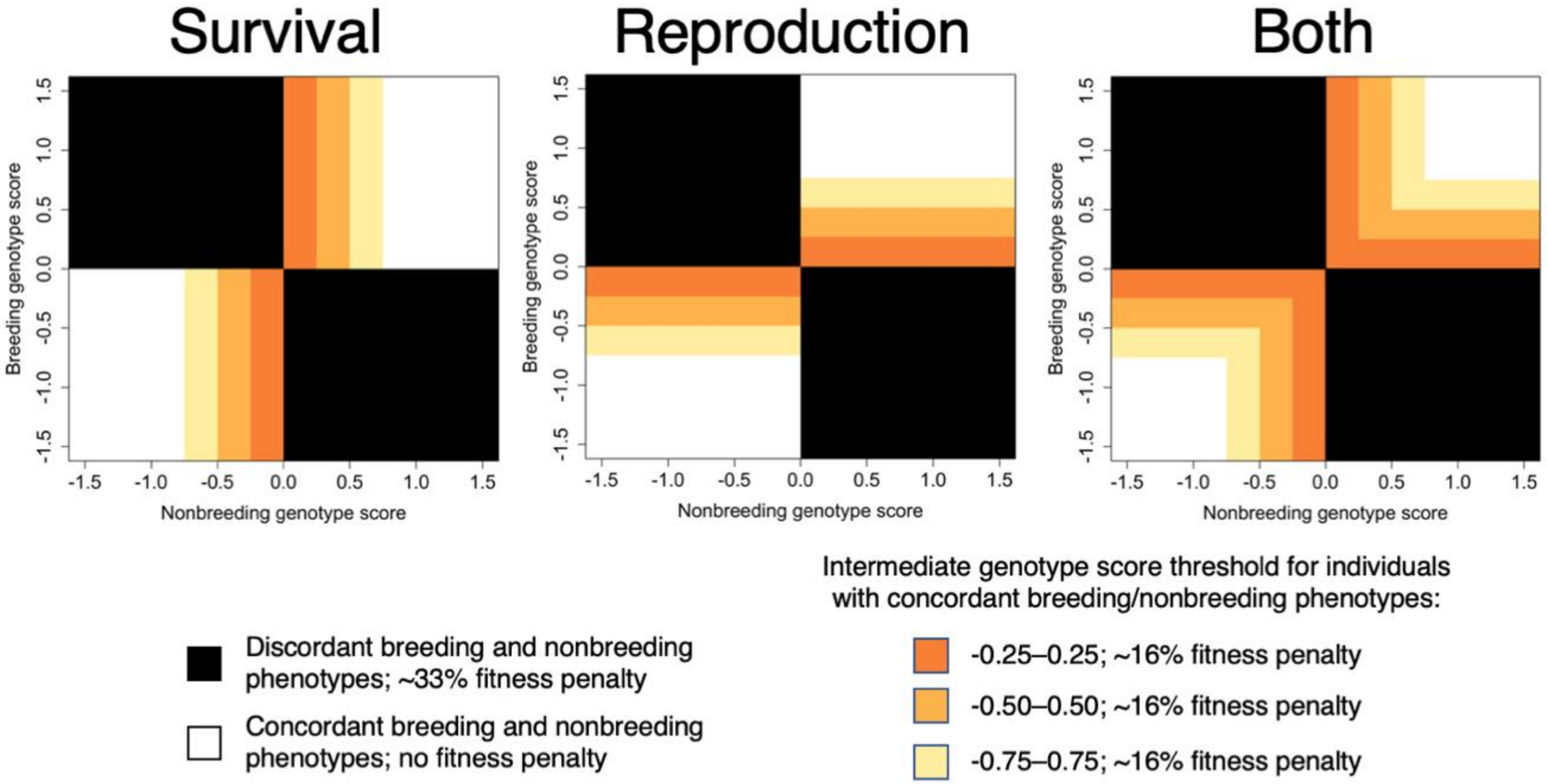

Figure D – 2: Graphic depiction of the fitness penalties imposed on individuals based on concordance of breeding and nonbreeding phenotypes and the intermediacy of individuals' genotype scores (applies to all scenarios except null, S1, R1, B1). Individuals with discordant breeding and nonbreeding phenotypes (black) experienced a 33% reduction in fitness. Individuals experienced a 16% reduction in fitness (survival, reproduction, or both survival and reproduction) in scenarios that included selection against individuals with concordant breeding and nonbreeding phenotypes, but with genotype scores near zero (-0.25–0.25, dark orange; -0.50–0.50, light orange; -0.75–0.75, yellow). Individuals with concordant breeding and nonbreeding phenotypes and with genotype scores outside of the intermediate genotype thresholds (white) did not experience any fitness penalties.

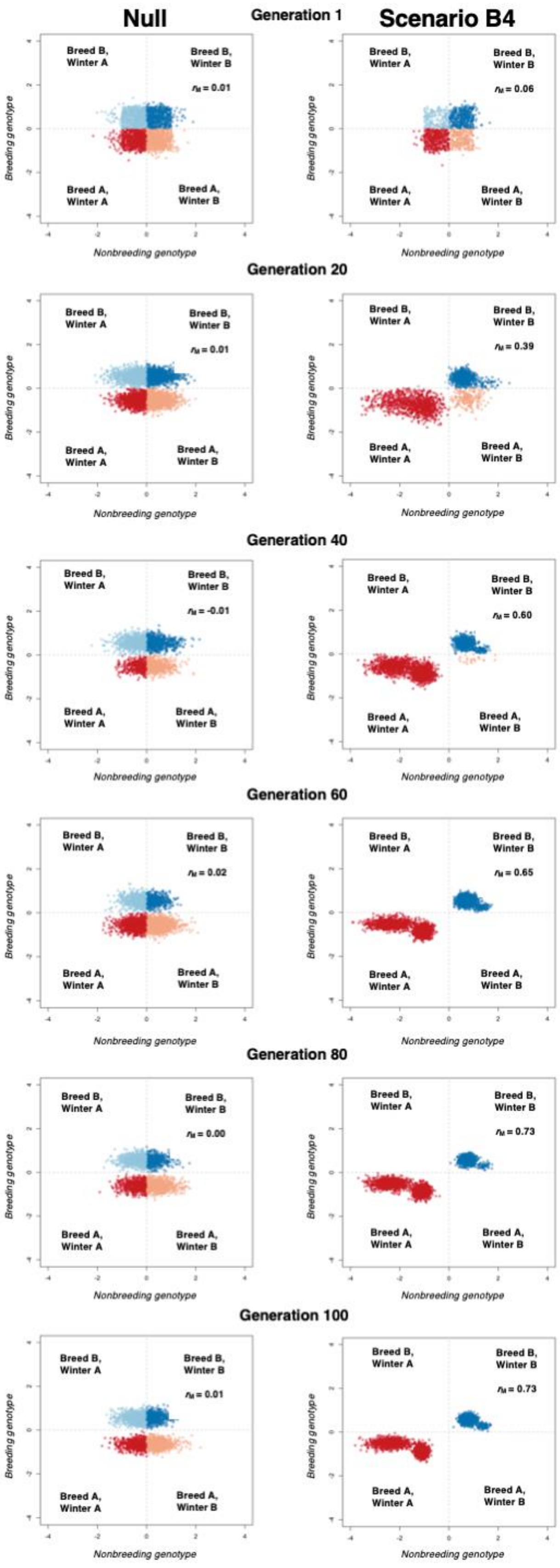
Null
Generation 1
Scenario B4
Breed B, Winter A
Breed B, Winter B
r_M = 0.01
Breed A, Winter A
Breed A, Winter B
Breeding genotype
Nonbreeding genotype
Breed B, Winter A
Breed B, Winter B
r_M = 0.06
Breed A, Winter A
Breed A, Winter B
Breeding genotype
Nonbreeding genotype
Generation 20
Breed B, Winter A
Breed B, Winter B
r_M = 0.01
Breed A, Winter A
Breed A, Winter B
Breed B, Winter A
Breed B, Winter B
r_M = 0.39
Breed A, Winter A
Breed A, Winter B
Generation 40
Breed B, Winter A
Breed B, Winter B
r_M = -0.01
Breed A, Winter A
Breed A, Winter B
Breed B, Winter A
Breed B, Winter B
r_M = 0.60
Breed A, Winter A
Breed A, Winter B
Generation 60
Breed B, Winter A
Breed B, Winter B
r_M = 0.02
Breed A, Winter A
Breed A, Winter B
Breed B, Winter A
Breed B, Winter B
r_M = 0.65
Breed A, Winter A
Breed A, Winter B
Generation 80
Breed B, Winter A
Breed B, Winter B
r_M = 0.00
Breed A, Winter A
Breed A, Winter B
Breed B, Winter A
Breed B, Winter B
r_M = 0.73
Breed A, Winter A
Breed A, Winter B
Generation 100
Breed B, Winter A
Breed B, Winter B
r_M = 0.01
Breed A, Winter A
Breed A, Winter B
Breed B, Winter A
Breed B, Winter B
r_M = 0.73
Breed A, Winter A
Breed A, Winter B
-4
-2
0
2
4

Figure D – 3: Plots depicting the evolved strength of migratory connectivity under the null scenario (left) and a scenario in which fitness penalties were imposed on both reproduction and survival in individuals breeding in region A and wintering in region B, or breeding in region B and wintering in region A. I imposed intermediate fitness penalties on individuals breeding in region A and wintering in region A, or breeding in region B and wintering in region B if their genotype scores were -0.75–0.75 (scenario B4). Individuals are represented by colored points and colored based on the combination of their breeding and nonbreeding phenotypes. The strength of migratory connectivity (r_M) estimated at each generation in the simulation is presented. Animated versions of these plots can be viewed at https://gunnarkramer.com/research/mc_simulation/.